The role of chemerin and chemerin receptors during acute inflammation



Sophia Valaris

Hertford College

University of Oxford

A thesis submitted for the degree of

Doctor of Philosophy in Pathology

Michaelmas 2017

Acknowledgements

Firstly, I would like to thank my supervisor, David Greaves, for awarding me this studentship and for giving me the opportunity to join your lab back in 2013. It has been an incredibly valuable experience which I will always treasure. I have learned so much during my time in the lab, having grown as a person and as a scientist. Thank you for always having the time to discuss data, project plans, science in general and finally, for your attention and comments on this thesis.

Secondly, I would like to thank my industrial supervisor, Adrian Moore, and my UCB day-to-day supervisor, Mike Wright, at UCB pharma, for all of your help and support throughout these four years. A special thanks to Mike for your help with using and understanding phage display technology and for making me feel so welcome in your group at UCB.

Next, I want to thank the entire Greaves lab, past and present, for all of your input, time, support and — most of all — your friendship. It has been an amazing experience working and spending my time with you. Gemma, thank you for being my supervisor and a pillar of support in my first year and Asif, for being a mentor and a friend who has always made the time to help. Dan, Lewis and Theo, thank you for always managing to cheer me up with your ridiculous conversations and making the atmosphere in the lab that bit more lively. Daniel, thank you for always having something witty to say in any situation. Carlota, thank you for bringing girl power into the lab, and for helping me with whatever I have needed, whether it was a chat or learning how to do a proper western blot. I would also like to thank all the FHS and rotation students, Max, Jamie, Krithi, Cherelle, Lisa and Poppy, for also making the lab a fun and lively place to come and work every day.

I would like to say thanks to all of my Oxford friends who have supported me, namely my first three Oxford friends, Thuy, Andy and Frankie, and then the ladies of 27 Warwick Street, who have always listened to my woes and would help me forget about them too.

Walid, thank you for your love, friendship and support when I have needed it most. Thanks for making sure that I always do my best but take time off when I need it, and for reminding me to give myself enough credit. Thank you for patience

when dealing with my moods, pushing me to try new things, and to travel to new places. And finally thank you for helping me to get used to LaTex, the program I used to write this thesis, and with the referencing disaster after!

Finally, I want to say a big thank you to all of my family. To Christina and Auntie Katie, for always making Greece the best place to come back home to. To Grandad, for always being there for me and for providing the place I call home in the U.K. when I visit now, and while I was studying in Newcastle. To my lovely Mam and Dad for the constant love and support I have had from you both throughout my life. Words cannot describe how thankful I am to you. Thank you.

Abstract

Cytokines play a major role in orchestrating the inflammatory process. This thesis focuses on one such cytokine, called chemerin. Chemerin is a multifunctional protein that is secreted as an inactive precursor, prochemerin, which becomes proteolytically cleaved at the C-terminus into the active signalling molecule, chemerin. Chemerin binds three G-protein coupled receptors: ChemR23, GPR1 and CCRL2, and acts as a chemoattractant, primarily via the ChemR23 receptor expressed on immature dendritic cells, natural killer cells and macrophages. The role of chemerin during inflammation remains controversial. However, multiple studies have reported elevated levels of chemerin in patients suffering from a plethora of inflammatory and metabolic diseases.

The need for proteolytic cleavage of chemerin's inactive precursor, prochemerin, results in a myriad of prochemerin-derived isoforms, with varying signalling ability. Current commercially available antibodies are not able to detect different different chemerin isoforms. Therefore, one of the aims of my work was to develop and characterise anti-chemerin antibodies derived from a naïve phage display library, which could recognise the inactive sequence of prochemerin and the C-terminus of active chemerin.

I set out to investigate the role of chemerin receptors during early stages of inflammation in a well-established model of acute inflammation. Prior to this, I surveyed the protein and mRNA expression of the ChemR23 receptor and the mRNA expression of CCRL2 and GPR1 chemerin receptors on leukocyte subsets. Following this, I investigated the role of the non-signalling chemerin receptor, CCRL2, using an acute inflammatory model of zymosan-induced peritonitis. Mice lacking the CCRL2 receptor displayed augmented inflammatory response compared to age-matched wild type mice. In early time points of this inflammatory model, the CCRL2 knockout mice displayed increased neutrophil and monocyte infiltration to the site of inflammation and augmented mediator production of CXCL1 partly caused by the increased levels of chemerin in the knockout mice. The use of a neutralising chemerin antibody and the pre-treatment of excess recombinant chemerin led me to this conclusion. These pro-inflammatory effects of chemerin were mediated via signalling through the

ChemR23 receptor. ChemR23 deficient mice display a reduction in neutrophil and monocyte recruitment to the site of inflammation in the same early time points of zymosan-induced peritonitis.

The final aim of this thesis was to investigated the behavioural phenotype of CCRL2 deficient mice after 3 years of working with them. Mice lacking the CCRL2 receptor exhibited increased anxiety behaviour under steady state conditions. Immunohistochemistry of their neuroanatomy showed no differences from age-matched wild type mice. However, wild type *in vitro* cultured microglia cells express the chemerin receptors.

Taken together the results from this thesis illustrate the pro-inflammatory effects of chemerin in early stages of inflammation. Furthermore, the non-signalling chemerin receptor CCRL2 plays a non-redundant role in dampening the effects of chemerin in early stages of inflammation. Further research should be undertaken to elucidate chemerin's role during chronic disease setting of inflammation, in order to suggest whether chemerin could be a beneficial therapeutic target against human disease.

Abbreviations

-/- Knock out gene

a.a. Amino acid sequence

AGEs Advanced glycation end-products

BAL Bronchoalveolar lavage fluid

BBB Blood brain barrier

BDNF Brain-derived neurotophic factor

BMDC Bone marrow derived dendritic cells

BMDM Bone marrow derived macrophages

BSA Bovine serum albumin

CNS Central nervous system

DCs Dendritic cells

DSS Dextran sodium sulfate - induced colitis

EAE Experimental autoimmue encephalitis model

ELISA Enzyme-linked immunosorbent assay

FBS Heat inactivated foetal bovine serum

G-CSF Granulocyte-colony stimulating factor

GPCR G-protein coupled receptor

hchemerin Human chemerin

HCl Hydrocholic acid

HEK 293 Human embryonic kidney 293 cells

HK Housekeeping genes

HPA Hypothalamic-pituitary-adrenal cortex

hprochemerin Human prochemerin

Iba-1 Ionized calcium-binding adaptor molecule 1

IHC Immunohistochemistry

ILCs Innate lymphoid cells

LDLs Low-density lipoproteins

LPS Lipopolysaccharide

M-CSF Macrophage-colony stimulating factor

mAbs Monoclonal antibodies

MAPKs Mitogen-activated protein kinases

NETs Neutrophil Extracellular Traps

NeuN Neuronal nuclei

NK Natural killer cells

NO Nitric oxide

oxLDL Oxidised low-density lipoproteins

PAMPs Pathogen-associated molecular patterns

PBS Phosphate buffered saline

PCR Polymerase chain reaction

pDCs Plasmacytoid dendritic cells

PECs Peritoneal elicited cells

phage Filamentous bacteriophage

RA Rheumatoid arthritis

RAGE Receptor for advanced glycation end-products

RT Room temperature

scFv Single chain variable fragment

SPR Surface plasmon resonance

TLRs Toll-like receptors

TMB 3 5 Tetramethylbenzidine substrate

VH Variable Heavy chain of an antibody

VL Variable Light chain of an antibody

Contents

1 Introduction **1**

1.1 Inflammation . . . 1
1.2 The activation of inflammation . . . 2
1.2.1 Pattern recognition receptors . . . 2
1.2.2 Tissue resident cells . . . 3
1.2.2.1 Tissue resident macrophages . . . 4
1.2.2.2 Mast cells . . . 5
1.2.2.3 Eosinophils . . . 6
1.2.2.4 Dendritic cells . . . 6
1.2.2.5 T cells, B cells and Innate lymphoid cells . . . 7
1.3 Endothelial cells . . . 8
1.4 Neutrophils . . . 10
1.5 Monocytes . . . 12
1.6 Macrophages . . . 13
1.7 Pro-inflammatory mediators . . . 15
1.7.1 Cytokines . . . 15
1.7.1.1 TNFα . . . 16
1.7.1.2 IL-6 . . . 16
1.7.2 Chemokines . . . 17
1.7.2.1 Neutrophil chemoattractants . . . 17
1.7.3 Pro-inflammatory eicosanoids . . . 18
1.8 Resolution of inflammation . . . 20
1.8.0.1 Pro-resolving lipid mediators . . . 21
1.8.0.2 Glucocorticoids and the Annexin A1 protein . . . 22
1.8.0.3 Anti-inflammatory Cytokines . . . 23
1.9 Antibody therapies for chronic inflammation . . . 23
1.10 Chemerin . . . 27
1.10.1 Discovery of chemerin and its receptors . . . 27

1.10.2 Structure and isoforms . . . 28
1.10.3 Chemerin receptor signalling . . . 29
1.10.3.1 ChemR23 (CMKLR1) . . . 29
1.10.3.2 GPR1 . . . 30
1.10.3.3 CCRL2 . . . 30
1.10.4 Chemerin expression . . . 32
1.10.5 Chemerin in inflammation . . . 34
1.10.5.1 *In vitro* activities of chemerin . . . 35
1.10.5.2 *In vivo* treatments and inflammatory models of chemerin 35
1.10.6 Chemerin as an adipokine . . . 36
1.10.7 Chemerin and angiogenesis . . . 37
1.10.8 Antibacterial effects of chemerin . . . 37
1.11 Original hypothesis for this thesis . . . 38
1.12 Experimental aims . . . 39

2 Methods and Materials **40**
2.1 Materials . . . 40
2.1.1 Reagents . . . 40
2.1.2 Animals . . . 40
2.2 Methods . . . 42
2.2.1 Panning a phage display library . . . 42
2.2.1.1 Panning against recombinant murine chemerin . . . 42
2.2.1.2 Panning against C23 peptide . . . 44
2.2.1.3 Phage binding ELISA for chemerin and chemerin peptides . . . 45
2.2.1.4 Mini-prep and Sequencing . . . 45
2.2.2 Cloning scFv genes onto mouse Fc vector . . . 45
2.2.3 Transfections of Freestyle^{TM} 293 cells . . . 47
2.2.4 Antibody purification . . . 47
2.2.5 Quantification of eluted antibody and ligand binding ELISAs . 47
2.2.6 Surface plasmon resonance . . . 48
2.2.7 DiscoverX β-arrestin recruitment assay . . . 49
2.2.8 C23 cleavage assay . . . 49
2.2.9 Western blot . . . 50
2.2.10 *In vivo* model of peritonitis . . . 50
2.2.11 Flow cytometry . . . 51

2.2.12 Cell counting using flow cytometry . . . 52
2.2.13 ELISA . . . 52
2.2.14 Bio-gel elicited peritoneal cells . . . 53
2.2.15 Murine bone marrow derived macrophages . . . 53
2.2.16 Murine bone marrow derived dendritic cells . . . 54
2.2.17 Bone marrow neutrophil isolation . . . 54
2.2.18 Human blood monocyte isolation . . . 55
2.2.19 ACEA xCELLigence real-time chemotaxis assay . . . 55
2.2.20 ACEA 96 well ECIS Electrical impedance sensing assay . . . 56
2.2.21 RNA isolation, reverse transcription and real-time qPCR . . . 56
2.2.22 Behaviour assays . . . 57
2.2.23 Tissue sectioning . . . 57
2.2.24 Immunohistochemistry staining . . . 57
2.2.25 Data and statistical analysis . . . 59

3 Developing antibodies against chemerin using phage display technology 61

3.1 Introduction . . . 61
3.1.1 Chemerin and its various isoforms . . . 62
3.1.2 Phage Display Technology . . . 63
3.1.2.1 Phage structure . . . 63
3.1.2.2 Library Construction . . . 64
3.1.2.3 Biopanning and Clone selection . . . 65
3.1.3 Rationale of study . . . 65
3.2 Results . . . 66
3.2.1 The development and generation of anti-chemerin antibodies . 66
3.2.1.1 Panning against recombinant full length chemerin using UCB phage library. . . . 66
3.2.1.2 Panning against C23 peptide using UCB naive human phage library separate. . . . 69
3.2.1.3 Surface plasmon resonance analysis of C23 pan . . . 71
3.2.1.4 scFv-Fc construct production and purification . . . 74
3.2.1.5 Surface plasmon resonance analysis of reformatted clones 76
3.2.2 Functional characterisation of antibody clones . . . 78
3.2.2.1 DiscoverX β-arrestin recrutiment in CHO-ChemR23 expression system . . . 78

3.2.2.2 The inhibition of chemerin chemotaxis using Bio-gel elicited peritoneal cells . . . 85
3.2.2.3 Human Neutrophil Elastase cleavage assay using the C23 peptide . . . 86
3.2.2.4 Western blot detection of chemerin within peritoneal lavage fluid . . . 91
3.3 Discussion . . . 92
3.3.1 Limitations and future work . . . 97

4 Characterising chemerin receptor expression across leukocyte subsets 98
4.1 Introduction . . . 98
4.1.1 Chemokine-like receptor 1 (ChemR23) . . . 98
4.1.2 G protein coupled receptor 1 (GPR1) . . . 99
4.1.3 CC-Chemokine receptor-like 2 (CCRL2) . . . 99
4.1.4 Rationale of study . . . 100
4.2 Results . . . 100
4.2.1 Bone marrow derived macrophages . . . 100
4.2.2 Bone marrow derived dendritic cells . . . 101
4.2.3 Bone marrow isolated Neutrophils . . . 103
4.2.4 Blood neutrophils and monocytes . . . 104
4.2.5 Bio-gel elicited peritoneal cells . . . 105
4.2.6 Resident populations of cell in the peritoneum . . . 106
4.2.7 mRNA expression of Chemerin and Chemerin receptors in murine tissues . . . 109
4.2.8 Protein expression of ChemR23 receptor on resident leukocytes subsets . . . 109
4.2.8.1 Lung tissue . . . 109
4.2.8.2 Liver tissue . . . 109
4.2.8.3 Spleen tissue . . . 110
4.2.8.4 Human blood monocytes . . . 115
4.2.9 Chemerin treatment in peritoneum . . . 116
4.3 Discussion . . . 118
4.3.1 Macrophages . . . 118
4.3.2 Monocytes . . . 120
4.3.3 Dendritic cells . . . 120

4.3.4 Neutrophils . . . 121
4.3.5 B and T cells . . . 122
4.3.6 Non-leukocyte cells . . . 123
4.3.7 Chemerin treatment *in vivo* . . . 124
4.3.8 Limitations of this study . . . 124

5 CCRL2, a non-signalling chemerin receptor during acute inflammation 126
5.1 Introduction . . . 126
5.1.1 Rationale for study . . . 128
5.2 Results . . . 129
5.2.1 Absence of non-signalling receptor, CCRL2, displays no overt difference in peritoneal resident leukocyte populations under naive conditions. . . . 129
5.2.2 Absence of non-signalling chemerin receptor, CCRL2, exacerbates inflammatory responses in zymosan-induced peritonitis. 130
5.2.3 Absence of non-signalling receptor, CCRL2, increases leukocyte recruitment to peritoneum during acute thioglycollate induced peritonitis. . . . 134
5.2.4 Chemerin blocking antibody treatment attenuates neutrophil recruitment to the local site of inflammation in *CCRL2*$^{-/-}$ mice. 136
5.2.5 Chemerin-treatment exacerbates neutrophil recruitment to local site of inflammation in wild type mice. . . . 138
5.2.6 Real-time chemotaxis of macrophages lacking CCRL2 and ChemR23 receptors. . . . 142
5.2.7 *In vitro* zymosan and chemerin stimulations of peritoneal mesothelium and resident cells. . . . 144
5.2.8 Absence of the chemerin signalling receptor, ChemR23, decreases leukocyte recruitment to the peritoneum during acute zymosan-induced peritonitis. . . . 145
5.3 Discussion . . . 149
5.3.1 The inflammatory phenotype of *CCRL2*$^{-/-}$ mice . . . 149
5.3.2 Other inflammatory models in the absence of CCRL2 . . . 150
5.3.3 Addressing the mechanism driving the inflammatory phenotype 151
5.3.4 Limitations of the study . . . 157

6 Investigating the behaviour of mice lacking CCRL2 receptor 160
6.1 Introduction . . . 160
6.1.1 Immunity, the central nervous system and behaviour . . . 160
6.1.2 Rationale of study . . . 163
6.2 Results . . . 164
6.2.1 Open Field assay . . . 164
6.2.2 Elevated O-Maze test . . . 165
6.2.3 Forced swim test . . . 166
6.2.4 Neuroanatomy of *CCRL2*-/- mice . . . 167
6.2.4.1 Neuronal staining . . . 167
6.2.4.2 Microglial staining . . . 167
6.2.5 *In vitro* cultured microglia cells express chemerin receptor . . . 169
6.3 Discussion . . . 170
6.3.1 Limitations of this study . . . 174

7 Summary and future directions 176
7.1 Key findings . . . 176
7.2 What is the role of chemerin in pathology? Can it be a therapeutic target in human disease? . . . 178
7.3 Future directions . . . 181
7.4 Conclusion . . . 182
Appendix . . . 183
Conference presentations . . . 183
Oral Presentations . . . 183
Poster Presentations . . . 183
Courses Attended . . . 183
Publications . . . 184
Abstract . . . 184

Bibliography 185

List of Figures

1.1 Endothelial activation and the transmigration of leukocytes across endothelium. 10
1.2 Arachidonic acid metabolism. 20
1.3 Polyunsaturated fatty acids (PUFA) metabolism. 22
1.4 Antibody structure 24
1.5 Processing of chemerin and receptor signalling pathways. 31

2.1 A round of phage panning. 43
2.2 Digest products of scFv-Fc plasmids contain scFv and mouse Fc vector. 46
2.3 In-house developed enzyme-linked immunosorbent assays (ELISAs) for antibody quantification and ligand binding. 48
2.4 Comparison between the linear vs $\log_{10}$ analysis of RT-PCR data. . . 58

3.1 Schematic representation of a scFv expressing bateriophage particle. . 64
3.2 Panning against recombinant murine chemerin using UCB phage libraries in a mixture. 68
3.3 Panning against C23 peptide [A^{139} - K^{162}] using UCB phage libraries separately. 70
3.4 CDR3 sequence diversity from Round 3 panning against C23 peptide [A^{139} - K^{162}] using UCB phage libraries separetly. 71
3.5 Group 1 selected scFv clones, in a human IgG1 format, which recognise the active sequence of the C23 & C17 peptide in a T200 SPR analysis. 73
3.6 Group 2 selected scFv clones, in a human IgG1 format, which recognise the sequence of the C23 peptide in a T200 SPR analysis. 74
3.7 Purified scFv -Fc clones and C23 peptide binding confirmed 75
3.8 Biacore binding profiles of group 1 selected clones in scFv-Fc format. 76
3.9 Biacore binding profiles of group 2 selected clones in scFv-Fc format. 77

3.10 Chemerin induced β-arrestin recruitment in ChemR23 expressing cells is blocked by titrated commercial polyclonal antibody but not Group 1 in-house clones. 80
3.11 Chemerin induced β-arrestin recruitment in ChemR23 expressing cells is blocked by 10μg/ml of commercial polyclonal antibody but not Group 1 in-house clones. 81
3.12 Group 1 scFv clones show binding to C17 peptide but not mchemerin in ELISA binding assay. 82
3.13 C17 peptide induces β-arrestin recruitment in ChemR23 expressing cells is not blocked by titrated commercial polyclonal antibody or by in-house Group 1 clones. 83
3.14 Streptavidin bound-C17 peptide induces β-arrestin recruitment in ChemR23 expressing cells is not blocked by commercial polyclonal or by in-house Group 1 clones. 84
3.15 Real time chemotaxis assay, using biogel macrophages with chemerin, shows no inhibition by anti-chemerin clones from chemerin pan. . . . 86
3.16 Optimisation of C23 Cleavage assay using human neutrophil elastase and cathepsin G 88
3.17 C23 Cleavage assay using human neutrophil elastase and cathepsin G 89
3.18 C23 Cleavage assay using human neutrophil elastase with co-transfected clones 90
3.19 Chemerin in murine peritoneal lavage fluid, on 15% Acrylamide SDS-PAGE gel, revealed by commercial monoclonal, clones A6 and B6. . . 92

4.1 ChemR23 and CCRL2 receptor expression on bone marrow-derived macrophages. 102
4.2 ChemR23 expression and function on bone marrow derived dendritic cells. 103
4.3 ChemR23 receptor expression is not detected on bone marrow neutrophils by flow cytometry and qPCR. 104
4.4 Expression of ChemR23 receptor on murine blood neutrophils and monocytes. 105
4.5 ChemR23 receptor expression on macrophage and monocyte populations but not on neutrophils in day 4 bio-gel peritoneal exudated cells. 107
4.6 ChemR23 receptor is expressed on peritoneal macrophage and dendritic cells under naive conditions. 108

4.7 mRNA expression of chemerin and chemerin receptors in murine tissues. 111
4.8 Lung leukocytes do not express the ChemR23 receptor under naive conditions. 112
4.9 The ChemR23 receptor is not expressed on leukocyte subsets in the liver under naive conditions. 113
4.10 The ChemR23 receptor is not expressed on leukocyte subsets in the spleen under naive conditions. 114
4.11 ChemR23 receptor is not expressed on human blood monocytes. . . . 115
4.12 Intraperitoneal chemerin treatment causes peritoneal recruitment of MHC class II expressing leukocytes. 117

5.1 Absence of non-signalling receptor, CCRL2, displays no overt difference in peritoneal resident leukocyte populations under naive conditions. . 130
5.2 The absence of non-signalling receptor, CCRL2, increases leukocyte recruitment to peritoneum during acute zymosan-induced peritonitis. 132
5.3 The absence of non-signalling receptor, CCRL2, increases leukocyte counts and inflammatory mediators in blood during acute zymosan-induced peritonitis. 133
5.4 The absence of non-signalling receptor, CCRL2, increases peritoneal leukocyte recruitment and inflammatory mediator production. 135
5.5 Chemerin blocking antibody treatment attenuates neutrophil recruitment to peritoneum in *CCRL2*-/- mice. 137
5.6 Recombinant chemerin pre-treatment exacerbates neutrophil recruitment and mediator production in the peritoneum of wild type mice. . 139
5.7 A lower concentration of recombinant chemerin pre-treatment exacerbates neutrophil recruitment and mediator production in the peritoneum of wild type mice. 141
5.8 Absence of ChemR23 inhibits leukocyte migration towards chemerin whereas the absence of *CCRL2* has no effect in real-time chemotaxis assay. 143
5.9 The CXCL1 production by WT and *CCRL2*-/- peritoneal mesothelium and resident cells show no differences following *in vitro* stimulations. . 145
5.10 The absence of chemerin signalling receptor, ChemR23, decreases leukocyte recruitment and inflammatory mediators to peritoneum during acute zymosan-induced peritonitis. 147

5.11 The absence of non-signalling receptor, ChemR23, increases leukocytes in spleen and inflammatory mediators in plasma, while reducing neutrophils in blood during acute zymosan-induced peritonitis. 148

6.1 Increased anxiety-like behaviour of *CCRL2*-/- mice in the open field test. 165
6.2 Increased anxiety-like behaviour of *CCRL2*-/- in the elevated O-Maze test. 166
6.3 Behaviour of *CCRL2*-/- mice in the forced swim test. 167
6.4 Neural architecture and quantification of neural nuclear stain show no differences in the $CCRL2^{-/-}$ mice. 168
6.5 Microglial distribution and quantification show no difference in $CCRL2^{-/-}$ mice. 169
6.6 mRNA levels of chemerin receptors tend to increase *in vitro* cultured microglial cells following 16 hr exposure to TLR and cytokine ligands. 170

7.1 The function of CCRL2 and ChemR23 in acute inflammation of zymosan-induced peritonitis. 179

Chapter 1

Introduction

1.1 Inflammation

The body is exposed to a countless number of opportunistic and pathogenic microorganisms everyday. Despite this, a healthy individual only becomes ill occasionally. The body has evolved a variety of effector cells and molecules to protect the host and support homeostatic tissue function; collectively they are called the immune system. Inflammation is the complex biological response actioned by these cells and molecules, triggered by noxious stimuli and conditions, such as infection and tissue injury. Acute inflammation is often characterised by the rapid influx of blood granulocytes, typically neutrophils, followed swiftly by monocytes, that mature into inflammatory macrophages [1]. These cells make up the first line of defence, defined as the innate immune system. They are able to mount a rapid and non-specific response for the removal of noxious stimuli [2]. Acute inflammation is established within minutes to hours, and its purpose is to quickly isolate and remove the dangerous causative agent, repair any local damage and restore homeostasis. During the ongoing inflammatory event, macrophages begin phagocytosing apoptotic neutrophils, a process called efferocytosis. This process promotes the switch to a pro-resolving macrophage phenotype. Resolution of inflammation is an active process to return homeostasis in the affected tissue upon removal of noxious stimuli. The process of resolution involves the elimination of granulocytes and mononuclear cell repopulation (macrophages and lymphocytes) to normal tissue pre-inflammation numbers and phenotypes.

If the innate inflammatory response fails to eliminate the invasive pathogen, four to seven days post infection, the adaptive immune system sets in. In the early events of infection, antigen presentation cells within the site of inflammation migrate to lymphoid organs to present the pathogen specific epitope to T cells. Epitope recognition by T cells establishes the adaptive immune response, which takes longer to set in,

but provides a longer lasting and antigen-specific form of immunity. The adaptive response includes the migration of activated T cells to target the specific antigen and the induction of B cell mediated specific antibody production.

The persistence of the acute inflammatory response or the dysregulation of mechanisms of the resolution phase can lead to chronic inflammation. Chronic inflammation generally has detrimental effects on the tissue architecture and is a predominant feature of many inflammatory diseases. The dysfunction in various pathways of inflammation, including the innate and adaptive arms are clearly linked to the chronic inflammation states seen in type 2 diabetes, cardiovascular diseases and rheumatoid arthritis [1].

In this introduction, I will try to briefly capture the basic processes in inflammation by highlighting both cells and pathways involved. I will discuss the therapeutic approaches being used to limit the immune response from causing excess damage during chronic inflammatory conditions. Finally, I will discuss the cytokine chemerin and its functions during inflammation and homeostasis.

1.2 The activation of inflammation

1.2.1 Pattern recognition receptors

The skin and mucosal epithelial lining of the airways and gastrointestinal tract are the first line of defense against invading pathogens or external injury. When pathogens or tissue injury breach these defences, they are sensed by tissue resident leukocytes, such as macrophages, dendritic cells and mast cells, which I will discuss later in greater detail. The sensing mechansim of noxious stimuli occurs via the recognition of pathogen-associated molecular patterns (PAMPS) or damage-associated molecular patterns (DAMPS) mediated by pattern recognition receptors (PRRs). These receptors, expressed extracellularly and intracellularly, include the family of receptors called Toll-like receptors (TLRs), C-type lectin receptors, nucleotide oligomerization domain(NOD)-like receptors (NLRs), and retinoic acid-inducible gene I-like receptors (RLRs) [3, 4]. These receptors are able to recognise molecular patterns associated with bacterial, viral, fungal, and parasitic cell outer membranes or by detecting cytosolic viral DNA and RNA [3]. In addition to pathogen molecules, endogenous host molecules are also ligands for TLRs and receptor for advanced glycation end products (RAGE) receptors. These molecules trigger a similar inflammatory response. Many of these endogenous TLR ligands are produced as a result of cell death and injury or by tumour cells; they include degradation products of the extracellular matrix (ECM),

heat-shock proteins, high-mobility group box 1 (HMGB1) proteins and chromatin-DNA. Activation of these receptors induces a variety of pro-inflammatory pathways including the MyD88- and TRIF-dependent pathways, which lead to the activation of transcription factor nuclear factor-κB (NF-κB) and mitogen-activated protein kinases (MAPKs) [3]. These mount the transcription of multiple pro-inflammatory molecules, such as cytokines and chemokines, for the activation and mobilisation of innate immune cells to the site injury. As well as recruiting innate cells, they also activate the surrounding tissue resident leukocytes, stromal cells and vascular endothelium to coordinate and enhance the recruitment of the innate immune system.

Each receptor can recognise a particular class of ligand which allows for a specific immune response to be mounted against different stimuli. For example, TLR2, an extracellular receptor, recognises β-glycans and zymosan glycans present on yeast cell wall. TLR4, an extracellular receptor, recognises lipopolysaccharides (LPS) present on Gram-negative bacterial cell walls. Activation of these receptors mount a canonical inflammatory response via MyD88-dependent NF-κB activation [3]. However, TLR3 an intracellular receptor, recognises double stranded viral RNA and mounts an anti-viral immune response by interacting with TIR-domain-containing adapter-inducing interferon-β (TRIF). TRIF induces a more potent NF-κB activation via TRAF6. This pathway promotes the production of both type I interferon and inflammatory cytokines [4]. The NLR group of receptors, which includes the NOD1,2 and NLRP1,3 receptors, recognises intracellular bacterial cell products and subsequently form a multi-protein complex termed the inflammasome. This complex leads to the activation of caspase-1 which is able to cleave the pre-formed inactive IL-1 cytokines into active isoforms. This promotes the release of IL-1 family of cytokines, including IL-1β, IL-18 and IL-33 [5].

These PRR receptors have evolved to protect the host and to activate the immune system against damage. However, inappropriate responses by these receptors are major contributing factors for acute and chronic inflammation and autoimmune diseases. For instance, the presence of endogenous ligands from chronic inflammatory tissue leads to the constant and augmented inflammatory response by signalling through the PRR receptors. The activation of the inflammatory response exacerbates the chronic state of inflammation rather than promoting its resolution.

1.2.2 Tissue resident cells

A plethora of tissue resident leukocytes are present throughout the peripheral tissues of the body. They reside there and work together to provide immune surveillance,

modulation of local immune responses, clearance of apoptotic cells and tissue maintenance post-inflammation and under homeostatic conditions. These leukocytes include cells from both the innate and adaptive immune system. They have the ability to phagocytose and kill pathogens, process their peptides to activate the adaptive immune response, release preformed pathogenic killing granules from their cytoplasm, and release inflammatory mediators to alert the immune system and modulate the immune response by producing various cytokines and lipid mediators. Together, these cells have the ability to orchestrate the biological response of inflammation to protect and preserve the host tissue damage from occurring. Dysregulation is these cells or pathways have all been linked to chronic inflammatory conditions.

Before discussing the various subsets of leukocytes residing in peripheral tissue, it is worth mentioning an important modulator of inflammation of non-leukocyte origin, the stromal cell. Although the primary functions of stromal cells are structural, their expression of PRRs and cytokine receptors allows them to produce and respond to external inflammatory stimuli [6]. With these functions, they are able to work alongside and provide support for the leukocytes in modulating inflammatory responses [6].

1.2.2.1 Tissue resident macrophages

Recent fate-mapping studies have shown that tissue-resident macrophages, such as microglia, alveolar and skin macrophages, originate from yolk sac or the foetal liver, and migrate to the peripheral tissue during embryonic development [7]. In adulthood, these cells are a self-renewing population governed by M-CSF, IL-34 or GM-CSF growth factors depending on the tissue specific location [8, 9, 10, 11]. They are an extremely heterogeneous population due to fact that they have developed niche-specific functions during development and adulthood that are necessary for the function and homeostasis of the particular tissue [12]. These cells express a wide array of PRRs and readily activate inflammation allowing them to act as sentinel cells in case of infection or injury. Depletion of resident macrophages significantly impacts chemokine production and the influx of neutrophils into site of infection within the peritoneal and pleural cavity [13, 14]. This signifies a vital role for resident macrophages in initiating an appropriate immune response. Interestingly, the removal of resident macrophages also can result in excessive neutrophil recruitment due to the administration of aggressive quantities of the inflammogen in a zymosan-induced peritonitis model. This effect is linked to the lack of IL-10 cytokine production by the resident macrophages [14]. This suggests that as well as initiating inflammation, they play an important role

in balancing the inflammatory response according to the nature and magnitude of the insult. In murine models of acute inflammation, there is a dramatic reduction in the numbers of F4/80^{high} cells [15]. They are presumed to adhere strongly to the tissue, which means their recovery in lavage fluid is low and also a proportion of F4/80^{high} cells migrate to draining lymph nodes [15]. During the resolution phase of inflammation, tissue resident macrophages clear cell debris and re-establish tissue homeostasis. Recent studies have shown that tissue resident macrophages preferentially phagocytose apoptotic cells via the phosphatidylserine receptor Tim-4 [16]. This is partly due to their ability to sequester the milk globule-EGF factor 8 (MFG-E8), which is necessary for apoptotic cell phagocytosis by the bone-marrow derived macrophages in later time points of inflammation. This process is considered a mechanism for maintaining tolerance by appropriately disposing of self antigens [17].

1.2.2.2 Mast cells

Mast cells are bone marrow-derived granular leukocytes that are present in most peripheral tissues at strategically important tissue barriers, including skin and mucosal tissue under physiological conditions. Mast cells are derived from the haemotopoietic stem cell (HSC) along the myeloid pathway from a granulocyte-monocyte precursor which differentiates into mast cells under the influence of growth factor SCF and IL-4 [18]. They are released into the circulation, where they are recruited to peripheral tissues to complete their maturation process under tissue specific conditions. As tissue resident cells, they perform homeostatic functions in blood flow and coagulation, smooth muscle contractions in peristalsis, mucosal secretion, wound healing and regulation of innate and adaptive immune responses [19].

They are best known for their role in allergy, due to the expression of high-affinity Fc receptor for IgE (FcϵRI). Cross-linking antigen bound IgE antibodies on their surface results in their activation and subsequently their degranulation; releasing preformed histamine and eicosanoid mediators extracellularly. Due to their expression of PRRs and complement receptors, recent studies have shown that mast cells play a central role in host defence against bacteria and parasites, through the release of cytokines and eicosanoid mediators, including leukotriene C_4, which recruits neutrophils, eosinophils and T helper 2 (T_H2) cells to the site of infection [20]. The role of mast cells in chronic inflammatory disease such as rheumatoid arthritis and coronary atheromas has been reported [21, 22].

1.2.2.3 Eosinophils

Eosinophils are bone marrow-derived granular leukocytes that share a common precursor, the $GATA1^+$ granulocyte-monocyte precursor, with basophils and mast cells [23]. Eosinophils obtained their name by strongly staining with the acidic dye, eosin, due to their rich cationic granule content. In human eosinophils, there are 4 main cationic proteins present, major basic protein 1, eosinophil cationic protein, eosinophil-derived neurotoxin and eosinophil peroxidase [23]. The granules store numerous cytokines, enzymes and growth factors. They also store pre-synthesised eicosanoids such as leukotrienes, thromboxane, and prostaglandins.

Eosinophils are released into the peripheral blood by bone marrow, spend a brief time in blood before they migrate to the thymus or gastrointestinal tract, where they reside under physiological conditions [24]. They can also migrate towards other peripheral tissues, such as skin, lung and gut by the release of appropriate stimuli, such as CCL11 that signals via the CCR3 receptor [24]. They express various PRRs and Fc receptors which induce degranulation and cytokine production. There are various T_H2 cytokines, such as IL-5, which induce degranulation, modulate survival and activation of eosinophils. Hence, the association of eosinophilic function with allergic pathologies [24].

Eosinophils are classically associated with the immunity against parasitic helminths infection; mice depleted of eosinophils fail to efficiently clear helminth infection [25]. The activation of eosinophils has become more commonly associated with allergies. Eosinophilia in lung tissue during the pathology of asthma has been shown to play a role in tissue damage due to excessive degranulation. Mice null for eosinophil promoting cytokines and CCR3 receptor have illustrated the pro-inflammatory impact of eosinophils in hyper-reactivity of airways and increase collagen deposition [26, 27, 28]. A similar effect is seen in hyper-reactive gastrointestinal mucosa pathologies [29]. The release of these granular components have evolved to promote efficient pathogen killing however, they can harm tissue architecture when released in an uncontrolled manner.

1.2.2.4 Dendritic cells

Dendritic cells reside in many peripheral tissues including lung, liver, spleen, skin, acting as sentinel cells, orchestrating immune responses and antigen presentation to the adaptive immune system. Dendritic cells (DCs) are continuously being developed in the bone marrow due to the demand for mature DC replenishment in peripheral

tissue. The common DC progenitors in the bone marrow give rise to plasmacytoid DCs, migratory and lymphoid resident $CD8^+$ or $CD11b^+$ DCs and monocyte-derived (conventional) DCs [30]. DCs that reside in the skin are generated from the foetal liver and yolk sac during embryonic development. Within the skin, they are a self-renewing population. Like other tissue resident cells, they too express PRR receptors and Fc receptors to carry out phagocytosis and initiate cytokine production. As well as killing pathogens, phagocytosis serves to cleave pathogenic antigens to allow for the display of antigen complexed with major histocompatibility complexes (MHCs) on DC membranes. Activated DCs migrate to lymphoid organs to present the antigen to naïve T cells. T cells, which bind the antigen in the context of MHCII, mount adaptive immune response and immune memory. Finally, cytokine production by DCs has the ability to modulate the inflammatory response similarly to macrophages, by providing a balance between the pro- and anti- inflammatory cytokine productions [30].

1.2.2.5 T cells, B cells and Innate lymphoid cells

There are various T and B cells residing in tissues also providing similar first defence support and tissue specific maintenance. These cells are important for alerting and activating the immune system about potential threats. The innate cells residing in peripheral tissue express the PPR receptors which enable them to recognise general molecular patterns associated with potential threats for the host. The adaptive cells resident in the periphery are typically memory T and B cells, which provide recall responses to reinfection or a particular pathogen [31]. There are also regulatory T cells residing in lung and skin tissues that are important for balancing the inflammatory response [32, 33, 34]. Furthermore, there are B cells, B1 cells, which produce low-specificity IgM antibodies against common pathogen associated molecules [35].

Finally, a small but significant population of tissue resident lymphocytes include the innate-lymphoid cells (ILCs). They are under-represented in lymphoid tissue, however, they are vastly distributed across various tissues, including intestines, lungs, skin, liver and adipose tissue. They play a role in maintaining tissue homeostasis and pathogen immunity. In the intestine and lung mucosa, ILCs seem to play a role in regulating epithelial barrier function and as they are located in regions of potential pathogen invasion, they are key players in mounting an immune response against it and ensuring tissue homeostasis under physiological conditions [36]. All ILCs develop from precursors in the bone marrow, however, parabiosis studies illustrate that ILCs populate their niches soon after birth and remain in their environments throughout

life, where they proliferate locally [37]. They do not express PRRs, instead they react to myeloid or epithelial cell derived cytokines and lipid mediators such as IL-12, IL-4, IL-25, IL-1β, protaglandins and leukotrienes [38]. They do not express the usual T cells receptors that recognise 'non-self' structure. However, they do express key transcription factors which contol their cytokine profile upon activation. For example, activation of ILC1s express T-bet transcription factor and produce IFN-γ to fight intracellular pathogens [39]. ILC2s express GATA-3^{high} and produce IL-5 and IL-13 inducing eosinophil accumulation and parasitic immunity [40]. ILC3s produce IL-22 and IL-17, important for fungal immunity [41].

1.3 Endothelial cells

The ultimate aim of acute inflammation is to send out signals for the recruitment of more professional killing cells to engage in the clearance of pathogens and/or tissue damage. Therefore, it is very important to allow access of circulating leukocytes into damaged tissue as rapidly as possible. This is why local endothelial cells activation is a very important step in inflammation.

Among the first cells to become activated, during an inflammatory response, are the endothelial cells lining the capillary vessels close to the site of infection. The vascular endothelium has a key function in acting as a barrier and as a signal transducer for metabolic or inflammatory factors. In non-inflamed tissues, vascular endothelial cells maintain the fluidity of the blood and control vessel-wall permeability by maintaining tight junctions with adjacent endothelial cells [42]. The activation of endothelial cells leads to the cardinal signals of inflammation; heat, redness, swelling, and pain described by Celsus. Endothelial activation occurs due to the release of pro-inflammatory mediators derived from tissue resident leukocytes in the site of inflammation; mediators such as histamine or pro-inflammatory cytokines including tumour-necrosis factor (TNFα) and interleukin-1 (IL-1)[43, 44]. These mediators bind corresponding receptors expressed on endothelial cells, leading to downstream activation signalling cascades. Histamine H1 GPCR receptor activation results in increased blood flow via Ca^{2+} mobilisation within cytoplasm [45]. Free Ca^{2+} activates the enzyme, phospholipase A_2, which cleaves the membrane phosphatidylcholine into arachadonic acid. This leads to the rapid generation of leukotrienes and prostaglandins within the eicosanoid pathway. Free arachadonic acid is rapidly converted by cyclooxygenase-1 (COX1) into prostaglandin H_2 and then PGI_2 which is a potent vasodilator that relaxes smooth muscle surrounding the vasculature [42, 46].

Free Ca^{2+} also enables the production of nitric oxide (NO) which works together with PGI_2 as a potent vasodilator. Additionally, PGI_2 and NO are also able to induce vascular permeability by loosening tight junctions between adjacent endothelial cells, allowing plasma leakage and tissue oedema [47].

The rise in intracellular Ca^{2+} leads to the presentation of pre-formed P-selectin, an adhesion molecule, onto the surface of the luminal membrane [45]. At the same time, a by-product of the arachadonic acid generation rapidly acetylates, generating an endothelial-cell derived acyl form of platelet-activating factor (PAF), which causes platelet aggregation and inflammatory activation [48]. The combined display of P-selectin and PAF causes circulating neutrophil tethering and rolling followed by integrin activation for the initiation of neutrophil extravasation between the junctions between two endothelial cells [49].

The activation of the transcription factor NF-κB results in the transcription of pro-inflammatory proteins including chemokines such as CXC-chemokine ligand 8 (CXCL8 or IL-8), adhesion molecule E-selectin and the expression of COX2 which enhances the actions of COX1 mentioned earlier [42]. The upregulation of adhesion molecules is particularly important to allow leukocyte binding and eventually transmigration to the inflamed tissue, see Figure 1.1. These include E-selectin, intercellular adhesion molecule-1(ICAM1) and vascular cell-adhesion molecule 1 (VCAM1). Neutrophils are recruited by CXCL8, and transiently adhere to the endothelium by the interaction of E-selectin and P-selectin via the L-selectin and P-selectin glycoproteins ligand-1(PSGL-1) expressed on the surface of leukocytes. Higher affinity binding occurs via intergin activation of VLA-4 and LFA-1 on leukocytes adhering to their corresponding ligands vascular cell-adhession molecule 1 (VCAM1) and intercellular adhesion molecule-1 (ICAM1) on the activated endothelial cells. These interactions initiate capture and tight binding of neutrophils. The expression of CXCL8 on the surface of endothelial cells or the presentation of other chemokines, via heparin sulphate proteoglycans, strengthens the adhesion causing arrest in rolling and inducing diapedesis, the transmigration of leukocytes through the endothelial layer [42, 50]. In later time points, the production of CCL2 and VCAM1 favours the recruitment of monocytes to migrate into the site of inflammation [51, 42].

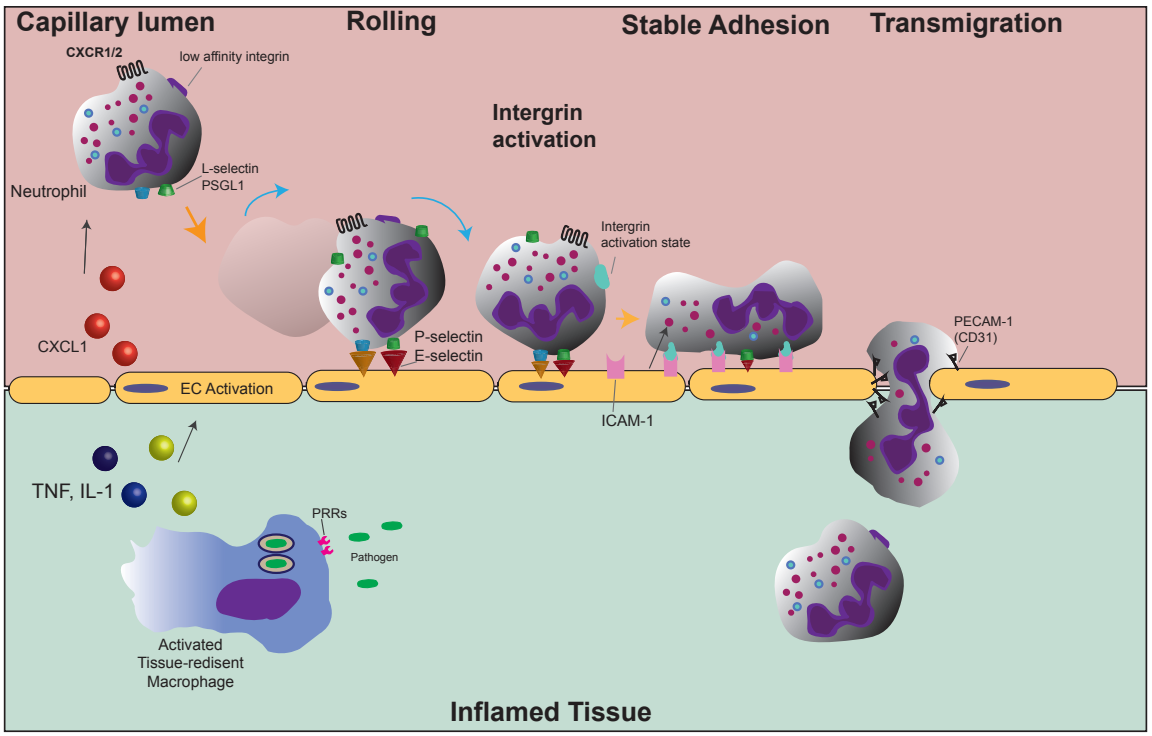


Figure 1.1: Endothelial activation and the transmigration of leukocytes across endothelium. Cytokines (TNF, IL-1) secreted by activated tissue resident macrophages, activate endothelium to express adhesion molecules, P-selectin and E-selectin and chemokines, CXCL1. Leukocyte transiently adhere to the endothelium, following secondary signals from pro-inflammatory mediators, such as chemokine activation, leukocytes activate and adhere strongly via VCAM and ICAM, which leads to transmigration through endothelial layer, via PECAM-1 interactions into inflamed tissue.

1.4 Neutrophils

Neutrophils are a polymorphonuclear leukocyte which are well recognised as one of the major players during acute inflammation. They are the first cells to be recruited from the circulation into the inflamed tissue with the aim of pathogen killing. Neutrophils are produced in the bone marrow by a process called granulopoiesis, largely dependent on the cytokine granule colony-stimulation factor (G-CSF) [52]. Due to their short lifespan, neutrophils are constantly being produced in the bone marrow. However, under physiological condition the majority of neutrophils are marginated in the bone marrow, lung and spleen organs, and only a limited number are patrolling in the blood circulation [53]. Neutrophil retention in the bone marrow is controlled by stromal cell production of CXCL12 which binds the CXCR4 receptor on the neutrophils [54]. The release of neutrophils from the bone marrow is mediated by the CXCR2 receptor which binds potent neutrophil chemoattractant chemokines, such as CXCL8, CXCL1, CXCL2 [54, 55]. Upon inflammatory insult, these CXC

chemokines produced from the site inflammation cause the release of neutrophils into the blood circulation. Pharmacological inhibition of CXCR2 in healthy and mouse disease models of inflammation showed significant reductions in neutrophilic accumulation [56, 57]. Circulating blood neutrophils are recruited to the site inflammation via these chemokines and undergo transmigration recruitment through vascular endothelial lining into the inflamed tissue via mechanism described above (Section 1.3).

The main function of recruited neutrophils is to eliminate pathogens from site of inflammation. Neutrophils are proficient phagocytic cells. Once in the site of inflammation, the activation of PRRs, Fcγ receptor and complement receptors expressed on neutrophils begin membrane ruffling which results in the membrane engulfing bacterial particles and microbes into a membrane bound structure called the phagosome. The complement system and opsonisation by IgG antibodies enhances phagocytosis. Primary and secondary granules fuse with phagosome releasing their anti-microbial proteases, including serine proteases such as elastase, cathepsin G, proteinease-3. Fusion of the neutrophil granules with the phagosome, results in the assembly of NADPH oxidase on the membrane of the phagosome generating an electron transport chain in the wall of the vacuole. This leads to the production of reactive oxygen species (ROS), such as $O_2^-$and H_2O_2, within the vacuole which are widely believed to enable the process of bacterial killing by activating the granule content of the phagosome, such as myeloperoxidase (MPO) [58]. This process is called respiratory burst. However, there is strong evidence which disagrees with the direct involvement of ROS in oxidative killing during phagocytosis [58, 59].

A recently described mechanism of bacterial killing by neutrophils is their ability to generate neutrophil extracellular traps (NETs). NETosis is a mechansim by which neutrophils release extracellular DNA traps, composed of decondensed chromatin, histones and granule proteins, ultimately resulting in neutrophil cell death [60]. NADPH oxidase and ROS formation seems to be necessary for efficient NET formations [61, 62]. The bactericidal content of the NETs mean that neutrophils have the ability to continue killing bacteria even after they die. The anti-microbial peptides, oxidants and proteases contained within the granules of neutrophils play a major role in bacterial killing. Most peptides are able to permeabilise or disrupt bacterial membranes, such as α-defensins and cathelicidins. Most of these peptides can also act as chemoattractants for more leukocyte recruitment. However, their secretion to the inflamed tissue environment can also harm tissue architecture and cause vast tissue damage typically seen in chronic inflammatory disease, such as artherosclerosis or rheumatoid arthritis [63, 64].

Although neutrophils are classically considered as pro-inflammatory, towards the end of their lifespan they can take on a pro-resolving phenotype. Apoptotic neutrophils express decoy receptors for inflammatory mediators, hence act as a sink to deplete the cytokine and chemokines within the site of inflammation [65]. Proteolytic degradation of inflammatory cytokines and chemokines is also a process which promotes resolution [66]. Furthermore, neutrophils secrete pro-resolving protein, annexin A1, when they are dying [67]. Annexin A1 reduces intergin activation on myeloid cells and promotes efferocytosis, neutrophil phagocytosis by macrophages [68]. Apototic neutrophils expose phosphatidylserine on their membranes which act as an 'eat-me' signal for phagocytosis by macrophages [63]. Phagocytosis of apoptotic neutrophils converts macrophages into an anti-inflammatory 'M2' phenotype, characterised by the release of IL-10 and transforming growth factor-β (TGF-β) cytokines [63].

1.5 Monocytes

The second set of leukocytes recruited to the site of inflammation are the circulating blood monocytes. Monocytes are mononuclear myeloid cells originating from the bone marrow, and are ultimately derived from the committed monocyte progenitor, which is the final progenitor in the haemopoetic stem cells development cascade [69]. The production of monocytes in the bone marrow is mostly influenced by the macrophage-colony stimulating factor (M-CSF) (or also known as CSF-1) that is produced by bone marrow and peripheral tissue stromal cells. The granulocyte-macrophage colony-stimulating factor (GM-CSF) is another factor involved in the development of mononuclear phagocytes but only during inflammatory states [70]. Monocytes exert functions that include clearance of cellular debris, promotion of angiogenesis, restoration of tissue integrity and transformation into macrophages and dendritic cells.

There are two distinct populations of circulating monocytes in the blood, the non-classical: remains 'patrolling' the vasculature, supporting endothelial cell function considered 'anti-inflammatory'. The other, which is called the classical monocyte, has the ability to migrate to tissue and lymphoid organs, considered 'pro-inflammatory'. The classical monocytes are Ly6C$^+$ CD43$^{\text{low}}$ monocytes (in mice), and CD14$^+$CD16$^{\text{low}}$ (in human). Monocyte release from the bone marrow is highly dependent on the CCR2 receptor expressed on classical monocytes [71]. Multiple inflammatory studies have illustrated the absence of CCR2 receptor results in the lack of classical monocyte mobilisation [72, 73, 74]. Ly6C$^+$ monocytes have a half-life of approximately 24

hours in the circulation. During this time, parabiosis experiments have revealed that under non-inflammatory conditions, they traffic into tissues or lymph nodes, convert into LyC6$^-$ monocytes or undergo programmed cell death [75]. Monocytes recruited into the site of inflammation are able to carry out pathogen killing via phagocytosis, production of ROS, NO and myeloperoxidase and secrete cytokines to promote activation of other cells [70]. Classical monocytes however, migrate into site of injury and differentiate into proinflammatory effector phagocytes, inflammatory macrophages or dendritic cells to combate pathogens and some drain through to the lymphatic system to alert the adaptive immune system [70].

The non-classical monocytes are Ly6C$^-$ CD43^{hi} (in mice) or CD14^{low}CD16$^+$ (in human). They express high levels of the chemokine receptor CX_3CR1, which allows them to underake continuous patrolling of the luminal side of the vascular endothelium at steady state as well as during inflammation [76]. Imaged by intravital microscopy techniques, Ly6C$^-$ monocytes slowly crawl along the luminal endothelium checking for damage and orchestating its repair. Exposure to bacterial insults leads to non-classical monocytes producing low levels of pro-inflammatory cytokines and high levels of anti-inflammatory, wound healing factors, such as IL1 antagonist, apolipoproteins ApoA and ApoE, whereas exposure to viral insults, results in the proinflammatory cytokine production [77]. Even though they are considered 'anti-inflammatory', they are found in high number in atherosclerotic plaques. Their recruitment into plaques is partially driven by the CCR5 chemokine receptor [78]. However, due to their role in removing damaged endothelial cells and scavenging lipids, such as oxidised low-density lipoportein (oxLDL), it is speculated that they are actually trying to repair the atherosclerotic endothelium, by promoting endothelial growth factors and collagen deposition [79, 80].

1.6 Macrophages

Macrophages are professional phagocytes, which are found in various sites around the body and play important roles in pathogen killing and apototic cell clearance. As stated earlier, tissue-resident macrophages are key activators of the inflammatory cascade in acute inflammation. Upon pathogen or tissue damage recognition, tissue macrophages express a range of cytokine and chemokines including TNFα, IL-8, IL-6, $PGE_2$and GM-CSF to name a few. This initial response is vital for the sequential recruitment of neutrophils and monocytes to the tissue. Classical Ly6C$^+$ monocyte

recruitment, mainly driven by CCL2 chemokine, become activated during the transmigration process through the endothelial cell wall. The influence of inflammatory cues, such as M-CSF, within the site of inflammation results in their differentiation into monocyte-derived inflammatory macrophages [70].

The monocyte-derived inflammatory macrophages become the larger population of macrophages in the site of inflammation. These macrophages have a pro-inflammatory'M1' phenotype and they secrete a range of pro-inflammatory mediators and induce clearance of infectious agents by phagocytosis and generation of ROS, NO and reactive nitrogen species for bacterial killing [81].

Chronic activation of these monocyte-derived inflammatory macrophages results in chronic inflammation where there is tissue damage and continuous inflammatory activation. In atherosclerosis, the 'inflammatory stimulus' is oxidised and modified low-density lipoproteins (LDLs). The accumulation of oxLDL in endothelial wall activates an inflammatory cascade which eventually results in the infiltration of monocytes into the subendothelial space which undergo differentiation into inflammatory macrophages. These phagocytose oxidised and modified forms of LDL, via their scavenger receptors CD36 and SR-A1, that have accumulated in the arterial wall [82, 83]. However, they cannot efficiently break the lipids down and there is no negative feedback loop to reduce the cholesterol uptake. This results in the formation of lipid laiden foam cells in the arterial wall. Foam cells become key drivers in the chronic inflammation of artherosclerosis, by secreting inflammatory cytokines, chemokines and matrix metalloproteases. Apoptotic foam cells undergo secondary necrosis, where they release their intracellular content into the arterial wall resulting in a continuous inflammatory activation and recruitment cycle which eventually leads to the formation of a necrotic core plaque with a fibrous cap on the luminal side [84]. The instability of this plaque rupture can result in life-threatening arterial occlusion.

Macrophages are highly responsive to cues within their niche. They are able to modify their behaviour by becoming more pro-inflammatory 'M1', or more anti-inflammatory 'M2'. The 'M2' like macrophage phenotype promotes wound healing, angiogenesis, secretion of anti-inflammatory cytokines and ultimately the resolution of inflammation. Unlike most other peripheral tissues, the tissue-resident macrophages in gastrointestinal mucosa are constantly replenished by circulating monocytes in the blood [85, 86]. Upon entering the lamina propria and muscularis of the gut, they convert to a 'M2' like phenotype, becoming hyporesponsive to bacterial ligands and maintaining homeostatic conditions necessary for this niche environment

[85, 86]. However, in chronic inflammation of tissue, macrophages can promote fibrosis. This process is driven by over activation of the 'M2' like phenotype due to inefficient clearance of insult during prolonged inflammation. In this situation, 'M2' like macrophages produce excessive tissue healing factors such as TGFβ and epidermal growth factor. This continuous supply of mediators leads to the proliferation of myofibroblasts which generates excessive extracellular matrix, collagen deposition and tissue remodeling which destroys normal tissue architecture [87].

Therefore, the balance of these macrophage phenotypes is necessary to maintain host tissue integrity. Resolution of inflammation, as mentioned earlier, is also driven by this switch to a 'M2' like phenotype upon phagocytosis of apoptotic neutrophils [88]. Even though tissue-resident macrophages preferentially phagocytose apoptotic cells, the large numbers of monocyte-derived macrophages in the site of inflammation means that they are involved in clearance and the resolution phase of inflammation as well [12].

1.7 Pro-inflammatory mediators

From the sections described above, it is evident that the inflammatory response is coordinated by a large range of mediators that form complex regulatory networks. These mediators are complex proteins and lipids that signal via their corresponding receptors expressed by cells to module cellular function during development, steady state and inflammation. These mediators induce cytokines, chemokine, growth factors, eicosanoids, complement proteins and peptides. In this section, due to the shear scope of the published literature, I will only focus on cytokines, chemokines and eicosanoids.

1.7.1 Cytokines

Cytokines are small secreted proteins that play a central role in coordinating the inflammatory response. There are over 100 genes encoding cytokine members which are secreted by the majority of cell types in the body [89]. The term 'cytokine' refers to interferons, interleukins, chemokines, mesenchymal growth factors, the tumour necrosis factor family, transforming growth factor family and adipokines. Their general functions are to promote growth and development and polarise immune responses towards pro- or anti-inflammatory. Their effects can manifest on one particular subset of cells to a whole array of them. Due to their functions, they have become attractive therapeutic targets for chronic inflammatory diseases and cancer.

1.7.1.1 TNFα

One important cytokine that has been successfully targeted therapeutically is tumour necrosis factor α (TNFα). TNFα was initially identified in the 1970s as an endotoxin-induced serum factor responsible for necrosis of tumours *in vivo* and *in vitro* [90]. It is a potent inflammatory mediator that activates innate cells, by stimulating cytokine production, activating adhesion molecules, proliferation in normal cells and apoptosis of dysregulated cells [91]. TNFα is a member of the TNF and TNF receptor superfamily of transmembrane proteins that now includes 30 receptors and 19 associated ligands. They all have diverse roles in cell differentiation, inflammation, immunity and apoptosis. TNFα is produced by macrophages and a plethora of other cell types, including activated endothelial cells. It is synthesised as a transmembrane precursor protein, which is transported from the recycling endosome to the cell surface. TNFα is released from the membrane as a soluble protein upon cleavage by TNFα converting enzyme, which is itself activated by metalloprotease cleavage [92]. The membrane protein complex that TNFα was initially attached to also acts as a pro-inflammatory signal for the cell itself, by triggering the pro-inflammatory production of other cytokines such as IL-12 [93].

TNFα mediates its actions through the TNFR1 and TNFR2 receptors. The TNFR1 receptor is widely expressed whereas the TNFR2 is predominantly on leukocytes and endothelial cells. Both single transmembrane glycoprotein receptors express a four cysteine-rich domain structure for TNF binding [94]. The TNFR1 contains intracellular death domain which activates upon ligand binding drives apoptosis via caspase activation. Unless there is alternative adaptor molecule recruitment to the cell surface prior to ligand internalisation which initiates pro-inflammatory cytokine production instead. TNFR2 binding promotes pro-inflammatory activation and cell survival [91].

1.7.1.2 IL-6

Another important pro-inflammatory cytokine is interleukin-6 (IL-6). It is expressed by an array of cells, including monocytes and macrophages, T and B cells, fibroblasts, and endothelial cells [91]. It has roles in B cell maturation into plasma cells, T cell activation, differentiation and regulation. It also has pro-inflammatory promoting abilities, as well as effecting lipid metabolism, and insulin resistance [95]. IL-6 signals through one ligand binding transmembrane glycoprotein receptor IL-6R, made up of a multi protein complex gp80 and CD126 with a signal transduction protein, gp130.

Activation of of IL-6R leads to signalling via JAK-STAT pathway which leads to STAT3 phosphorylation. STAT3 is a commonly induced transcription factor following cytokine signalling [91]. IL-6 is synthesised under stress conditions and TNF or IL1β signalling. Mice deficient in IL-6 displays impairment in innate and adaptive immunity to viral and bacterial pathogens [96, 97]. IL-6 has been shown to skew T cell differentiation to T_H2 by upregulating the cytosolic molecules NFATc2 and SOCS1 to produce IL-4 and suppress IFNγ production [98]. Additionally, IL-6 inhibits TGF-β from inducing regulatory T cell differentiation from naïve $CD4^+$ T cells. Instead the combination of IL-6 and TGF-β generates T_H17 cells [99].

1.7.2 Chemokines

Chemokines are a group of small proteins cytokines, characterised by a conserved cysteine residue containing tertiary structure. In humans and mice, there are approximately 50 chemokines, divided into four classes C, CC, CXC and CX_3C, the nomenclature of which is derived from the position of their key cysteine residues [100]. Chemokines signal through a family of seven-transmembrane, G protein-coupled receptors (GPCRs) [100]. The G proteins are made up of trimeric associated subunits which undergo conformational changes in the carboxyl terminus of the receptor to mediate G-protein signalling cascade. For instance, G-protein αi receptor activation causes the exchange of GDP for GTP that is bound to G protein α subunits. This causes the α subunit dissociation from the G $\beta\gamma$ subunits. Both these moieites engage with intracellular signalling molecules leading to the Gαi mediated sigalling cascades, including MAPK and STAT3 activation. These cascades usually result in cell activation and cytoskeletal re-arrangement for cellular migration [101].

Chemokines can be broadly classed as homeostatic or pro-inflammatory. Chemokines that are primarily pro-inflammatory are produced by cells to mobilise and recruit leukocytes to sites of injury. Chemokines induce intergrin expression on target leukocytes to allow diapedesis across the endothelium to occur. The homeostatic role of chemokines involves leukocyte homing into particular regions of tissue, such as bone marrow, lymph nodes and spleen. They can also induce T cell differentiation and angiogenesis [91].

1.7.2.1 Neutrophil chemoattractants

CXCL8, also known as IL-8, was the first human chemokine to be described for its ability to chemoattract human neutrophils [102]. The analogous murine chemokines

are CXCL1 (also known as KC), CXCL2 and CXCL5. They mediate their signalling primarily through the CXCR2 receptor but also through the CXCR1 receptor, both of which are expressed on neutrophils. Their signalling promotes neutrophil activation, migration and adhesion to the activated endothelium. Neutrophil activation leads to intergrin conformational changes into the active state of the $\alpha 1 \beta 2$. These changes generate a higher affinity towards endothelial adhesion factors such as ICAM1 [103]. The coordinated response between cytokines and chemokines is necessary for appropriate responses. For instance, the growth factor G-CSF, secreted by activated tissue resident macrophages, stimulates stromal bone marrow cells to produce CXCL1 and CXCL2 and downregulate CXCL12. This switch in chemokine production allows for neutrophil release into circulation [104]. The directed production of these chemokines in the periphary is necessary for leukocyte accumulation and transmigration through the endothelium [104]. Activated endothelium releases CXCL1 and CXCL2 from granular vesicle compartments as well as displaying them on their surface for neutrophil interaction and activation [105]. Inhibition of CXCR2 and CXCR1 receptors in murine studies shows a significant decrease in neutrophil accumulation [106]. Likewise, recombinant administration of CXCL1 and G-CSF leads to augmented neutrophil accumulation [104]. Pharmacological inhibition of CXCR2 in patients with severe asthma or cystic fibrosis illustrated that is was a safe therapeutic intervention which decreased neutrophil inflammation in the airways as well [107, 108].

1.7.3 Pro-inflammatory eicosanoids

Eicosanoids are locally acting bioactive signalling lipids, which constitute a complex network of regulators in response to external stimuli during homeostatic and inflammatory condition. Eicosanoids are produced from the metabolism of arachidonic acid and other polyunsaturated fatty acids (PUFAs) by cyclooxygenase, lipoxygenase and cytochrome P450 enzymes. These functions include control of smooth muscle contractions, vascular permeability and platelet aggregation.

The two main classes of pro-inflammatory eicosanoids are leukotrienes and prostaglandins. Both are generated by hydrolysis of membrane phospholipids by phospholipase A2 into arachidonic acid (AA) upon cell stimulation and Ca^{2+} mobilisation. These products are subsequently converted into leukotrienes (LTs), protaglandins (PGs), prostacyclins (PCs) and thromboxanes (TXAs) (Figure 1.2).

Leukotrienes are potent pro-inflammatory mediators exert negative effects in chronic inflammatory conditions such as asthma. The LTs are derived from AA via the 5-lipoxygenase (5-LOX) which converts AA into LTA_4, an inactive intermediate precur-

sor for the other leukotrienes. LTA_4 hydrolysis generates to LTB_4, the most potent leukotriene in this pathway [109]. LTA_4 can be conjugated to LTC_4 by LTC_4 synthase and sequentially to LTD_4 [110], refer to Figure 1.2. LTB_4 stimulate neutrophil activation, chemotaxis and degranulation by signalling through GPCR receptor LTB_4 receptor 1 and 2 (Blt1). The other LT produces act to cause smooth muscle contractions in the airways and increase vascular permeability [111].

Prostaglandins are another important lipid mediator within the eicosanoid group. They too are AA-derived pro-inflammatory mediators, generated from the actions of cyclooxygenase enzymes. AA is converted into PGG_2 and then PGH_2 through the actions of COX-1 and COX-2. PGH_2 can then be converted into various other modified prostanoid, including PGE_2, PGI_2, PGD_2 and PGF_{2a} [112]. PGH_2 can also be converted into TXA_2 by COX-1 coupling with thromboxane synthase (TXS), refer to Figure 1.2. These mediators are produced in low levels under homeostatic conditions and increase under inflammatory conditions. Under homeostatic conditions, macrophages produce TXA_2, however, LPS exposure shifts the ratio to favour PGE_2 production [113]. Additionally, PGs can be produced in almost any cell type and they signal via GPCRs. PGD_2 acts as a chemoattractant, via the CRTH2 GPCR receptor, for T_H2 cells, eosinophils and basophils [114].

The two cyclooxygenase isoforms, COX-1 and COX-2, are the targets of nonsteroidal anti-inflammatory drugs (NSAIDs), commonly used to manage the clinical symptoms of inflammation. NSAIDs bind and inactivate the COX enzymatic activity by inhibiting their active site thus, inhibiting prostanoid formation. The peroxidase activity of both proteases is uneffected by the NSAIDs [113]. Studies in both COX-1 and COX-2 knockout (KO) mice showed attenuated inflammatory responses. In general, there seems to be a co-dependence on the expression of both for them to work efficient [113]. COX-2 deficient mice showed considerable improvement in synovial inflammation and joint destruction in a collagen-induced arthritis model, whereas the depletion of COX-1 in this model displayed no difference compared to the controls [116]. However, in a serum-transfer model of arthritis, COX-1 derived PGI_2 was shown to make striking contributions to the initiation and perpetuation of the arthritis [117].

PGE_2 acts via the EP4 receptor to increase arterial dilation and microvascular permeabilty [113]. PGI_2 plays a role in cardiovascular homeostasis as a potent vasodilator and an inhibitor of platelet aggregation and smooth muscle proliferation. PGI_2 is constantly produced by endothelial cells and vascular smooth muscle cells [113]. Its receptors are also expressed by peripheral sensory nerves and in the spinal

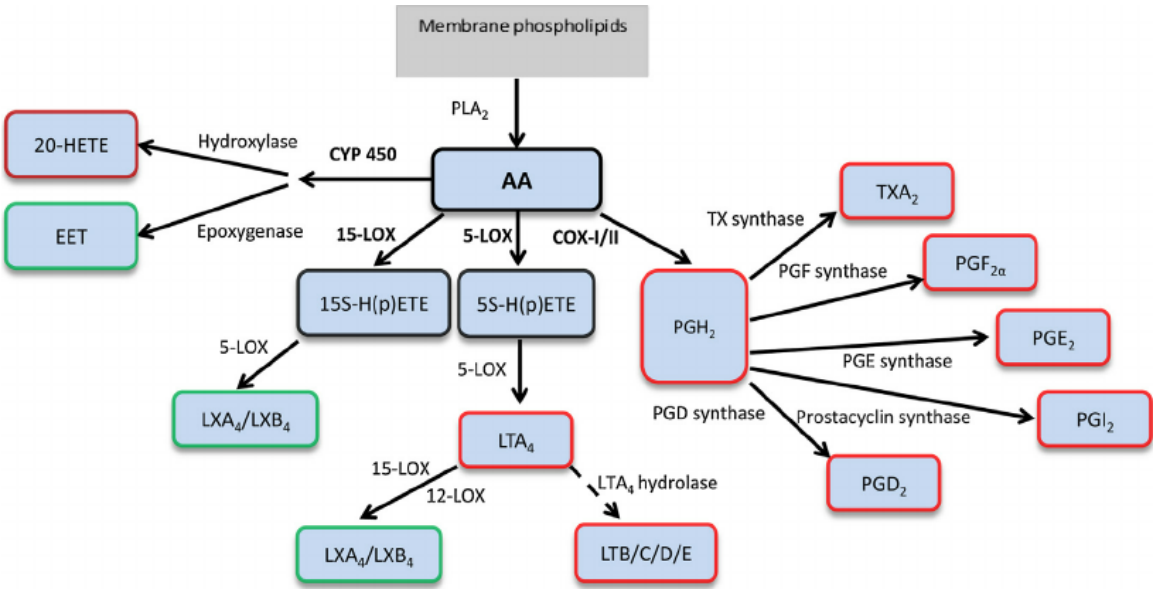


Figure 1.2: Arachidonic acid metabolism. Arachidonic acid (AA) is oxidized by lipoxygenases (LOX), cyclooxygenases (COX) and cytochrome P450 (CYP 450) to produce either pro-inflammatory (red border) or anti-inflammatory and pro-resolving (green border) metabolites. Dashed arrow represents incomplete description of reaction sequence. 20-hydroxyeicosatetraenoic acid (20-HETE); epoxyeicosatetraenoic acid (EET); hydroperoxyeicosatetraenoic acid (H(p)ETE); lipoxin (LX,); leukotriene (LT); prostaglandin (PG); phospholipase A (PLA); thromboxane (TX). Taken from [115]

cord and thus, PGE_2 also stimulates pain during inflammation; a common feature of inflammation [118, 119]. PGI_2 receptor KO mice illustrate an accelerated atherogenesis due to enhanced platelet accumulation and leukocyte adherence to endothelium in both LDL and ApoE KO models [120, 121].

1.8 Resolution of inflammation

Inflammation is a very important biological process to ensure host survival in events of infection or injury. The successful outcome of inflammation is the removal of noxious stimuli and the return to homeostatic conditions. However as mentioned earlier, the prolonged or over-activation of inflammatory process can also become detrimental to host survival [1]. In the past, the resolution of inflammation was considered to be a passive process by the eventual dampening of the pro-inflammatory mediators initially produced [122]. Now, there is strong evidence supporting the notion that the resolution of inflammation is an actively orchestrated process. A range of anti-inflammatory and pro-resolution mediators form complex regulatory networks coordinating the return to tissue homeostasis. These events include the clearance of

apoptotic cells and tissue debris, the restoration of normal vascular permeability and blood flow, tissue repair and recovery from fever and pain [122, 1].

1.8.0.1 Pro-resolving lipid mediators

The best studied pro-resolution compounds are lipid mediators, lipoxins, resolvins, maresins and protectins. They share some of the eicosanoid biosythesis pathways with the pro-inflammatory leukotrienes which are synthesised by lipoxygenase family members. However, the majority of pro-resolution molecules are mainly derived from multiple omega-3 and omega-6 PUFAs in addition to AA; illustrated in Figures 1.2 and 1.3 in green. The beneficial effects of aspirin treatment are due to its ability to inhibit acetylation of COX-2. This drives the lipid biosynthesis pathways to favour the actions of lipoxygenase enzymes, which can generate pro-resolving lipid mediators (Figure 1.2, 1.3) [122, 123, 124]. For a more in depth discussion about these mediators please refer to reviews from [122, 125].

Cell producing pro-inflammatory mediators undergo a 'class switch' in their eicosanoid biosynthesis towards the production of pro-resolving mediators [125, 123, 124]. During inflammation, high production of PGE_2 and PGD_2 stimulates the increased transcription of 15-lipoxygenase (LOX) in leukocytes, neutrophils and macrophages. The 15-LOX enzyme generates lipoxins, lipoxin A_4 and lipoxin B_4, thus creating a negative feedback loop for high production of pro-inflammatory PGE_2 [126].

Neutrophils recruited to inflamed sites interact with other cells in their environment, including leukocytes, endothelial cells, epithelial cells and platelets, this can induce a switch in their inflamatory phenotype to produce a different lipid profile. In blood vessels, activated neutrophils produce pro-inflammatory LTB_4 whereas in a resolving inflammatory site they produce lipoxins and resolvins [122]. In mucosa, lipoxins are generated by neutrophils obtaining the precursor for lipoxins, 15-hydroxyeicosatetraenoic acid (15-HETE), by interacting with the mucosal epithelial cells [127]. The 15-HETE is processed by the lipoxygenases in the cytoplasm of the activated neutrophils which are able to generate to lipoxinA_4 [127]. Likewise in blood vessels, the leukocyte-platelet interactions allows the transfer of 12-lipoxygenase found in platelets. 12-LOX enzyme is able to convert LTA_4 intermediate precursor found in neutrophils and other cells into anti-inflammatory lipoxins [128].

Furthermore, macrophage phagocytosis of apoptotic neutrophils causes a switch to this pro-resolving phenotype. Lipoxin A_4, resolvin E1 and resolvin D1 produced by macrophages signal via their corresponding GPCRs; lipoxin A_4 binds FPR2, resolvin E1 binds ChemR23 and resolvin D1 binds GPR32. These lipid mediators are able to

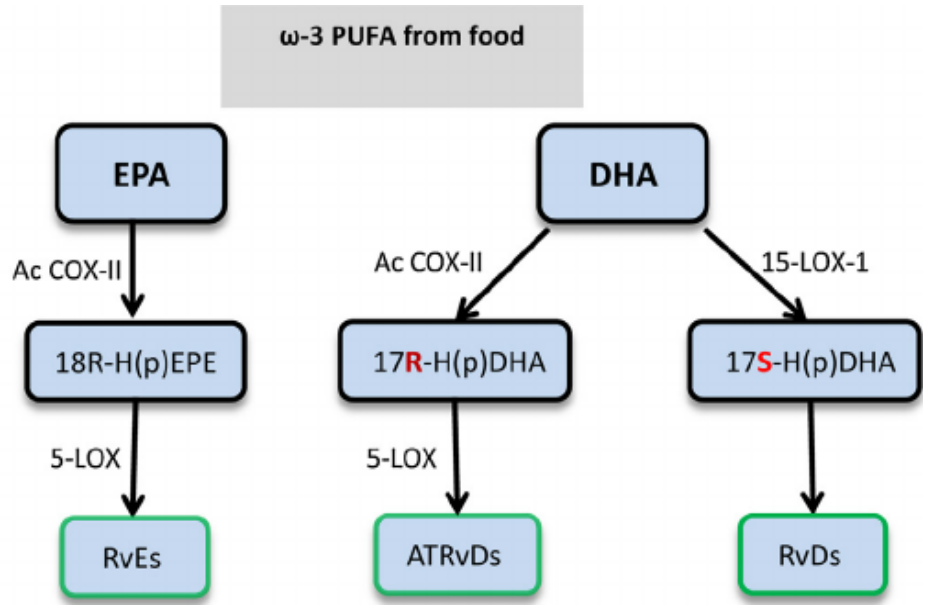


Figure 1.3: Polyunsaturated fatty acids (PUFA) metabolism. Eicosapentaenoic acid (EPA) is oxidized by acetylated cyclooxygenase II (Ac COX-II) and subsequently by 5-lipoxygenase (5-LOX) to the resolvins of the E series (RvEs). Docosahexaenoic acid (DHA) is oxidized by either Ac COX-II or 15-LOX-1. Green border indicates pro-resolving metabolites. Aspirin-triggered resolvin of the D series (AT-RvD); hydroperoxyoctadecadienoic acid (H(p)ETE); D-series resolvin (RvD). Taken from [115]

inhibit pro-inflammatory mediator secretion, thus reducing the recruitment of leukocytes to site of inflammation. They also inhibit the degranualtion of neutrophils and promote the phagocytic activity of macrophages for further apoptotic cell clearance and return to tissue homeostatis [129, 130].

1.8.0.2 Glucocorticoids and the Annexin A1 protein

Glucocorticoids are another group of endogenous anti-inflammatory ligands which work in concert to induce pro-resolution pathways. Synthetic glucocorticoids are regularly used in therapeutic application for chronic inflammatory conditions such as asthma, rheumatoid arthritis and psoriasis. Classical endogenous glucocorticoids, include cortisol and corticosterone, which are released from the adrenal glands to dampen the inflammatory process [131]. Additionally, the glucocorticoid regulated protein annexin A1 has been shown to regulate the inflammatory response and promote the resolution phase of inflammation. Annexin A1 is produced and stored in leukocytes populations including macrophages, monocytes and neutrophils. In neutrophils, annexin A1 is stored in granules which fuse upon attachment to the endothelium [132]. In the presence of high intracellular concentrations of Ca^{2+}, annexin A1

binds to phosphatidylserine [133]. When phosphatidylserine is presented on the surface of apoptotic neutrophils, promoting efferocytosis, membrane bound annexin A1 can also interact with its GPCR, ALX (human) and FPR2 (mouse), thus promoting the resolution and phagocytic phenotype of macrophages [134]. Moreover, a recent study illustrates that pro-inflammatory cytokine TNF-α upregulates pro-resolving receptors for annexin A1 [135] allowing the enhancement of the pro-resolution signals. Finally, treatment of annexin A1 in LDL receptor KO mice on a western diet reduced the artherosclerotic plaque burden, illustrating its beneficial effects in chronic models of inflammation [136].

1.8.0.3 Anti-inflammatory Cytokines

The process by which these pro-resolving mediators enhance the resolution of inflammation largely depends on their ability to inhibit the production of pro-inflammatory cytokines and chemokines, by switching to the production of anti-inflammatory cytokines, like TGFβ and IL-10. These cytokines are pro-resolving mediators in their own right. IL-10 is produced by pro-resolving macrophages in a resolving environment and also by Treg, T_H2 and dendritic cells [137]. Treatment with the cytokine IL-10 can convert a pro-inflammatory macrophage into a 'M2' like pro-resolving phenotype via STAT 3 signalling [138]. As a result it diminishes mRNA and protein levels of TNFα and IL-1β [138]. TGFβ enhances mechanisms involved in tissue repair and the production of IL-10 by macrophages [137].

It is important to highlight that there is a high degree of overlap in these pro-resolving pathways, in which mediators synchronise the return to tissue homeostasis. For instance, resolvin E1 stimulates the production of lipoxin A_4 and both lipoxins and resolvins promote macrophage IL-10 production [139].

1.9 Antibody therapies for chronic inflammation

In the past, therapeutic drugs were dominated by low molecular organic chemical molecules, which are absorbed via the gut. The current therapeutics dominating treatment of inflammatory disease and cancers are injectable proteins, primarily monoclonal antibodies (mAbs) [140]. The concept of using antibodies for treatment of disease dates back to the 1890s: Emil Adolf von Behring discovered the ability of small doses of diphteria or tetanus toxin produce a transferable immunity between animals via serum. This was later attributed to the presence of functional antibodies following immunisation [141]. The production of antibodies was revolutionised by the

discovery of the hybridoma technique in the 1970s by Köhler and Milstein, which provided a method for isolating monoclonal antibodies against specific targets. Splenic B cells of an immunised animal were fused with mouse myeloma cells to create an immortal B cell line, a hybridoma, producing the antibody of interest [141].

Antibodies are immunoglobulin protein structures, produced by B cells and plasma cells. They comprise of 4 polypeptide chains (2 heavy and 2 light chains) that come together to form a Y shaped molecule. Antibodies contain a variable region on each heavy and light chain of the polypeptide chain [142]. Within these, there are 3 hypervariable regions defined as complementarity-determining regions (CDRs) in heavy and light variable regions. During B cell maturation, these CDR regions undergo genetic recombination, thus creating unique CDR sequences in each B cell clone. These CDR regions are responsible for the antigen interaction and binding affinity [142] (Figure 1.4).

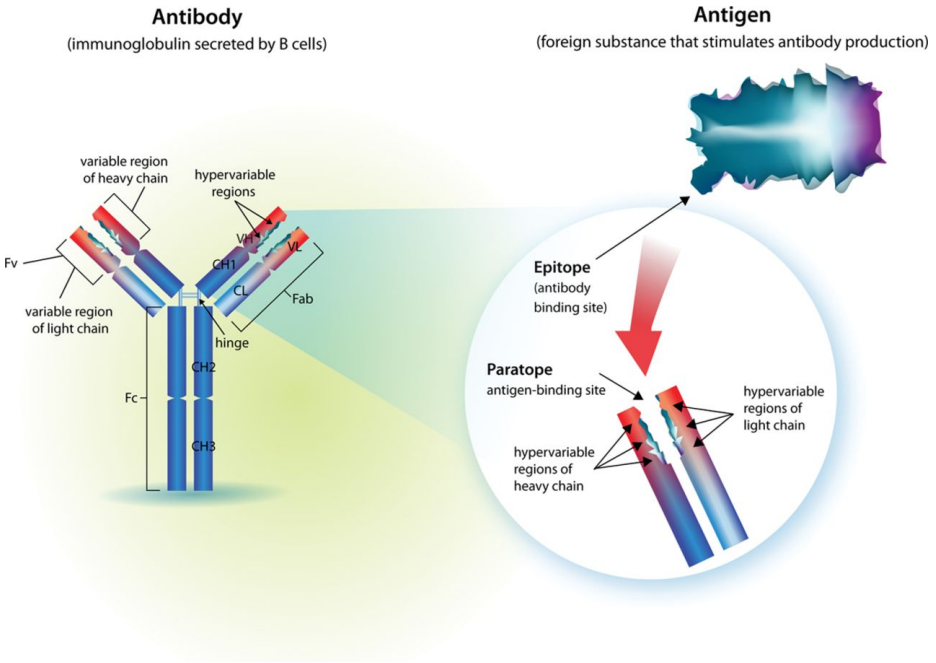


Figure 1.4: Antibody structure. The hypervariable regions (VH and VL) of the antigen-binding fragment (Fab) region of the antibody specifically bind an antigen. The fragment (Fc) region of the antibody is responsible for effector function by binding the Fc receptors on effector cells, linking the humoral (antibody) response to a cellular response. CH indicates heavy chain, constant domain; CL, light chain, constant domain; Fv, variable fragment; VH, heavy chain, variable domain; and VL, light chain, variable domain. Taken from Foltz *et al.* [142].

In nature, antibodies are found soluble in the circulation or bound to B cell membrane as part of the B cell receptors for particular antigen. There are 5 immunoglobulin isotypes produced by B cells, but the most abundant one is the IgG isotype. IgG

typically acts in the secondary (specific) phase of immune response. There are four IgG subclasses (IgG1-IgG4) in humans, and IgG1 most abundant subclass, followed by the IgG2,3,4. Their half lives are 20-21 days with the exception of IgG3 which is 7 days [142]. IgGs are the most common class of immunoglobin molecule used for the generation of therapeutic monoclonal antibodies. The Fc region is responsible for effector function by binding Fc receptors on effector cells or cross-linking for a cellular response.

Antibodies can swiftly provide therapeutic molecules to target disease-associated molecules. They provide high levels of specificity and affinity towards target molecules thus, providing fewer adverse effects than small molecule therapies. Antibodies are able to target diverse molecules, and by making modification to the antibody structures by genetic engineering, they provide purpose built structures for therapeutic use. Before any of the genetic engineering technology was developed murine anti-CD3 was the first mAb to be approved for use for treating acute allograft rejection in 1986 [142]. Accumulating clinical evidence indicated that the use of murine mAb was creating a host immune response due to the species differences. This was causing therapeutic inefficacy for long-term administration [141]. This prompted the development of recombinant DNA strategies to create a more humanised mAbs, thus, reducing the immunogenicity of mAbs.

A good example of how advances in genetic engineering technology has helped the development of more diverse antibodies structures to improve therapeutic use is the development of anti-TNFα mAbs. TNFα was an attractive therapeutic target, particularly for rheumatoid arthritis. Rheumatoid arthritis (RA) is a common autoimmune disease, associated with chronic inflammation of the joints which causes cartilage and bone damage [143]. Early *in vitro* studies showed that synovial fibroblasts from RA patients produced a wide variety of cytokines, chemokines and growth factors [144], the addition of anti-TNF antibody to the cultured synovial fibroblasts significantly reduced the expression of a wide variety of these pro-inflammatory mediators; such as IL-1, IL-6, IL-8 and GM-CSF [145]. This indicated a potential hierarchical role of TNFα in inducing the production of pro-inflammatory mediators. To improve on murine mAb structures, the generation of chimeric mAbs was developed, in which the murine Ig constant domains were replaced with the corresponding human Ig constant domains. Chimeric antibodies are approximately 70% human [141]. This strategy was implemented to produce, infliximab, the first anti-TNF mAb therapy for use in RA. With these genetic modifications, infliximab is able to bind human TNF with high

affinity and specificity and is much less immunogenic in patients [146]. Infliximab is still used in the clinic today.

Developments in antibody engineering, made it possible to further decrease the murine content of the variable regions, by replacing the hypervariable loops of a human antibody with the murine hypervariable loops of interest, using an approach called CDR grafting [141]. This created the 'humanised' antibodies which are 85-90% human and thus less immunogenic than chimeric antibodies. However, with the use of this method, directed mutagenesis approaches are needed to be used to restore the affinity of the original murine mAbs [141].

The first fully human mAb, adalimumab, is an anti-TNF mAb developed from phage display technology, and was approved for clinical use in RA in 2002 [142]. Phage display technology is a *in vitro* antibody discovery method, where large repertoires of antibody variable regions are displayed on the surface of bacteriophage particles. For more information about phage display technology, please refer to Chapter 3. Adalimumab was derived from a murine mAb template, which was paired with a repertoire of human light chains and heavy chains to create two phage display libraries. The combined human and light chains from the phage selected clones yielded a binding clone against human TNF. Following affinity maturation techniques, directed CDR mutagenesis, a higher affinity version of the phage-derived clone was established [146]. The phage-derived human variable sequences were fused with human IgG1κ constant domain sequence. Despite the human origin of adalimumab, it still elicits an immune response in approximately 5% of RA patients treated with this antibody [146].

Finally, another anti-TNF biologic is Certolizumab pegol, developed by UCB Pharma. It is a humanised antigen-binding fragment (Fab) of a monoclonal antibody that has been conjugated to a polyethylene glycol moiety. It is currently used for the treatment of RA and Crohn's disease. Crohn's disease is also an autoimmune disease, characterised as a chronic relapsing inflammatory bowel disease. The original clone was selected from a hybridoma for human TNFα binding. The CDRs from the murine mAb were inserted in to a human Fab IgG framework along with several other structural residues of the variable domain to maintain affinity [147]. This Fab structure was then PEGylated in order to extend the half life of the Fab molecule [147]. The lack of an Fc region on this molecule minimises the potential Fc-mediated effects such as complement-dependent cytotoxicity (CDC) or antibody dependent cell-mediated cytotoxicity (ADCC). *In vitro* studies have shown that the other Fc conjugated therapeutic antibodies still cause adverse CDC and ADCC whereas cer-

tolizumab pegol does not [148]. Another beneficial aspect of the PEGylation of the Fab is that it does not cross the placenta during pregnancy [147].

The biological purpose of the Fc region of an antibody is to exert an effector function either through the binding C1q complement fragment for CDC or activating cell cytotoxicity ADCC via binding Fcγ receptor [149]. The constant regions of the Fc fragment from the four IgG isotypes exert different potencies of CDC and ADCC, with IgG3 and IgG1 being the most active and IgG2 being the most inert [149]. Considering the activities of the Fc regions is very important in respect to designing a therapeutic antibody. In mAb therapies directed against cancers, in which the desired effect is to deplete a particular cell type by targeting specific cell markers, the ADCC or CDC activities are favourable. Therapeutic mAbs with this mode of action are rituximab and alemtuzumab. They are both used in the therapy of B cell lymphomas, targeting B cell by CD20 and CD52 receptors respectively [150, 151]. Rituximab is also used in a subset of patients with MS and RA. A neutralising mAb is desired in the elimination of soluble mediators, such as the anti-TNF mAbs discussed above or anti-vascular endothelial growth factor (VEGF) antibodies[150].

1.10 Chemerin

1.10.1 Discovery of chemerin and its receptors

Chemerin was first discovered as a retinoid-induced gene in psoriatic skin lession in 1997. Its expression was upregulated following treatment with a synthetic retinoid tazarontene and specific retinoic acid receptor agonists. Hence, they named it Tazarotene-induced gene 2 (TIG2) and the gene as retinoic acid receptor responder gene 2 (RARRES2)[152]. Subsequently, chemerin expression was identified in multiple tissues including liver, pancreas, small intestine, ovary and prostate via northern blot.

Chemerin binds three GPCR receptors. The first evidence of the biological function of chemerin came with the discovering of the orphan GPCR that chemerin signals through, known as chemokine-like receptor 1 (CMKLR1) or Chemerin Receptor 23 (ChemR23) [153] in 2003. The second receptor described to be bind and signal chemerin is G protein-coupled receptor 1 (GPR1). GPR1 was first described in 1994 in human hippocampus, but was not linked to chemerin until 2008 [154]. The last receptor to be associated with chemerin is chemokine (CC motif) receptor-like 2 (CCRL2) which was first discovered in humans in 1998, then known as human chemokine receptor (HCR). The link to chemerin was not made until 2008 when Zabel *et al.* investigated the cell biology mechanism of this chemerin receptor binding [155].

Since then chemerin has been identified throughout the human body and analysis of its function seems to point towards a multifunctional role as a chemokine, an adipokine, an anti-bacterial peptide and a growth factor.

1.10.2 Structure and isoforms

The structure of chemerin is unknown, however, the predicted structure of chemerin indicates it may be structurally similar to other chemokines, cystatin (a cysteine protease inhibitor) and cathelicidins (bacterial peptide precursor). The predicted chemerin structure has a disordered carboxyl-terminus (C-terminus), an antiparallel β-pleated sheet wrapped around an amino-terminal α-helical domain [156]. Chemerin is translated as a 163 amino-acid (a.a.) pre-proprotein that is secreted as 143 amino acid (approximately 18kDa) called prochemerin. Prochemerin has low biological activity at the chemerin receptors and requires proteolytic cleavage of the C-terminal inhibitory sequence, consisting of 6 a.a., indicated in Figure 1.5. The proteolytic cleavage is performed by various serine proteases, from the coagulation, fibrinolytic and inflammatory cascades. The most active chemerin isotype is the a.a. sequence of chemerin$^{20\text{-}157}$, mainly generated by neutrophil-derived elastase and carboxy-peptidase B and N [153, 157]. The C-terminus is responsible for inducing the signalling activities at the ChemR23 receptor. Investigations with the C-terminal 9 a.a. peptide of the active chemerin sequence, C9$^{148\text{-}157}$, illustrated a lower potency but comparable receptor activation [153]. All the known chemerin isoforms generated are shown in Table 1.1. Further cleavage of the chemerin molecule generates smaller derived peptides, these exhibit other functional activities and will be discussed in later sections.

Protease	Cleavage substrate	Product	Chemotaxic bioactivity	Reference
Elastase	Chemerin^{163}	Chemerin^{157}	High	[158]
		Chemerin^{155}	Inactive	
Cathepsin-G	Chemerin^{163}	Chemerin^{156}	High	[158, 159, 160]
		Chemerin^{148}	Inactive	
Proteinase-3	Chemerin^{163}	Chemerin^{155}	Inactive	[161]
Mast cell chymase	Chemerin^{156}	Chemerin^{154}	High	[158, 159, 160]
	Chemerin^{157}			
Plasmin	Chemerin^{163}	Chemerin^{158}	Low	[159]
Factor XIIa	Chemerin^{163}	Undetermined		[157]
Cathepsin K & L	Chemerin^{163}	Chemerin^{157}	High	[162]
		Chemerin^{125}		
		Chemerin^{158}	Low	[159]
		Chemerin^{155}	Inactive	
Carboxypeptidase B & N	Chemerin^{163}	Chemerin^{157}	High	[157]

Table 1.1: Proteolytic cleavage of human chemerin by different proteases.

1.10.3 Chemerin receptor signalling

1.10.3.1 ChemR23 (CMKLR1)

The first chemerin receptor to be identified was the ChemR23 or CMKLR1 receptor [153]. The ChemR23 receptor shares nucleotide homology with CXCR1 receptor, C3a, C5a and N-formyl peptide related receptors. The ChemR23 receptor is coupled to Gα_io family of G proteins. Receptor activation via chemerin and chemerin peptides induces Gα_i protein activation, β arrestin recruitment and receptor internalisation, which results in cAMP inhibition, phospholipase C activation, calcium mobilisation, as well as activation of ERK and MAPK pathways [163, 164]. Ultimately, chemerin signalling via this receptor induces chemotaxis of ChemR23$^+$ cells [153, 165]. It is broadly expressed on leukocyte and non-leukocyte cells for more details please refer to Chapter 4. Tables 1.2 and 1.4 illustrate the previously reported phenotypes of ChemR23 knockout mice in the current literature.

ChemR23 is also reported to be a receptor for the pro-resolution lipid derived from eicosapentaenoic acid, Resolvin E1[166]. Signalling via the ChemR23 receptor induces phosphorylation of Akt, ERK and PI3K downstream cascades. Resolvin E1 regulates leukocyte migration by reducing epithelial cell adherence and enhancing macrophage phagocytosis of apoptotic neutrophils [130, 167] as discussed in Section 1.8.0.1.

1.10.3.2 GPR1

The second chemerin signalling receptor described was GPR1. GPR1 induces classic GPCR signalling cascades but with less potency when compared to ChemR23 [154, 164]. For instance, GPR1 displays lower β-arrestin recruitment and ERK phosphorylation compared with ChemR23 receptor. Chemerin-derived C-terminal peptides compete with chemerin in binding GPR1 receptor, however, this is not the case with the ChemR23 receptor [164]. There has been a report illustrating that C9 C-terminal peptide can induce stronger β-arrestin recruitment than chemerin, suggesting that GPR1 may be able to bind and signal with C-terminal derived peptide more favourably if they are generated *in vivo* [164]. However, these results has not been seen by others [168]. GPR1 is expressed in the central nervous system and by non-leukocyte subsets, such as smooth muscle cells and stromal cells in adipose tissue [169, 168, 170]. Table 1.4 illustrates the metabolic phenotype of GPR1 knockout transgenic mice reported in the current literature.

1.10.3.3 CCRL2

The third chemerin receptor is CCRL2. It is described as a 'non-signalling' GPCR that binds chemerin with low nanomolar affinity. It does not convey any downstream signalling due to the lack of a classic DRYLAIV motif and it does not internalise upon chemerin binding [164, 171, 155]. It also does not seem to bind the C-terminal C9 peptide. It has been suggested that the chemerin binding to the CCRL2 receptor occurs through the N-terminus [164, 171]. One accepted hypothesis for the role of CCRL2 is to display chemerin on the surface of cells for paracrine ChemR23$^+$ cells [155, 171]. The expression of CCRL2 was first described in primary neutrophils, monocytes and differentiated macrophages [172]. However, studies have shown that it is widely expressed in many tissues on leukocyte and non-leukocyte subsets. Exposure to inflammatory stimuli, results in CCRL2 upregulation by cells expressing the receptor [173]. For more information on the expression and role of CCRL2 during inflammation, including my own investigations, the reader is referred to Chapter 5. Table 1.3 illustrates the phenotypes of CCRL2 knockout mice in the current literature.

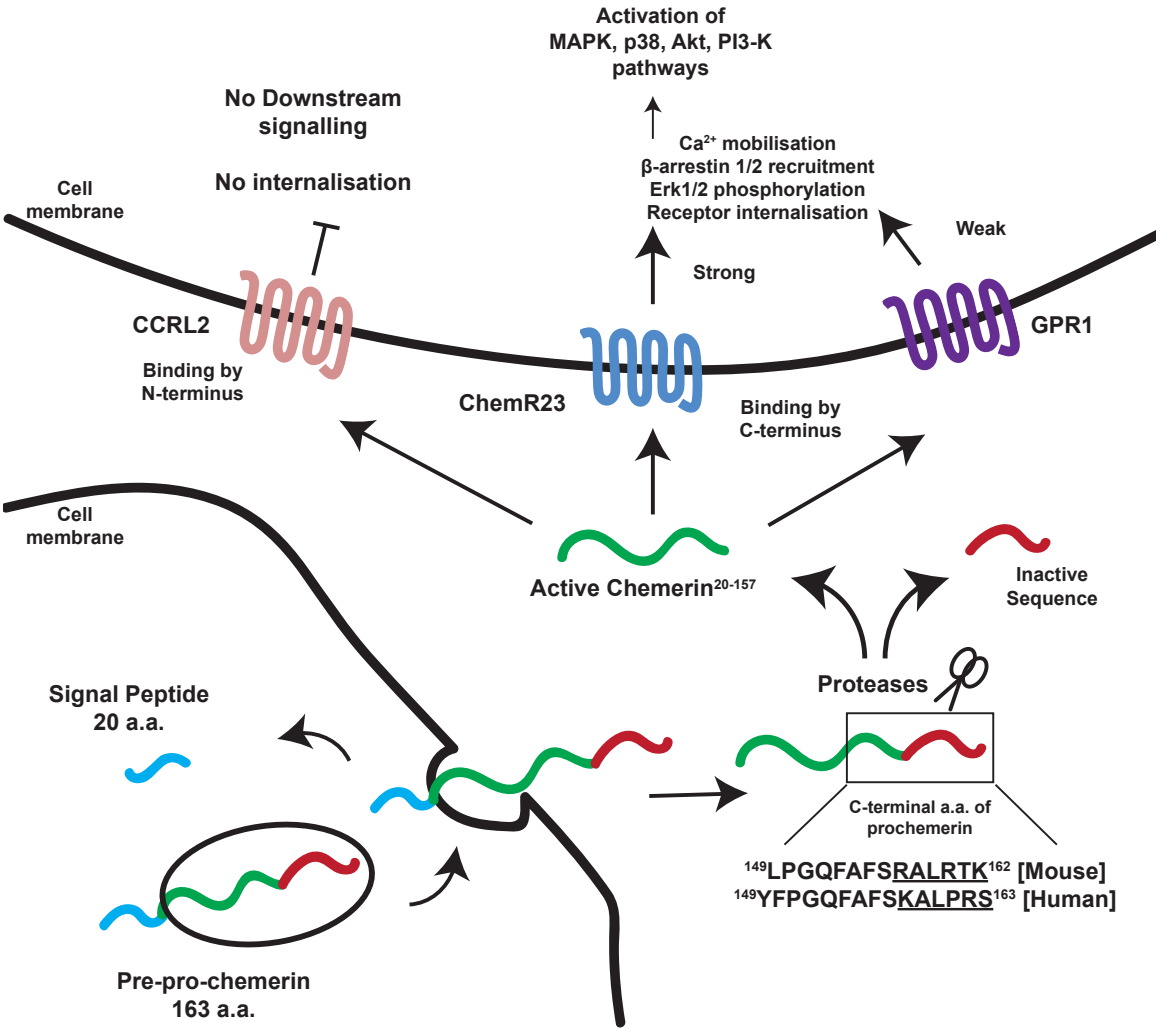


Figure 1.5: Processing of chemerin and receptor signalling pathways. Chemerin is depicted with the N-terminus on the left and C-terminus on the right. When pre-prochemerin is released, the membrane-bound signal peptide (blue) is released and the extracellular protein becomes the inactive precursor called prochemerin. This is then cleaved at various locations by proteases (Table 1.1), releasing the inactive prochemerin a.a. sequence (red) and creating the active chemerin fragments (green). Active chemerin can bind to three GPCRs, CCRL2, ChemR23, and GPR1. ChemR23 and GPR1 demonstrate Gαi downstream signalling while CCRL2 is an non-signalling GPCR. Adapted from image in Ferland *et al.* [174]

ChemR23 knockout mice

Author & Year	Background strain	Inflammation Phenotype of KOs	Model used	Reference
Cash 2008	129S6SvEv	↑	Zymosan (10μg) induced peritonitis	[175]
Luangsay 2009	C57BL/6	↑	LPS-induced lung inflammation	[176]
Graham 2009	C57BL/6	↓	EAE model of MS disease	[177]
Bondue 2011	C57BL/6	↑	Viral lung pneumonia model	[178]
Demoor 2011	C57BL/6	↓	Chronic cigarette smoke induced lung inflammation	[179]
Dranse 2015	C57BL/6	↓	DSS-colitis model	[180]
Provoost 2016	C57BL/6	↓ ↑	Diesel exhaust particle-induced acute lung inflammation Dust-mite induced lung allergy model	[181]

Table 1.2: Inflammatory phenotype of previously reported ChemR23 knockout mice.

CCRL2 knockout mice

Author & Year	Background strain	Inflammation Phenotype of KOs	Model used	Reference
Zabel 2008	C57BL/6	↓	Mast-cell driven subcutaneous anaphylaxis	[155]
Otero 2010	C57BL/6	↓	OVA-induced lung allergy	[182]
Monnier 2012	BALB/c	↓	LPS-induced lung inflammation	[171]
Mazzon 2016	C57BL/6	↑	EAE model of MS disease	[183]
Del Prete 2017	C57BL/6	↓	CIA & Serum transfer-induced arthritis	[184]
Regan-Komito, Valaris 2017	C57BL/6	↑	Zymosan (100μg) induced peritonitis	[185]

Table 1.3: Inflammatory phenotype of previously reported CCRL2 knockout mice.

Metabolic phenotype of chemerin and receptors

Gene knockout	Author & Year	Background strain	Phenotype of KOs	Reference
Chemerin	Takahashi 2011	C57BL/6	Impaired glucose tolerance	[186]
ChemR23	Rouger 2013	C57BL/6	No glucose intolerance; Mild obesity; no defect in adipogenesis	[187]
GPR1	Rouke 2014	C57BL/6	Impaired glucose tolerance	[170]

Table 1.4: Metabolic phenotypes of chemerin and its receptors.

1.10.4 Chemerin expression

Chemerin is expressed in a range of different tissues, including the liver, lung, skin, pituitary, ovary, kidney, and white adipose tissue [153]. It is primarily considered

to be produced in the liver and adipose tissue, however, the range of tissues and cells has grown to include epithelial, endothelial cells, chondrocytes and platelets [176, 188, 189, 157]. Under resting conditions, the inactive form, prochemerin, is present at relatively high concentrations in plasma (100-200ng/ml), in healthy control groups [190]. The source of prochemerin in plasma is unknown but it is considered to be produced by the liver and adipose tissue [178, 191].

Retinoic acid and similar analogues, such as vitamin D, have been implicated in the induction of chemerin production [152]. In a study treating endothelial cells with various pro-inflammatory mediators, retinoic acid was the most efficient inducer of chemerin production by endothelial cells [192]. Retinoic acid signalling induces peroxisome proliferator-activated nuclear receptor γ (PPARγ). Bone marrow mesenchymal stem cells express chemerin and its ChemR23 receptor during adipogenesis. The forced expression of PPARγ does not completely rescue proliferation and adipogenesis following chemerin knockdown [193]. Forced expression of PPARγ in fibroblasts stimulated chemerin expression. Sequence analysis showed that there is a PPARγ response element sequence within the chemerin promoter which was confirmed with chromatin immunoprecipitation [193].

Chemerin is associated with osteoclast differentiation and in the context of bone development chemerin can act as a growth factor. The expression of chemerin was induced by the treatment of stromal cells with vitamin D and dexamethasone, a glucocorticoid, for their differentiation into osteoclasts [194]. Haematopoietic stem cells also secrete chemerin protein and express ChemR23 receptor. Blocking of chemerin via a neutralisation antibody, blocks the differentiation of haematopoietic stem cells towards osteoclastogenesis, resulting in a lack of matrix resorption and reduced marker gene expression [195]. Furthermore, the pro-inflammatory stimulation of the chondrocytes and adipocytes display augmented production of chemerin [189, 196]

Moreover, endometrial stromal cells from pregnant, fertile non-pregnant, or menopausal women treated with sex hormones, such as progesterone and 17β-oestradiol show a significant up-regulation of chemerin secretion. However, levels of chemerin released from the pregnant stromal cells were significantly higher than the non-fertile and menopausal cells [197]. This indicates that even though the sex hormones contribute to the production of chemerin in these stromal cells, there is likely another factor involved in inducing production [197].

1.10.5 Chemerin in inflammation

In addition to psoriatic skin lesions, chemerin expression has been identified in multiple inflammatory exudates, such as in secondary ovarian ascite fluid and synovial fluid from RA patients [153]. Elevated levels of chemerin in plasma have been observed in a myriad of different inflammatory diseased patients. These include patients with cardiovascular disease, metabolic syndrome, systemic lupus erythematosus, RA, Crohn's disease and in obesity [198, 199, 200, 191]. There have been multiple reports about the correlation of chemerin levels as a biomarker to predict atherosclerotic changes and cardiovascular events [198, 201, 202]. Furthermore, RA patients undergoing anti-TNF or anti-IL-6 therapy display significant reductions in serum chemerin levels [203, 204].

The first recognised function of chemerin was to promote chemotaxis of immature dendritic cells and macrophages via the ChemR23 receptor [153]. ChemR23 is also expressed on pDCs and natural killer (NK) cells which were also able to migrate towards chemerin *in vitro* and *in vivo* models of lung inflammation in a ChemR23-dependant manner [205, 206, 178]. Elevated levels of chemerin during colitis model of inflammation also induces ChemR23$^+$ NK cell recruitment [207]. Dermal endothelial vessels of lupus erythematosus skin lesions and inflamed dental endothelium expressing chemerin are associated with the recruitment of ChemR23$^+$ pDCs [205, 206].

During pregnancy, chemerin is expressed in the endometrial stromal cells in high levels, which supports the migration of blood NK cells through both the decidual endothelial cell and stromal cell layer into the endometrium tissue [197]. The numbers of uterine NK cells present during early pregnancy is important for successful embryo development, particularly in respect of vascular remodeling [197].

Moreover, chemerin seems to be an alternative mediator to action cell-tissue homing for ChemR23$^+$ into particular regions of a tissue. Tissues such as secondary lymphoid organs, skin and endometrium all have marginal zones in which particular subsets of DCs and NK cells reside [205, 197]. Adipose tissue contains a resident macrophage population and the lack of chemerin in a chemerin KO mouse illustrates a reduction in adipose tissue resident macrophages [186].

The transmigration through a vascular endothelial wall is an important mechanism of action to enable the efficient chemotaxis of cells. Chemokines are able to activate migratory leukocytes and endothelial cells to express the adhesion molecules, integrins, to enable rolling, binding and diapedesis into inflamed tissue. Like most classic chemokines, chemerin treatment induces intergrin activation in a ChemR23-dependent manner in macrophages and dendritic cells [165, 192]. Chemerin-stimulated

adhesion is dependent on increased avidity of VLA-5($\alpha5\beta1$) and VLA-4($\alpha4\beta1$) towards VCAM-1 and fibronectin adhesion molecules [165], enabling their migration to site of inflammation.

1.10.5.1 *In vitro* activities of chemerin

Similar to other pro-inflammatory cytokines, chemerin stimulation of chondrocytes and fibroblast-like synoviocytes can induce pro-inflammatory mediator production of TNFα, IL-8, IL-6 and matrix metalloproteases [189, 188]. While another study has only illustrated the production of CCL2 and the expression of TLR4 receptor in synovial fibroblasts treated with chemerin [208]. Similarly, human microvascular endothelial cells and vascular smooth muscle cells treated with bioactive chemerin increased the mRNA of proinflammatory mediators, generated ROS and MAPK phosphorylation, stimulated smooth muscle proliferation via NADPH oxidase [209]. However, there has been one published study illustrating an anti-inflammatory effect of chemerin on human umbilical vein endothelial cells (HUVECs) by inhibiting pro-inflammatory cytokine production and adhesion molecule expression via NO production [210]. In addition to this, chemerin treatment of lung epithelial cells has been shown to inhibit the CCL2 mRNA and protein production [211].

Moreover, peritoneal macrophages treated with a C-terminal derived chemerin peptide, C15, were shown to establish a 'M2'-like phenotype and produce pro-resolving mediators [175]. However, a similar study using activated peritoneal macrophages stimulated with chemerin showed no alterations in the pro-inflammatory cytokine profile they were generating [212].

1.10.5.2 *In vivo* treatments and inflammatory models of chemerin

Due to conflicting findings from *in vitro* and *in vivo* studies in the published literature, the role of chemerin, during inflammation, is still unclear. Numerous murine models of inflammation have been used to study the role of chemerin and in this section I will describe a selection of them and their key findings. Treatment with recombinant chemerin in a model of dextran sodium sulfate (DSS)-induced colitis displayed enhanced disease and inflammatory outcome, which was associated with the suppression of 'M2'-like phenotype genes in macrophages at the site of inflammation [207]. ChemR23 KO mice in a model of cigarette smoke-induced and diesel exhaust particle-induced lung inflammation displayed remarkably attenuation in chemokine production, total cell recuitment and T cell accumulation [179, 181]. Additionally, in a murine model of multiple sclerosis, experimental autoimmune encephalomyelitis

(EAE), ChemR23 null mice or mice treated with a ChemR23 antagonist developed less severe clinical and histological disease and displayed lower inflammation in the central nervous system (CNS) [177, 213]. These results were associated with a reduction in macrophage infiltration.

While there is much evidence to support a pro-inflammatory role for chemerin/ChemR23, there are also a number of *in vitro* and *in vivo* studies to suggest an anti-inflammatory role of chemerin. Luangsay *et al.* used a LPS-induced murine model of acute lung inflammation demonstrated that ChemR23-deficient mice show an increase in the recruitment of neutrophils and an increase in inflammatory cytokine production. Pretreatment with chemerin in wild type mice prior to inducing this model showed reduced lung inflammation [176]. Another study, using intranasal administration of chemerin in a murine model of allergic asthma inhibited the production of the chemokine CCL2 and subsequent recruitment of inflammatory dendritic cells into the airways. This mechanism seemed to be associated with chemerin inhibiting the production of CCL2 following LPS exposure in lung epithelial cells [211]. In a model of zymosan-induced peritonitis, the treatment of a C-terminal chemerin peptide, C15, displayed anti-inflammatory properties by preventing the recruitment of neutrophils and monocytes and reduced the expression of pro-inflammatory mediators [175]. *In vitro* treatment with C15 peptide, macrophages reduced their pro-inflammatory cytokine production and inhibited neutrophil integrin activation [175, 214]. However, the use of C15 peptide in an acute lung inflammatory model had not observed effect [176].

1.10.6 Chemerin as an adipokine

Chemerin has a significant role in adipogenesis. Pre-adipocytes express the ChemR23 receptor and chemerin during differentiation into mature adipocytes. Blocking of chemerin impairs this differentiation [215, 216, 199]. Mice on a high-fat diet expressed higher levels of chemerin and ChemR23 receptor by adipocytes [215, 199]. Treating adipocytes with chemerin induces ERK1/2 phosphorylation, lipolysis and glucose uptake by enhanced insulin signalling [215]. In fact, chemerin-deficient mice displayed impaired glucose tolerance due to increased hepatic glucose production and impaired insulin secretion [186]. The absence of chemerin leads to a downregulation of a significant transcription factor, MafA, in pancreatic β islet cells that is necessary for their efficent function [186]. This result indicates that chemerin regulates glucose homeostasis in a tissue-dependent manner in mice.

A study by Rourke *et al.* reported that animals lacking the GPR1 chemerin receptor also displayed glucose intolerance and decreased insulin sensitivity, indicating both ChemR23 and GPR1 may be important for the observed effects of chemerin on glucose homeostasis [170]. In contrast, Rouger *et al.* reported animals lacking ChemR23 displayed no differences in glucose tolerance or insulin sensitivity and only obesity in aged ChemR23 knockout mice [187]. Hence, the exact role of chemerin and its receptors on glucose homeostasis remains unclear *in vivo*, with some studies proposing chemerin drives metabolic dysfunction while others supporting a protective function for chemerin by increasing glucose uptake and insulin sensitivity.

There is a significant correlation between elevated levels of plasma chemerin with body fat, serum triglycerides and a negative correlation with high density lipoprotein cholesterol (HDL) in human studies. In addition to elevated levels of C-reactive protein [217]. These epidemiological findings indicate an association of chemerin with low grade inflammation and dyslipidemia seen in obesity.

1.10.7 Chemerin and angiogenesis

ChemR23 is expressed by human and murine vascular endothelial cells, and its expression is upregulated by pro-inflammatory mediators, such as TNFα and IL-6 [218]. Studies have also shown that chemerin activates key angiogenic pathways and induces angiogenesis *in vitro* [218, 219]. These signalling pathways include the dose-dependent induction of gelantinolytic matrix metalloproteases 2 and 9, as well as activating PI3K/Akt and MAPKs pathways involved in angiogenic and cell survival cascades [218, 219].

A successful pregnancy depends on efficient assembly of vascular remodelling and placenta development. Decidual endothelial cells in the endometrium express the ChemR23 receptor and once treated with chemerin, they undergo capillary-like tube formations. Thus, this suggests that chemerin expressed in the uterus can participate in the complex decidual vessel remodelling that accompanies foetal development [197].

1.10.8 Antibacterial effects of chemerin

Chemerin is predicted to have a structural similarity to the cathelicidin/cystatin family of proteins. This family of proteins is comprised of antibacterial polypeptide cathelicidins and inhibitors of cysteine proteinases (cystatins). Cathepsin K and L from this family of proteins cleave chemerin triggering previously discussed, chemotaxis of ChemR23$^+$ cells whilst also displaying antibacterial activity against Gram

negative *Enterobacteriaceae* and *Klebsiella pneumoniae* [162]. Cathepsin K and L are able to cleave chemerin into the active chemerin$^{20\text{-}157}$ isoform but also cleave to release 38-residue from the C-terminal chemerin peptide to generate chemerin$^{20\text{-}125}$, with no functional pro-migratory ability. However, both active chemerin$^{20\text{-}157}$ and chemerin$^{20\text{-}125}$ display comparable antibacterial activity [162]. The N-terminal region of chemerin is responsible for the antibacterial effects seen, particularly the a.a. residues Val^{66}-Pro^{85}. The general mode of action exerted by antibacterial peptides is their ability to dock on specific components on bacterial cell wall causing subsequent pore formation. The antibaterial effects observed by chemerin-derived peptides are caused by direct bacterial lysis [220]. These effects have also been demonstrated in a 3-D skin culture environment, in which chemerin is naturally highly produced by keratinocytes and inhibited by the use of a chemerin blocking antibody [220].

1.11 Original hypothesis for this thesis

Chemerin is undoubtedly a multifunctional cytokine, which exerts its effects in a plethora of tissue sites around the body and in immunological conditions. Considering the current literature, the function of chemerin during inflammation seems to be situation-dependent. For a successful inflammatory event, there has to be the correct balance of activation and inactivation signals; hence the function of a protein is never only beneficial, there is a yin and a yang. Most of the current literature focuses on the role of chemerin in longer term disease models of lung, gut and CNS pathology. These models are important to illuminate mechanistic features of adverse pathological conditions in humans, yet there has not been a detailed investigation into the role chemerin and its receptors play during the early onset of inflammation. The acute phase of inflammation can illuminate impairments that may subsequently become augmented within a chronic inflammatory setting.

The original hypotheses for this thesis are:

1. That it is possible to develop antibodies that recognise only prochemerin for more accurate epidemiological assessment.
2. ChemR23 receptor is expressed by tissue resident leukocyte subsets.
3. Chemerin has a function during acute inflammation.
4. The non-signalling receptor, CCRL2, plays a role during acute inflammation.

1.12 Experimental aims

Due to the lack of commercially available tools to measure different isoforms of chemerin, my first experimental aim was to develop and characterise antibodies, that recognise chemerin and prochemerin, derived from UCB Pharma phage display library.

The second aim was to investigate the expression of chemerin receptors on leukocyte subsets under steady state conditions.

The third aim was to investigate the role of non-signalling receptor, CCRL2, and the signalling receptor, ChemR23, in an acute inflammatory model of zymosan-induced peritonitis.

Finally, the fourth aim was to investigate behavioural differences in CCRL2 null mice that I had observed during the first 3 years of my DPhil studies.

Chapter 2

Methods and Materials

2.1 Materials

2.1.1 Reagents

Recombinant murine chemerin, C5a, goat anti-chemerin polyclonal, rat anti-chemerin monoclonal were purchased from R& D systems (Abingdon, UK). Chemerin peptides: murine C17 (AGEDPHGYFLPGQFAFS), N-terminal biotinylated murine C17, murine C9 (FLPGQFAFS), murine C23 (AGEDPHGYFLPGQFAFSRALRTK), N-termnal biotinylated murine C23, N-terminal biotinylated murine C23 and FLAG tagged at the C-terminus were ordered from Peptide Protein Research (London, UK).

HRP- labelled goat anti-M13 phage antibody and rProtein A GraviTrap 10 prepacked gravity-flow columns purchased from GE Healthcare Life Sciences. Rabbit anti-FLAG antibody was purchased from Abcam (UK). HRP-conjugated Goat anti-rabbit or anti-mouse secondary was purchased from Biorad (UK). Human neutrophil elastase and cathepsin G from Merk Millipore (UK). BD FACS^{TM} Lysing solution and BD Pharm Lyse^{TM} (Lysing Buffer) from BD Biosciences (UK). Bio-gel polyacrylamide beads (P-100 fine 45-90 m) were purchased from Biorad (Hertfordshire, UK). CIM-16 and 96 well E-plates plates were purchased from Cambridge bioscience (Cambridge, UK). Zymosan- A (Z4250), Thioglycollate brewers broth, eppendorf LoBind microcentrifuge tubes and all other laboratory chemicals were purchased from Sigma Aldrich (Dorset, UK).

2.1.2 Animals

All animal studies were conducted with approval from the Dunn School of Pathology Local Ethical Review Committee and in accordance with the UK Home Office regulations (Guidance on the Operation of Animals, Scientific Procedures Act, 1986).

Experiments on animals were performed under the PPL 30/3035. All animal experiments were planned with consideration of the 3Rs ie. Replacement, Reduction and Refinement at every stage. Statistical power calculations were performed to ensure that all experiments used the minimum number of animals required to obtain a statistically significant result. Replaced animal experimentation with *in vitro* alternatives when possible and refined the experimental method(s) to improve animal welfare and minimise suffering

All mice used in these experiments were all housed and bred in the Pathology Support Building. Animals were fed a standard laboratory chow diet and water *ad libitum*. Animals were housed on a standard 12 hour light cycle followed by a 12 hour dark cycle under pathogen-free conditions. C57Bl/6J mice strain were obtained from in-house colony maintained in our animal facility (referred to as wild type (WT) animals). CCRL2 knockout mice were from Jackson laboratory, backcrossed onto a C57Bl/6J genetic background for 12 generations (original genetic background were 129S6/SvEv strain). 129S6/SvEv mice strain were from our own in-house colony. ChemR23 knockout mice were from Paradigm Pharmaceuticals and were on a 129S6/SvEv strain background.

Antigen	Isotype	Clone	Fluorophore	Supplier	Validation
B220	RA3-6B2	Rat IgG2a	APC	Biolegend	✓
CD11b	M1/70	Rat IgG2b	PercP	Biolegend	✓
CD19	6D5	Rat IgG2a	Brilliant violet 421	Biolegend	✓
CD3	17A2	Rat IgG2b	PE	Biolegend	✓
CD45	30-F11	Rat IgG2b	APC/Cy7	Biolegend	✓
ChemR23	477806	Rat IgG2b	PE	R&D	✓
hChemR23	84939	Mouse IgG3	PE	R&D	✓
F4/80	CI:A3-1	Rat IgG2b	FITC	Bio-rad	✓
F4/80	CI:A3-1	Rat IgG2b	Alexa Fluor 647	Bio-rad	✓
Ly6C	HK1.4	Rat IgG2c	APC	Biolegend	✓
Ly6C	HK1.4	Rat IgG2c	FITC	Biolegend	✓
Ly6B.2	7.4	Rat IgG2a	Alexa Fluor 647	Biolegend	✓
Ly6G	1A8	Rat IgG2a	PE	Biolegend	✓
Ly6G	1A8	Rat IgG2a	Pacific blue	Biolegend	✓
Siglec-F	E50-2440	Rat IgG2a	Alexa Fluor 647	Biolegend	✓

Table 2.1: Flow cytometry antibodies used throughout this thesis. Validation from suppliers for flow cytometry.

2.2 Methods

2.2.1 Panning a phage display library

2.2.1.1 Panning against recombinant murine chemerin

In phage display technology, multiple rounds of antigen exposure to an antibody phage display library is required in order to enrich for specific binding clones. These repeated rounds of exposure and selection from a library is called 'biopanning' or 'panning', a summary of the steps is depicted in Figure 2.1. Here I will briefly describe the protocol for phage library panning.

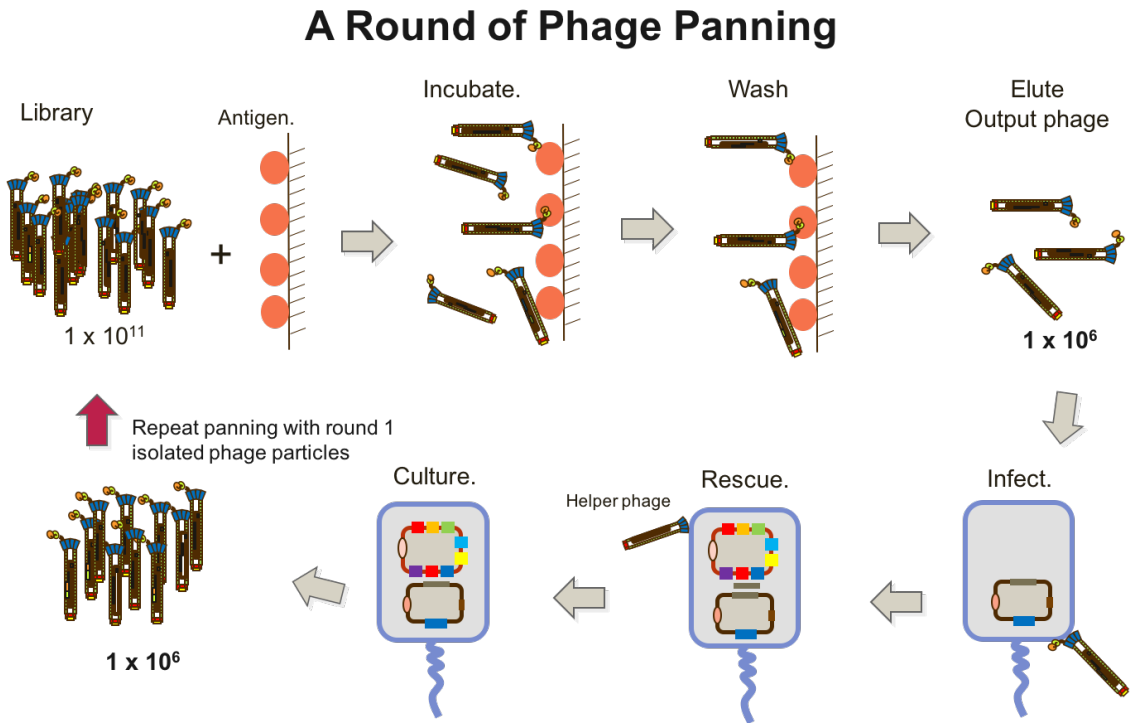


Figure 2.1: A round of phage panning. Taken from UCB phage display team.

The protein of interest is immobalised to high binding plastic surface. Recombinant murine chemerin[T^{17}-S^{156}](R& D) was immobalised on a nunc-immunotube (Thermo Scientific) at a concentration of 12μg/ml by incubating at 4°C overnight. The immunotube was blocked with 3% Bovine serum albumin BSA in phosphate buffered saline (PBS) for 1 hour at room temperature (RT). Concurrently, the human naïve phage library that was created by UCB's phage display team, was also blocking in a 1:1 ratio of phage library and phage blocking solution (3% BSA 3% Milk powder in PBS) for 1 hour at RT. The phage library was provided as a mixture of 10 different libraries, with 100μl from each one. Following, the blocking of the immunotube, the blocked phage library was added to the immunotube (approximately 2ml) and placed on a rolling mix shaker for 1 hour at RT. In round 1 panning, the immunotube was washed 5× with 0.1% Tween-20 PBS and 2x PBS to remove the non-binding phage from the tube. Bound phage was eluted by adding 500μl of 0.1M HCl (Sigma) to the dried immunotube for 10 minutes. The acid was removed from the immunotube and placed into 500μl Tris 1M buffer (pH7.4, Sigma) to neutralise phage suspension. Eluted phage was added to a flask of TG-1 stain *E.coli* culture, in log phage, for infection at 37°C standing for 1 hour. Infection of phage can occur better in static conditions. Following 1 hour incubation, the bacterial culture was

cultured on 2TY agar plates with 1% Glucose and 100μg/ml Carbenicillin (Novagen) at 30°C overnight. Carbenicillin resistance is provided by the phage particles that have infected the TG-1 bacteria.

The rescue of phage for round 2 panning involved collecting all bacterial colonies from agar plates and centrifuging 200 $\times g$ for 15 minutes. The pellet of cells was added to 2Ty conditioned media (1% Glucose and 100μg/ml Carbenicillin). Once at log phage, (optical density of 0.4-0.8), the culture was infected with helper phage with a multiplicity of infection of 20. Culture was left to stand for 1 hour at 37°C. Culture was centrifuged and resuspended in 2TY media with 100μg/ml carbenicillin and 50μg/ml kanamycin and incubated to grow overnight at 30°C at 250rpm. Phage is naturally secreted by the TG-1 *E.coli* into the supernatant overnight.

The bacterial culture was centrifuged at 200$\times g$ for 10 minutes. The supernatant was collected and centrifuged at 7700$\times g$ for 20 minutes. The supernatant was collected, added to a polyethylene glycol (PEG) solution (2.5M NaCl, 20% PEG) in a 1:5 dilution and incubated on ice for 1 hour. The PEG solution forces the phage out of solution to allow purification. Solution was centrifuged at 200$\times g$ for 10 minutes and the pellet was resuspended in 5ml of PBS. This solution contained the phage particles selected for round 1 panning. Using this solution of round 1 selected phage clones, the panning process was repeat twice more. In the following rounds, the washing step was increased to 15$\times$ washes with with 0.1% Tween20 PBS and 2x PBS in order to be more stringent and wash off weaker phage binders to the antigen. Round 2 and 3 95 bacterial colonies were picked and grown as individual cultures. The monoclonal phage was purified from them following the helper phage rescue. The monoclonal phage isolated from the individual bacterial colonies were tested in a Chemerin or a C17 peptide binding ELISA to test their binding specificity.

2.2.1.2 Panning against C23 peptide

The panning against C23 peptide was carried out as described above with a few variations. The biotinylated peptide was immobalised onto a nunc-96 well plate at a concentration of 10μg/ml via high affinity binding with streptavidin (10μg/ml). The 96-well plate was used because the 10 phage libraries were kept separate; 5 κ libraries and 5 λ libraries. Due to the need for the streptavidin immobalisation, round 2 and 3 panning was carried out with neutravidin, which has the same high affinity binding with biotin and removes the potential streptavidin binding phages from the round 1. Round 3 phage output were tested in C23 peptide, C17 peptide and chemerin binding ELISA to test specificity of clones using streptavidin as a control.

2.2.1.3 Phage binding ELISA for chemerin and chemerin peptides

Using high-affinity binding nunc-96 well plates, chemerin (2μg/ml) and streptavidin (1μg/ml) are immobalised by overnight incubation at 4°C. Isolated monoclonal phage were blocked by 1 hour incubaion with 3% Milk powder at RT. Following 3%BSA block for the 96 well plates, C23 or C17 peptide (1μg/ml) were incubated in the streptavidin plates for 30 minutes at RT. Plates were then washed 5× 0.1% Tween-20 PBS, then incubated with the blocked monoclonal phage for 1 hour at RT. Plates were washed and then incubated with a peroxidase (HRP)-conjugated anti-M13 phage particle antibody (GE Life technologies) at a 1:5000 dilution for 1 hour at RT. Following a final wash step, 3,5 Tetramethylbenzidine (TMB) substrate (Sigma) was used to reveal the assay using an absorbance plate reader at 490/630nm.

2.2.1.4 Mini-prep and Sequencing

In order to sequence phage plasmids to assess the antibody sequences, the monoclonal phage colonies are grown overnight. The DNA from the bacterial cultures is isolated using QIAprep spin miniprep kit. This method is based on an alkaline lysis step of bacterial cells followed by DNA absorption into silica in the presence of high salt and eluting the DNA plasmid. The procedure was carried out following the manufacturer's instructions. Sequencing was then carried out using the sanger sequencing method, which entails the use of flanking primers external to the scFv genes on the DNA phage plasmid isolated from mini-preps. Primers were designed in-house UCB, so they can not b disclosed. The sequences were analysed using AlignX software.

2.2.2 Cloning scFv genes onto mouse Fc vector

The transcriptionally active polymerase chain reaction (TAP) method used for the construction of a human IgG format of clones cannot be disclosed due to it being intellectual property of UCB Pharma. The scFv genes were cloned onto a mouse Fc vector (UCB) in order to take forward for functional analysis.

The scFv DNA associated on the phage vector was amplified by the PCR protocol for selected clones.

PCR recipe: 5μl Buffer, 3μl $MgSO_4$, 5μl dNTPs, 5μl of Forward and Reverse phage vector primers (UCB), 1μl of template DNA and 1μ KOD Hot start DNA polymerase.

PCR conditions: 98°C for 1 min, 98°C for 30 seconds, then 25 cycles of 55°C for 30 seconds, 72°C for 30 seconds, followed by 72°C for 1 min and 4°C infinite hold.

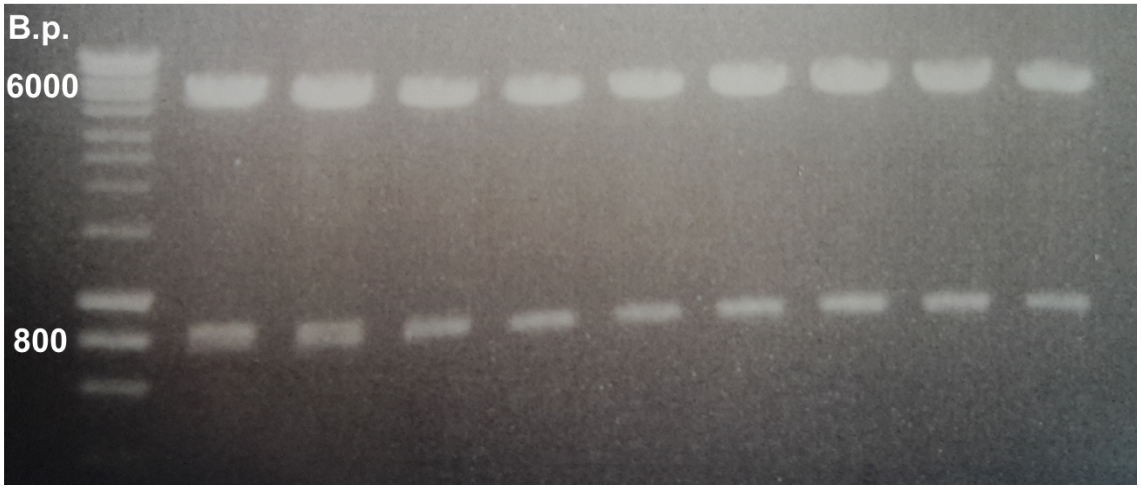


Figure 2.2: Digest products of scFv-Fc plasmids contain scFv and mouse Fc vector. 1.5% agarose gel with digest products of scFv-Fc plasmids, contain scFv at 850 base pairs and Fc vector at 6000 base pairs.

The scFv DNA PCR products were run through a PCR purification column, QIAqick PCR purification kit (Qiagen). The scFv genes were cut from phage vector by restriction endonucleases NcoI and NotI using Buffer H (New England Biolabs) from a 2 hour digest at 37°C. The digest products were run on a 1.5% agarose gel for 43 min at 90V, the scFv band was cut out and extracted from the gel by QIAEX II Gel Extraction kit (Qiagen). Ran another gel to determine quantity of DNA; approximately 20ng DNA in 5μl of a sample eluted in 22μl.

The extracted scFv genes were then ligated onto a mouse Fc vector (UCB) using a ratio of 3:1 due to the smaller molecular size of the scFv genes. Ligation was completed with T4 ligase buffer and T4 ligase (New England Biolabs) at 4°C overnight.

The ligation products were used to transform XL1 Blue *E.coli* strain (Stratagene, US) with the clones scFv Fc vectors by heat shock method at 42°C for 45 second and SOC media (Sigma) treatment. Bacterial were cultured on 50μg/ml kanamycin enriched agar overnight 37°C. Individual colonies were picked out and cultured in LB Broth enriched with kanamycin. The plasmids were purified from QIAgen plasmid Giga Kit (Qiagen) according to manufacturer's instructions. The plsamids were sequenced to confirm the scFv clones were consistent prior to construct reformatting and a digest was done to confirm the existance of both scFv genes and Fc vector (Figure 2.2).

Recipe for agarose gel: 0.7g Ultra pure agarose, 70 ml TAE buffer, 7μl Ethidium Bromide

2.2.3 Transfections of Freestyle^{TM} 293 cells

The constructs were transfected into Freestyle^{TM} 293 expression cell system (ThermoFisher scientific) following the manufacturer's instructions. Briefly, Freestyle^{TM} 293-F are a suspension cell culture used for generating large amounts of mammalian recombinant proteins. Optimal cell density for transfection is 1×10^6 cells/ml in 30 ml of Freestyle^{TM} 293 Expression medium within a 125ml polycarbonate vent-cap Erlenmeyer shaker flask. I used 35μg of scFv plasmids with 70μl of Lipofectamine 2000 (a ratio of 1:2) and incubated for 30 min prior to adding it to the cell culture flask. The culture was incubated for 4-6 days in a 125rpm shaker incubator at 8% CO_2 and 37°C.

2.2.4 Antibody purification

Cell supernatants were collected and antibodies were purified using the rProtein A GraviTrap^{TM} of 10 pre-packed gravity-flow columns (GE Healthcare Life science) according to the manufacturer's instructions. Columns were equilibrated and then cell supernantants were added. Antibodies were bound to the Protein A resin in the columns. Following a couple of wash steps, the antibodies were eluted using an acid based elution buffer (0.1 M glycine-HCl, pH 2.7) into a basic solution (1M Tris-HCL, pH 9) for neutralisation. Solution was eluted in a volume of approximately 12ml. In order to concentrate the eluted antibody, I used Vivapsin 20 MWCO 10,000 or 50,000 spin columns (GE Healthcare Life science) that concentrate solutions and exchange buffer by membrane ultrafiltration. Solution is spun at 200×g for 15-20 min, then 15ml of PBS is added and spun down till it reaches 0.5ml-1ml final volume. The addition of PBS is repeated twice.

2.2.5 Quantification of eluted antibody and ligand binding ELISAs

Protein presence was assessed by ND-1000 spectrophotometer (Nanodrop, Thermo Scientific) on the Protein Abs setting and BCA assay kit (Thermo Scientific). An in-house enzyme-linked immunosorbent assay (ELISA) was developed to assess concentration of protein samples. Antibody samples and a serial dilution of mouse IgG were immobalised on high-binding plastic nunc-96 well plates overnight at 4 °C. Plate was blocked with 3% BSA PBS buffer for 1 hour at RT, washed 3× in 0.1% Tween20 PBS wash buffer and treated with anti-mouse antibody conjugated with a HRP (Biorad). Plates were washed and then revealed with TMB substrate (Figure 2.3a). Absorbance

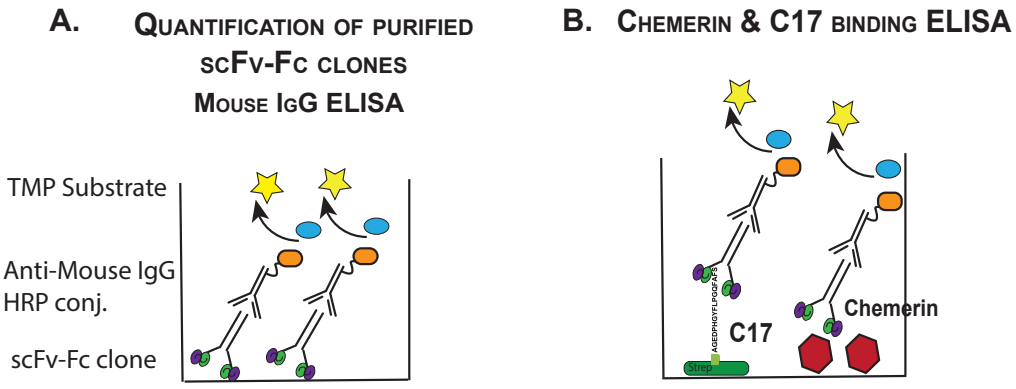


Figure 2.3: In-house developed enzyme-linked immunosorbent assays (ELISAs) for antibody quantification and ligand binding. A. A direct ELISA for the quantification of scFv-Fc clones by serial dilution of mouse IgG. **B.** A direct ELISA to assess ligand binding capacity of scFv-Fc clones to chemerin and C17 peptide.

measurements were taken using a PHERAstar microplate reader at 430/640nm and antibody samples by extracting the values against the ploted serial dilution of mouse IgG. The ligand binding capacity of the purified antibodies was assessed using a chemerin and C17 peptide in-house developed ELISA (Figure 2.3b). Strepavidin (1μg/ml) and chemerin (2nM) were incubated in 96 well high-binding plastic plates. Following blocking with 1%BSA, the steptavidin coated plates were incubated with biotinylated C17 peptide (27nM) for 30 minutes. Then the scFv clones were incubated with serial diluted clones (top concentration 50μg/ml) for 1 hour at RT. Then followed the procedure described above and in Figure 2.3 to reveal the scFv-Fc clones binding to the ligands.

2.2.6 Surface plasmon resonance

Surface plasmon resonance experiments were performed using Biacore 3000 and T200 instrument. Immobalisation of peptides and proteins to the CM5 sensor chip, involved the activation of carboxymethyl groups on the dextran-coated chip by reaction with N-hydroxysuccinimide, followed by covalent bonding of the ligands to the chip surface via amide linkages and blockage of excess activated carboxyls with ethanolamine. The HBS-EP buffer was used as running buffer and analyte-binding buffer. In the Biacore 3000 and T200, C17 and C23 peptides (33nM) were immobalised on the chip by binding to covalently bound streptavidin (1μg/ml; 19nM) to sensor chip flow cells. Chemerin (62.5nM) was immobalised by covalent bonding to flow cell on chip. The human IgG and the scFv-Fc clones were flown over the top of the ligands at increasing concentrations or one concentration. The reverse format was also attempted, where

scFv-Fc clones were immobalised on the sensor chip and the ligands were flown over the top. Dissociation values (Kd) were calculated by using a two-site binding analysis from plotting the dissociation relative unit from each antibody concentration. A two-site binding analysis assumes that there is association of one or two binding sites on a molecules; i.e. the two scFv fragments on a Fc portion.

Using a mouse antibody capture kit (GE life technologies) an anti-mouse antibody (30μg/ml) was covalently bound to the flow cells. Then the scFv-Fc clones and a mouse IgG (30mug/ml) were flown over the each flow and were captured on the surface. One concentration of the ligands were flown over each flow cells; chemerin (2.0μM), non-biotinylated C17 and C23 (30μM). There was limited success with this method to confirm the Kd values from the previous.

2.2.7 DiscoverX β-arrestin recruitment assay

Recruitment of β-arrestin to murine CMKLR1(ChemR23) was measured using the Discoverx Path-Hunter eXpress β-Arrestin GPCR Assay following the manufacturers protocol. Briefly, CHO-K1 cells stably expressing murine CMKLR1 (ChemR23) were seeded into 1/2 area 96 well plates (5,000 cells/well) and incubated at 37°C, 5% CO_2 for 48 hours. Chemerin (2nM) or C17 peptide (27nM) were treated with serial diluted anti-chemerin polyclonal antibody (top conc: 10mug/ml) (R& D) and scFv-Fc clones (top conc: 50μg/ml) in a sealed polypropylene dilution plate at 37°C for 1 hour. Cells were then stimulated with vehicle (Cell assay reagent), chemerin and chemerin peptides or the antibody treated solutions at the indicated concentration for 90 min at 37°C, 5% CO_2. Cell lysis and detection of total recruited β-arrestin was determined following the manufacturers protocol. Luminescence measurements were taken using a PHERAstar microplate reader.

2.2.8 C23 cleavage assay

The C23 peptide is a prochemerin C-terminal peptide, which contains the active C-terminus sequence of chemerin and the 6 a.a. inhibitory sequence of prochemerin. Multiple serine proteases are able to cleave the C-terminus of prochemerin to generate active chemerin. Some of the clones generated from the phage panning were able to bind to the 6 a.a. sequence, which led to the investigation into whether they could sterically hinder the cleavage activity of elastase and cathepsin G at the C-terminus of this peptide. A N-terminal biotinylated C23 peptide with a FLAG-tagged C-terminus was used for this assay. The FLAG tagged peptide (150ng/ml) was incubated in

LoBind eppendorf tubes (Sigma) in HBSS buffer with scFv-Fc clones or mouse IgG (10μg/ml or otherwise indicated) for 1 hour at 37°C. Human neutrophil elastase (15mU/ml) or cathepsin G (3mU/ml) were added to the solution for 1 hour at 37°C. This solution was then added to a BSA-blocked streptavidin coated 96-well plate for immobalisation of the biotinylated C23 peptide. Plate was washed 4× with 0.1% Tween-20 PBS solution. Wells were treated with a rabbit anti-FLAG antibody (1:5000 dilution) for 1 hour at RT. Following a wash step, a secondary HRP-conjugated anti-rabbit antibody (Biorad) was incubated for 1 hour at RT. Plate was washed and then TMB substrate, 1-StepTM Ultra TMB-ELISA, was added to reveal the presence of a FLAG signal. Absorbance measurements were taken using a PHERAstar microplate reader. A schematic representation of assay can be seen in Chapter 3, Figure 3.16.

2.2.9 Western blot

Peritoneal samples were concentration by Viva-flow columns (MW 3,000; GE life sciences). Samples (30 μg total protein) were separated using a 15% SDS-PAGE gel (120 V for 90 minutes) and transferred (200 mA for 110 minutes) onto Hybond ECL nitrocellulose (GE healthcare, Buckinghamshire, UK). Membranes were blocked with 5% Milk powder in Tris-buffered saline supplemented with 0.1% Tween20 (TBS-T) for 1 hour at RT. After blocking, membranes were incubated with rat anti-chemerin monoclonal (R& D) or A6 and B6 scFv-Fc in-house clones (both 1:500) diluted in 3% Milk/TBS-T for 2 hours at RT or overnight at 4°C. Membranes were then incubated with a HRP-conjugated anti-rat secondary antibody or anti-mouse secondary (1:10,000) for 1 hour at RT. Protein bands were visualised by incubating the membranes for 5 min with Millipore Immobilon Western Chemiluminescent HRP ECL subsequent exposure to x-ray film over a range of exposure times. To confirm equal protein loading between samples, bound antibodies were removed by incubating the nitrocellulose membranes in stripping buffer (60 mM Tris-HCl pH 6.8, 2% SDS, 0.8% β-mercaptoethanol) for 30 min at 50°C. Membranes were then blocked with 5% Milk in TBS-T for 1 hour at RT and then incubated with mouse anti-actin (1:1000) diluted in 5% Milk/TBS-T for 1 hour. Protein detection was then conducted as detailed above.

2.2.10 *In vivo* model of peritonitis

10 mg of Zymosan A (Sigma-Aldrich) was weighed out and dissolved in 50 ml of sterile PBS. This suspension or 4% Thioglycollate broth (Sigma-Aldrich) was vortexed

thoroughly and the Falcon tube was inverted repeatedly between each injection to ensure a uniform suspension was injected. 0.5 ml of inflammatory stimuli (100μg zymosan) was injected intraperitoneally (i.p.). Recombinant murine chemerin (0.5 or 4μg) or goat anti-chemerin polyclonal antibody or goat IgG control (100ng) (R& D) were diluted to the required concentrations with PBS. Pre-treatments of these reagents were administered 1 hour (or otherwise indicated) by i.p. injection using a 0.5 ml insulin syringe (BD). Animals were administered the inflammatory stimuli for a duration of 1-16 hours. Mice were sacrificed at indicated time, after inflammatory stimuli injection, by CO_2 euthanasia followed by cervical dislocation for confirmation. A small incision was made along the abdomen and the skin was pulled back to expose the peritoneum. Ice cold PBS supplemented with 2mM EDTA (5 ml) was injected into the peritoneal cavity using a 5 ml syringe and a 25G needle. The cavity was massaged firmly but gently with the side of a 19G needle. The same needle attached to a 5 ml syringe was carefully inserted into the abdomen avoiding internal organs and blood vessels. The contents were gently mixed and the peritoneal exudate fluid was slowly removed and lavage fluid was immediately transferred to 15 ml falcon tubes on ice.

Blood was collected by opening the peritoneum, moving the small and large intestine to one side to reveal the posterior vena cava. Blood was collected by EDTA coated 1ml syringes with 23G needles from the posterior vena cava vein. The blood collected was placed into an EDTA coated tube, mixed vigorously and placed on ice. Spleens were also collected into ice-cold PBS and stored on ice.

2.2.11 Flow cytometry

Cells (5 x 10^5) or 300 μl of peritoneal lavage fluid was placed into polypropylene tubes and pelleted by centrifugation at 200 xg for 5 mins at 4C. These were then resuspended in 50 μl of FACS buffer (PBS containing 2% FCS, 25 mM HEPES and 5 mM EDTA) supplemented with mouse IgG (116 mug/ml) and mouse SeroBlock FcR (6.6 μg/ml AbD Serotec, Oxford, UK) and left on ice for 10 min to allow Fc receptor blocking. Specific staining was conducted by the addition of 50 μl antibody cocktail in FACS buffer for 30 minutes on ice. The antibodies used throughout this thesis are listed in Table 2.1, and positive staining was determined using the appropriate isotype controls. Cells were then washed with 1 ml FACS buffer before being resuspended in 1% PFA fixative buffer and analysed using a Dako Cyan ADP flow cytometer (Beckman Coulter Ltd, High Wycombe, UK) and FlowJo software (V10, Tree Star, Ashland, USA).

For whole blood staining, 50 μl of blood was placed into polypropylene tubes containing 50 μl blocking solution as detailed above, and left on ice for 10 min. Antibody staining was then conducted by the addition of 50 μl antibody cocktail and incubation for 30 minutes on ice. Next 3 ml of 1x BD FACS^{TM} lysing solution (BD Biosciences) was added to each sample and tubes left for 15 min at RT to allow red blood cell lysis. Cells were then pelleted by centrifugation at 200$\times g$ for 5 min, washed twice with 1 ml FACS buffer and then resuspended in 1% PFA for analysis.

Lung and livers were dissected in to smaller pieces using a scalpel. They were places in 1% BSA PBS buffer containing 1mg/ml collagenase D (Roche) for 1 hour at 37°C and 5% CO_2. Tissue homogenate was then passed through 70μm cell strainer. Similarly, spleens were dissected in half and mashed through a 70μm cell strainer, using 1% BSA PBS solution to filter through the cell content. Cells from the tissues are spun down at 200 μg for 5 min, resuspended in in 2mls 1x BD Pharmalyse lysis buffer (BD Biosciences) and incubated at RT in the dark for 15 mins. Cells were spund down and resuspended in 1 ml of FACS buffer and placed 100μl in to polypropylene tube spin down and resuspended in 50μl of blocking solution. Then followed the normal FACS protocol described above.

2.2.12 Cell counting using flow cytometry

For peritoneal elicited cells, 50 μl of CountBright^{TM} Absolute Counting Beads (ThermoFisher Scientific, Paisley, UK) were added to 300 μl of lavage fluid. Samples were analysed by gating separately on beads (which have high side scatter) and cells in the flow cytometry software, and obtaining the number of events in each gate. For other samples, including blood, spleen, liver and lung, cells were resuspended in 300μl of fixative buffer in the final resuspension step of the flow cytometry protocol then 50μ of counting beads are added. The number of cells per ml of sample was then calculated using the following equation:

$$\text{Cells/ml} = \frac{\text{Cell events}}{\text{Bead events}} \times \frac{\text{Bead concentration}}{\text{Volume in sample}} \times 1000.$$

For cells recruited in the peritonitis models, the resulting number was multiplied by 5 to calculate the absolute number of cells recruited to the cavity, as this factor represents the volume (ml) of lavage fluid used to collect the cells.

2.2.13 ELISA

Sandwich ELISAs for CCL2, CXCL1, IL-6 and chemerin (R& D systems) were performed according to manufacturers guidelines. 96 well high binding plates (Nunc)

were coated with 100 μl capture antibody diluted to required working concentration in PBS overnight at RT. The next day, plates were washed 3 times with 300 μl ELISA wash buffer per well (PBS supplemented with 0.05% Tween). Non-specific binding was blocked with 300 μl 1% BSA per well for a minimum of 1 hour. During this blocking step, 7 point standard curves were prepared in Eppendorf tubes in 1% BSA (in PBS) and samples were diluted to ensure they were within the linear part of the standard curve. After blocking, plates were washed 3 times, and 100 μl of standards or samples were added to the plate and incubated for 2 hours at room temperature. Plates were washed again and 100 μl biotinylated detection antibody diluted to working concentration (as per manufacturer's instructions) in 1% BSA (in PBS) was added per well and incubated for 2 hours. Plates were washed 3 times and 100 μl of Streptavidin-HRP diluted 1:40 in 1% BSA (in PBS) was added per well for 20 minutes. Plates were washed 3 times and 50 μl of one-step Ultra TMB (Thermo Fisher) was added. The reaction was stopped with 50 μl 3M H_2SO_4 20 minutes later or when the standard curve had changed colour. Plates were read at 450 nm and at 630 nm using a PHERAstar FS plate reader (BMG Labtech). Absorbance at 630 nm was subtracted to correct for optical imperfections in the plate. Unknown values were interpolated using a 4-point linear regression analysis in Graphpad Prism 7.

2.2.14 Bio-gel elicited peritoneal cells

Male C57BL/6J and 129S6SvEv mice or CCRL2$^{-/-}$ and ChemR23$^{-/-}$ mice were injected intraperitoneally with 1 ml of sterile 2% Bio-gel polyacrylamide beads (P100 fine, 45-90 μM, Sigma) suspended in PBS. After four days, mice were sacrificed and the elicited cells collected by peritoneal lavage with 10 ml ice cold PBS containing 2 mM EDTA. The cellular composition of this population was determined by flow cytometry as described in Figure 4.5.

2.2.15 Murine bone marrow derived macrophages

Bone marrow macrophages (BMDM) were generated as previously described by Marim *et al.* [221]. Briefly, fresh bone marrow cells from tibiae and femurs of C57BL/6J or otherwise stated mice (8-12 weeks) were flushed out and filtered through 70μ cell strainer, and spun at 200$\times g$ in Thermo Scientific Sorvall ST16R centrifuge. Cells were resuspended and cultured in DMEM media supplemented with 10% heat inactivated foetal bovine serum (FBS), 10% L929 cell-conditioned media as a source of

macrophage colony stimulating factor, 100 U/ml penicillin, and 100 μg/ml streptomycin for 7 days. 4x10^6 bone marrow cells were seeded into 10ml of medium in 100mm petri dishes (Sterilin, Abergoed UK.) and on day 3 an additional 5ml of medium was added. Cells were harvested by lightly scraping to lift cells off surface.

Cell were seeded into 6 well plates at a concentration of 1x10^6/ml. They were then exposed to TLR ligands and cytokines for 16 hours in a 37°C 5% CO^2 incubator. The TLR ligands and cytokines were added to cells at a final concentration of: LPS 100μg/ml, IFNγ 20ng/ml, Poly I:C 10μg/ml, zymosan 10μg/ml, flagellin 500ng/ml, IL-4 20ng/ml and IL-13 20ng/ml.

2.2.16 Murine bone marrow derived dendritic cells

Bone marrow dendrtic cells (BMDC) were generated as previously described [222]. Briefly, fresh bone marrow cells from tibiae and femurs of C57BL/6J mice (8-12 weeks) were flushed out into RPMI media (Sigma). Cells were filtered through 70μ cell strainer, and spun at 200$\times g$. Cells were resuspended in 2mls of Red Blood cell lysis buffer (Sigma) for 2-3 min at RT followed by 10ml of RPMI. Cells were pelleted and cultured in RPMI media supplemented with 10% FBS, 3% X63-GM-CSF cell-conditioned media as a source of granulocyte colony stimulating factor, 100 U/ml penicillin, and 100 μg/ml streptomycin, 1%L-glutamine, 1% non-essential amini acids and 1% sodium pyruvate for 7 days. Bone marrow cells were seeded into 12ml of medium in two 90mm tissue culture plates (Corning UK.) On day 3 and 6, an additional 5ml of medium was added. Cells were harvested by lightly scraping to lift cells off surface. Maturation of BMDC was achieved by adding 1μg/ml of LPS to culture overnight on day 6.

2.2.17 Bone marrow neutrophil isolation

Isolation of murine bone marrow neutrophils was conducted as previously described [223]. Briefly, the femur and tibia were isolated from male C57BL/6J mice with the surrounding tissue carefully removed. The bones were then flushed through with RPMI containing 10% FCS and 2 mM EDTA. The bone marrow cells were then gently resuspended using a pasteur pipette, passed through a 70 μm cell strainer to remove any remaining tissue or cell clumps and pelleted by centrifugation at 250 xg for 5 min at 4C. Red blood cells were then lysed by hypotonic lysis (20 ml 0.2% NaCl followed by 20 ml 1.6% NaCl) and the remaining cells pelleted by centrifugation at 250$\times g$ for 5 min at 4C. After washing with RPMI containing 10% FCS and 2 mM

EDTA, cells were resuspended in 1 ml PBS and layered onto a Histopaque gradient consisting of Histopaque 1077 (3ml) on top of Histopaque 1119 (3 ml) and centrifuged at 400×g for 30 min at RT. Neutrophils were then collected from the interface of the Histopaque layers using a pasteur pipette, pelleted by centrifugation at 250×g for 5 min at 4°C and then resuspended in 1 ml chemotaxis buffer and counted. Cell density was then adjusted to 5 x 10^5 cells/sample for flow cytometry. Neutrophil purity was also determined by flow cytometry (Figure 4.3).

2.2.18 Human blood monocyte isolation

Blood was collected into EDTA coated blood tubes. Peripheral blood mononuclear cells (PBMCs) were isolated by density gradient centrifugation. Monocytes were isolated by depletion of non-monocytes by negative selection using Monocyte Isolation kit II (MACS, Miltenyi Biotec, UK) following the manufacturer's instructions. Non-monocytes are indirectly magnetically labeled and anti-biotin monoclonal antibodies conjugated to MIcroBeads as secondary labeling reagent. The magnetic labeled non-monocytes are depleted by retaining them in them in the MACS column by the magnetic field from the MACS separator, and thus allowing the unlabeled monocytes to pass through.

2.2.19 ACEA xCELLigence real-time chemotaxis assay

Real-time chemotaxis analysis was performed using the ACEA RTCA-DP intrument as previously described by Iqbal *et al.* [224]. Briefly, vehicle, recombinant C5a (10nM), chemerin (5-10nM) and C17 peptide(20nM), or chemerin (5nM) pre-treated with anti-chemerin polyclonal (R& D) or scFv-Fc in-house antibody clones (both at 10μg/ml) for 1 hour at 37°C , were make up in chemotaxis buffer (RPMI 1640 supplemented with 0.5% BSA and 25mM HEPES) at the desired concentration and added 160μl to the lower chamber of a CIM-16 plate. The upper chamber was subsequently attached and 50μl of pre-warmed chemotaxis buffer was added to the upper chamber wells for equilibration and a background reading on the RTCA-DP system. Bio-gel elicted peritoneal cells or BMDM (50μl - 4×10^5 cells/well) were added to the upper well chamber. The plate was then placed into the RTCA-DP system.

Cell Index (CI) measurements were recorded every 5 seconds over 3-4 hours. CI is an arbitrary measure of cell adherence to the lower chamber of the transwell plate. Cell adherence causes electric current impedance thus, inversely correlating to the CI. CI is the electrical resistance at a given time point taken away from the background

CI resistance taken at time point zero. Chemotaxis traces are displayed as raw Delta CI where wells are normalised to 1 at the start of the reading or as maximum CI minus the minumum CI signal pooled from individual experiments.

2.2.20 ACEA 96 well ECIS Electrical impedance sensing assay

The ACEA Biosciences RTCA-SP intrument was used to analyse differences in cell adhesion and spreading of BMDC in response to GPCR activating ligands. Day 7 immature and mature BMDCs were resuspended in chemotaxis buffer at a cell density of 1×10^6 cells/ml. 50μl of chemotaxis buffer was added to 96 well E-plate and a background measurement was taken. 50μl of cells were then seeded into wells (50,000 cells/well) and cells were left at 37°C, 5%CO_2 for 2-3 hours to adhere until the CI had reached a stable plateau. Cells were then stimulated with vehicle, recombinant C5a and chemerin (10nM) (R& D), at which time the CI measurements are recorded every 5 seconds for 1-2 hours after addition of the agonists. Data is displayed as Delta CI, as traces are normalised to 1 at the point of addition. The Maximum and minimum CI are subtracted to obtain the Delta CI (Max-Min) response.

2.2.21 RNA isolation, reverse transcription and real-time qPCR

Total RNA was extracted using RNeasy Mini kit (Qiagen, UK) as instructed by the manufacturer. Briefly, cell or tissue were lysed by addition of 500μl RLT buffer and manual disruption. Total RNA extracted from lysates by filtering through silica-membrane RNeasy spin columns. The eluted RNA concentration and purity of samples was determined using ND-1000 spectrophotometer (Nanodrop, Thermo Scientific) at 260/280 nm and 260/230 nm. cDNA was synthesized from 500-800ng of total RNA using QuantiTect Reverse Transcription kit (Qiagen, UK) following the manufacturers instructions. cDNA was amplified for 15 minutes at 42°C and then 3 minutes at 95°C. Real time quantitative PCR was performed using SYBR Select Master Mix (Applied Biosystems, Life technologies) in the Step One Plus Real time PCR System (Applied Biosystems). Chemerin and chemerin receptor primers were from QuantiTect Primer Assay (Qiagen), except for β-actin primers (5→ 3): Actin Fwd CCAACAGCAGACTTCCAGGATT, Actin Rev CTG- GCAAGAAGGAGTG-GTAACTG. The thermal profile included an initiation step for 2 minutes at 50°C and 95°C followed by 40x cycles of 15 seconds at 95°C and 1 minute at 60°C. Cycle

threshold (Ct) values were determined by the StepOne software v2.3 and the mRNA content of samples was inferred by normalising to the housekeeping β-actin or the average of 3 housekeeping genes: actin, 18S and GAPDH genes. Relative expression results were plotted as mRNA expression over housekeeping genes ($2\wedge(-\Delta Ct)$). Sample that were compared to a basal or saline treatment were normalised to $\log_{10}$(N-fold). The differences between the linear and log scale analysis is illustrated in Figure 2.4. Samples that were not analysed by N-fold (i.e. Figure 2.4 a-b) were maintained in a linear scale due to the exaggerated negative log values generated with low cycle values (i.e. Figure 2.4 c-d).

2.2.22 Behaviour assays

All the behaviour tests were captured on video and were analyse later by 3 independent investigators blinded to the genotype of the mouse. During the testing, all efforts were made to minimise mouse discomfort. Mice were brought to testing room at least 30 minutes prior to starting the test session to allow for habituation. Unless otherwise specified, standard light (approximately 50 lux) and quiet conditions were maintained throughout the experiments. For more details on the three individual behavioural assays performed refer to Chapter 6.

2.2.23 Tissue sectioning

A group of 8-12 week old WT and *CCRL2*$^{-/-}$ mice were euthanised by intraperitoneal injection of a barbiturate. Tissues were perfused and fixed with 4% paraformaldehyde and brain tissues were collected and stored in fixative solution at least 10× the volume of the tissue overnight at 4°C with occasionally swirling. Brain tissues were washed with PBS and the stored in 15% then 30% sucrose solution for 2-3 days in 4°C for cryoprotection until tissues sink. Tissue is then embeded in Tissue-Tek OCT (optimum cutting temperature) solution (VWR, UK) and then stored at -80°C until sectioning. Tissues were cryosectioned using Leica 3050s Cryostat at -18°C at 10μm. Sectioned tissues were placed onto gelatinised slides, dried overnight at RT and stored in -20°C.

2.2.24 Immunohistochemistry staining

Slides were dried in a 37°C over for 15 min, then antigen retrieval was carried out by incubating slides in a coplin jar of Citrate buffer for 1 min in the microwave.

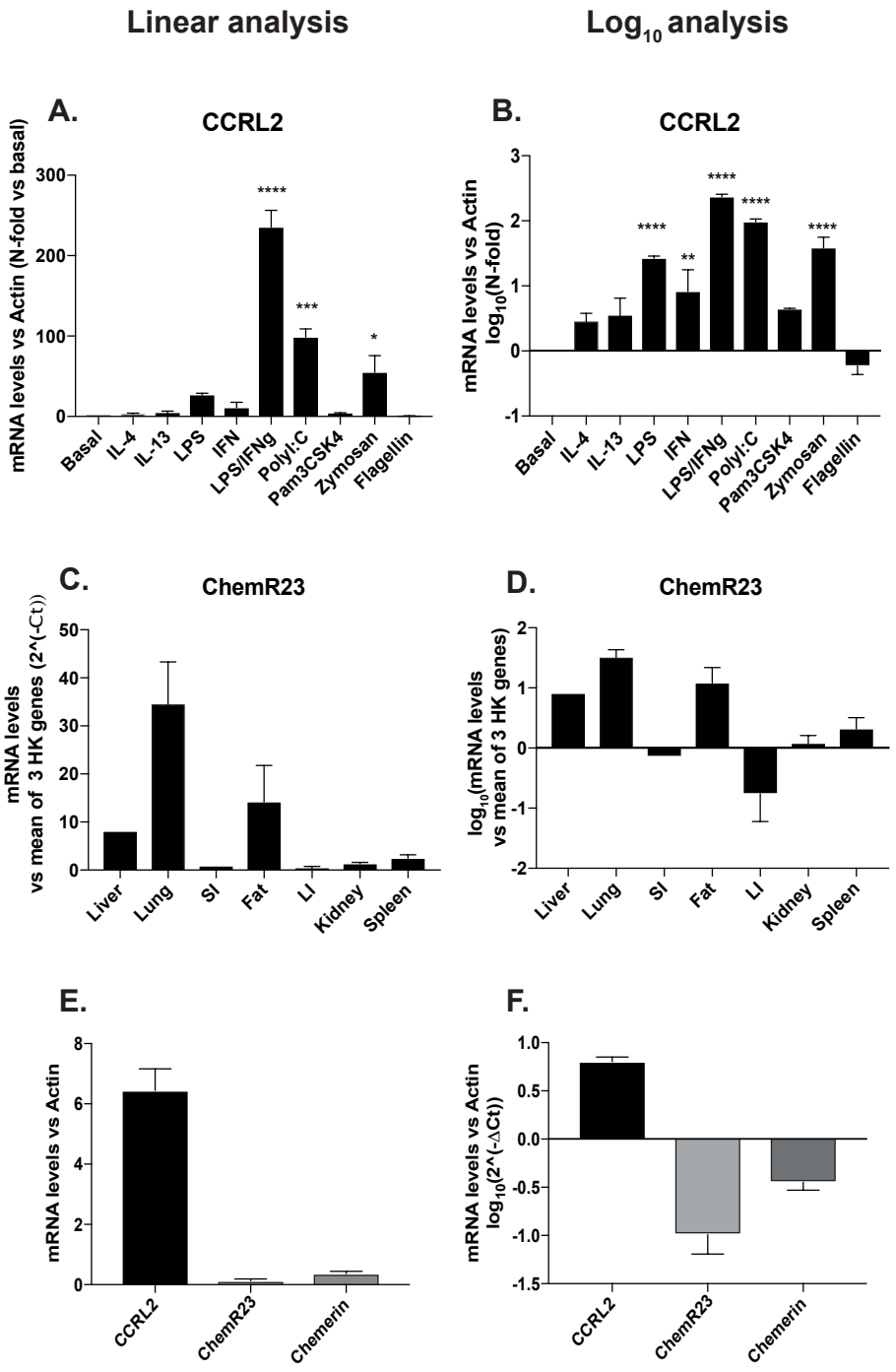


Figure 2.4: Comparison between the linear vs $\log_{10}$ analysis of RT-PCR data. In the left column is the relative arbitrary units of mRNA levels in linear scale and on the right are these values plotted on Log_{10} scale. **A-B.** mRNA expression of CCRL2 versus β-actin in bone marrow derived macrophages treated with various TLR and cytokine ligands are all compared to the basal sample by N-fold comparison. **C-D.** mRNA expression of ChemR23 versus the mean of 3 housekeeping genes in various tissues. **E-F.** mRNA expression of CCRL2, ChemR23, and chemerin versus β-actin in bone marrow isolated neutrophils.

Slides were washed by PBS to remove the OCT. Slides are quenched to block endogenous peroxidase activity with 1% H_2O_2 in methanol for 10 min (300ml methanol + 3ml H_2O_2 from 30% stock). Slides washed with PBS. Slides were put on sequenza clips and washed 2× for 5 min with PBS. Slides were blocked for non-specific protein binding with 10% serum (from the secondary antibody i.e. goat serum) in 0.1% Tween20 PBS for 1 hour at RT. Slides in the sequenza clips are covered with a volume of 120μl/sequenza clip. Sections were incubated with either primary (rabbit) antibody, anti-NeuN antibody ([EPR12763], ab177487, Abcam, UK) or anti-Iba1 antibody ([EPR16588], ab178846, Abcam, UK), at 1:1000 dilution in 1% serum overnight at 4^{o}C in the sequenza clips. Sections were washed 3× in PBS and then incubated with secondary biotinylated goat anti-rabbit (Vector laboratories) diluted 1:200 in 1% goat serum PBS for 2 hours at RT. Vectastain^R ABC-HRP kit (Peroxidase, Standard) (Vector Laboratories) was made up according to manufacturer's instructions, (mixing solution A 1:100 with solution B 1:100 in PBS) at least 30 min before use at RT. Sections were washed 3× for 5 min in PBS, and then incubated with ABC mixture for 1 hour at RT. Sections were washed in 2× in PBS for 5 min and removed from sequenza clips and racked into a solution of 0.1M phosphate buffer. Sections were incubated in 3,3'-Diaminobenzidine (DAB) peroxidase substrate staining kit (Vector Laboratories), then washed 0.1M phosphate buffer. Sections were counter stained by 5 min incubation in acidified water, then 10 min in Cresyl violet then dehydrated in increasing concentrations of alcohol (80%, 90%, 95%, 2× 100%). Sections were then cleared in xylene 2× 5 min and sections were mounted with DPX permanent mounting medium (remove bubbles). Slides were dried overnight and sections were quantified under bench-top Leica DME light microscope.

2.2.25 Data and statistical analysis

All data presented in this thesis were analysed using GraphPad Prism (Version 7, La Jolla, CA). All data are expressed as mean + or ± SEM, as detailed in each figure legend. The test used for each individual data set is specified in the corresponding figure legend. For comparisons between two groups only, a Students t-test was applied. For multiple comparisons with only a single variable, a one-way ANOVA with Dunnetts multiple comparisons correction was applied. The Dunnett's comparisons is the appropriate multiple comparisons test to apply for the comparison of every mean with a control mean, according to GraphPad statistics guidelines. For comparisons with two variables, a two-way ANOVA with Sidaks multiple comparisons correction was applied. A P value of <0.05 was taken to be statistically significant. According

to the guidelines of the GraphPad statistics guidelines, the Sidak method has a bit more power than the Bonferroni method. Furthermore, the Sidak method assumes that each comparison is independent of the others, however, if this assumption is independence cannot be supported, then the Bonferroni method is more applicable, which does not assume independence. In the data presented in this thesis, due to the independence of each individual mouse for comparisons of two variables the Sidak's multiple comparisons test was applied. Finally, to ensure the appropriate numbers of animals per study and in consideration of the 3Rs the use of power calculations was employed. Statistical power is used to calculate the minimum sample size required to reasonably detect an effect of a given size.

Chapter 3

Developing antibodies against chemerin using phage display technology

3.1 Introduction

Chemerin is a 16-18kDa protein with chemotactic and adipogenic properties. It is secreted as an 143 a.a. long inactive precursor called prochemerin$^{20\text{-}163}$. Prochemerin becomes an active signalling molecule, named chemerin$^{20\text{-}156}$, when it is cleaved at the C-terminus via various serine proteases. Prochemerin can be cleaved by many different proteases and thus, produces a variety of different isoforms with varying signalling potencies at its receptors. Additionally, chemerin is cleaved further, into shorter chemerin derived peptides, which can still display functional ability [175, 162, 153]. The various isoforms of chemerin have been identified in *in vitro* and *in vivo* tissue samples using mainly chromatography and mass spectrometry techniques. However, the detection of chemerin by current commercially available antibodies and ELISA kits does not discriminate between the various isoforms of chemerin. There have been a few groups that have developed in-house antibodies against chemerin isoforms via animal immunisation [158, 225], but these are not commercial available. The conflicting literature about the role of chemerin during inflammation, could be due to the generation of various isoforms causing alternative effects. The aim of this chapter was to develop our own in-house anti-chemerin antibodies to detect murine prochemerin and chemerin C-terminus.

3.1.1 Chemerin and its various isoforms

Chemerin is translated as an inactive pre-protein, pre-prochemerin$^{1\text{-}163}$, this undergoes N-terminal cleavage before its secreted as an inactive precursor, prochemerin$^{20\text{-}163}$ [226]. Once secreted, prochemerin becomes active molecule, called chemerin, upon cleavage of the C-terminus end [157, 153]. Chemerin acts as a chemoattractant and an adipokine, by signalling via a G-protein coupled receptor GPCR, ChemR23 (CMKLR1)[153, 216]. Chemerin binds to another two GPCR receptors, GPR1 and CCRL2 [154, 155]. Hepatocytes and adipocytes have repeatedly been named the primary producers of chemerin however, there are various other tissues which express chemerin, these include ovaries, placenta, skin epidermis, large and small intesine, lymph nodes and lungs [216, 169, 227, 176].

Investigations into *in vitro* and *in vivo* samples have shown that the presence of different isoforms of human chemerin (hchemerin), exerting varying signalling potencies at the ChemR23 receptor, refer to Table 1.1. These isoforms are produced by various serine proteases from granulocytes, the coagulation and fibrinolytic cascades [153]. Generally *in vitro* studies have shown that human prochemerin$^{20\text{-}163}$ is cleaved into hchemerin$^{20\text{-}156 \text{ or } 157}$ by neutrophil elastase, cathepsin G, K and L, plasminogen [159, 158]. hChemerin$^{20\text{-}156}$ or ^{157} have the highest potency of the chemerin isoforms at the ChemR23 receptor [157, 228, 162]. Mast cell tryptase cleaves human prochemerin^{163} to hchemerin^{158} isoform which has a low potency at the ChemR23 receptor [159]. Further processing at the C-terminus of this isoform and of hprochemerin$^{20\text{-}163}$, by carboxypeptidase N or B produces hchemerin$^{20\text{-}156 \text{ or } 157}$ [157]. In addition to protease driven activation of chemerin, there are proteases which cause deactivation of the chemerin isoforms, including hchemerin^{155}. The proteases responsible for the deactivation include the cleavage by mast cell chymase, angiotensin converting enzyme as well as elastase [161, 229, 158]

Inflammatory exudates have been useful in revealing these various isoforms of chemerin. These have usually been detected using gel filtration chromatography, PAGE separation, and mass spectrometry techniques. The analytes detected include the hchemerin^{155} isoform present in serum[159] and the hchemerin^{157} isoform present in haemofiltrate and ovarian ascites [153]. Instead of using these techniques, Zhao *et al* developed their own in-house antibodies against isoforms of human chemerin. They used them to quantify the prevalent isoform of chemerin in various human samples. The prevelant isoform in plasma was the inactive hprochemerin^{163}. The hchemerin^{158} isoform was found to be most prevelant in the cerebrospinal fluids of cancer and non-cancer CNS diseased patients and in the synovial fluid of various

arthritic diseased patients[225]. They also reported the presence of the carboxypeptidase B and N in both cerebral and synovial fluid, which would allow the conversion of the hchemerin^{158} isoform into the active hchemerin^{157} isoform; that has a higher potency at the ChemR23 receptor. A comprehensive list of all the isoforms generated by different proteases can be seen in Table 1.1.

Synthetic peptides corresponding to the C-terminus of chemerin have been used to decipher the most relavent structure in chemerin to activate ChemR23 receptor. The C-terminal peptide C9$^{148\text{-}157}$ is able to activate the ChemR23 receptor *in vitro* in a low nanomolar range [153]. Another C-terminal peptide, murine C15$^{140\text{-}154}$, has been reported to induce anti-inflammatory effects in murine macrophages and in a murine model of zymosan-induced peritonitis [175]. These peptides have not been detected *in vivo* or *in vitro* cultures , however, there have not been any tools developed to directly detect them.

3.1.2 Phage Display Technology

Phage Display technology, first described by G. Smith in 1985, is a method for presenting polypeptides on the surface of filamentous bacterophages (phage) [230]. Due to the phage phenotype and genotype being physically linked, these phage particles are used as expression vectors which can rapidly and inexpesively be amplified by infecting bacterial cell cultures. Later, this technology became a platform for an *in vitro* antibody discovery method, where diverse libraries of antibodies are displayed on the surface of filamentous bacteriophage particles, with each antibody encoded and displayed on an indiviual phage. The antibodies are displayed in smaller formats in comparison to the normal IgG structure; these being the Fab antibody binding fragment, Fv fragment variable, and single chain variable fragments (scFv). A scFv contains a Variable Heavy chain (VH) connected by a linker to a Variable Light chain (VL) and is the most commonly used format for a phage display library [231].

3.1.2.1 Phage structure

The commonly used filamentous bacteriophage particles for this technology are *Escherichia coli* specific f1, fd and M13 phage. The peptides and antibodies can be displayed on the surface of the phage structural proteins, pIII and pVIII. pVIII is the major coat protein and occurs in nearly 3000 copies, therefore it is used to enhance detection signal of peptides. However, expressing peptides on pVIII prevents its functionality unless the peptides are 6-7 residues long and do not contain cysteine

a.a. [232, 233]. pIII is the minor coat protein, which has 3-5 copies on the surface of the particle, and it can support the expression of most larger proteins as a pIII fusion. The pIII loses its functionality by expressing the desired protein however, this is overcome by incubation with a helper phage during the amplification stage or by modification to the protein coat [233]. The phage particle contains the wild type genome of viron and a copy of a fusion gene occuring as an insert in phage genome or a phagemid; a vector containing a functional origin of replication for phage and its host antibiotic resistance. The helper phage will provide all structural proteins for the phage with the phagemid, but the helper phage has been engineered to contain an impaired origin of replication so that only the phage with the phagemid will replicate [231].

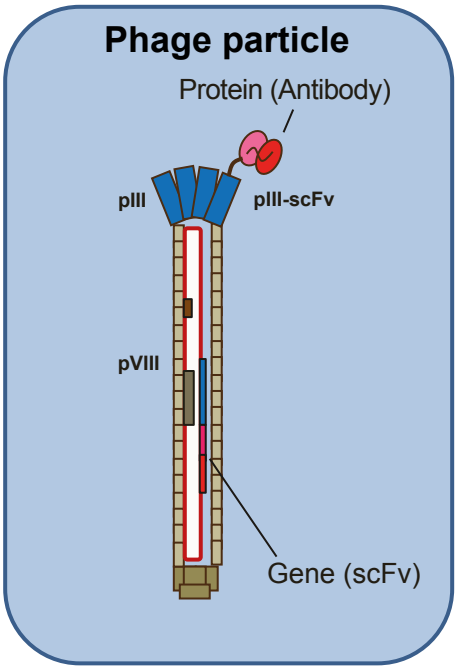


Figure 3.1: Schematic representation of a scFv expressing bateriophage particle. The gene of the single chain variable fragment (scFv) is in the phage genome. The scFv is being expressed on the surface of the pIII coat protein. Image obtained from phage display team in UCB.

3.1.2.2 Library Construction

Immune libraries are used to produce high quantity and high affinity antigen-specific antibodies to provide good analytical tools. The sources of V genes commonly used are the antibodies present in an immunised animal or the B cells present in the peripheral blood or spleen in humans. The advantage of these types of libraries is that the generated antibodies will have undergone affinity maturation by immune system, producing high affinity antibodies particularly against the antigen of interest.

However, immunisation of animals is time consuming and each antigen requires the construction of a new antibody library, and tend to yield smaller number of antibodies that cannot be used to target other antigens [234]. There are also limitations to immunisations as there could be a lack of immune response to a self or toxic antigen. Naive libraries use a source of V genes from non-immunised human or animal donor B cells. This generally provides a larger and more diverse repertoire of clones, with efficient but lower affinity antigen-specific antibodies due to the lack of *in vivo* affinity maturation. The V genes are isolated from B cells present in lymphoid tissues, including the spleen, lymph nodes, tonsils or bone marrow. The advantage of using a naive library is that the large repertoires of clones provides the possibility of isolating higher affinity antibodies to self, unimmunogenic or toxic antigens, such as the vipera ammodytes meridionalis neurotoxin, vipoxin [235]. The limitation of the naive libraries is also the size of the repertoire and the general lower affinity of clones. To overcome this disadvantage, induced combinatorial diversity increases diversity and potential binding affinities by rearranging the heavy and light variable chains already existing in the library. Another method is by generating semi-synthetic libraries, using the existing CDR regions of the V genes, to construct randomised versions of the hypervariable antibody-binding sites of existing clones by polymerase chain reaction (PCR) or oligonucleotide directed mutagenesis [236, 237]. This increases the diversity of the library and may yield higher affinity clones.

3.1.2.3 Biopanning and Clone selection

Once a phage display library has been constructed, with each phage particle expressing a individual clone, there is a process of selection out of the library against a ligand of interest. This process is called biopanning (or panning); the procedure of specific binder selection encompasses repeated cycles of incubation, washing, amplification and re-selection of the bound phage. The ligand of interest is immobilised on a solid surface, which can be a simple multi-well plate or immunotube [235], magnetic beads [238] or even whole cells [134]. The multiple rounds of selection cycles are necessary to enrich for high-specificity and affinity-binding clones, which are commonly detected with simple dot blot assays or ELISA at the initial stage [235].

3.1.3 Rationale of study

Conflicting reports from the literature, about the role of chemerin in inflammation could be due to the various isoforms present at particular sites of inflammation. There are no commercially available antibodies against the various isoforms

of chemerin. Therefore, the main aim of this chapter was to develop tools able to detect murine prochemerin$^{20\text{-}162}$, murine chemerin$^{20\text{-}156}$ and C-terminus derived peptides$^{140\text{-}156}$ in samples from homeostatic and inflammatory conditions. To achieve this, UCB pharma's naive human phage display library was panned against murine chemerin$^{20\text{-}156}$, and a prochemerin peptide 'C23'$^{140\text{-}162}$; containing the C-terminus of murine prochemerin. Following the biopanning procedure, the selected clones from UCB's phage display library, were evaluated for binding affinity and functional ability in order to determine whether they would be useful in investigating the role of chemerin during inflammation.

3.2 Results

3.2.1 The development and generation of anti-chemerin antibodies

3.2.1.1 Panning against recombinant full length chemerin using UCB phage library.

The phage display group, in UCB Pharma, have developed 5 naïve λ and κ phage display libraries from a collection of healthy human tissues. Each library was mixed together in equal proportion to pan against the active isoform of murine chemerin [T^{17} - S^{156}] (R& D); the a.a. sequence of this protein is depicted in Figure 3.2a. Recombinant murine chemerin (mchemerin) [T^{17} - S^{156}] was immobalised on a high binding nunc-immuno tube and the phage panning was carried out as described in Chapter 2, section 2.2.1.1. The *E.coli.* colonies from the Round 2 output were picked, grown individually, and the phage were isolated from the cultures. The phage was then tested in a chemerin-binding phage ELISA, methods described in 2.2.1.1. In the left panel of Figure 3.5b, the phage ELISA shows 6 scFv clones binding recombinant murine chemerin [T^{17} - S^{156}].

The total Round 2 phage output was re-panned, and the Round 3 phage output was retested in chemerin-binding phage ELISA (Figure 3.2c). The blue wells represent a monoclonal scFv phage binding. The left panel shows the 93 scFv monoclonal phage binding to chemerin and the right panel is a negative control with BSA.

Due to the importance of the C-terminus for chemerin signalling via its GPRC receptors [153], I was searching for a scFv clone able to bind to the C-terminus of mchemerin. To address that, I assessed the Round 3 scFv phage in a C17 peptide-binding phage ELISA. The C17 peptide$^{140\text{-}157}$ contains the active portion of chemerin's C-terminus. Out of 95 phage tested 2 wells were positive in the left panel of Figure

3.2d. After sequencing the scFv clones, the two hits were shown to be the same clone. This is a common occurrence in the phage panning, the number of repeated binding scFv clones increases the more rounds of panning undertaken. The round 3 phage output was sequenced and there was a large number of clones which were only half scFv, containing only the linker and the Variable Light region. Figure 3.2e shows the clones run on a 10% agarose gel with the full scFv (VH-VL) at 850bp and the half scFv clones as 450bp. Figure 3.2f shows the proportion of half scFv (VL only) compared to the full scFv (VH-VL) clones within the round 3 clone output.

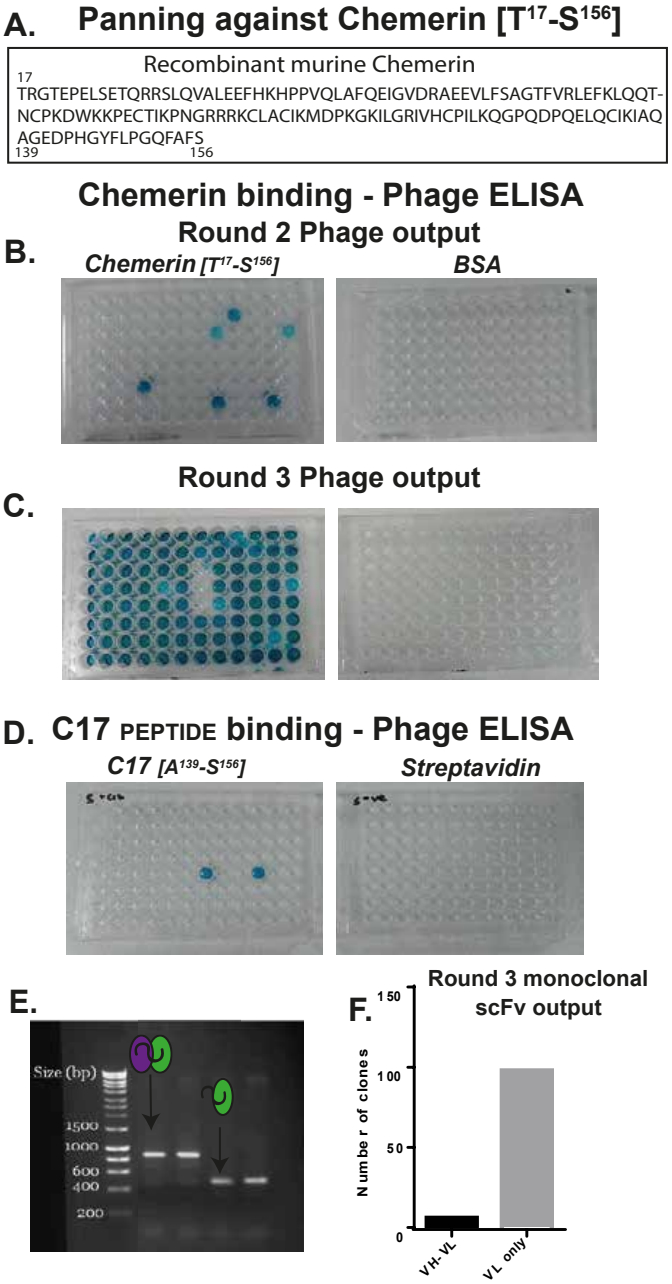


Figure 3.2: Panning against recombinant murine chemerin using UCB phage libraries in a mixture. The UCB phage libraries, in an mixture, were panned against 12μg/ml of immobilised recombinant murine Chemerin [T^{17} - S^{156}] (R& D) on a nunc-immuno tube. **A**. amino acid sequence of recombinant murine chemerin [E^{21} - S^{156}]. In sections B - D, blue wells signify monoclonal scFv phage binding and right panel is coated with 5%BSA or 1μg/ml streptavidin as a control for the left panel. **B**. 95 monoclonal scFv clones from Round 2 output were tested in a chemerin binding - phage ELISA; left panel contains Chemerin [T^{17} - S^{156}]. **C**. 95 monoclonal scFv clones from Round 3 output were tested in a chemerin binding - phage ELISA; left panel is Chemerin [T^{17} - S^{156}]. **D**. 95 monoclonal scFv clones from Round 3 output were tested in a C17 peptide binding phage ELISA; left panel shows Strepatavidin-C17 peptide [A^{139} - S^{156}]. **E**. Four scFv output clones, which bind chemerin, were run on the 10% agarose gel ; 800bp is the full scFv (VH-linker-VL), 450bp is half a scFv (linker-VL). **F.** Total number of round 3 scFv clones that were the full scFv (VH-linker-VL) and half the scFv (linker-VL).

3.2.1.2 Panning against C23 peptide using UCB naive human phage library separate.

I panned the UCB phage display libraries against the murine C-terminal prochemerin peptide, C23 [A^{139} - K^{162}]; the a.a. sequence is displayed in Figure 3.3a. C23 peptide was selected because it contains both the 6 a.a. inhibitory sequence of the prochemerin isoform and also for the active C-terminal sequence of mchemerin. Theoretically, scFv clones recognising prochemerin or the C-terminus of active chemerin could be developed using this peptide. Due to the issues faced by the previous pan against chemerin in Figure 3.2, where a large proportion of the scFv clones were VL only, I panned all 10 UCB phage λ and κ libraries separately against C23 peptide. Using a peptide means that immobalisation onto plastic is challenging, therefore, I used the C23 peptide with a biotinylation site at the N-terminus of the peptide. The biotinylated-C23 was immobalised using streptavidin coated wells, similarly described in [239]. Following the biopanning procedure and phage isolation, the round 3 phage output was tested in a C23 peptide-binding phage ELISA. On the left panel of Figure 3.3b, the 93 blue wells signify monoclonal scFv phage binding to the C23 peptide, on the right panel is streptavidin alone, there are only 4 scFv phage clones are binding. The round 3 output phage were also tested in the chemerin-binding phage ELISA and the C17 peptide-binding phage ELISA. The blue wells, illustrated in the ELISA plates Figure 3.3c and d, signify that some scFv clones are able to bind the two different isoforms of chemerin as well as the C23 peptide they were raised against.

Following Sanger sequencing, using flanking primers external to the scFv genes, the scFv clones binding C23 from the round 3 output were found to be highly diverse. The spread in the CDR3 lengths of the VH chain, from each scFv positively binding clones, provides a visual representation of the diverse output (Figure 3.4a). Out of 118 scFv clones, found to positively bind C23 from our priliminary phage ELISA data, 88% of the clones VH CDR3 sequences are only identified once. Figure 3.4 illustrates an example of a subsection of the diverse VH CDR3 a.a. sequences.

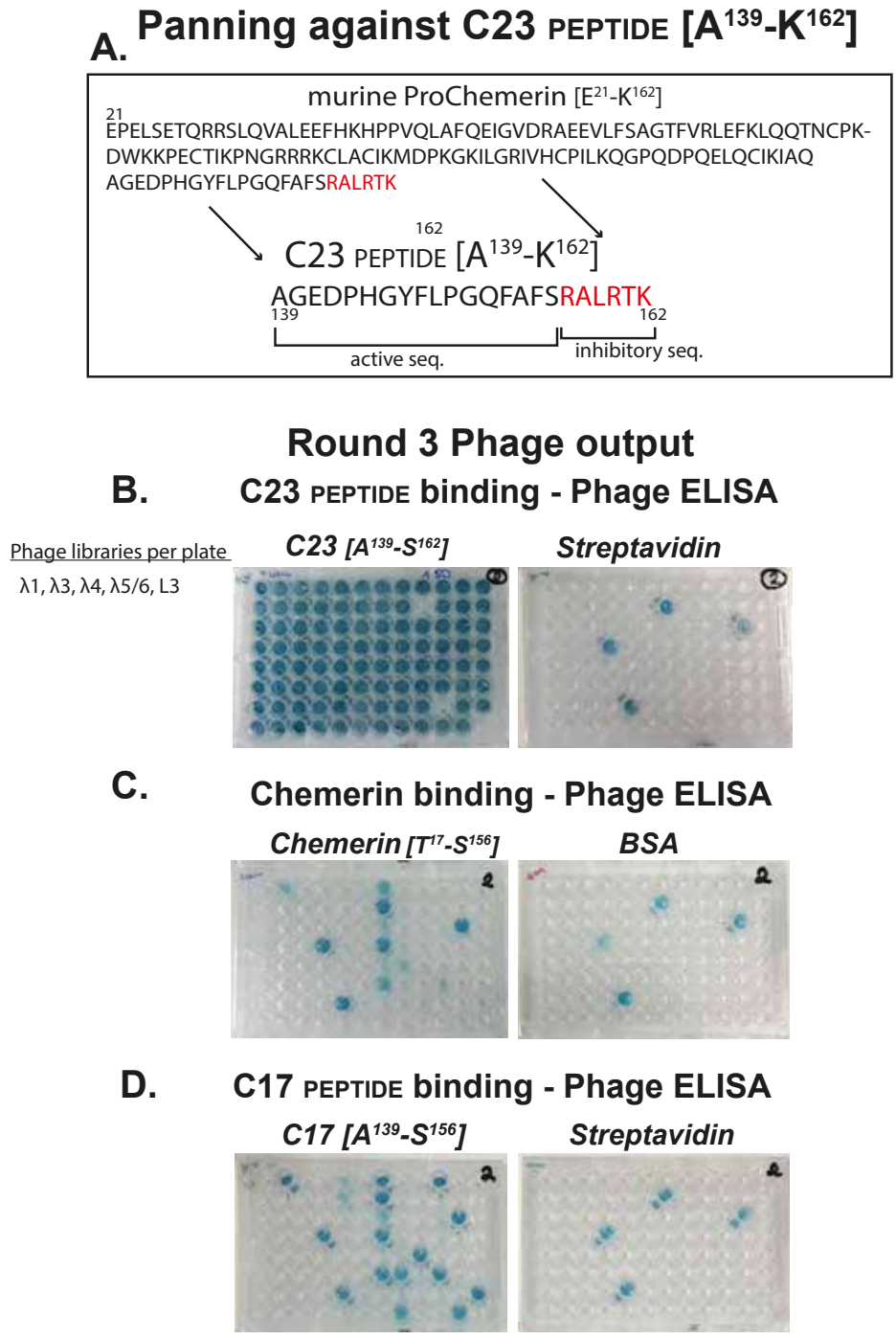


Figure 3.3: Panning against C23 peptide [A^{139} - K^{162}] using UCB phage libraries separately. The UCB phage libraries were separetely panned against 1μg/ml biotinylated C23 peptide [A^{139} - K^{162}], which was immobalised on a nunc-immuno plate by streptavidin. **A**. The a.a. sequence of murine prochemerin [E^{21} - K^{162}] and C23 peptide used as for this panning. In sections B - D, blue wells signify monoclonal scFv phage binding and right panel is coated with 1μg/ml streptavidin as a control for the left panel. **B**. 95 monoclonal scFv clones from Round 3 output were tested in a C23 peptide binding - phage ELISA; left panel contains C23 peptide [A^{139} - S^{156}]. **C**. 95 monoclonal scFv clones from Round 3 output were tested in a Chemerin binding - phage ELISA; left panel contains Chemerin [T^{17} - S^{156}]. **D**. 95 monoclonal scFv clones from Round 3 output were tested in a C17 peptide binding - phage ELISA; left panel contains C17 peptide [A^{139} - S^{156}].

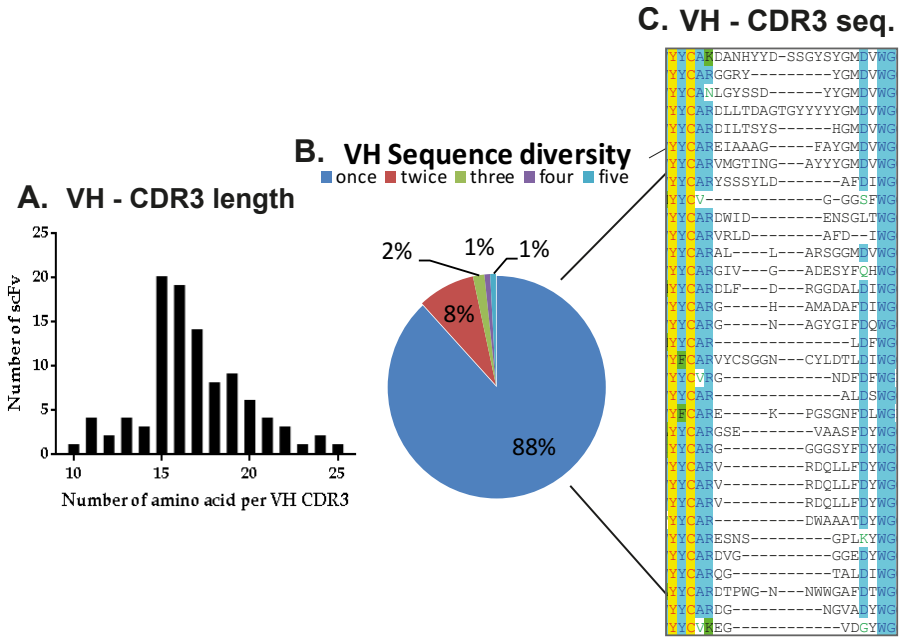


Figure 3.4: CDR3 sequence diversity from Round 3 panning against C23 peptide [A^{139} - K^{162}] using UCB phage libraries separetly. The scFv clones from the Round 3 output of the C23 peptide [A^{139} - K^{162}] pan, were sequenced using Sanger sequencing method; it was found that 118 scFv clones, that could bind C23 peptide, had high diversity in the CDR3 region of the VH. Data was analysed using the AlignX sequencing program; **A**. depicts the number of scFv clones and their varying VH CDR3 a.a. length amounts the clones which bind the C23 peptide. **B**. The pie chart represents the number of repeated sequences out of 118 scFv clones binding C23 peptide; 88% sequences were seen once. **C**. AlignX sequencing program helped us analyse the large number of sequences obtained and here is a sample of unique VH CDR3 sequences obtained from the Round 3 output.

3.2.1.3 Surface plasmon resonance analysis of C23 pan

The C23-binding phage, from Round 3 panning, were converted from a phage scFv format into a human IgG1 format by using a two step transcriptionally active PCR (TAP) method developed by the UCB phage display team, Figure 3.5a. These re-formatted human IgG1 antibodies were used to evaluate the clones binding capacity towards two mchemerin peptides (Figure 3.5); C17 [A^{139} - S^{156}] containing the active sequence of the C-terminus and C23 [A^{139} - K^{162}] containing the active and inhibitory sequence of prochemerin C-terminus. The binding affinites of the clones was assessed by surface plasmon resonance (SPR) analysis in a Biacore T200 instrument. A total of 95 IgG1 reformatted clones were evaluated in one SPR run. The 10 best binding clones were selected out of 20 binding clones observed from the SPR traces. These 10 were selected according to their unique sequences and their binding profiles generated by the SPR. Figure 3.5c contains the binding profiles of group 1 selected clones. These recognise the active sequence of the C-terminus; clones A9, A7, C9 recognise

both C17 and C23 peptide. Clone A1 seems to recognise the C17 peptide, rather than the C23 peptide in this instance. Figure 3.5d contains the binding profile of group 2 selected clones. These recognise the inhibitory sequence of C23 peptide rather than the C17 peptide. Clones B6, A6, F9 and A4 do not bind C17 peptide and favour binding to the C23 peptide. B7 and C6 only partially bind to C17 but show higher binding afinity towards C23 peptide.

These 10 clones were carried forward in a scFv-mouse Fc vector from UCB. The mouse Fc vector belongs to UCB, however, it was easier to use this format out of UCB. Because the TAP method for generating the human IgG1 constructs was not in the public domain, it would of been more complicated to use them out of UCB. Furthermore, I was interesting in using a murine based fragment for future use in *in vitro* murine systems and *in vivo* inflammation models.

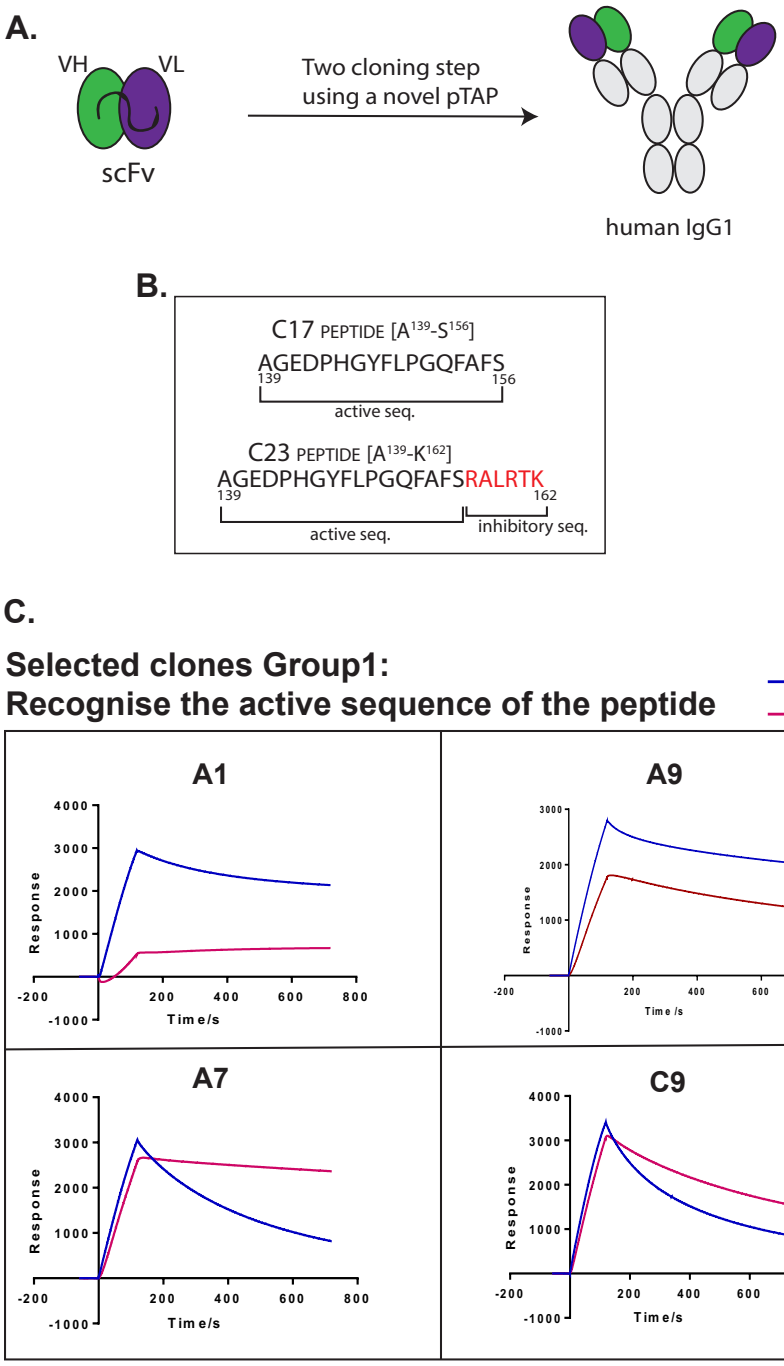


Figure 3.5: Group 1 selected scFv clones, in a human IgG1 format, which recognise the active sequence of the C23 & C17 peptide in a T200 SPR analysis. A. scFv clones were constructed into a human IgG1 format using a transcriptionally active PCR method; each scFv clone was cut out of phage vector, amplified and barcoded in the primary TAP step, in the following TAP step the constant regions of IgG are constructed onto the barcoded scFv fragments from primary step; transfection of the TAP products in 293 Freestyle^{TM} cells results in the production of the clones in a human IgG1 format. B. The a.a. sequence of the biotinylated C17 and C23 peptide used for SPR analysis T200 Biacore. C. Group 1 Selected clones; The binding profiles of 4 selected clones which seem to recognise the active C17 sequence of the C23 peptide.

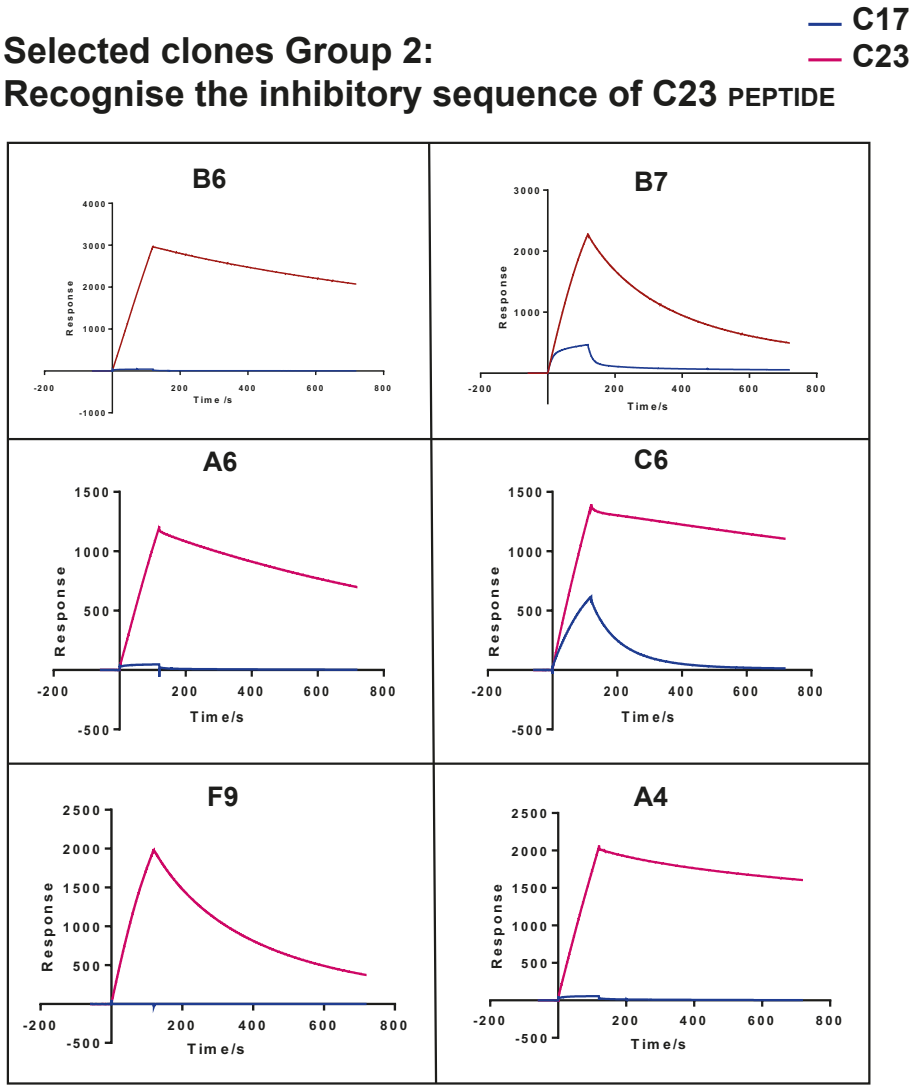


Figure 3.6: Group 2 selected scFv clones, in a human IgG1 format, which recognise the sequence of the C23 peptide in a T200 SPR analysis. The biacore binding curves of the selected clones which only recognise the C23 peptide are shown.

3.2.1.4 scFv-Fc construct production and purification

Following the cloning of the selected scFv clones into the mouse Fc vector from UCB, human embryonic kidney(HEK 293) 293 Freestyle^{TM} cells were transfected with the scFv-Fc constructs. The scFv-Fc clones were purified from the 6 day culture supernatants using Protein A gravity columns (GE). Following the antibody purification, the antibody concentrations were quantified preliminarily using the nanodrop and then a mouse IgG1 indirect ELISA. By making a serial dilution of mouse IgG1 for a standard curve, the concentration of antibody per sample following purification was quantified. On average a concentration of 1μg/ml was purified according to

the ELISA. However, the clone A4, showed minimal production following multiple transfections, which resulted in the conclusion that it was difficult clone for mammalian transfection and production. The Figure 3.7a depicts a schematic diagram of the IgG ELISA used to quantify the purified scFv clones and a 4-10% SDS-PAGE gel coomassie stained gel with 7μg of scFv-Fc purified samples. In addition, a C23 binding ELISA was carried out to illustrate the purified scFv clones could still bind C23 peptide.

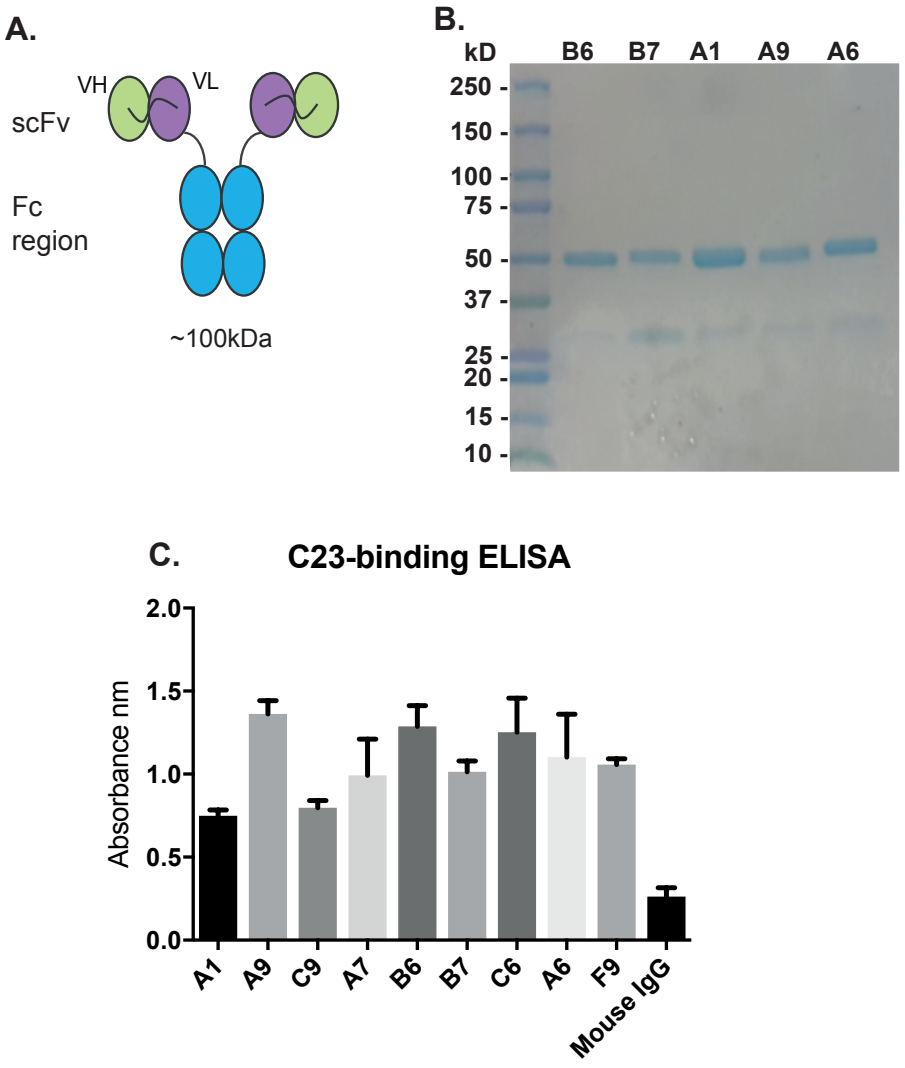


Figure 3.7: Purified scFv-Fc clones and C23 peptide binding confirmed. A. Diagram of scFv-Fc construct. **B.** 7μg of the scFv-Fc constructs were run on a 4-10%SDS page gel, under reduced conditions, stained with coomassie blue protein stain. The reduced size of the scFv-Fc is 50kDa. **C.** A C23 peptide binding ELISA, using 1μg/ml per clones, was used to determine binding was still obtainable in this format.

3.2.1.5 Surface plasmon resonance analysis of reformatted clones

Due to the different clone format, I wanted to clarify the binding profiles and affinities of the clones in this scFv-Fc construct format. Here I used a Biacore 3000 instrument, where increasing concentrations of the antibodies were flowed over the immobilised peptides and full length mchemerin protein. These results were confirmed by two independent experiments. Interestingly, the binding profiles differ from the previous SPR experiment with the clones in a IgG format. A7 was not included in this panel of investigation as it did not seem to bind very strongly in the ELISA so was not included. The dissociation constants, Kd, of each clone are included in Tables 3.1 and 3.2. These were calculated using a Two-site binding analysis in the binding curved generated in the SPR assay. This analysis allows the prediction of the two scFv portions of the scFv-Fc construct engaging in binding (Hi) as well as a single one (Lo). The points fit on a two site binding curve correctly, suggesting that the ligand proximity allows the engagement of both scFv portions.

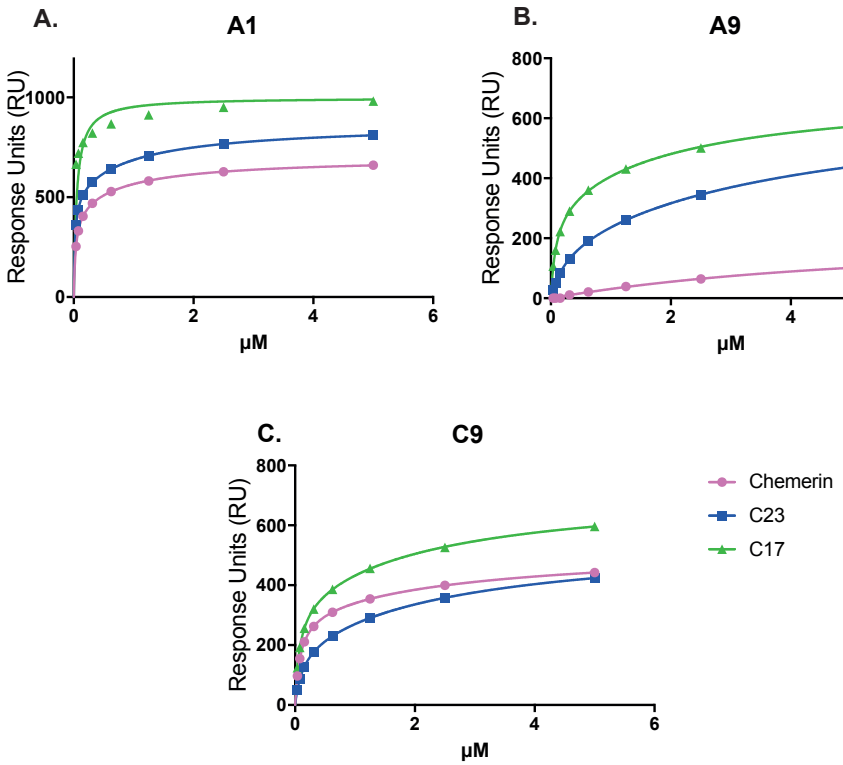


Figure 3.8: Biacore binding profiles of group 1 selected clones in scFv-Fc format. Chemerin, C23 and C17 peptides were immobilised on a T200 Biacore chip and increasing concentrations of scFv clones were flowed over them. Representative experiment of 2. **A.** Clone A1 binding profile **B.** Clone A9 binding profile **C.** Clone C9 binding profile.

Table 3.1: Kd values from Two site binding curve for Group 1 clones

Clone	Kd value μM	C23	C17	Chemerin
A1	Lo	1	0.05	0.88
	Hi	0.02	0.05	0.03
A9	Lo	4.2	2.1	17.2
	Hi	0.25	0.084	9.5
C9	Lo	2.8	2.4	3
	Hi	0.13	0.072	0.086

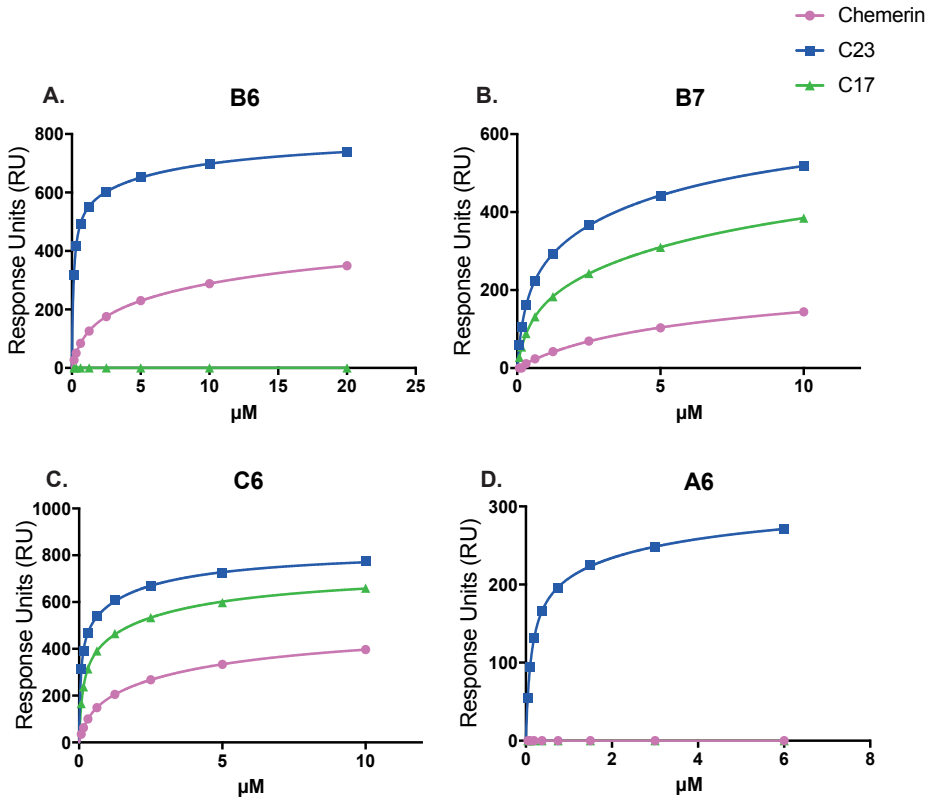


Figure 3.9: Biacore binding profiles of group 2 selected clones in scFv-Fc format. Chemerin, C23 and C17 peptides were immobilised on a T200 Biacore chip and increasing concentrations of scFv clones were flowed over them. Representative experiment of 2. **A.** Clone B6 binding profile **B.** Clone B7 binding profile **C.** Clone C6 binding profile **D.** Clone A6 binding profile.

Table 3.2: Kd values from Two site binding curve for Group 2 clones. NB= no binding

Clone	Kd value μM	C23	C17	Chemerin
B6	Lo	7.67	0.0	17.1
	Hi	0.13	NB	1.0
B7	Lo	6.3	9.8	4.4
	Hi	0.32	0.40	4.4
C6	Lo	2.1	3.2	5.2
	Hi	0.05	0.12	0.38
A6	Lo	3.6	NB	NB
	Hi	0.13	NB	NB

In order to validate the Kd values obtained from this SPR experiment, it was necessary to reverse the SPR set up, by immobilising the antibody clones on the chip and flowing one concentration of each analyte over the top of them. This would confirm the binding specificity and dissociation constant of the clones. During the course of these investigations, I was faced with some technical difficulties, including the antibody decay off the chip, and the lack of efficient dissociation from one ligand to the next. These issues meant that accurate readings could not be obtained. The crude results I was able to obtain was that these experiments were showing reduced chemerin and increased C17 peptide association. The C17 peptide was not dissociating efficiently, thus, making it impossible to obtain correct readings with the different analytes (data not shown).

3.2.2 Functional characterisation of antibody clones

3.2.2.1 DiscoverX β-arrestin recrutiment in CHO-ChemR23 expression system

Given that there was evidence to suggest the selected clones bind to chemerin and peptides, I was interested in investigating whether the scFv clones exhibited any functional activity. My first set of investigation were to assess the clones ability to inhibit the activity of full length recombinant murine mchemerin and C17 peptide at the ChemR23 receptor. The DiscoverX β-arrestin recruitment assay uses modified CHO cells have a small peptide fused to the GPCR of interest, the ChemR23 receptor, and the complementing fragment to the small peptide is fused to β-arrestin2. Upon activation, the GPCR binds to β-arrestin forcing complementation of the enzyme fragments. The addition of a luminescent substrate allows quantification of GPCR activation. A serial dilution of mchemerin [T^{17} - S^{156}] (R& D) was used to choose the appropriate EC-80 concentration to test the inhibitory activity of anti-chemerin

antibodies (Figure 3.10a). Using a commercial goat polyclonal antibody (R& D) as a positive control, chemerin inhibition at the ChemR23 receptor is achieved, Figure 3.10b. The in-house Group 1 selected antibodies, that recognise the active sequence of C23 peptide, show no inhibition of mchemerin at the ChemR23 receptor (Figure 3.10c-f). In Figure 3.11, I compare the luminescent reading from each clone at a concentration of 10μg/ml. The commercial polyclonal is the only antibody showing a significant inhibition of β-arrestin recruitment by 2nM chemerin.

The binding profiles detected by the first SPR data, suggest Group 1 clones binding to chemerin, however as stated earlier, there were some discrepancies when attempting to verify these binding profiles. Using a simple ELISA binding assay for chemerin (2nM) and C17 peptide (27nM), I tested the titrated Group 1 antibodies and found that in the ELISA, they could not bind chemerin. However, they were all able to bind C17 peptide in the ELISA (Figure 3.12).

Next, I wanted to assess whether the clones could inhibit the activity of the C17 peptide at the ChemR23 receptor using the DiscoverX assay, due to the binding data from SPR and ELISA (Figure 3.8, 3.12). The standard curve is right shifted compared to chemerin, suggesting that C17 peptide is less potent but display equal efficiency by reaches the same degree of activation at the receptor in high concentrations (Figure 3.13a). The Group 1 clones do not display any significant inhibitory activity towards the C17 peptide, Figure 3.13 c-d, neither does the commercial polyclonal in Figure 3.13b. Due to the ELISA binding assay and the SPR data, where the Group 1 clones were binding to C17 peptide, it was expected that the Group 1 clones would be able to inhibit the C17 peptide's ability to activate the ChemR23 receptor.

It was hypothesised that Group 1 clones were not able to recognise and bind 'free' C17 but they needed it to be immobilised or bound to bigger molecule. In order to achieve a bound form of C17, that is still able to activate the ChemR23 receptor, I tested streptavidin bound C17 in the DiscoverX assay, where the free floating streptavidin would create a tetramer of bound C17 peptides. In Figure 3.14, there seems to be a slight inhibition of β-arrestin recruitment at high concentrations of the Group 1 clones A1 and the commercial polyclonal. Yet there is no significant inhibition in any of the clones tested.

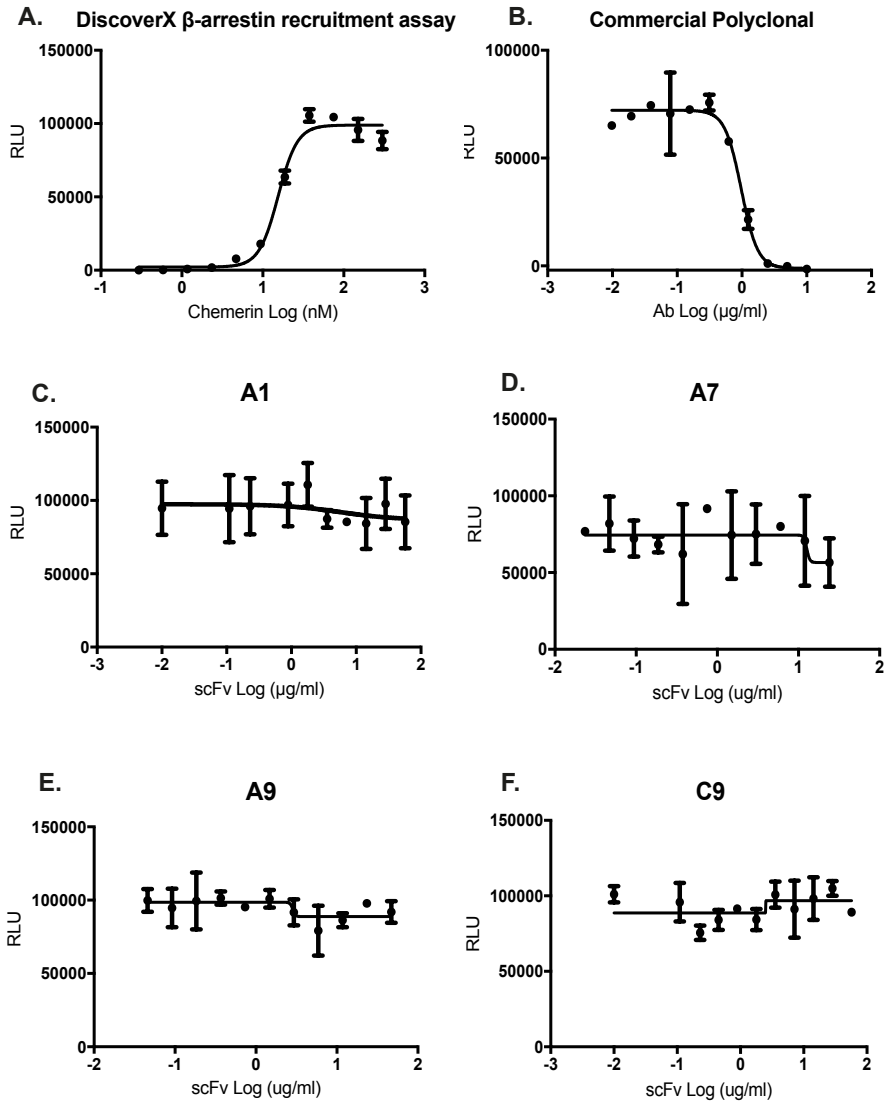


Figure 3.10: Chemerin induced β-arrestin recruitment in ChemR23 expressing cells is blocked by titrated commercial polyclonal antibody but not Group1 in-house clones. Group 1 clones and commercial polyclonal anti-chemerin (R& D) were incubated with 2nM Chemerin (R& D) before being added to ChemR23 expressing CHO cells from Discoverx systems, where β-arrestin recruitment is measured by luminescence. Representative of 2 experiments. **A.** Serial dilution of murine Chemerin (R& D) induced β-arrestin recruitment. The β-arrestin recruitment by chemerin with a titration of **B.** Commercial polyclonal. **C-F.** 2nM chemerin induced β-arrestin recruitment with a titration of A1, A7, A9, C9 clones respectively. Representative of 2 individual experiments.

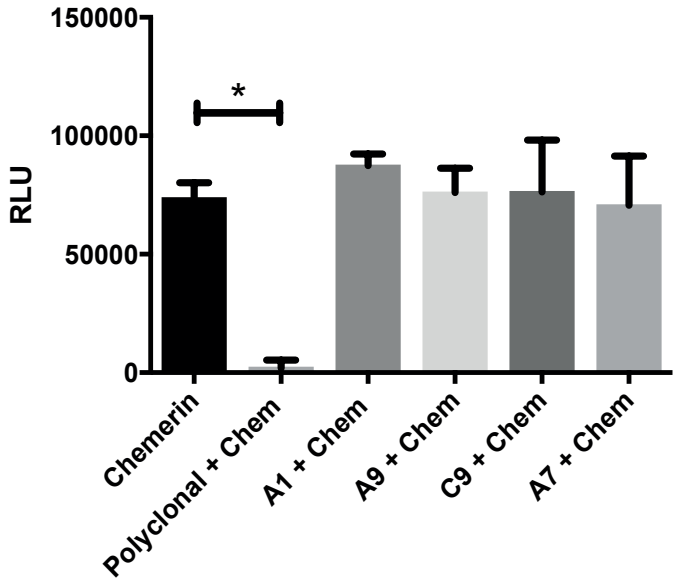


Figure 3.11: Chemerin induced β-arrestin recruitment in ChemR23 expressing cells is blocked by 10μg/ml of commercial polyclonal antibody but not Group 1 in-house clones. Group 1 clones and commercial polyclonal anti-chemerin (R& D) were incubated with 2nM Chemerin (R& D) before being added to ChemR23 expressing CHO cells from Discoverx systems, where β-arrestin recruitment is measured by luminescence. Statistical analysis with one-way anova, $(*) = p < 0.05$, $n = 2$

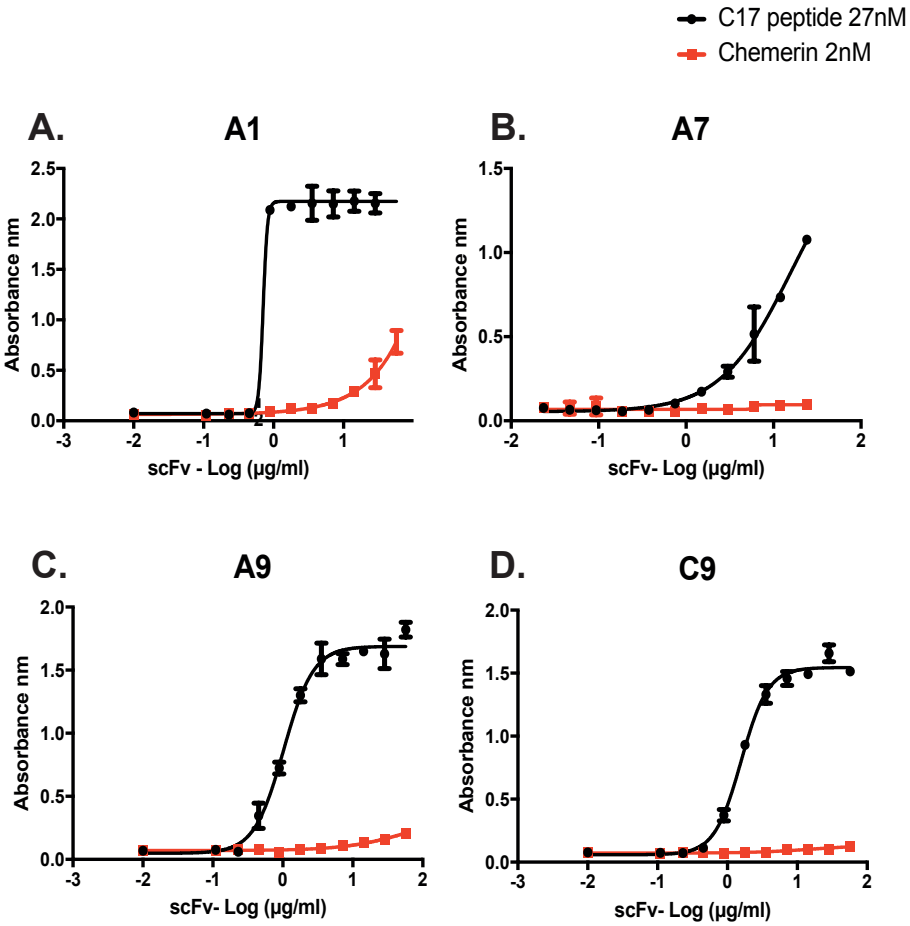


Figure 3.12: Group 1 scFv clones show binding to C17 peptide but not mchemerin in ELISA binding assay. Chemerin and C17 peptide were immobilised on a nunc 96 well plate, either by overnight incubation and streptavidin-biotin interaction respectively. They were then incubated with scFv group 1 clones that were detected with an anti-mouse IgG HRP tagged secondary antibody. **A-D.**Group 1 clones titrated A1, A7, A9, C9 respectively. Top concentration is 50μg/ml.

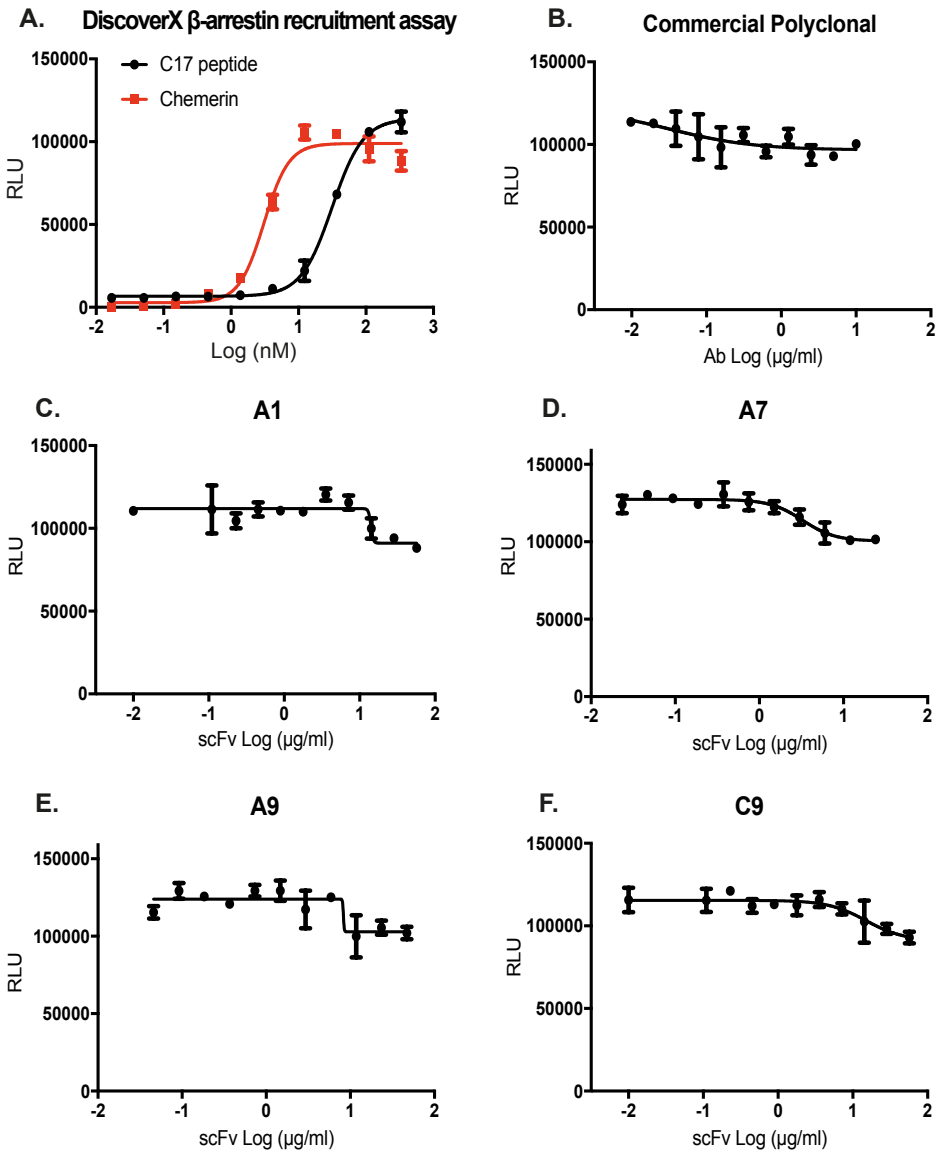


Figure 3.13: C17 peptide induced β-arrestin recruitment in ChemR23 expressing cells is not blocked by titrated goat antibody or by in-house group 1 clones. Group 1 clones and commercial polyclonal anti-chemerin (R& D) were incubated with C17 peptide (27nM). These were then added to ChemR23 expressing CHO cells from Discoverx systems, where β-arrestin recruitment is measured by luminescence. Representative of 2 experiments. **A.** Serial dilution of murine Chemerin (R& D) and C17 peptide. The β-arrestin recruitment by C17 peptide with a titration of **B.** Commercial polyclonal. **C-F.** Group 1 clones; A1, A7, A9, C9 clones respectively.

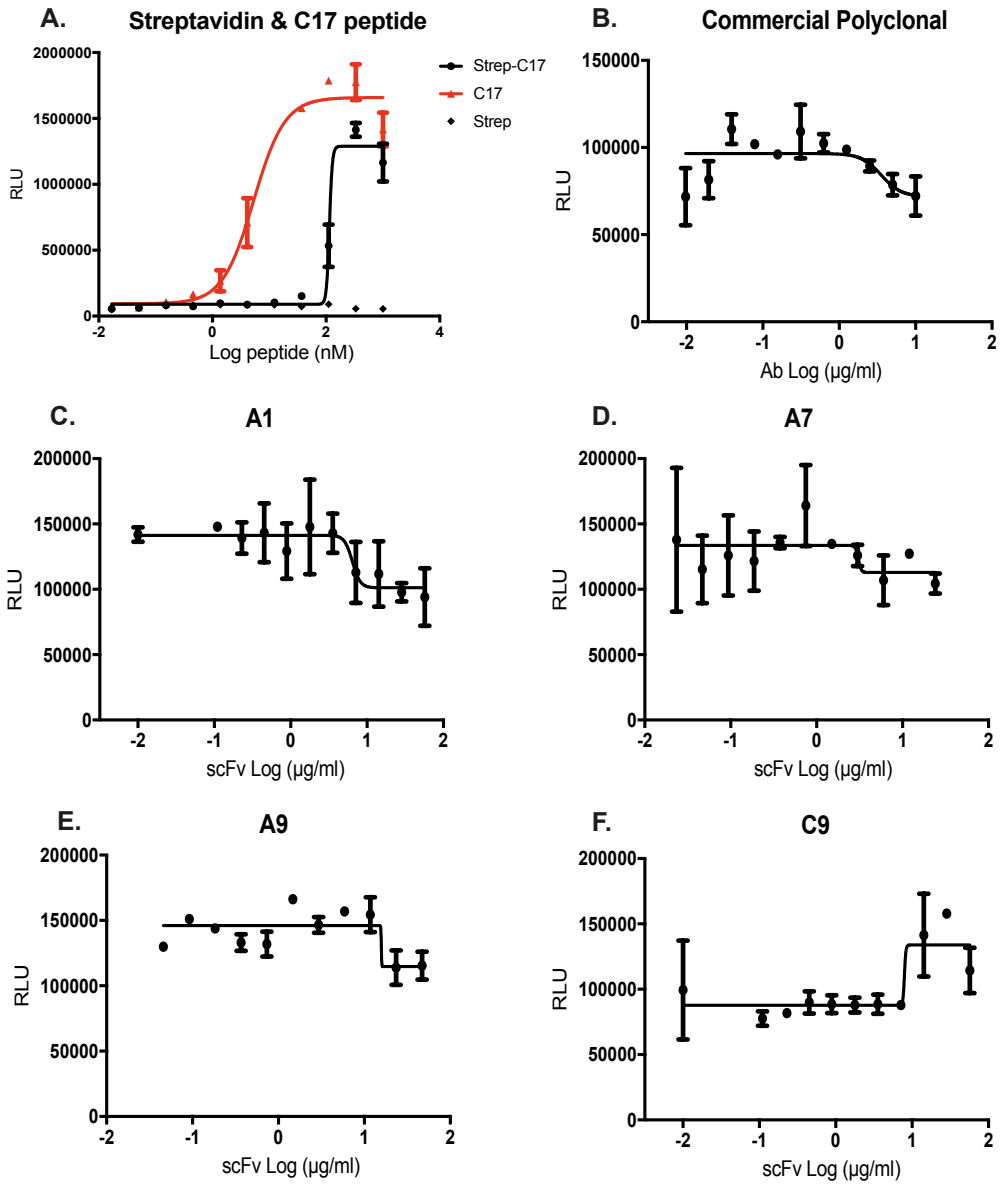


Figure 3.14: Streptavidin bound-C17 peptide induces β-arrestin recruitment in ChemR23 expressing cells is not blocked by commercial polyclonal or by in-house group 1 clones. Group 1 clones and commercial polyclonal anti-chemerin were incubated with streptavidin bound-C17 peptide (1μg/ml, 27nM respectively). They were all added to the ChemR23 expressing CHO cells from Discoverx systems, where β-arrestin recruitment is measured by luminescence. Representative of 2 experiments. **A.** Serial dilution of C17 peptide, streptavidin bound C17, and streptavidin. The β-arrestin recruitment of streptavidin-bound C17 with a titration of **B.** Commercial polyclonal **C-F.** Group 1 clones; A1, A7, A9, C9 clones respectively. Representative of 2 individual experiments.

3.2.2.2 The inhibition of chemerin chemotaxis using Bio-gel elicited peritoneal cells

Due to the lack of chemerin binding and inhibitory functions in the β-arrestin recruitment assay from the Group 1 clones from the C23 pan, I decided to clone the scFv clones from the chemerin pan (Figure 3.2) on the the Fc vector. Because these clones had been selected from the library by panning using the full length mchemerin, I suspected that they may have had an ability to block functional responses to chemerin. Therefore, using a real-time chemotaxis assay, I assessed their ability to inhibit chemerin chemotaxis by ChemR23$^+$ cells. Day 4 Bio-gel elicited peritoneal cells were used as a primary cells source of ChemR23$^+$ cells. The macrophage and monocyte populations from this source of cells express ChemR23 receptor, making them appropriate to carry out chemerin chemotaxis studies (Figure 4.5). Chemerin was pre-treated with the clones derived from the chemerin pan and the commercial anti-chemerin polyclonal antibody (R& D) for an hour at 37^{o}C, prior to placing into the bottom wells of the transwell system. In the top well, the Bio-gel cells (4×10^5 cells per well) were added and migration was measured by ACEA xCelligence ECIS chemotaxis system, where the cells adhesing to the bottom side of the transwell system gives a cell index reading. Figure 3.15 shows that there is chemotaxis towards C5a (control) and chemerin. The inhibition of chemerin chemotaxis is only achieved by pre-treatment with commercial polyclonal. The clones # 1,3,6 do not exhibit inhibition of chemerin migration of these macrophages. These results are representative of 2 independent experiments, with differing concentrations of chemerin (2.5nM). Subsequent Biacore anaylsis of these clones revealed weak affinity towards chemerin (data not shown) making this result less surprising.

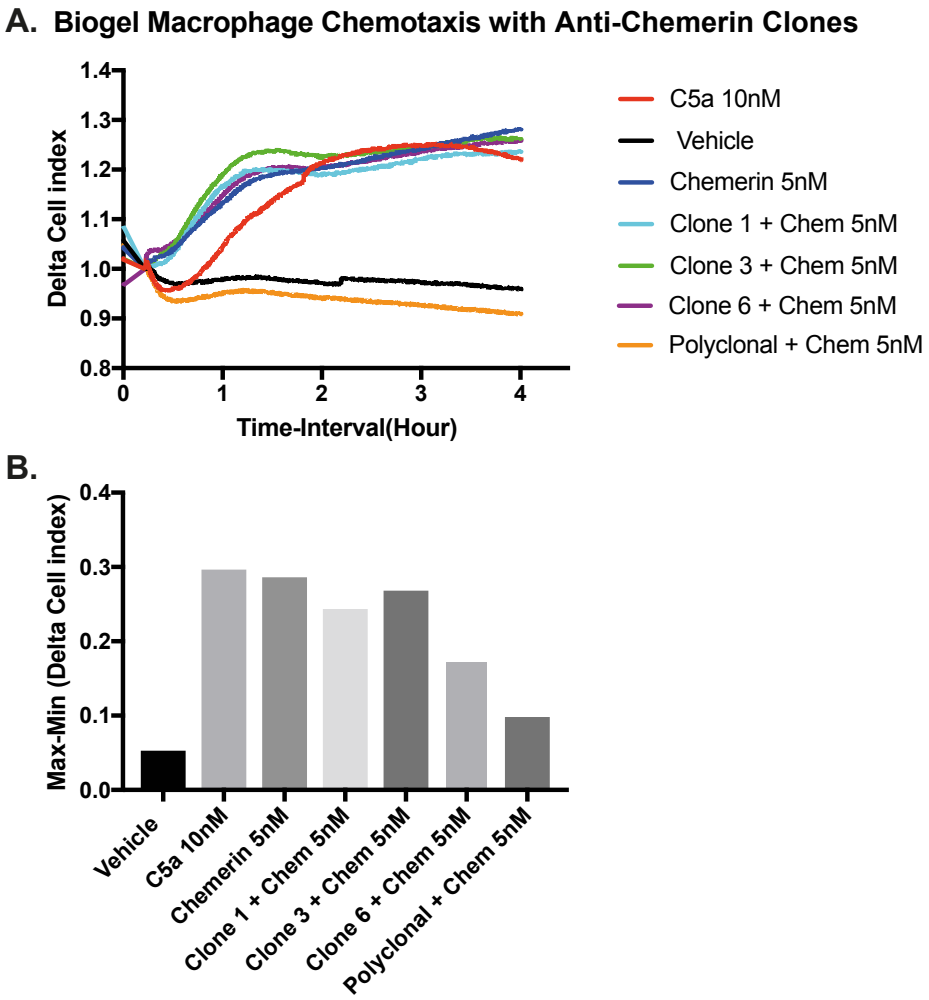


Figure 3.15: Real time chemotaxis assay, using biogel macrophages with chemerin, shows no inhibition by anti-chemerin clones from chemerin pan. A. Original traces of biogel macrophage chemotaxis towards C5a(10nM) and chemerin(5nM). Chemerin chemotaxis is inhibited by polyclonal anti-chemerin but not by clones # 1,3,6 which were selected from the chemerin pan 3.2. **B.** Max-Min of Delta Cell index values of the real time chemotaxis shows inhibition of chemotaxis only by polyclonal anti-chemerin n=2

3.2.2.3 Human Neutrophil Elastase cleavage assay using the C23 peptide

Group 2 selected clones recognising the inhibitory sequence of C23 peptide, should theoretically be able to detect prochemerin. To this effect, it was hypothesised that some of these clones may be able to prevent the activation of prochemerin into active chemerin, by blocking the cleavage site of inactive protein. To test this, I developed an *in vitro* assay employing the C-terminal peptide C23 that is FLAG tagged on its C-terminus. The FLAG-tagged C23 peptide is added to a HBSS solution with human neutrophil elastase and incubated for various time points. This solution is then added to an ELISA plate coated with streptavidin, where the peptide is immobilised to the

plate by the N-terminus. Following the wash steps, an anti-FLAG tag antibody is used to detect the presence of the FLAG sequence on the peptide. The lack of a FLAG signal suggests that human neutrophil elastase or cathepsin G (millipore merk) are able to cleave the C-terminus of C23 (Figure 3.16a,b). The detection of the FLAG signal decreased with increasing concentrations of each enzyme(Figure 3.16d,e).

During the course of optimising this experiment, it became apparent that the C23 peptide was sticking to the normal eppendorf plastic tubes. Figure 3.16c shows a time series experiment, where the C23 peptide being detected by FLAG tag decreases over time, where as in low binding tubes the signal is maintained through out the time series.

Once the optimisation of the C23 cleavage was complete, the C23 peptide was pre-treated with Group 2 clones, for 1hr in 37°C, before treating with the protease, in order to see if the cleavage of C23 peptide was prevented. The initial experiments had shown that clone B7 Figure 3.17a and B6 (not shown) either from a crude supernatant or from purified sample were able to inhibit the removal of the FLAG signal. However, the following experiments concluded that this was not the case, and the clones from Group 2 as well as clones from Group 1 including A1 and C9 were unable to inhibit the cleavage of C23 peptide by both proteases; elastase and cathepsin G.

In order to confirm that the C23 peptide was being cleaved at the inhibitory sequence rather than other sites on the peptide, the same samples that were used for FLAG signal detection were also analysed for the maintenance of the C17 sequence within the C23 peptide. This was done by using the Group 1 selected clone, A1, to detect the presence of the active sequence of the C23 peptide. As a control, I used the C17 peptide (150ng/ml concentration). The 'C23 only' sample displays a lower absorbance value than the C17 sample even though they were both the same concentration (150 ng/ml) (Figure 3.17c,e). This could be due to the fact that A1 clone can detect the C17 peptide better and than the C23 peptide. The C17 portion of the peptide all seem to be present in the elastase treated samples, when comparing the C23 only sample to the rest (Figure 3.17c). This indicates that the elastase is not cleaving the peptide past the prochemerin sequence. However, all the cathepsin G treated samples display no detection of the C17 portion. This suggests that the cathepsin G may be cleaving the C23 in further regions within the C-terminus.

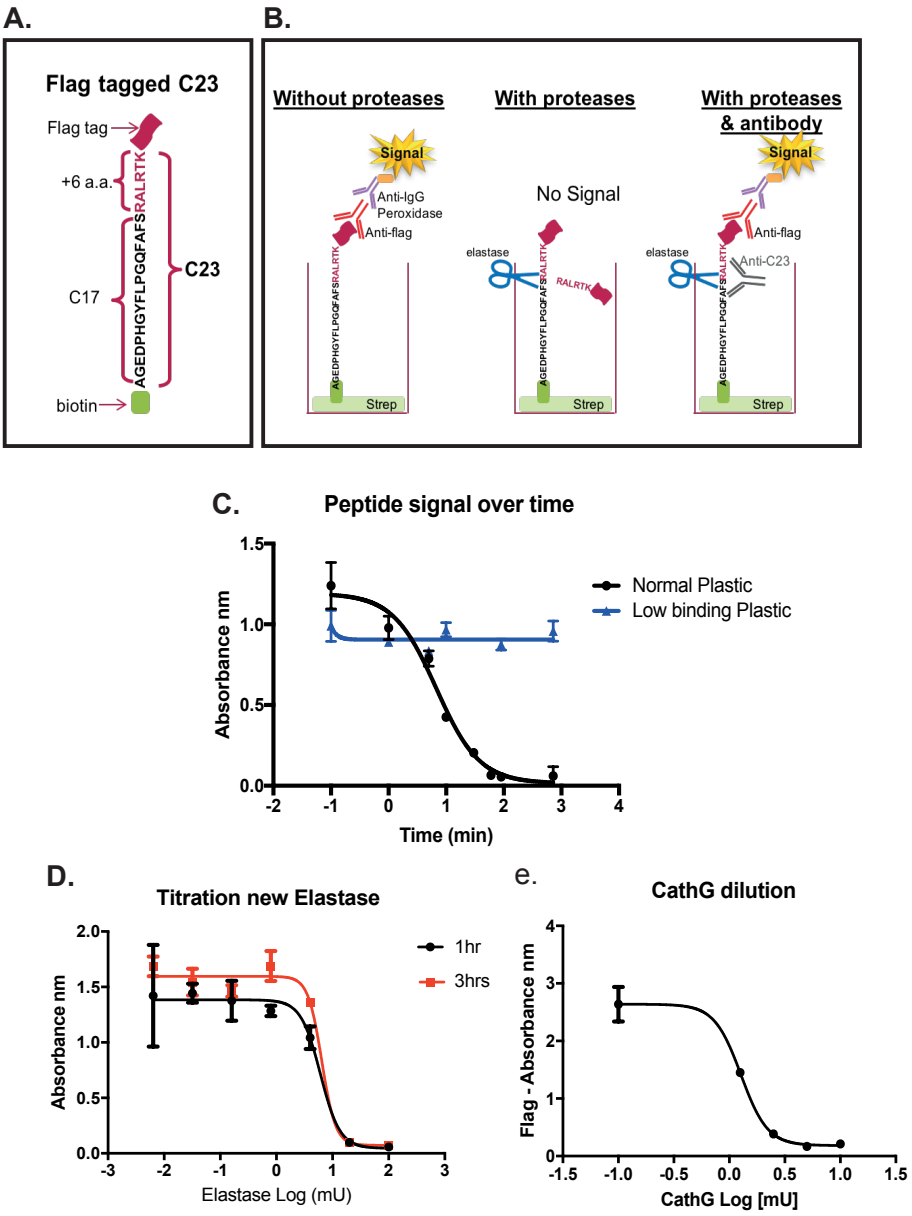


Figure 3.16: Optimisation of C23 Cleavage assay using human neutrophil elastase and cathepsin G A. Flag tagged C23 peptide sequence B. Diagrammatic representation of the C23 Cleavage assay C. C23 peptide binding on eppendorf plastic overtime vs low binding plastic eppendorf tubes. Samples were frozen immediately after time point and signal was detected using an anti-flag antibody. D. Titration of human neutrophil elastase (mUnits) with 150ng/ml C23-Flag peptide. E. Titration of cathepsin G (mUnits) with 150ng/ml C23-Flag peptide

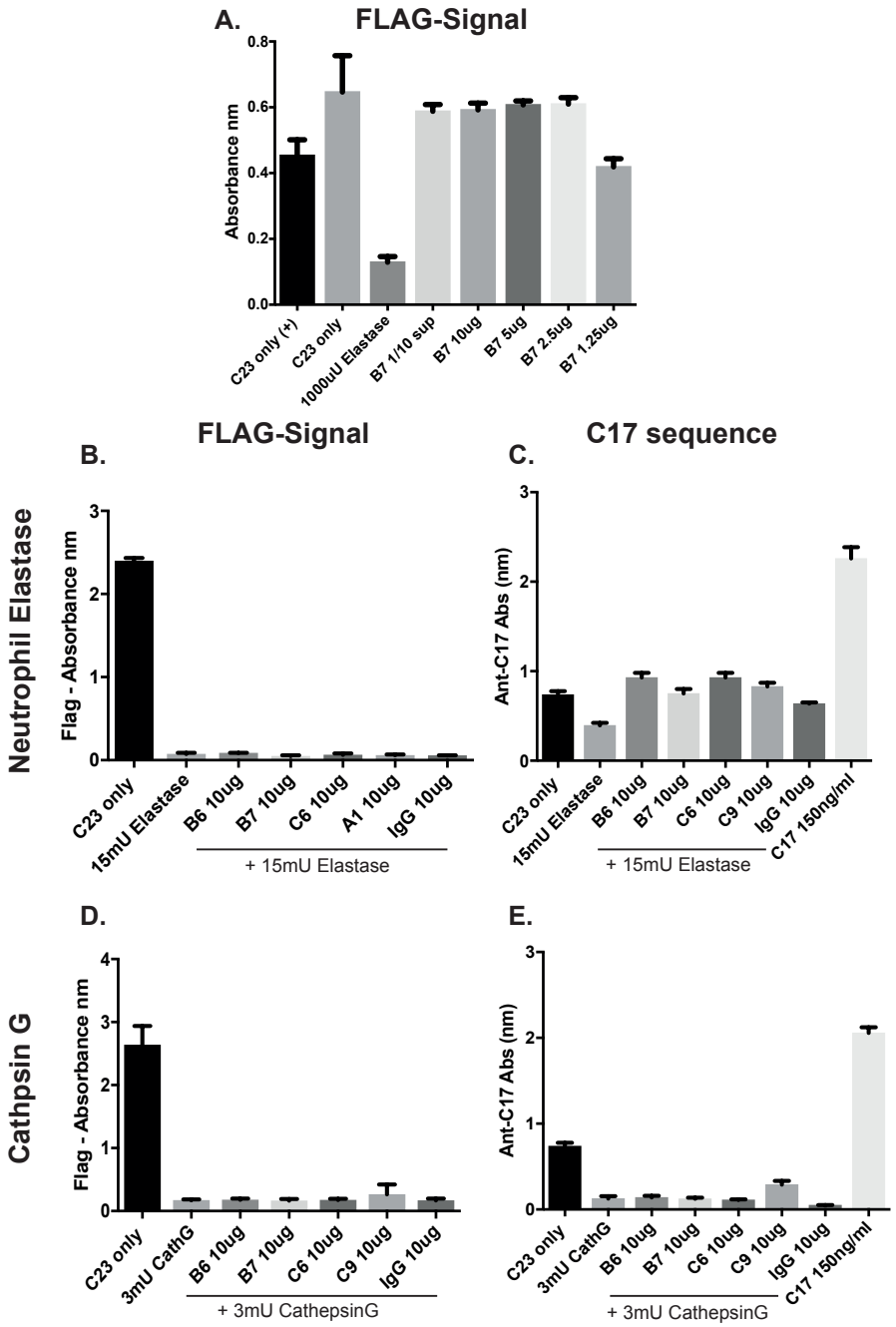


Figure 3.17: C23 Cleavage assay using human neutrophil elastase and cathepsin G A. C23-Flag peptide was protected from cleavage by the purified form of clone B7 at varying concentrations as well as from the crude cell supertatants n=2. Following numerous repeats, this result was not repeated. The results are now depicted in B& D Flag signal for neutrophil elastase and cathepsin G respectively. C & D. illustrate the binding of the C17 sequence in the C23-Flag peptide revealed by A1 clone. This was done to determine whether the proteases were cleaving the C23 peptide in a earlier a.a. sequence.

Due to the lack of inhibitory cleavage activity at the C23 peptide, I decided to produce a polyclonal pool of the antibodies by the co-transfection of two plasmids,

expressing individual scFv clones. The co-transfection would create a polyclonal pool of the two antibodies but also generate a 'bivalent' construct, where one clone would expressed on one clone on one half of the Fc region and the other clone on the other side of the Fc arm. The co-transfection of two independent plasmids has been carried out to create a fully functional IgG1 antibody [240]. Here, I co-transfected the clone A1, which recognises the active region of the C23 peptide with clones B6 and A6, which recognise the region of the inactive sequence of C23. Together these clones could possibly be able to increase the affinity to prochemerin and prochemerin peptide C23. Additionally, A1 was also co-transfected with clone # 6, which was one of the clones selected from the chemerin pan, that is meant to recognise chemerin. Biacore data suggest that # 6 has low binding affinity to chemerin (data not shown) however, in combination with the A1 clone I was hoping to increase it's binding ability to chemerin. In this instance, it would have acted as a control for clone able to inhibit cleavage.

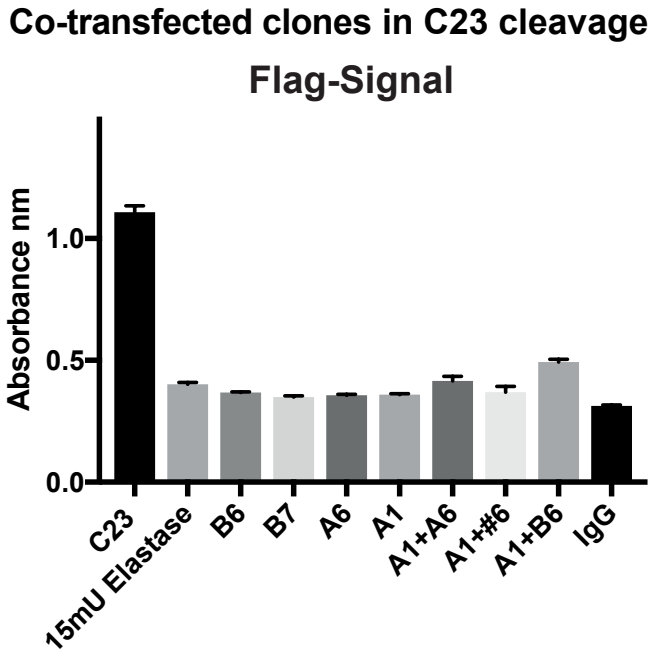


Figure 3.18: C23 Cleavage assay using human neutrophil elastase with co-transfected clones Using human neutrophil elastase(15mU) with 10μg individually expressed clones as well as co-transfection of two plasmids of two individual clones, A1+B6, A1+ # 6, A1+A6. As the individually expressing clones, the co-transfected clones we not able to inhibit the activity of the neutrophil elastase on the C23 peptide.

3.2.2.4 Western blot detection of chemerin within peritoneal lavage fluid

Peritoneal lavage fluid and plasma samples, from mice and humans, under homoeostatic or inflammatory states contains chemerin, see Figure 5.3, 5.2 and [241]. In our experiments the quantification of chemerin was achieved using R& D commercial ELISA kit. Using the group 2 clones, I was interested to assess whether the clones I had developed would be able to detect chemerin or prochemerin in these *in vivo* samples. Samples were run on a 4-15% SDS-PAGE gel and incubated with clone A6 and B6, and a commercial anti-chemerin monoclonal. As a control, I also ran a 15μg of recombinant chemerin (R&D), but neither the commercial monoclonal nor the A6 and B6 clones were able to detect it. The ponceau S protein stain of the membrane, following the transfer, reveals that there was much less protein in the lane with the recombinant chemerin. This could explain the lack of bands seen in lane 4 by all 3 antibodies used. Figure 3.19a, depicts most of the gel after incubation with clone B6. It is clear that there is a lot of non-specific binding by the in-house clones, within the peritoneal fluid. Chemerin is between 16-18kDa in size [153], however, the prochemerin may have a higher molecular weight, hence in Figure 3.19b, I have highlighted the two bands seen at 17kDa and 22kDa for clones A6 and B6. The commercial monoclonal shows bands at 16kDa. This could potentially mean that the clones, A6 and B6, are binding prochemerin. However, they could also be binding non-specifically to other proteins of a similar molecular weight present in the peritoneal fluid, as there is not differences in the band density between the $CCRL2^{-/-}$ and WT samples (2,3 respectively) during inflammation. The commercial monoclonal displays higher levels of chemerin in the WT.

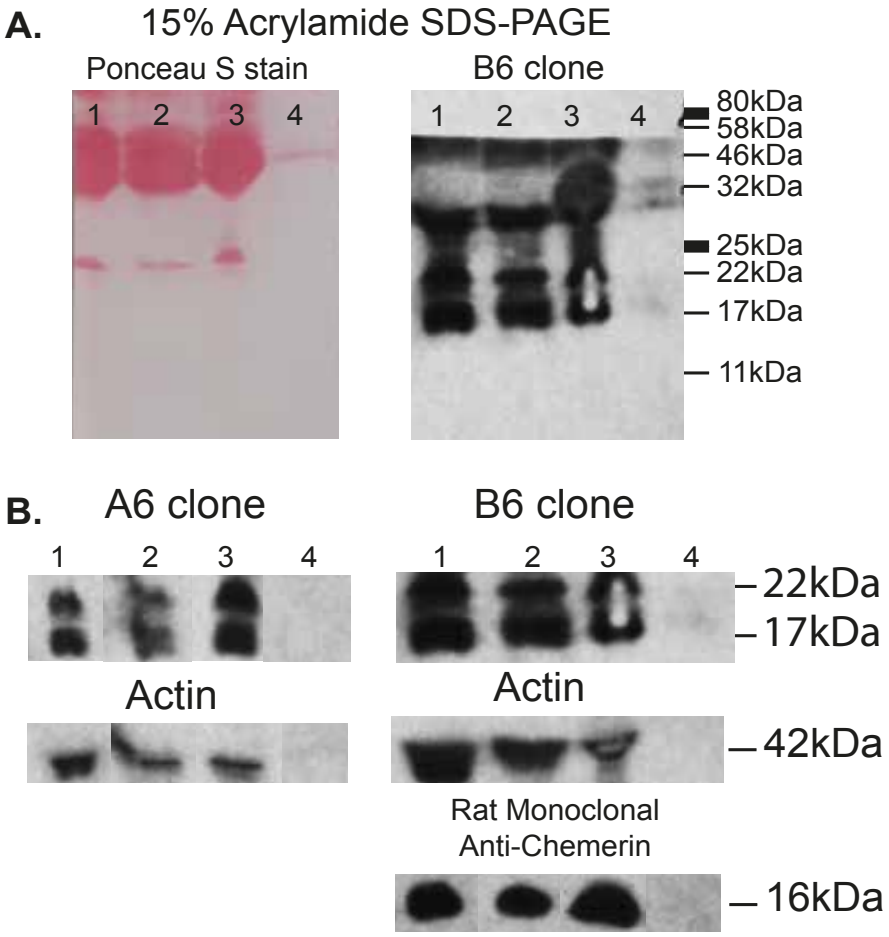


Figure 3.19: Chemerin in peritoneal lavage fluid from mice, on 15% Acrylamide SDS-PAGE, revealed by rat monoclonal, clones A6 and B6. Samples 1-3 are all peritoneal lavage fluid; 1.129S6 WT under naive conditions, 2. CCRL2 -/- 2hr ZIP, 3. 129S6 WT 2hr ZIP and 4. 15μg of recombinant chemerin (R& D). A. 15% Bis-Acrylamide SDS-PAGE gel with Ponceau S stain, B6 clone, showing low specificity across the peritoneal lavage samples, and no binding to recombinant chemerin. B. 15% Bis-Acrylamide SDS-PAGE gel (with no β-mercaptoethanol in samples) with A6, B6, commercial monoclonal anti-chemerin(R& D) and actin. For all the blots the recombinant chemerin is not revealed.

3.3 Discussion

The main aim of this study was to develop antibodies to detect murine prochemerin$^{20\text{-}162}$, murine chemerin$^{20\text{-}156}$ and C-terminus derived peptides$^{140\text{-}156}$. To achieve this, I panned UCB naive phage display library against recombinant active chemerin and a prochemerin peptide C23, which allowed for the selection of clones that recognised the 'active' sequence and the 'inactive' sequence of the C-terminus of prochemerin. With these clones, I had hoped to be able to quantify chemerin and prochemerin from *in vivo* samples, inhibit the activity of chemerin and C-terminal derived peptides at the

ChemR23 receptor and inhibit the cleavage of prochemerin to chemerin. I conclude that, most likely due to low binding affinity and lack of specificity, these scFv clones did not display functional activity nor did they allow the quantification of chemerin isoforms from *in vivo* samples.

Phage display is a quick and useful method of *in vitro* antibody discovery, which was the reason for employing this method to develop the antibodies of interest for this study. There are a myriad of anti-chemerin antibodies commercially available yet they do not distinguish between the different isoforms of chemerin. The chemerin literature is lacking an effective set of tools to distinguish between the various proteolysed produces of chemerin during inflammation. Without the correct tools, conflicting conclusion are reached [176, 207]. Given the nature of chemerin proteolysis during inflammation, it would be a useful contribution to the field to have tools to detect the active or inactive isoforms of chemerin. Furthermore, these tools could reveal the function of the isoforms and the natural proteolytic cascades chemerin undergoes.

Phage display panning is a simple method, used to isolate specific binders to the antigen target of interest. Repeated rounds of antigen exposure to the phage library allows the enrichment of higher affinity binding phage from within the library [242]. This is the reason there are low numbers of phage binding chemerin being detected in round 2 compared to round 3 phage output, 6 and 93 respectively (Figure 3.2).

Advances in library construction have resulted in theoretical diversity surpassing 1×10^{10} [243, 244]. The diversity for UCB's naive library, following induced combinatorial diversity of the heavy and light chains by electroporation, created a total of 2×10^{11} sequences in the library with highly diverse variable regions (data unpublished). This could be why I detected a high number of unique hits, 103 hits, from the preliminary ELISA in both the chemerin and C23 peptide panning (Figure 3.2, 3.4). The first biacore SPR analysis, where the phage-scFv were constructed onto a IgG1 format, was necessary for selecting the binders for the C17 and C23 peptides. Unfortunately, in this instance, the clones were not tested against the full length mchemerin. The binding profiles were re-analysed in the scFv-Fc construct format. I was able to obtain values for the dissociation constants to address the binding affinities of the selective clones. The Kd values were calculated using a Two-site binding analysis. When both portions of the scFv-Fc construct become engaged, the stronger Kd value (Hi) is generally in the nanomolar range; this is considered a moderate to high affinity for an antibody [245]. The weaker Kd value (Lo) generated in this analysis signifies the engagement of one scFv from the Fc portion; this value was generally in the micromolar range, which is considered low affinity binding.

The concentration of chemerin, used in Biacore 3000 assay for immobilisation on the CM5 chip was 62.5nM (Figure 3.8) in this instance, there was weak to moderate chemerin binding. However, the chemerin-binding ELISA does not display binding by Group 1 clones which bind in the SPR. Even though chemerin is immobilised to plastic, the concentration is much lower at 2nM, which could account for the discrepancy. Moreover, the reverse set up in the SPR resulted in low affinity binding to chemerin (33nM) (data not shown). Additionally, free chemerin was not blocked by the Group 1 clones to inhibit activity at the ChemR23 receptor. This suggests that the immobilisation of chemerin at high concentrations may have enabled binding by these clones. Similar results seen with the C17 peptide or streptaviden bound peptide, with no inhibitory effects observed (Figure 3.13, 3.14). Due to the limited amount of purified antibodies produced, I did not perform a titration of chemerin and C17 peptide against one concentration of the clones. This would have revealed whether the concentrations selected was optimal for antibody activity and binding.

The inhibition of elastase cleavage activity against the C23 peptide, was also investigated using the Group 2 clones. Blocking the cleavage of prochemerin into active chemerin may be of desirable effects in some instances of inflammation. Group 2 clones were good candidates to display this function, according to the SPR analysis (Figure 3.6, 3.9), they identify the inhibitory prochemerin sequence of the C23 peptide. Binding at the cleavage site of the peptide should theoretically inhibit protease activity of proteases such as neutrophil elastase. Early studies of this assay revealed that clone B7, was able to inhibit the activity of human neutrophil elastase, by maintaining the FLAG signal on the C-terminus of the peptide. However, multiple attempts to recapture this effect failed (Figure 3.17). In order to confirm that the protease activity was not cleaving the peptide sequence downstream, I used one of Group 1 clone, A1, to identify the active region of the C23 peptide. This revealed that, cathepsinG was able to cleave the active sequence of C23 peptide, where as elastase processing maintained the active sequence of C23 (Figure 3.17).

The use of antibodies to inhibit the cleavage of proteins has previously been reported to show promising therapeutic applications in cancer, viral cell cyle and Alzheimer's disease [246, 247, 248]. Trastuzumab is one such humanised monoclonal antibody, used therapeutically in the treatment for breast cancer. Trastuzumab target HER-2, a member of the epidermal growth factor receptor tyrosine kinase family. A subset of breast cancer patients over express HER-2 receptor, this overexpression correlates with poor breast cancer prognosis [249]. HER-2 undergoes proteolytic cleavage

that results in the release of the extracellular domain and the production of a truncated membrane-bound fragment, called p95. The phosphorylation of p95 stimulates growth and proliferative response in the cancer cell [250]. The proteolytic cleavage of HER-2 receptor is induced by a matrix metalloprotease activator called APMA [251]. Treatment with trastuzumab or a broad-spectrum metaloprotease inhibitor blocks the basal and induced HER-2 cleavage and consequently the p95 phosphorylation. This inhibitory effect of the trastuzumab is not shared by another antibody which recognises a different epitope of the HER-2 [251]. Overall the treatment of trastuzumab inhibits the expression of HER-2 receptor and the growth of HER-2 expressing breast cancer cells [249]. Furthermore, a couple of studies have developed antibodies against the cleavage site of amyloid precursor protein, to prevent the over accumulation of amyloid β peptide, a characteristic neuropathological feature of the Alzheimer's disease. An IgG2 antibody as well as various intrabodies have been developed to inhibit the cleavage activities of β-secretase by steric hindrance due to binding on the cleavage site on the precursor [252, 248]. Intrabodies, which in this study were in a scFv format are able to bind intracellular amyloid precursor protein, where as the IgG2 antibodies can only prevent membrane bound cleavage [252, 248]. Intrabodies are becoming promising therapeutic tools in neurodegenerative diseases, such as Parkinson's and Huntington's disease [253]. Intrabodies include single chain Fv (scFv), single-domain antibodies (VH or VL) or camelid nanodies, containing a a heavy-chain-only fragment (VHH). The manipulation of disulfide bonds within intrabodies ensures their stability within the cytoplasm of cells [254]. Phage display technology has played a key part to the development of many of these reagents[253].

One of the aims of my investigations was to develop an antibody that could recognise the inactive sequence of prochemerin for quantification in *in vivo* samples. However, the binding specificity of the clones was also revealed as being low. The treatment of group 2 clones, A6 and B6 on a SDS-PAGE containing *in vivo* peritoneal samples, revealed bands in the expected molecular weight of chemerin and prochemerin (16-22kD) but also in multiple bands at higher molecular weights. This reduces the possibility that these clones specifically identify prochemerin. Moreover, the commercial ELISA kit reveals changes in the amount of chemerin present in the peritoneum. The amount of chemerin increases slightly in the WT during inflammatory conditions and increases significantly in the *CCRL2*$^{-/-}$ mice during inflammation, seen in chapter 5, Figure 5.2. Furthermore, prochemerin is expected to be present in the peritoneum under naïve conditions [153]. However, in the western blots, no

differences were seen from the A6 and B6 clones in the molecular weight region highlighted. This was also true by the commercial monoclonal antibody, which is likely to be the capture antibody used in the R&D ELISA kit.

The binding affinity and specificity of the selected anti-chemerin clones, from this study, have not been as efficient as desired. However, with the correct manipulation using affinity maturation techniques, phage display technology has been used to develop important immunotherapeutic tools. Mutagenesis of specific regions on selected clones can drastically increase the desired affinity and specificity. Alanine-scanning mutagenesis can be used in order to reveal the relevant residues necessary for binding or function [255], and thus further modification of these can result in more desired effects. Another important method for creating higher binding affinity and specificity is by affinity maturation. The sequences of the variable heavy and light genes from antibody candidates already selected, from a library or an immunisation, are cloned to perform random mutagenesis of the CDR regions or of the full-length of the variable regions. These mutated VH and VL sequences can then be cloned onto phage plasmid vectors to generate a highly diversified and higher quality library for the specific target antigen [255]. Subsequently, the phage display rounds of selection on the target of interest will enrich for strong binders within this library. Bioinformatic analysis of the rescued clones is necessary to ensure the quality of the sequence and to identify residue redundancy within epitode binding sites [255, 256].

Monoclonal antibody therapies are becoming the new generation of commonly used therapy to treat disease. With the above techniques in mind, the creation of phage display libraries is enabling the selection and development of high affinity monoclonal antibodies for therapeutic and diagnostic use [231]. A useful aspect of phage display technology is its use in isolating already existing antibodies in patients with autoimmune diseases. These autoimmune antibodies generated in disease can become useful tools in treatments of other diseases. An example of this is the isolation of antibodies against the $\alpha_{IIb}\beta_3$ integrin from patients suffering from thrombocytopenic purpura (AITP) and polytransfused Glanzmann thrombasthenia (GT). The human platelet membrane glycoprotein IIb-IIIa complex is a member of β_3 subclass of integrin receptors, which mediates platelet aggregation, by binding adhesive proteins to form bridges linking adjacent platelets, thus enabling clotting. The anti-$\alpha_{IIb}\beta_3$ integrin-binding antibodies were isolated from a combinatorial library of scFv created from B cells and serum antibodies of patients from both AITP and GT [257]. It was found that there is molecular diversity of the humoral immune response against $\alpha_{IIb}\beta_3$ integrin within these patients. The $\alpha_{IIb}\beta_3$ antibodies isolated from this study

have been preferentially selected against the activated form of the integrin. This would be an attractive therapeutic reagent for acute coronary syndromes. Current $\alpha_{IIb}\beta_3$ antagonists do not specifically recognise the activated form of integrin, thus, causing uncontrollable bleeding in patients [258, 257, 259].

3.3.1 Limitations and future work

The obvious limitation to this study is the lack of high affinity and specificity binding reagents, as illustrated from the SPR analysis of Figure 3.8, 3.9, the functional testing and the western blots of *in vivo* peritoneal exudates. It would be interesting to identify protein bands in the 17-22kDa range that the clones A6 and B6 were binding to within the peritoneal lavage fluid. This could be achieved by cutting the bands out and analysing the proteins present in the mass spectrometer. Moreover, it would be useful to produce our own recombinant prochemerin to run on the SDS-PAGE along side lavage fluid.

Given more time, it would have been interesting to carry out an affinity maturation study, on the C23-binding clones, followed by re-panning against the C23 peptide. This may very well have enhanced the affinity of these clones. Alternatively, immunisation of an animal may be favourable to generate the high specificity, followed by *in vitro* affinity maturation or the creation of a scFv phage display library from the immunised animal to find clones to differenciate between the different forms of chemerin [158, 225].

Another way in which to achieve inhibitory activity of chemerin receptor would have been to develop antibodies directly against the chemerin receptor of interest i.e. ChemR23. After having completed the studies reported in this thesis chapter, Peyrassol *et al.* described the development of two anti-human ChemR23 receptor nanobodies by genetic immunisation of llamas and phage display technology [260]. The engineered bivalent nanobodies were able bind human ChemR23 with moderate efficacy and act as antagonists of chemerin and C9 peptide-induced intracellular calcium mobilisation responses. Furthermore, the fluorescently-labeled nanobodies were able to detect ChemR23 on the surface of human monocyte-derived macrophages and dendritic cells.

Chapter 4

Characterising chemerin receptor expression across leukocyte subsets

4.1 Introduction

Chemerin is a chemoattractant ligand with reported pro and anti-inflammatory properties during inflammation. Chemerin also plays a significant role in adipocyte differentiation and angiogenesis. These actions of chemerin are mediated through 3 GPCR receptors, these being: ChemR23(also known as CMKLR1), GPR1, and CCRL2 (also known as HCR, CRAM-A or-B, ACKR5). ChemR23 and GPR1 are both classic G αi signalling GPCR receptors and CCRL2 is a non-signalling receptor.

4.1.1 Chemokine-like receptor 1 (ChemR23)

The ChemR23 receptor shares nucleotide homology with chemokine and complement receptors. Chemerin signalling via ChemR23 receptor induces is classic downstream GPCR signalling which ultimately leads to the chemotaxis of ChemR23$^+$ cells [153].

ChemR23 is expressed on a broad range of murine tissues associated with haematopoietic and immune function, including: thymus, bone marrow, spleen and lymphoid organs [261, 262]. Its expression is also detected on variety of human and murine leukocytes including the monocyte-derived macrophages, immautre dendritic cells, plasmatocytoid dendritic cells (pDCs), natural killer (NK) cells [163]. NK cell and pDCs are key immnue cells for anti-viral immunity and both cells types migrate to inflamed tissue in a ChemR23 induced manner [206, 205].

As well as leukocytes, non-leukocyte cells also express the ChemR23 receptor. Adipocytes express ChemR23 receptor and high levels of chemerin. In these cells, chemerin is important in inducing adipocyte differentiation and in regulating lipid and glucose homeostasis [263, 215, 264]. Human endothelial cells upregulate their

ChemR23 expression by treatment with pro-inflammatory cytokines [218]. During proinflammatory conditions, chemerin induces the production of metalloproteases and promotes angiogenesis via ChemR23 receptor [218] vascular endothelial cells [168]. ChemR23 is also detected in oral and lung epithelial cells [130, 176], osteoclasts [265], vascular smooth muscle cells [124, 266]. Finally, ChemR23 receptor influences the proliferation and migration of vascular smooth muscle cells[124, 266].

The ChemR23 receptor has been detected via mRNA and protein expression. Protein expression has been identified using both anti-human and anti-mouse ChemR23 commercially antibodies enabling both flow cytometry, western blot and immunohistochemistry (IHC). This is in addition to the RT-qPCR techniques for the detection of receptor mRNA.

4.1.2 G protein coupled receptor 1 (GPR1)

GPR1 is another receptor for chemerin and shares 40% sequence homology with ChemR23 [267, 268]. Chemerin binding induces receptor internalisation, phosphorylation of ERK1/2 MAP kinase and induces calcium mobilisation to a lesser extent than ChemR23 and predominantly induces β-arrestin2 activation [154, 164]. GPR1 is expressed in the central nervous system, skin, smooth muscle cells, and adipose tissue, predominantly by the non-adipocyte stromal vascular fraction [267, 268, 169, 168, 170]. Both mRNA and protein expression of GPR1 expression has been reported in the past [170, 168]. The protein expression of GPR1 receptor has been identified using anti-GPR1 commercially antibodies which enable both western blot and immunohistochemistry (IHC) [168]. There is limited information about it's functions upon chemerin binding, as it is the least studied receptor out of all the chemerin receptors.

4.1.3 CC-Chemokine receptor-like 2 (CCRL2)

CCRL2 is a non-signalling receptor that binds chemerin with low nanomolar affinity and does not convey any downstream signalling or chemerin internalisation [164]. The mRNA expression of CCRL2 was first described in primary neutrophil, monocytes and differentiated macrophages [172]. However, mRNA studies have shown that it is widely expressed in many tissues on leukocyte and non-leukocyte subsets. Exposure to inflammatory stimuli, results in CCRL2 upregulation by cells expressing the receptor [173]. For more detailed information on the expression and role of CCRL2 during inflammation, go to Chapter 5.1. For a long time, the expression of CCRL2 was only

detectable by quantitative PCR, and most protein expression was detected by in-house developed antibodies [155]. However, very recently there have been numerous human and mouse anti-CCRL2 antibodies released commercially and one clone has already been used to detect CCRL2 in a recent publication [184].

4.1.4 Rationale of study

The chemerin binding receptors are widely expressed throughout haematopoietic and non-haematopoietic tissues, in both immune and non-immune cells. Previous work has illustrated that chemerin plays a role in inflammatory disease pathologies. Therefore, in order to aid my investigations into addressing the role of chemerin and its receptors in acute inflammation, the objective for this chapter was to characterise the protein expression of ChemR23 on murine leukocyte subsets, and to investigate the mRNA expression of ChemR23, GPR1 and CCRL2 receptors in murine immune cell subsets and tissues.

4.2 Results

4.2.1 Bone marrow derived macrophages

Macrophages play a key role in a plethora of immune pathologies, due to their ability to orchestrate the inflammatory response against pathogens and their role in restoring tissue homeostatis [269]. Monocyte-derived human macrophages were some of the first cells shown to express ChemR23 and CCRL2 receptors [262, 153, 173]. Bone marrow derived macrophages (BMDM) are a pure *in vitro* cultured population of macrophages, as seen in Figure 4.1a. The protein expression of the ChemR23 receptor is detected on 7 day cultured BMDM using flow cytometry. Sixteen hour treatments of LPS (0.1μg/ml) and IL-4 (20ng/ml) displayed no significant differences in the expression of ChemR23 receptor compared to basal (Figure 4.1b,c). Furthermore, the mRNA expression of the chemerin receptors, ChemR23, GPR1 and CCRL2, was analysed in 7 day cultured BMDM following 16 hour exposure to various TLR and cytokine ligands. These mRNA samples were a kind gift from Dr Carlota Recio. The expression of ChemR23 is variable between individual experiments, hence, the large standard error in both mRNA and geometric mean fluorescence. ChemR23 tends to be upregulated by IL-13, LPS/IFNγ, PolyI:C and zymosan (Figure 4.1d) with large error bars. The mRNA expression of CCRL2 is significantly unregulated in LPS, LPS/IFNγ, PolyI:C and zymosan treatment in BMDM (Figure 4.1e).

4.2.2 Bone marrow derived dendritic cells

Dendritic cells play a prominent role as sentinels and antigen presentation cells. Studies have shown that ChemR23 and CCRL2 receptors are expressed on dendritic cell subsets, which suggests that their functions may be influenced by chemerin signalling [153, 176, 205, 182]. Bone marrow derived dendritic cells (BMDC) are cultured by 7 day *in vitro* culture of bone marrow cells in GM-CSF enriched media. On day 6 dendritic cells are matured by an overnight treatment of LPS (1μg/ml). Specific dendritic cell markers are used to compared the tissue cultured immature and matured BMDC (Figure 4.2). Mature BMDC show downregulation of CD11c, upregulation of MHC-II and CD80, as described in [270]. The ChemR23 protein expression shows no major difference between matured and immature BMDC (FIgure 4.2c). Other studies have reported a reduction in the expression of ChemR23 by matured dendritic cells, therefore I wanted investigate the responsiveness of immature and matured BMDCs to chemerin in a real-time 96 well ACEA ECIS impedance assay (Figure 4.2d). This impedance system provides a real-time measure of the cytoskeletal rearrangements upon GPCR activation (validated by Dr Gemma White, personal communication). The response to chemerin (10nM) shows no difference between immature and mature BMDC, confirming the flow cytometry data in Figure 4.2c. However, the mature BMDC response to C5a, an anaphylatoxin and a potent chemoattractant, displays a decreased signal. The expression of C5aR is downregulated upon LPS maturation [271, 272], which could explain the decreased response C5a in impedance assay, seen in Figure 4.2e.

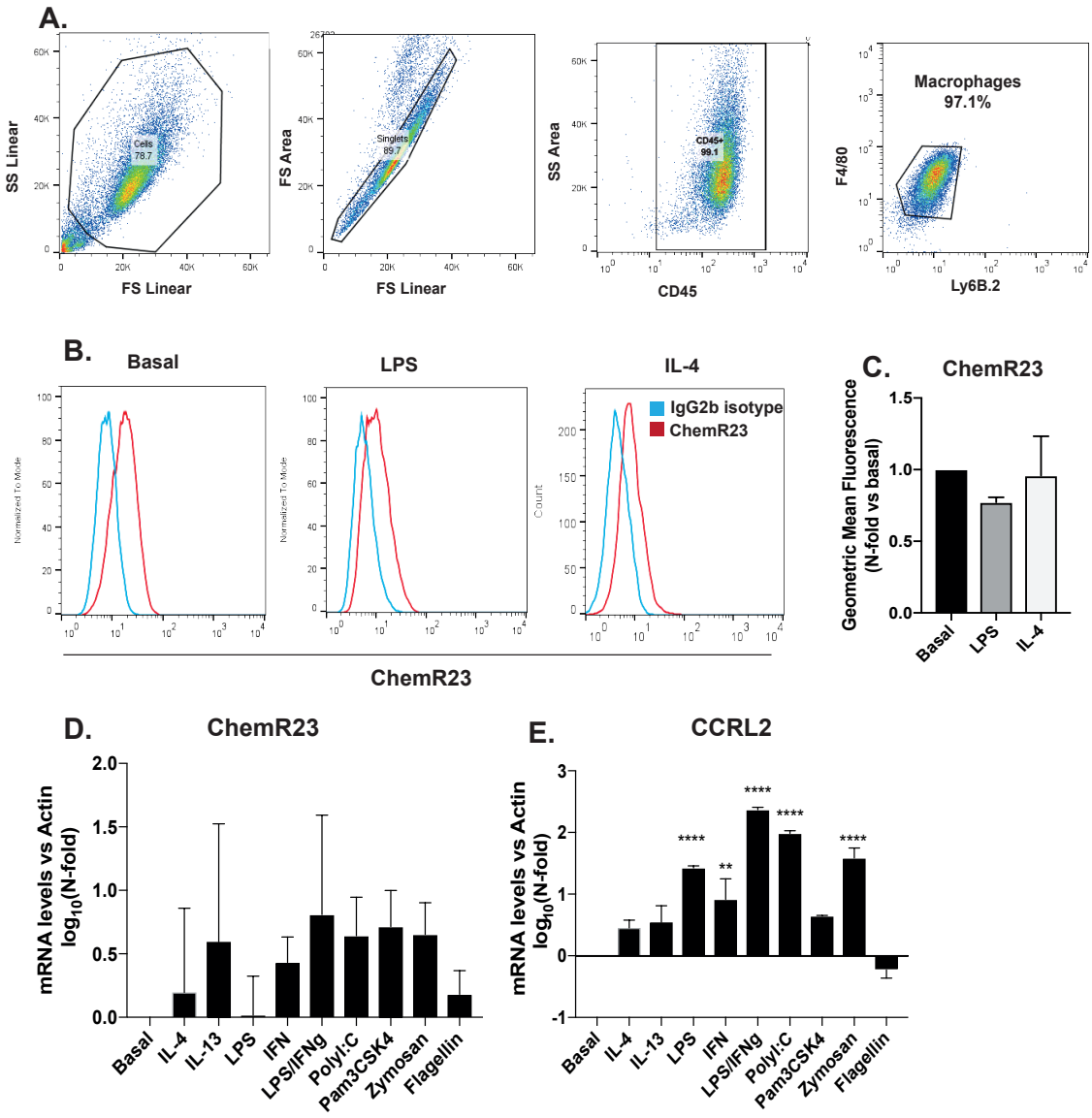


Figure 4.1: ChemR23 and CCRL2 receptor expression on bone marrow-derived macrophages. Day 7 cultured bone marrow derived macrophages (BMDM) were grown in L929 cell-conditioned media. **A.** Representative flow cytometry plots of macrophage linage analysis. **B.** Representative histogram plots of ChemR23 receptor expression on BMDM under basal conditions, 16 hour treatment of LPS (0.1μg/ml) and IL-4 (20ng/ml). **C.** Geometric mean fluorescence of ChemR23 expression on BMDM varies between treatments. **D-E.** The mRNA levels of ChemR23 and CCRL2 receptors of BMDM stimulated with TLR and cytokine ligands for 16 hours, were obtained by qPCR, normalised to Δcycle value of actin and basal samples. **D.** Treatments show subtle differences in mRNA expression of ChemR23 with IL-13(20ng/ml), LPS/IFNγ(0.1μg/ml and 20ng/ml respectively) and PolyI:C (10μg/ml). **E.** mRNA levels of CCRL2 receptor show significant increases following LPS/IFNγ , PolyI:C and zymosan (10μg/ml) when compared to the basal levels. Error bars represent S.E.M. n=2-4/bone marrow preps. Statistical significance was assessed using an ordinary one-way ANOVA test. $*$ P $\leq$0.05, $***$P$\leq$0.001, $****$P$\leq$0.0001.

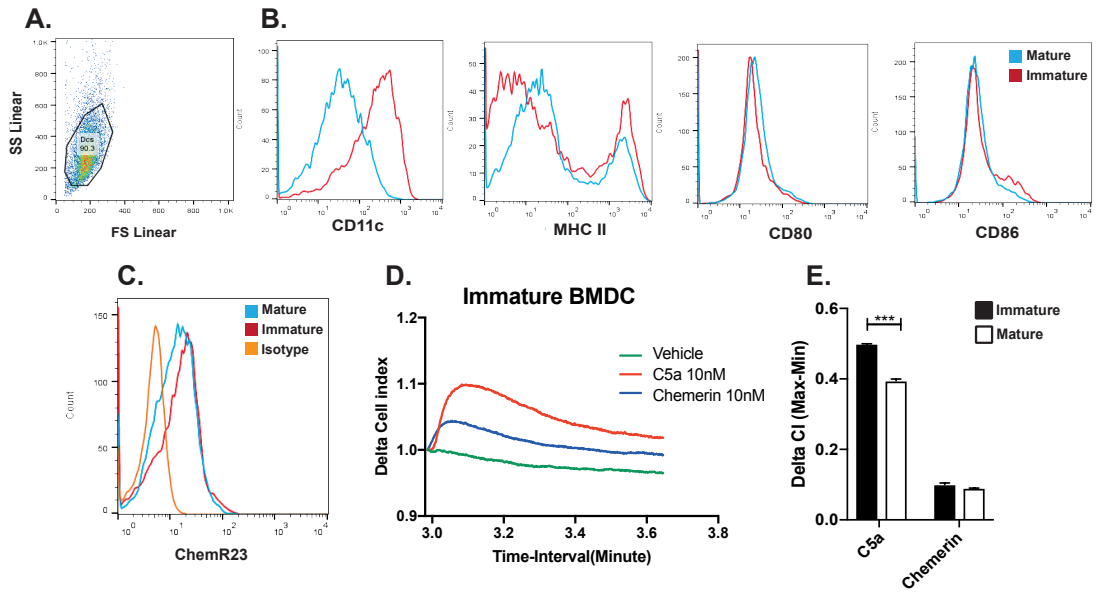


Figure 4.2: ChemR23 expression and function on bone marrow derived dendritic cells. Day 7 cultured bone marrow derived dendritic cells (BMDC) were grown in X63-GMCSF cell conditioned media and maturation of BMDCs was achieved by addition of LPS (1μg/ml). **A.** Representative flow cytometry plots of cultured BMDC. **B.** Representative histogram plots of dendritic cell markers for immature, in red, and mature in blue. **C.** Representative histogram plot of ChemR23 receptor by $CD11c^{+}MHCII^{+}$ immature, in blue, and mature, in red, BMDC show no significant differences in expression. Representative of 3 independent experiments. **D.** Cells were allowed to adhere for 4hrs in 96 well ECIS plates, then treated with 10nM of C5a or Chemerin (R%D). Delta cell index correlate with cytoskeletal re-arrangement and recordings were taken every 5 seconds. Representative traces of immature BMDM stimulation in this system. **E.** The max-min Delta cell index of chemerin stimuation in immature and mature BMDC show no significant difference, where as stimulation with C5a shows a decreased response in mature BMDC. Error bars represent S.E.M. of 2 independent experiments.

4.2.3 Bone marrow isolated Neutrophils

Neutrophils are a pre-eminent member of the innate immune system and are the first line of defence against pathogens in the early stages of the inflammatory process. Due to my interest in studying acute inflammation, I wanted to investigate the expression of chemerin receptors by neutrophils. The bone marrow is a rich source of neutrophils and their isolation is a relatively straight forward process. Using a histopaque centrifugation separation protocol, neutrophils were isolated from WT and *ChemR23*$^{-/-}$ bone marrow, Figure 4.3a. The protein and mRNA expression of the ChemR23 receptor is not detected on WT neutrophils when analysed by flow cytometry and qPCR (Figure 4.3b,c). There is detectable mRNA expression of CCRL2 and minimal mRNA expression of chemerin.

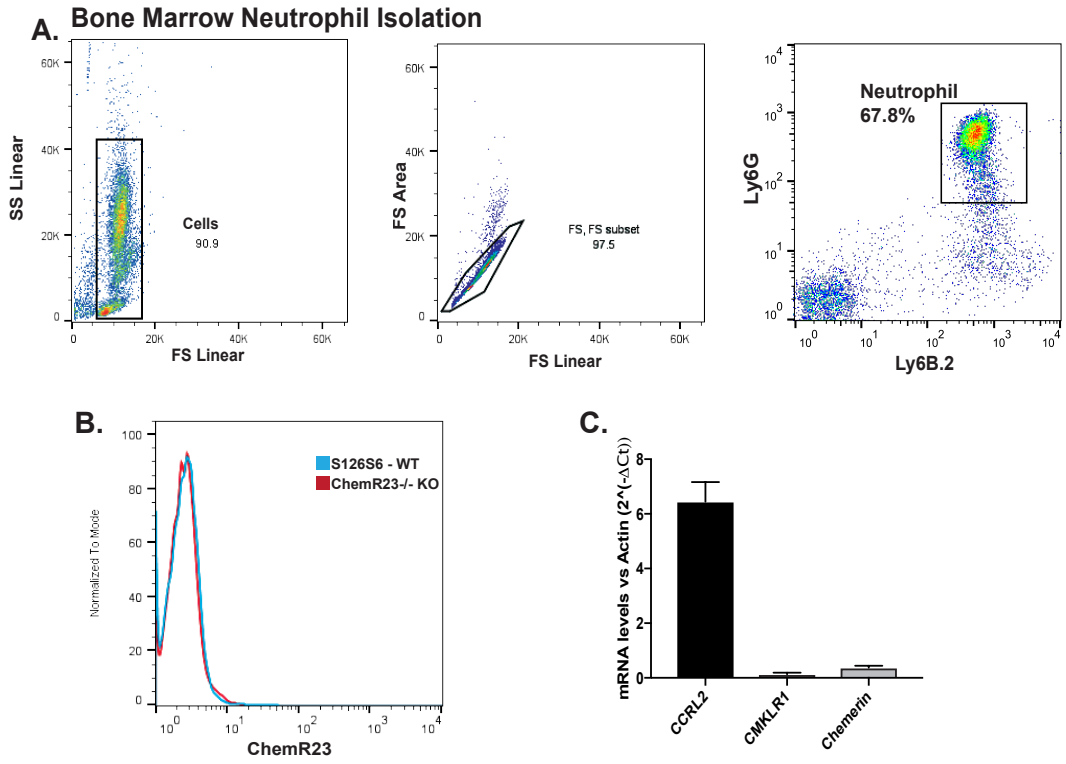


Figure 4.3: ChemR23 receptor expression is not detected on bone marrow neutrophils by flow cytometry and qPCR. 8-10 week old male *ChemR23*-/- and 129S6 WT mice were euthanised and their bone marrow was collected from the tibia and femurs. Bone marrow neutrophils were isolated by a histopaque centrifugation technique. **A.** Representative flow cytometry plots of bone marrow isolated neutrophils. **B.** Bone marrow neutrophils show no ChemR23 receptor protein by flow cytometry. **C.** BM neutrophil mRNA levels of chemerin, CCRL2 and ChemR23 receptors were analysed by Δcycle value of actin in qPCR, from WT mice. The CCRL2 receptor and low levels of chemerin mRNA are detected. However, mRNA levels for ChemR23 receptor are very low. Error bars are S.E.M. of 3 independent WT neutrophil preps.

4.2.4 Blood neutrophils and monocytes

To study a mature population of neutrophils, that has been released from bone marrow, I decided to investigate ChemR23 mRNA expression on blood neutrophils. Blood neutrophil and monocyte populations were sorted by staining with CD45, a pan leukocyte marker, CD11b, a myeloid specific marker, Ly6G and Ly6C (Figure 4.4a,b). Using *ChemR23*$^{-/-}$ blood cells as a control, both neutrophils and monocytes do not display ChemR23 receptor protein expression, Figure 4.4c.

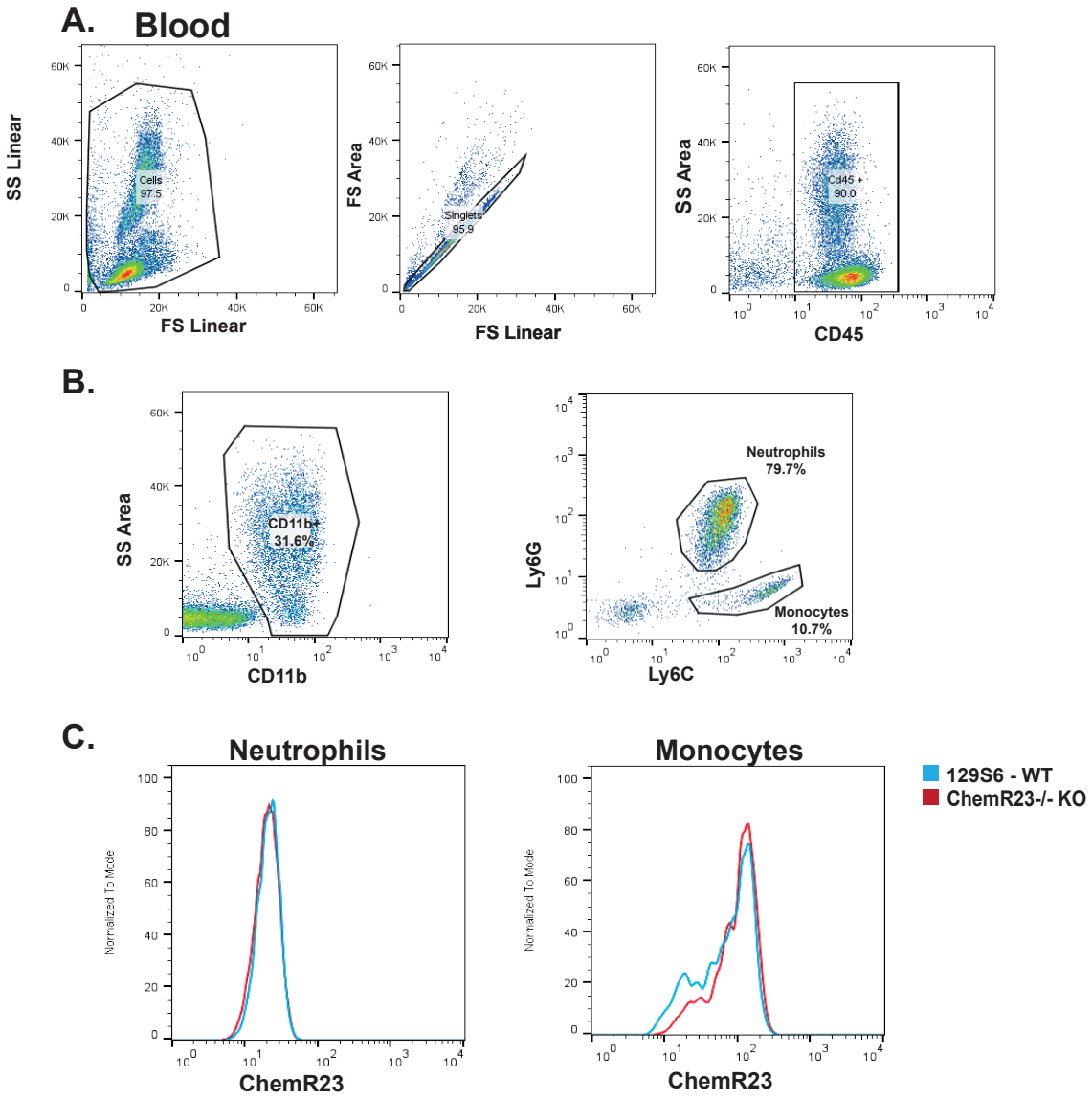


Figure 4.4: Expression of ChemR23 receptor on murine blood neutrophils and monocytes. 8-10 week old male *ChemR23*-/- and 129S6 WT mice were euthanised and blood was collected via the posterior vena cava in EDTA coated tubes. **A.** Representative flow cytometry plots for murine blood using pan-leukocyte marker CD45. **B.** Representative flow cytometry plots of murine blood neutrophils and monocytes, by CD11b, Ly6C and Ly6G cell markers from $CD45^+$ cells. **C.** Blood neutrophils and monocytes, from WT in blue, do not show expression of ChemR23 when compared to *ChemR23*-/- in red. Representative of 3 animals/group.

4.2.5 Bio-gel elicited peritoneal cells

The peritoneal cavity provides an easily accessible site for harvesting moderate numbers of resident peritoneal macrophages in mice. The purification of large numbers of elicited macrophages is usually achieved by the injection of Bio-gel polyacrylamide beads into the peritoneal cavity, which produces an mild inflammatory response

[273, 274]. Although Bio-gel is typically used for eliciting macrophages at 4 day post injection, I noticed a large number of neutrophils in the Bio-gel elicited peritoneal cells, as seen in Figure 4.5a. These elicited peritoneal cells allowed me to determine the protein expression of ChemR23 receptor in a mixed population of recruited cells. The macrophages and monocytes, in 4 day of Bio-gel injection, express ChemR23 receptor, whereas the recruited neutrophils do not. The mRNA levels of the ChemR23 and CCRL2 receptors are highly expressed in this mixed cell population, while the levels of chemerin are very low. Finally, the lack of the CCRL2 receptor does not affect the expression pattern of ChemR23 by the macrophages, monocytes and neutrophils in these elicited peritoneal cells (Figure 4.5d).

4.2.6 Resident populations of cell in the peritoneum

The peritoneal cavity consists of a diverse population of resident leukocytes. Approximately 70% of the resident leukocyte population are F4/80^{+} macrophages. Resident peritoneal macrophages express high protein levels of the ChemR23 receptor, Figure 4.6b. Moreover, there is a subset of resident dendritic cells, which also express the ChemR23 receptor (Figure 4.6c). Peritoneal lavage also consists of B and T cells, approximately 15% and 5% of the total leukocytes respectively. CD19^{+}MHCII^{+} staining was used to identify B cells and CD3^{+}MHCII^{-} for the T cell population. Neither B nor T cells express the ChemR23 receptor in the peritoneum by flow cytometry (Figure 4.6c).

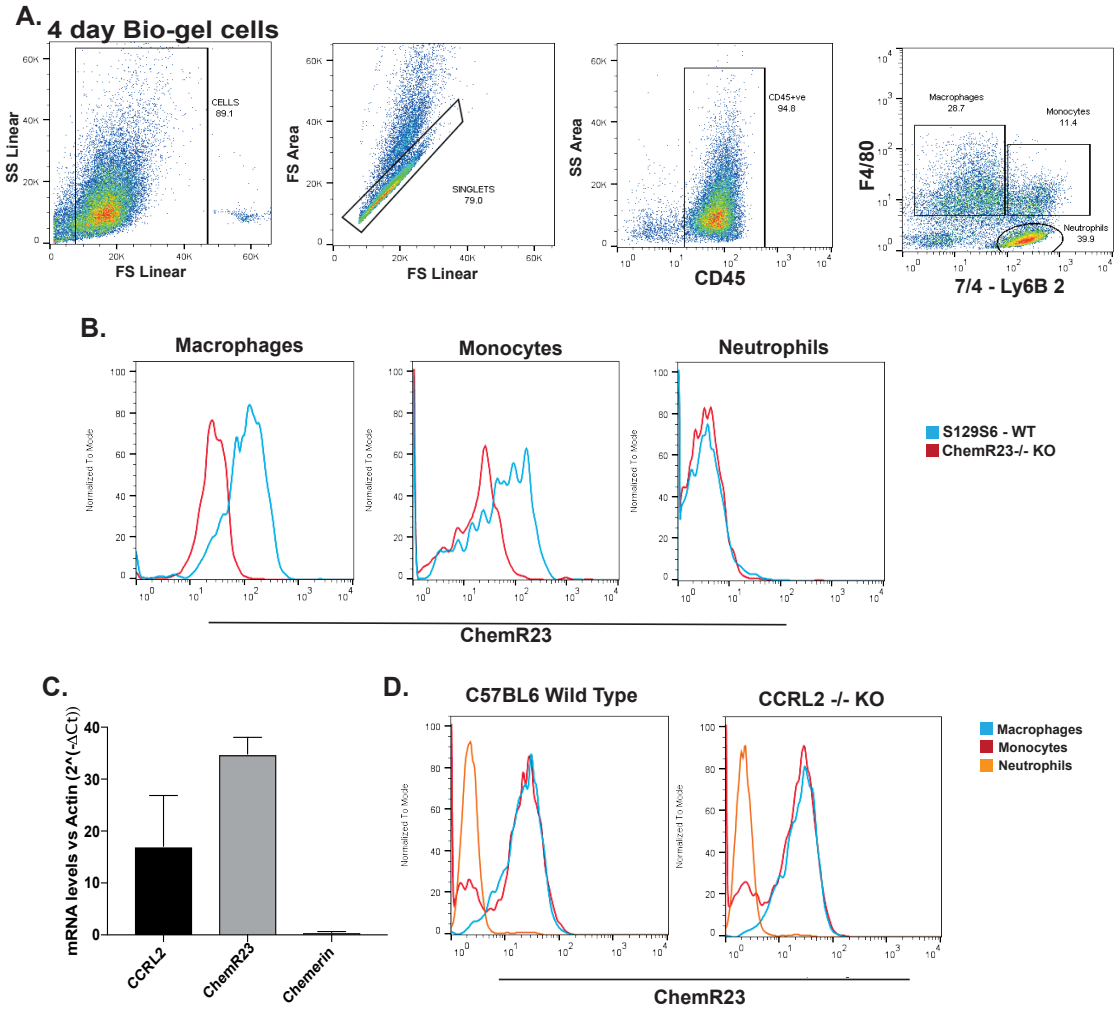


Figure 4.5: ChemR23 receptor expression on macrophage and monocyte populations but not on neutrophils in day 4 bio-gel elicited peritoneal cells. 8-11 week old male WT or otherwise specified genotype of mice were injected i.p. with 2% Bio-gel (polyacrylamide beads), and sacrificed 4 days later. Peritoneal cavities were lavaged with ice-cold PBS supplemented with 2mM EDTA. **A.** Representative flow cytometry plots of cell populations from 4 day bio-gel peritoneal cells. **B.** Representative histogram plots of positive staining for the ChemR23 receptor on macrophages and monocytes, and negative staining for the ChemR23 receptor on the neutrophil population when comparing WT, in blue, to *ChemR23*-/- mice, in red (n=2/group). **C.** mRNA expression of chemerin receptors and chemerin were analysed by qPCR from WT bio-gel elicited peritoneal cells. ChemR23 showed highest mRNA expression normalised to the ΔCt of actin. Error bars represent S.E.M. of 2 individual WT. **D.** Bio-gel elicited peritoneal cells from C57BL6 WT and *CCRL2*-/- mice also showed ChemR23 expression on macrophage and monocytes (n=2/group).

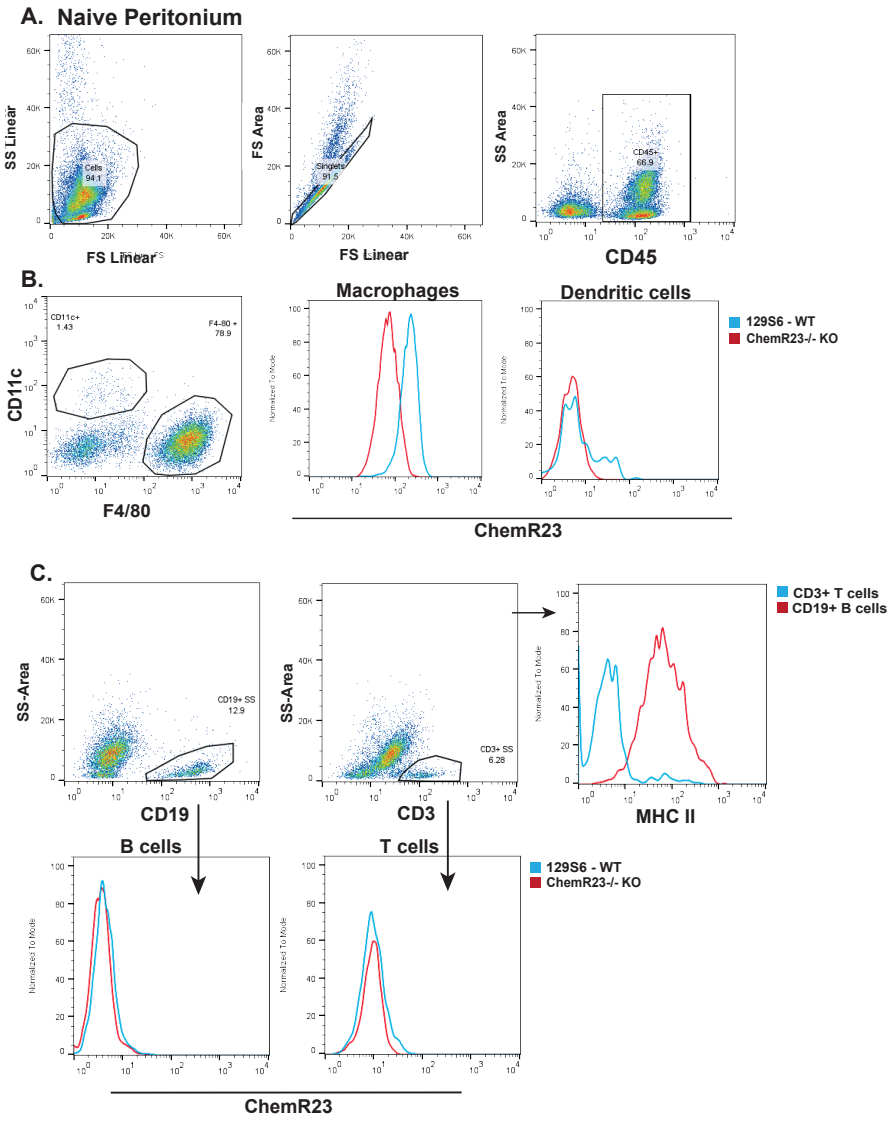


Figure 4.6: ChemR23 receptor is expressed on peritoneal macrophage and dendritic cells under naive conditions. 8-10 week old male *ChemR23*-/- and 129S6 WT mice were euthanised, their peritoneal cavities were lavaged with ice-cold PBS supplemented with 2mM EDTA and peritoneal cells were stained for flow cytometry. **A.** Representative flow cytometry plots of peritoneal cells sorted for CD45 pan-leukocyte marker. **B-C.** Histograms illustrating ChemR23 receptor on selected population of cells with 129S6 stain WT, in blue compared to *ChemR23*-/- in red. **B.** After sorting for CD45 positive cells, ChemR23 receptor expression was seen on macrophage and dendritic cell populations, identified using a F4/80 and CD11c stain. **C.** After sorting for CD45 positive cells, B cells and T cells showed no ChemR23 expression. B cells and T cells were identified by CD19 and CD3 respectively, which were confirmed by the expression of MHCII on B cells, in red and T cells in blue.Representative of 3 animals/group.

4.2.7 mRNA expression of Chemerin and Chemerin receptors in murine tissues

Wanting to confirm and extend published reports, I did a small survey of the mRNA chemerin and chemerin receptor expression in tissues from wild type mice by qPCR; the tissues included were liver, lung, small intestine, fat, large intestine, kidney and spleen. These mRNA samples were generously provided by Dr. Carlota Recio. CCRL2, ChemR23 and chemerin are expressed in all the tissues tested. The genes of interest were normalised to the average of cycle value of 3 housekeeping (HK) genes from each tissue sample; these were β-actin, 18S, and GAPDH, as described in [275]. Both CCRL2 and ChemR23 are highly expressed in the lung and fat. CCRL2 is also expressed in kidney and spleen at a moderate level. Chemerin is highly expressed in liver, lung and fat as previously reported. Finally, GPR1 is only detected in fat of these samples and in low levels in lung and large intestine.

4.2.8 Protein expression of ChemR23 receptor on resident leukocytes subsets

4.2.8.1 Lung tissue

Previous studies have shown that lung tissue expresses chemerin and its receptors and that the ChemR23/chemerin system plays a role during lung inflammation [176, 178, 181]. In Figure 4.7, I also found that there were large amounts of mRNA of ChemR23 receptor expressed in the lung. Therefore, I wanted to survey the expression of ChemR23 receptor by resident leukocyte subsets in the lungs, using flow cytometry. Resident lung macrophages, stained positive for SiglecF$^+$ CD11c$^+$ F4/80$^+$, do not express the ChemR23 receptor. CD11b$^+$ cells neutrophil and monocytes, identified by Ly6G and Ly6C staining, also do not express ChemR23 receptor. Finally, ChemR23 is not detected on resident T and B cells in the lung.

4.2.8.2 Liver tissue

The liver is an important sensory organ for pathogen or tissue damage recognition [276]. It is also a significant chemerin producing organ [277] which is confirmed in Figure 4.7c. Hence, I was interested in assessing the ChemR23 expression by resident leukocyte subsets in the liver, using flow cytometry. CD11b selected myeloid cells, were selected to identify macrophages and dendritic cells residing in the liver, F4/80$^+$ and CD11c$^+$ respectively. Both populations do not express the ChemR23 receptor. Within the CD11b$^+$ cells, neutrophils and monocytes in liver tissue, were

also identified by Ly6G and Ly6C markers. ChemR23 expression on both populations is negative. Finally, T and B cells, residing in the liver, identified by B220 and CD3 staining, also do not express ChemR23 receptor by flow cytometry.

4.2.8.3 Spleen tissue

The spleen is a key organ for iron metabolism and erythrocyte homeostasis. However, it also plays a cruicial role as a secondary lymphoid organ by enabling the innate and adaptive immunity to engage an appropriate immune response [278]. In Figure 4.7, I found that mRNA of chemerin and its receptors CCRL2, and ChemR23 were expressed in the spleen. For this reason, I was interested in identifying possible leukocytes subsets resident in the spleen that expressed the ChemR23 protein receptor. Spleen leukocytes were selected by CD45 marker in the flow cytometric analysis, as seen in Figure 4.10a. Dendritic cells and macrophages resident in the spleen, selected by $CD11c^+$ and $F4/80^+$ markers respectively, demonstrated no ChemR23 expression. Furthermore, B and T cells selected by CD19 and CD3 staining and confirmed with $MHCII^+$ staining on the B cells, showed no ChemR23 receptor expression (Figure 4.10c).

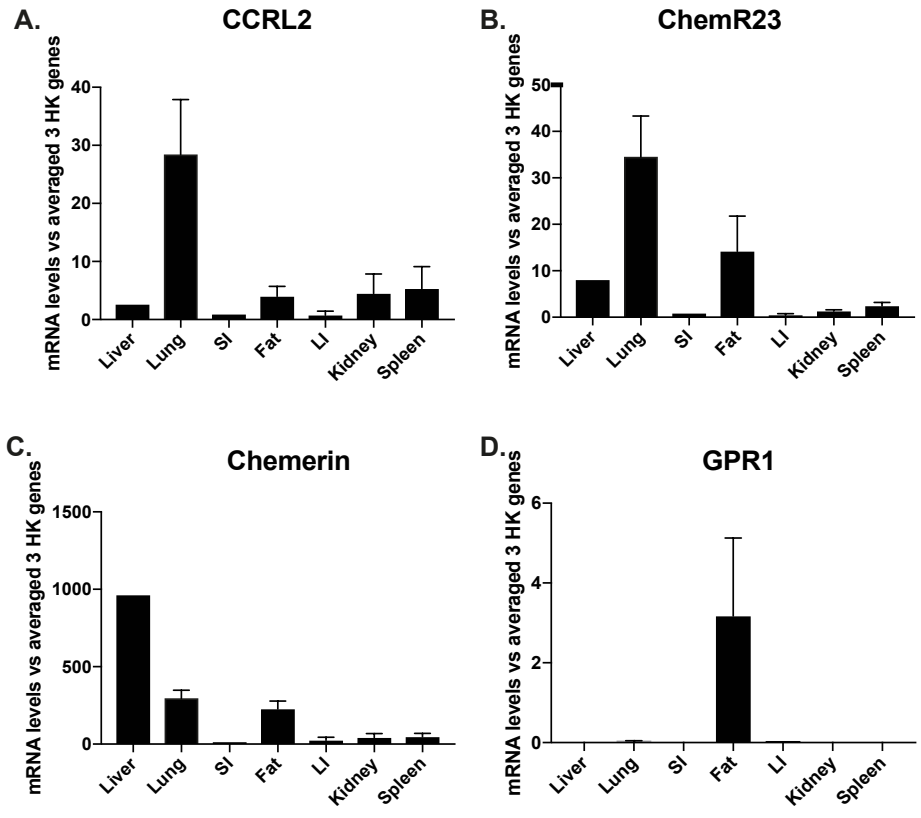


Figure 4.7: The mRNA expression of chemerin and chemerin receptors in murine tissues. 8-10 week old male WT mice were sacrificed and tissues were collected for mRNA extraction with RNA isolation kit (Qiagen). The mRNA levels of chemerin and its receptors were assessed by qPCR, and normalised to the average Ct value of 3 housekeeping(HK) genes. **A.** The CCRL2 receptor mRNA expression is highest in lung tissue. **B.** The ChemR23 receptor mRNA expression is highest in lung and fat tissue. **C.** The chemerin mRNA expression is highest in liver then lung and fat. **D.** GPR1 mRNA expression is highest in fat followed by low expression in the large intestine. Error bars represent S.E.M. of 3 WT mice.

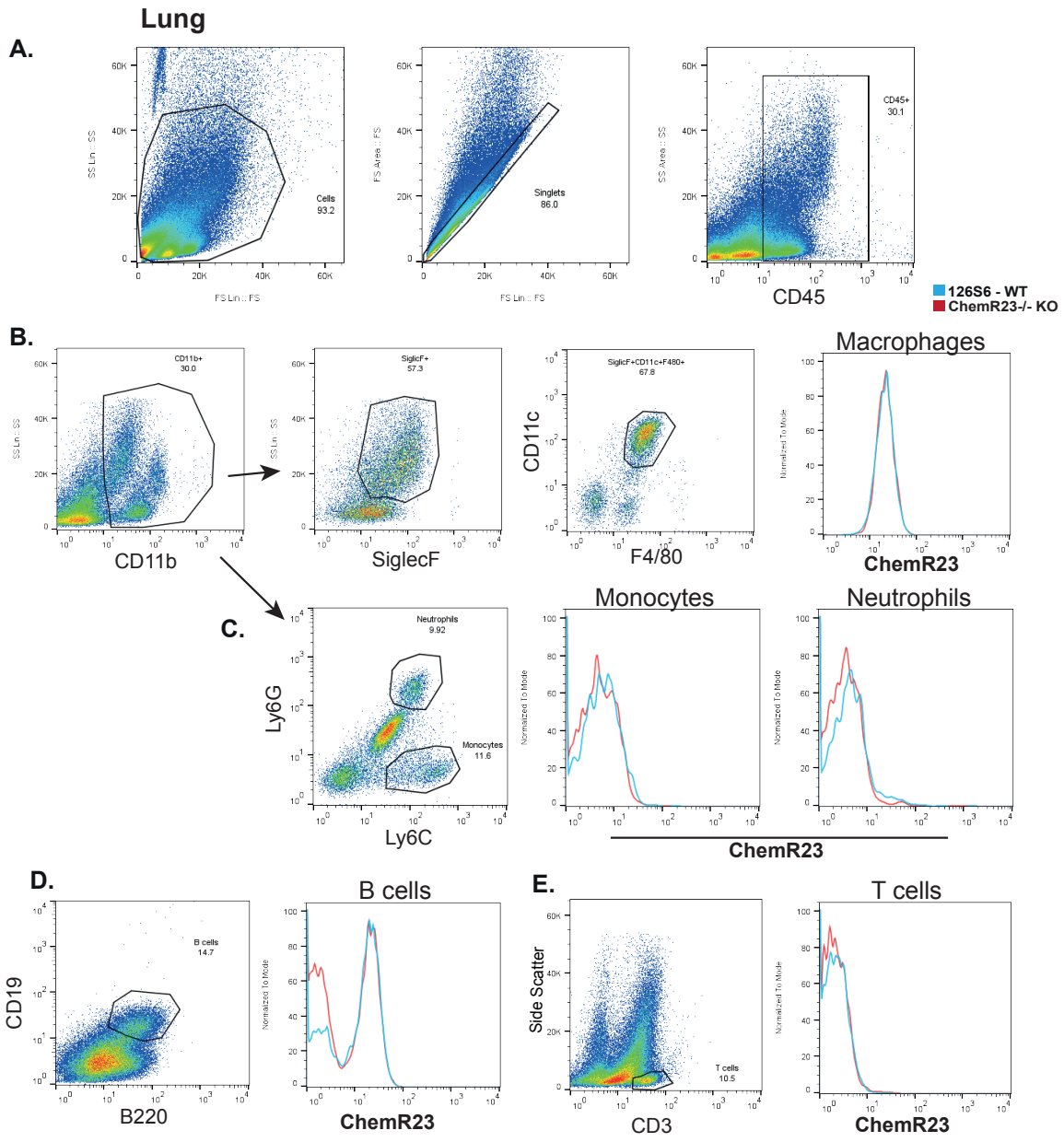


Figure 4.8: Lung leukocytes do not express the ChemR23 receptor under naive conditions. 8-10 week old male *ChemR23*-/- and 129S6 WT mice were euthanised and lungs were collected in ice-cold PBS. Following a collagenase I digest and a blood lysis step, a single cell suspension was achieved for flow cytometry staining. **A.** Representative flow cytometry plot of lung single cell suspension and CD45 pan-leukocyte marker. **B-E.** The histograms illustrating ChemR23 receptor, on selected populations of cells, show 126S6 strain WT, in blue, compared to *ChemR23*-/-, in red. **B.** By selecting cells expressing CD11b myeloid specific marker, from the CD45 positive cells, macrophages are identified by positive staining for Siglec F, CD11c, F4/80. ChemR23 expression on lung macrophages show no positive expression of ChemR23 receptor. **C.** By selecting cells expressing CD11b myeloid specific marker, neutrophils and monocytes in lung tissue are identified by Ly6G and Ly6C markers . ChemR23 expression on both populations is negative. **D.** B cells are identified from CD45 positive cells, by expressing both CD19 and B220 markers. ChemR23 is not expressed on B cells resident in lung tissue. **E.** T cells are identified from CD45 and CD3 positive cells. T cells resident in lung tissue do not express ChemR23 receptor. Representative of 2 animals/group.

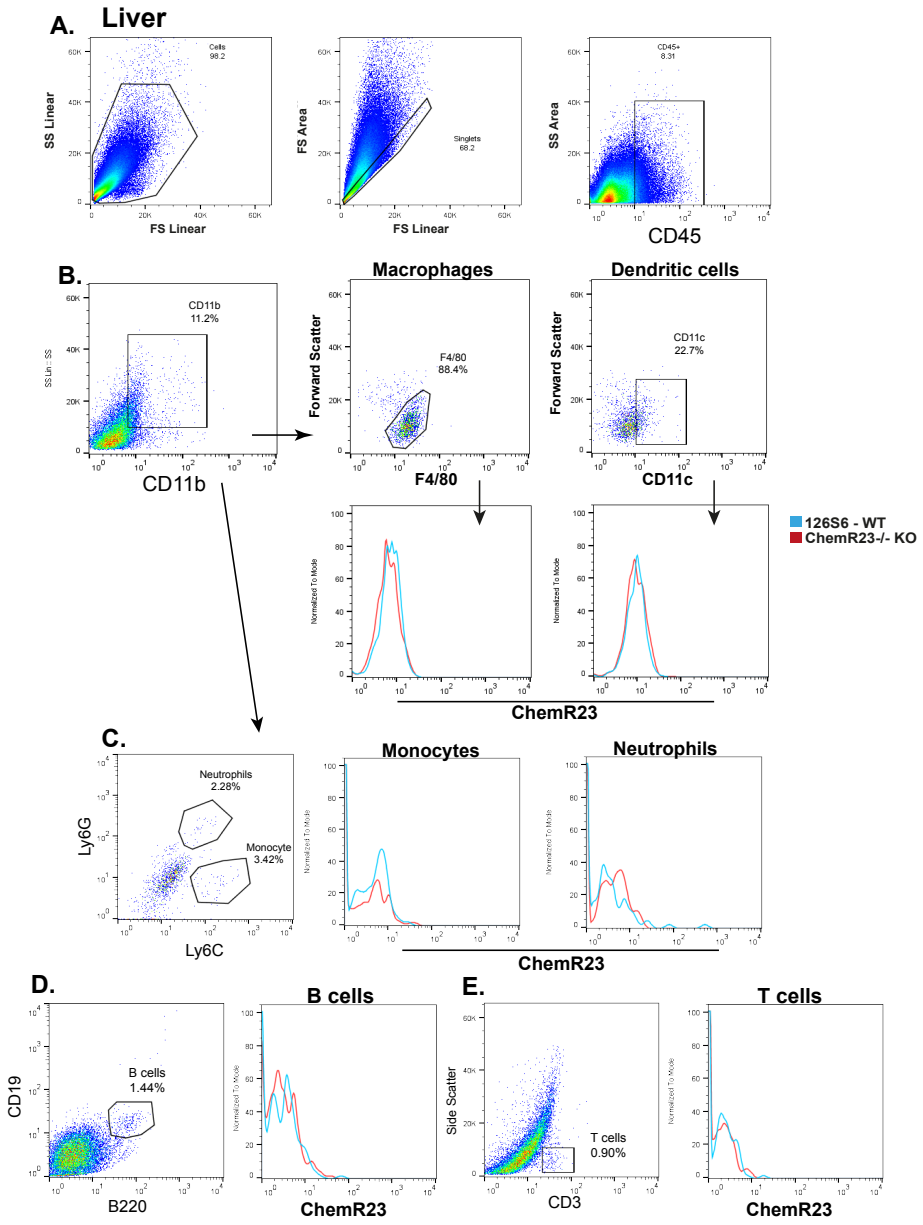


Figure 4.9: The ChemR23 receptor is not expressed on leukocyte subsets from liver under naive conditions. 8-10 week old male *ChemR23*-/- and 129S6 WT mice were euthanised and livers were collected in ice-cold PBS. Following a collagenase I digest and a blood lysis step, a single cell suspension was achieved for flow cytometry staining. **A.** Representative flow cytometry plot of lung single cell suspension and CD45 pan-leukocyte marker. **B-E.** The histograms illustrating ChemR23 receptor, on selected populations of cells, show 126S6 strain WT, in blue, compared to *ChemR23*-/-, in red.**B.** By selecting cells expressing CD11b myeloid specific marker, from the CD45 positive cells, macrophages and dendritic cells are identified by positive staining for F4/80 and CD11c respectively. ChemR23 expression on liver macrophages and dendritic cells show no positive expression of ChemR23 receptor. **C.** By selecting cells expressing CD11b myeloid specific marker, neutrophils and monocytes in liver tissue are identified by Ly6G and Ly6C markers. ChemR23 expression on both populations is negative. **D.** B cells are identified from CD45 positive cells, and expressing both CD19 and B220 markers. ChemR23 is not expressed on B cells resident in lung tissue. **E.** T cells are identified from CD45 and CD3 positive cells. T cells resident in liver tissue do not express ChemR23 receptor. Representative of 2 animals/group.

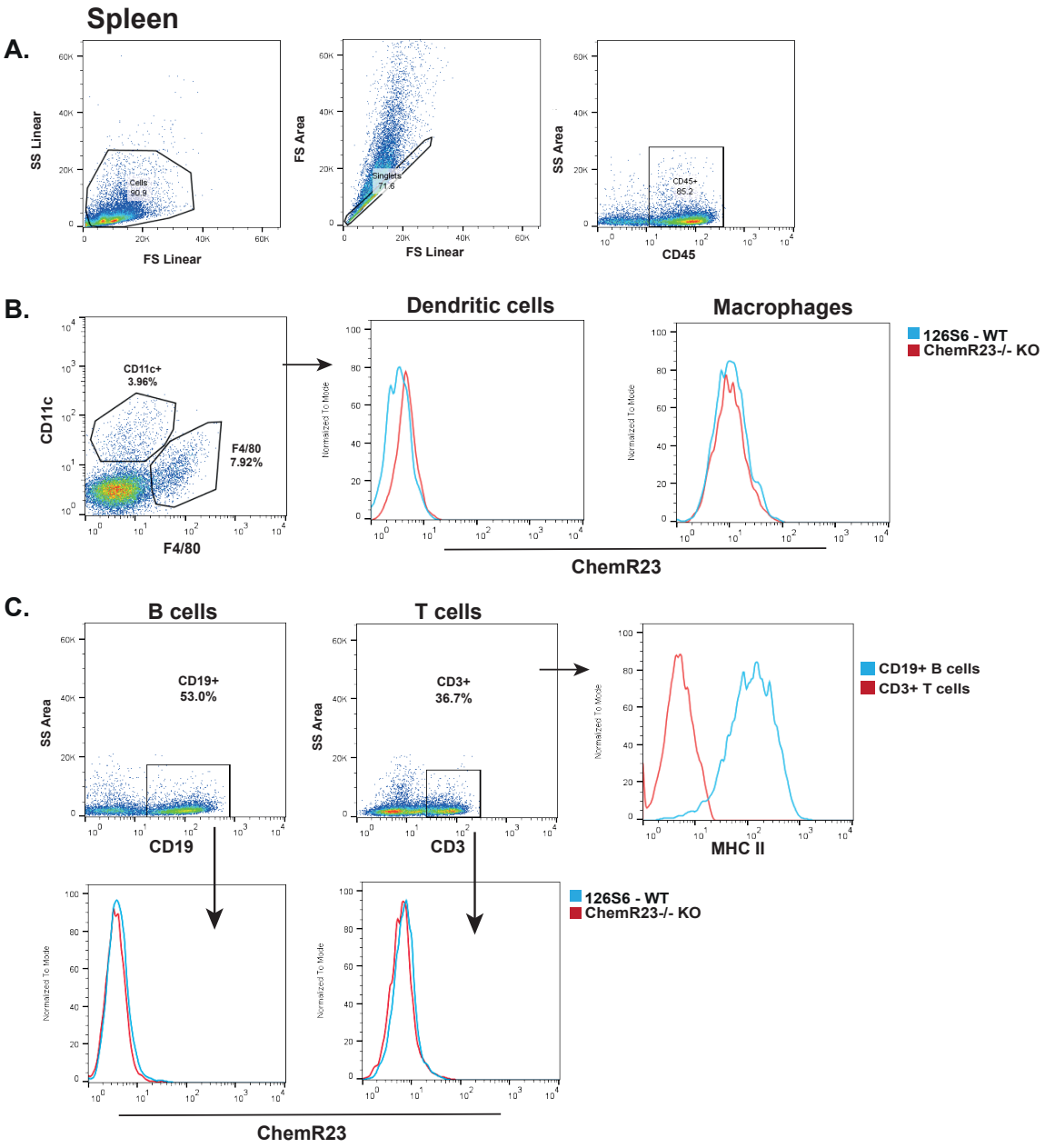


Figure 4.10: The ChemR23 receptor is not expressed on leukocyte subsets in the spleen under naive conditions. 8-10 week old male *ChemR23*-/- and 129S6 WT mice were euthanised and spleen were collected in ice-cold PBS. Following filtration and a blood lysis step, a single cell suspension was achieved for flow cytometry staining. **A.** Representative flow cytometry plot of lung single cell suspension and CD45 pan-leukocyte marker. **B-C.** The histograms illustrating ChemR23 receptor, on selected populations of cells, show 126S6 strain WT, in blue, compared to *ChemR23*-/-, in red. **B.** By selecting cells expressing CD11b myeloid specific marker, from the CD45 positive cells, macrophages and dendritic cells are identified by positive staining for F4/80 and CD11c respectively. ChemR23 expression on spleen macrophages and dendritic cells show no positive expression of ChemR23 receptor. **C.** B cells and T cells are identified from CD45 positive cells, by the CD19 and CD3 markers respectively, which were confirmed by the expression of MHC II on B cells, in blue and T cells in red. ChemR23 is not expressed on B cells or T cells resident in spleen tissue. Representative of 3 animals/group.

4.2.8.4 Human blood monocytes

In the literature, there have been conflicting reports of ChemR23 expression on human blood monocytes [279] however the majority of published data support that ChemR23 is expressed on human blood monocytes [280, 281, 205]. Due to the fact that I did not detect the ChemR23 receptor on the murine blood monocytes, in Figure 4.4, I was interested to assess whether human blood monocytes express the ChemR23 receptor. Using a negative selection using monocyte isolation kit II, human monocytes were isolated from whole blood, as seen in Figure 4.11a. The ChemR23 receptor was not detected on the surface or intracellularly in human monocytes. There is only a small 'shoulder' seen in the permeablised samples.

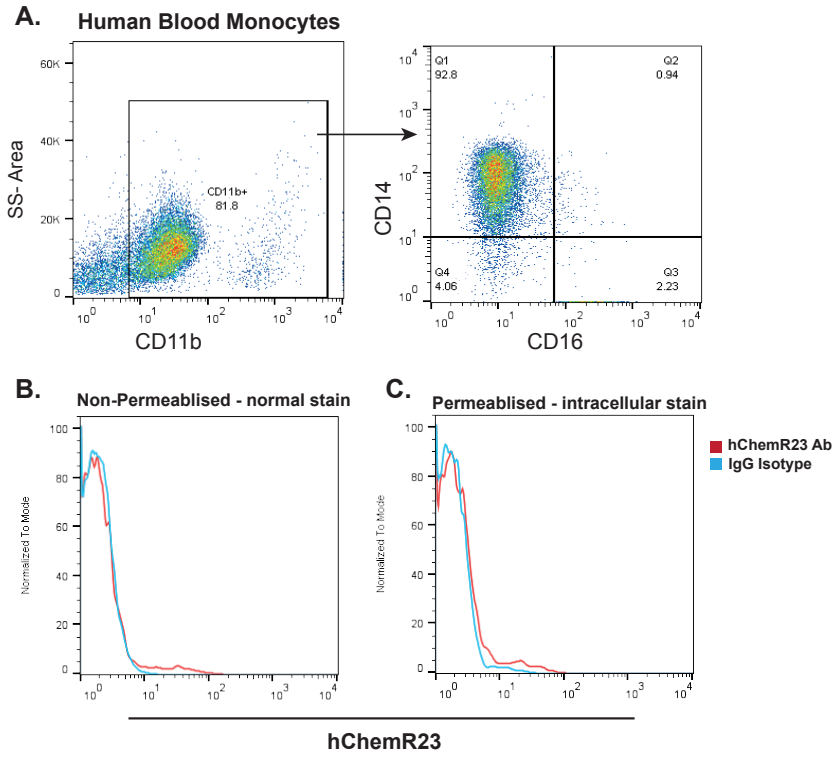


Figure 4.11: ChemR23 receptor is not expressed on human blood monocytes. Donor blood was collected in heparin coated tubes and processed using a MACS human negative selection monocyte isolation kit II. **A.** Representative flow cytomerty plots of blood isolated monocytes stained with CD11b and CD14. **B-C.** Monocytes do not express ChemR23, either on the surface or intracellularly, when compared to isotype, in blue. Representative of two donors.

4.2.9 Chemerin treatment in peritoneum

Given that resident peritoneal macrophages and dendritic cells were the cell types with detectable ChemR23 protein receptor by flow cytometry, I was interested in investigating the effects of recombinant active chemerin on the resident cell populations of the peritoneum. One hour post injection, the chemerin treated group display a significantly increase in total $CD45^+$ leukocytes in the peritoneum (Figure 4.12b). In order to confirm that the injected chemerin was functional, I assessed the expression of ChemR23 by peritoneal macrophages from the PBS and chemerin treated group. The chemerin treated group showed significant decrease in the geometric mean of $ChemR23^+$ cells compared to the PBS treated group (Figure 4.12c). This suggests that the active recombinant chemerin bound to the ChemR23 and the receptor was internalised.

In order to discover the cell types responsible for the increase in total leukocytes to the peritoneum following chemerin treatment, I decided to split the $CD45^+$ cells into $MHCII^{mid}$ or ^{high}. With this, I found that $MHCII^{mid}$ cells are significantly increased and from this group of cells, the dendritic cells are significantly elevated in the chemerin treated group. Whilst the total number of macrophages remain unchanged between groups. The $MHCII^{high}$ cells are not significantly increased, and similarly B cells are also not significantly elevated. However, the pDCs are significantly elevated in the chemerin treated group. From the literature, it is known that pDCs express ChemR23 and migrate towards chemerin [205], further confirming that the chemerin injected had functional signalling ability. Finally, there is no neutrophil recruitment and a non-significant increase in monocyte recruitment to the peritoneum following chemerin treatment.

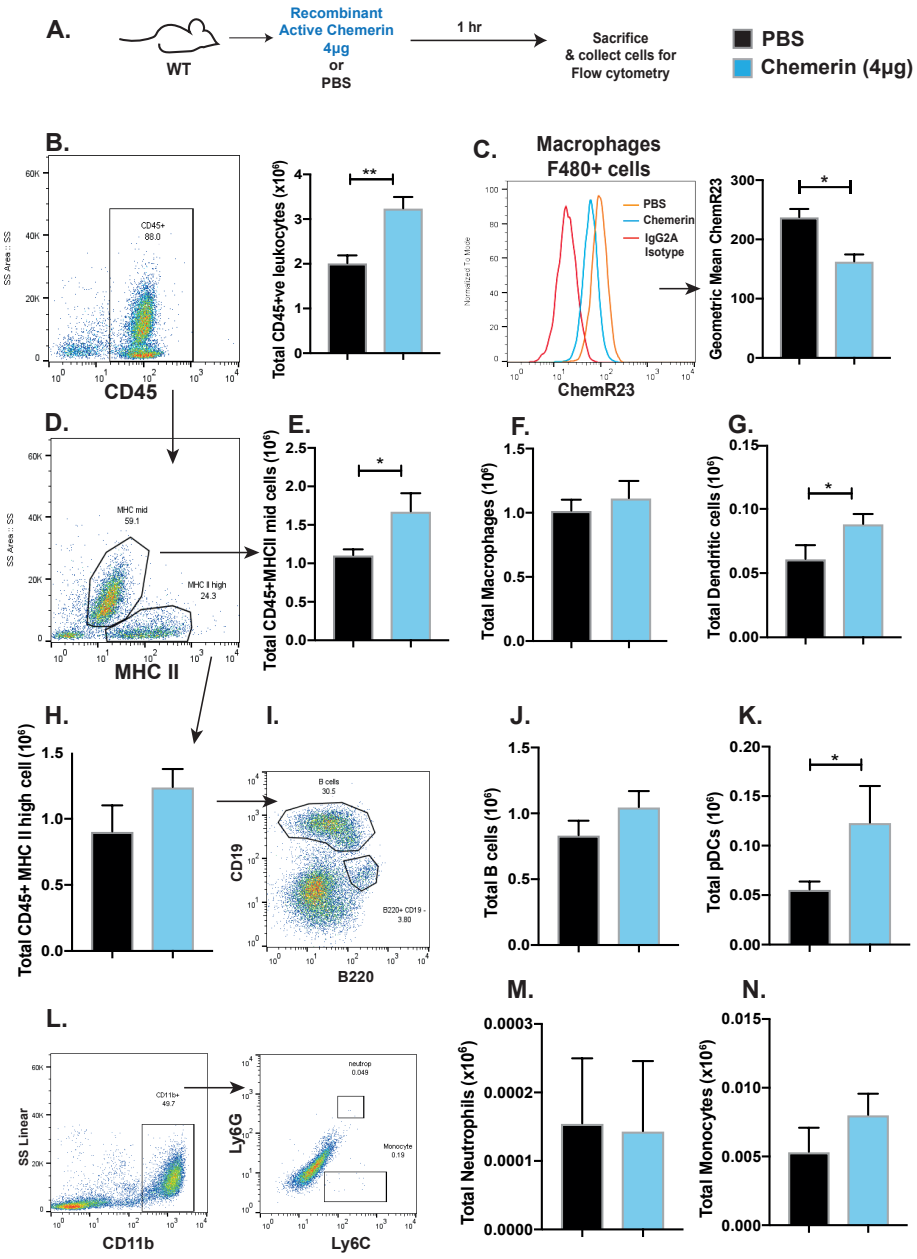


Figure 4.12: Intraperitoneal chemerin treatment causes recruitment of MHC class II expressing leukocytes to the peritoneum. 8-11 week old male WT mice were injected i.p. with 4.0μg of recombinant murine chemerin (R&D) or PBS. One hour following treatment, mice were euthanised and their peritoneums were lavaged with ice-cold PBS, supplemented with 2mM EDTA. **A.** Flow diagram of experiment outline. **B.** Representative flow cytometry plot of pan-leukocyte marker, CD45, gating. **C.** Peritoneal macrophages, expressing ChemR23, show significant decrease in ChemR23 receptor expression following chemerin-treatment. **D-G.** Flow cytometry plot of side scatter and MHCII receptor shows two groups of leukocytes in peritoneum: MHCII^{mid} and MHCII^{high}. Total MHCII^{mid}-expressing cells and dendritic cells (CD11c^{+}) are significantly increased following chemerin-treatment where as there is no observed difference in macrophages (F4/80^{+}). **H-K.** Total MHCII^{high} cells and B cells (CD19^{+}B220^{+}) showed no significant difference between treatments, where as pDCs (B220^{+}) were significantly increased in the chemerin-treated group. **L-N.** Peritoneal neutrophils and monocytes were identified by CD11b, Ly6G and Ly6C staining. There was no significant neutrophil or monocyte recruitment following chemerin treatment. Error bars represent S.E.M. of 5-7 mice/group. Statistical significance was assessed by unpaired t-test. $*$ P $\leq$0.05, $**$P$\leq$0.01.

4.3 Discussion

Chemerin binds three GPCR receptors with high affinity. The main aim of this chapter was to better characterise the expression of chemerin receptors on various leukocyte subsets. Firstly, because chemerin has been reported to play a role in various inflammatory processes and pathological disease models. Secondly, because I was able to detect the mRNA expression of chemerin, ChemR23 and CCRL2 receptors in tissue consisting a large proportions of tissue resident leukocytes (Figure 4.7). The aim of the chapter was achieved by assessing mRNA and protein expression of the chemerin receptors by *in vitro* primary cell cultures and by *in vivo* flow cytometry analysis of resident leukocyte populations in various tissues. I decided to focus on the protein expression of the ChemR23 receptor, due to the fact that it has the strongest binding affinity for chemerin, and it engages the strongest downstream signalling responses compared to the other receptors [164]. GPR1 receptor has a strong affinity for chemerin, but has weaker downstream signalling [164]. Additionally, my data, from Figure 4.7, shows that mRNA expression of GPR1 is only detectable in adipose tissue. Hence, GPR1 was only assessed via qPCR through out this chapter. Finally, during the time I was carrying out these experiments there was a lack of an effective commercially available antibody against the CCRL2 receptor, which means that in this chapter, CCRL2 is always assessed by qPCR.

4.3.1 Macrophages

Macrophages are an important tissue resident cells found in most tissues, whose main roles are to orchestrate the immune response against invasive pathogens, promote and engage in tissue repair processes. It has been well documented that macrophages express the chemerin receptors of ChemR23 and CCRL2 [165, 173]. I was interested in assessing the changes in the expression of chemerin receptors by BMDM cultured cells following the exposure of TLR and cytokines. In Figure 4.1, BMDMs are stimulated with pro-inflammatory TLR ligand, LPS, and 'alternative' activating IL-4 cytokines display modest and non-significant changes in protein and mRNA expression of ChemR23 when compared to basal conditions. The mRNA levels of ChemR23 receptor following LPS/IFNγ are elevated. However, due to the large variations between individual experiments, it is difficult to draw a conclusion above the expression pattern from my results. Previous studies report conflicting results regarding the expression pattern of ChemR23 under various pro or resolution conditions. Zabel *et al.* showed peritoneal macrophages treated with LPS display a decrease in

ChemR23 [282]. While Herová *et al.* describes the upregulation of protein and mRNA of ChemR23 by human monocyte-derived macrophages [281]. In my experiments, I observe an modest increase in ChemR23 mRNA by BMDM treated with LPS, as does Herová *et al.* but this is not reflected in the flow cytometry protein expression data. Normally mRNA and protein expression patterns are thought to correlate due to the fact that ultimately mRNA gets processed and translated into amino acid chains at the ribosome and subsequently folded into functional proteins. However, there is not always a strong correlation between mRNA and protein abundance probably due to limitations with the techniques used or the time points selected for analysis [283]. However, due to the modest changes in mRNA and protein levels I observe with the LPS treatments, it may have been more useful to assess the protein expression of ChemR23 with LPS and IFNγ instead. The combination of the two may induce a greater protein expression of ChemR23, which would coincide with elevated mRNA levels.

Moreover, Herová *et al.* reported a decrease in ChemR23 expression over time with IL-4 treatment [281], which my results do not reflect (Figure 4.1c). Zabel *et al.* shows increased ChemR23 expression following TGFβ stimulations, another 'alternatively' activating cytokine. It is obvious that the expression patterns differ between publications. The cell types used to test the expression pattern of protein may introduce variations in the results. Thus, I cannot conclude that the polarisation stimulations strongly induce the expression of ChemR23 in BMDM from these results.

However, in contrast to the ChemR23 expression, BMDM treated with pro-inflammatory TLR ligands display a significant elevated levels of CCRL2 receptor by mRNA expression; these ligands include LPS, LPS/IFNγ, PolyI:C, and zymosan. These results are in agreement with BMDCs treated with proinflammatory agents [173]. Unfortunately, I have not assessed the protein expression of CCRL2 on BMDM, due to the lack of an effective anti-CCRL2 antibody during the time I was undertaking the experiments. Nonetheless, mRNA and protein upregulation of CCRL2 following pro-inflammatory stimulations have consistently been described in various cell types including peritoneal macrophages, mast cells and endothelial cells [284, 155, 171]. mRNA levels of GPR1 are not detected in the BMDM with or without TLR and cytokine treatments, which suggests that the GPR1 receptor is not expressed on macrophages.

Peritoneal resident macrophages are known for being ChemR23$^+$ cells and thus have been used to uncover the signalling pathways involved in ChemR23 and chemerin activation [165, 282, 212]. As in the literature, I too show that peritoneal macrophages under naive conditions and in 4 day Bio-gel elicited cells, express high levels of protein

and mRNA for the ChemR23 receptor, Figure 4.6 and 4.5. Under naive conditions, resident macrophages act as sentinel cells for pathogen recognition and also in maintaining tissue homeostasis. While 4 day Bio-gel elicted macrophages are monocyte-derived macrophages which are repopulating the peritoneal cavity following the mild inflammatory insult, in order to restore tissue homeostasis [285]. This suggests there might be a tendency for the expression of ChemR23 during the resolution phase of inflammation. This would fit with the data of Zabel *et al.* but not by Herová *et al.* as stated earlier [282, 281].

Due to the high levels of ChemR23 mRNA expression in lung, liver and spleen detected by qPCR in Figure 4.7, I was expecting to find that the macrophages would be one of the cell types expressing the ChemR23 receptor. However, macrophages resident in the lung, liver and spleen do not express ChemR23 receptor via flow cytometric analysis in Figure 4.8, 4.9, 4.10. To the best of my knowledge, there have not been any publications stating otherwise about macrophages resident in the liver and spleen. However, there have been two conflicting reports about the expression of ChemR23 by alveolar macrophages [178, 279].

4.3.2 Monocytes

Monocytes are a vital part of the immune response, by travelling to sites of injury and differentiating into macrophages and dendritic cells. There have been conflicting reports of the expression of ChemR23 by monocytes [214, 279, 205, 153]. I did not observe ChemR23 expression on blood monocytes in agreement with Zabel *et al.* [279] (Figure 4.4). Similarly, human monocytes also do not express the ChemR23 receptor intracellularly or on their surface, in disagreement with Herová *et al.* and Vermi *et al.* It must be noted that I only assessed $CD14^+$ human monocytes. Additionally, the recruited monocytes present in the peritoneum, 4 days post injection of 2% Bio-gel, display ChemR23 protein expression (Figure 4.5).

Aside from blood, there is a small resident population of monocytes in the lungs and liver, therefore, under naive conditions I assessed the ChemR23 receptor in these tissues. Similarly to resident macrophages, the monocytes in lung and liver do not express ChemR23 receptor.

4.3.3 Dendritic cells

Dendritic cells are an important link between the innate and adaptive immunity. In agreement with previous publications, Figure 4.2 illustrates immature BMDCs ex-

pressing ChemR23 receptor. They also reported the downregulation of ChemR23 expression following maturation [192, 205], yet I observe no major change in the protein expression of ChemR23 upon LPS maturation. For further validation, I measured the functional responses to chemerin, these remained unchanged between immature and mature BMDCs in the 96 well ACEA ECIS impedance assay. This further confirms the lack of changes in ChemR23 between immature and mature BMDCs in my data.

Even though, monocyte-derived dendritic cells are predominently shown to express the ChemR23 receptor, dendritic cells are also tissue resident leukocytes in many tissues. Luangsay *et al.* documented the expression of ChemR23 on splenic dendritic cells [176]. Vermi *et al.* identified ChemR23^{+} resident dendritic cells in secondary lymphoid organs and skin by immunohistochemistry [205]. In the naïve peritoneal cavity, I too observe a subset of resident dendritic cells expressing the ChemR23 receptor (Figure 4.6). I expected to find expression of ChemR23 on resident dendritic cells in liver and spleen tissue. Yet, in both liver and spleen, I did not detect the expression of ChemR23 by resident dendritic cells (Figure 4.10, 4.9).

4.3.4 Neutrophils

The majority of the literature supports that neutrophils do not express the ChemR23 receptor [227]. However, there are a couple of papers showing the expression of ChemR23 on neutrophils [280, 286, 287]. All papers that have shown the expression of ChemR23 on neutrophils, either report it at low levels of expression or have used high concentrations of the anti-ChemR23 antibody (personal communication with Dr. Cash, [214]. Recall that my investigations for the ChemR23 receptor on bone marrow isolated neutrophils, circulating blood neutrophils and from mature neutrophils recruited to the peritoneum in 4 day Bio-gel elicited peritoneal cells, all showed no ChemR23 expression by qPCR and flow cytometry (Figure 4.3, 4.4, 4.5). Considering my data, I conclude that neutrophils do not express the ChemR23 receptor. Freire *et al.* reported that ChemR23 (or ERV-1 receptor as they call it in this paper) is identified in low levels from healthy neutrophils, whilst the receptor becomes over-expressed in neutrophils stimulated with TNF-α or LPS or from type 2 diabetes patients. However in Figure 4.5, I have used 2% Bio-gel, which can be considered as a mild inflammatory stimulus, to elicit larger numbers of peritoneal cells. The neutrophils present in the peritoneal exudate in this instance also do not express the ChemR23 receptor. While Bio-gel is not a comparable model for a type 2 diabetes environment, it can still be considered a pro-inflammatory insult due to the fact

that there are large numbers of neutrophils being recruited. Concurrently, I am able to detect large amounts of ChemR23 receptor on both macrophage and monocytes within the same Bio-gel elicited peritoneal cell samples. This further encourages me to conclude that neutrophils lack the ChemR23 receptor.

Interestingly, I can detect mRNA expression of CCRL2 receptor in bone marrow isolated neutrophils. Migeotte *et al.* also reported strong expression of CCRL2 on neutrophils [173]. Other atypical chemokine receptors, such as D6, are expressed by non-leukocyte and leukocyte cell types, including neutrophils [288]. In order to confirm that the lack of CCRL2 receptor does not affect the distribution of ChemR23 receptor on leukocytes, Bio-gel elicited peritoneal cells from *CCRL2*$^{-/-}$ mice were compared to C57BL6J WT elicited peritoneal cells. The *CCRL2*$^{-/-}$ recruited cells display no difference in the expression of the ChemR23 receptor. Moreover, GPR1 is not detected by qPCR on bone marrow isolated neutrophil or from 4 day Bio-gel elicited peritoneal cells.

Furthermore, there is a small population of neutrophils present in liver under naïve conditions. Similar to the blood and bone marrow neutrophils, I observe no ChemR23 expression by the neutrophils in the liver, Figure 4.9. Finally, the neutrophils present in the lungs may very well be actively engaging with pathogens due to the lung epithelial exposure with the outside environment. However, they also do not express the receptor (Figure 4.8).

4.3.5 B and T cells

B and T cells are the cornerstone of the adaptive immune response. Following antigen presentation usually by antigen presentation cells, T cells mount an antigen specific cell-mediated immunty, and concurrently activate their counterpart B cells to mount a humoral immunity against the antigen. B cells also have the ability to act as antigen presentation cells, due to their high MHCII expression. Both T and B cells are found in the peripheral tissue under resting conditions. B1 cells, an innate-like B cell population, are the principle lymphocytes in the peritoneum. They produce low specificity IgM antibodies against common pathogen associated molecules [35]. Upon inflammatory insult they have been found to migrate to spleen and produce IgM and IL-10 cytokine [289]. T cells in peripheral tissues are generally resident memory T cells, which are poised to respond to previously encountered antigens. Within this T cell resident population, there are effector memory T cells and regulatory T cells. These have been observed in peritoneal cavities of dialysis patients, human lung and skin in non-inflamed conditions [32, 33, 34]. As stated before, the spleen

is a secondary lymphoid organ, and so T and B cells are optimally positioned for antigen-presentation cell trafficking and priming. The liver contains a lymphoid cell population as well. T cells have a 1:3.5 proportion of $CD4^+$:$CD8^+$ respectively and the majority of B cells are of the innate-like CD5+ B cell populations [276].

To the best of my knowledge, B cells have not been reported to express the ChemR23 or the CCRL2 receptor [153, 173], except for one paper which found that immature bone marrow B cells express the CRAM-A, a CCRL2 splice variant, while mature blood B cells express the CRAM-B splice varient [290]. There have been mixed reports into whether T cells express ChemR23. Some papers detect low levels of mRNA expression of ChemR23 by T cells [262, 280, 153] whereas others show no ChemR23 protein expression [205, 282, 176]. Additionally, T cells have been found to express mRNA of CCRL2 receptor [173], but peritoneal and lung BAL fluid T cells do not express the CCRL2 protein by flow cytometry [155, 182]. In my results, I only investigated the ChemR23 protein expression on T and B cells. I am unable to detect ChemR23 on either B or T cells in the naïve peritoneum, lung, liver and spleen (Figure 4.6, 4.8, 4.9, 4.10).

4.3.6 Non-leukocyte cells

Given the role of chemerin and ChemR23 receptor during inflammation, and the expression of ChemR23 receptor in haematopoietic tissues, such as the lung, liver, and spleen, I expected to find ChemR23 being highly expressed on resident leukocyte populations. However, under naïve conditions the resident leukocytes in these tissues, do not express the chemerin receptor ChemR23. This suggests that the main cell types expressing the ChemR23 receptor are non-leukocyte cell types. In liver, hepatocytes have been shown to express ChemR23, which is downregulated during in fatty liver disease [291]. Similarly, in a pneumonal-viral lung infection model, Bondue *et al.* finds that the non-leukocyte cell population in lung exert the anti-inflammatory propertied of ChemR23 receptor. In an adoptive transfer study of the model, they found that wild type bone marrow reconstitution into *ChemR23*$^{-/-}$ mice, augmented the inflammatory response [178]. As stated in the Introduction 4.1.1, there are large amount of non-leukocyte cell types which do express the chemerin receptors, including adipocytes, vascular smooth muscle cells, endothelial and lung epithelial cells [263, 266, 218, 176].

4.3.7 Chemerin treatment *in vivo*

The peritoneum is the only site *in vivo* that I can detect the ChemR23 receptor on leukocyte subsets. Given the chemoattractant properties of chemerin via the ChemR23 receptor, I was interested in investigating the effects of recombinant active chemerin on the resident peritoneal population and on cell recruitment to peritoneum. The chemerin treated groups display significantly elevated levels of total leukocytes, MHCII^{mid}, dendritic cells and pDCs. The pDCs and NK cells are well characterised ChemR23^{+} cells, which are able to migrate towards active chemerin *in vitro* [205, 206]. In a DSS-induced colitis study in which chemerin was administered i.p., there were no significant cell recruitment into the colon tissue even with elevated chemerin levels, however, they did not assess the peritoneal cavity for cell recruitment [207].

Furthermore, MHCII^{mid} cells are increased following chemerin treatment. The cells in this category, include the macrophages, whose cell numbers remain unchanged, and the dendritic cells which are significantly increased in the chemerin treated groups. However, this increase in dendritic cells does not account for the total increase in MHCII^{mid} cells. The cell types that would be included in this category and were not investigated, could be eosinophils, mast cells and NK cells.

Additionally, there was no recruitment of neutrophils to the peritoneum following chemerin treatment, this further supports their lack of ChemR23 receptor. Moreover, there is a non-significant increase in monocyte recruitment also suggesting the lack or low levels of ChemR23 receptor expression on circulating monocytes.

Finally, I am able to confirm that chemerin injected into the cavity bound ChemR23, causing receptor internalisation in ChemR23^{+} peritoneal macrophages. However, the *in vivo* effects of the downstream signalling are not clear from this experiment. I did not investigate the effects chemerin has on the cytokine production in local site of the injection and whether this altered the cell populations in the cavity. In agreement with multiple publications, when treating BMDM with various doses of chemerin, there are no changes in cytokine production (data not shown) [176, 212].

4.3.8 Limitations of this study

One significant limitation to this study is that I have only used one anti-ChemR23 antibody for flow cytometry. The anti-ChemR23 antibody that other publications have used are either in-house developed or a different clone. Therefore, each antibody will have varied affinity and binding towards a different epitope on the protein. In order to confirm the leukocyte subset ChemR23 expression results from this chapter, I

should repeat the flow cytometric analysis with at least one more ChemR23 antibody following antibody titration of the antibody concentration.

Another limitation to this chapter is the fact that I did not have an working anti-CCRL2 antibody (clone: 498321 from R& D) therefore, I could not make a clear comparison between the expression of CCRL2 and ChemR23 receptors on leukocyte subsets. The papers which have published results with the protein expression of CCRL2 by flow cytometry have utilised an in-house generated antibody. However, recently there have been more CCRL2 antibodies commercially available, and a recent publication utilised one such commercially available CCRL2 antibody (LS-C184185-100, Source BioScience) to detect protein CCRL2 by flow cytometry [184].

A further limitation to this chapters is that I did not study pDCs and NK cells which are reported to express the ChemR23 receptor. These cells are present in the blood and tissues residence in low numbers. In addition, under non-inflamed conditions, I am not able to detect many ChemR23^{+} cells in tissues by flow cytometric analysis. However, I did not investigate the *in vivo* expression of ChemR23 on leukocytes during inflammation nor during later time points of the resolution phase of inflammation. Under inflammatory conditions, I may be able to detect the recruitment of ChemR23^{+} pDCs and NK cells. During the resolution phase of inflammation, it would have been interesting to assess whether ChemR23 receptor is expressed on more pro-resolution phase phenotypes of cells.

Finally, a useful tool to follow the expression of ChemR23, CCRL2 or GPR1 receptors would be using transgenically engineered mice. To achieve this, a method of CRISPR Cas9 technology could be used to add a N terminal epitode tag to endogenous chemerin receptor genes [292] or by knocking in a GFP receptor gene into the chemerin receptor gene loci as was done for CX_3CR1 receptor [293].

Chapter 5

CCRL2, a non-signalling chemerin receptor during acute inflammation

5.1 Introduction

C-C chemokine receptor-like2 (CCRL2) is a seven transmembrane G protein receptor that shares significant homology (containing 40% of its amino acid sequence) with known chemoattractant receptors, including CCR1, CCR2, CCR3, CCR5 [294, 295]. CCRL2 lacks the DRYLAIV motif usually located in the second transcellular loop, which is crucial for G-protein signalling [296]. There has been one report of CCRL2 signalling with a number of CC-chemokines [297], but these findings have been contested and not reproduced by other groups [182, 155]. CCRL2 binds chemerin, without inducing downstream signalling and without internalising the bound chemerin. These investigations were carried out by using L1.2 and HEK293 transfected cells or bEND.3 and HUVEC endothelial cell lines [155, 171, 164]. Taken together, the published literature is consistent with a model in which CCRL2 acts as an 'atypical' or non-signalling receptor devoid of ligand scavenging properties.

Most conventional chemokine receptors, studied in detail, share conserved signalling pathways leading to calcium mobilisation and chemotaxis, by triggering classic downstream signalling through $G\alpha_i$ coupling mediated by a highly conserved DRYLAIV motif in the second intracellular loop of the receptor [101]. Atypical receptors fail to sustain activation of these signalling pathways in response to binding of ligands [298, 296]. Their characteristic function is to bind and scavenge CC and CXC chemokines by internalising them. These receptors have been shown to play relevant role in dampening inflammation [299], these include Duffy antigen/receptor for chemokine (DARC), D6, CCX Chemokine receptor (CXX-CKR), CXCR7, and C5aR-like receptor 2 (C5L2).

CCRL2 mRNA expression has been reported by a range of different cell types and tissues, including the spleen, lymph node, bone marrow, lung and heart [294]. mRNA and protein expression of CCRL2 has been detected in neutrophils, monocytes, macrophages, dendritic cells, mast cells, microglia, astrocytes, T cells and NK cells [300, 173, 182, 172, 155]. It is also expressed on endothelial and epithelial cells [171, 182]. CCRL2 is upregulated in activated cells; LPS, IFN-γ, Poly(I:C) and TNFα treatments all rapidly upregulate mRNA and protein expression in monocytes, dendritic cells, mast cells, neutrophils and endothelial cells [155, 182, 171, 301]. It is also found to be upregulated in neutrophils found in the synovial fluid of rheumatoid arthritic patients [302]. Upregulation of this non-signalling receptor suggests that it plays a role during inflammatory conditions.

The role CCRL2 receptor plays during inflammation has not been definitively determined, as there have been several published studies with conflicting results. Zabel *et al.* demonstrated that mice lacking CCRL2 receptor displayed reduced ear swelling and leukocyte recruitment in a mast cell-dependent, IgE-induced passive cutaneous anaphylaxis model. *In vitro* cultured mast cells from *CCRL2*$^{-/-}$ displayed no overt differences in chemotaxis, degranulation and cytokine secretion responses. However, *in vivo* the adoptive transfer of WT mast cells were able to induce a sufficient IgE-dependent inflammatory response. Hence, linking a role for CCRL2 in mast cell activation. The lack of chemerin signalling and lack of internalisation upon chemerin binding has prompted a popular hypothesis, by Zabel *et al.* for the function of CCRL2: to concentrate chemerin on the surface of cells in order to present it to ChemR23 expressing cells [155, 171], one of chemerin signalling receptors [165, 303]. This hypothesis was based on experiments where CCRL2 expressing endothelial cells binding chemerin promoted chemerin signalling and the adhesion of ChemR23 expression L1.2 lymphoid cells [155, 171]. This adhesion was found to be depended on $\alpha 4\beta 1$ integrins, which are induced by chemerin stimulated integrin clustering reported by Hart *et al.* [165].

Furthermore, Monnier *et al.* displayed that the lack of CCRL2 resulted in elevated plasma levels of chemerin under naive conditions and following treatment of LPS, however, the chemerin was in its inactive, prochemerin, form which meant it had reduced chemotactic activity. This was associated with impaired *in vivo* recruitment of ChemR23^{+} NK cells into LPS inflamed lungs of *CCRL2*$^{-/-}$ mice at a single time point. This study further supported the hypothesis that CCRL2 concentrates chemerin to present it to ChemR23 cells.

Similarly, *CCRL2*$^{-/-}$ mice challenged with ovalbumin (OVA) in the induced lung allergy model had reduced leukocyte recruitment and lower T_H2 cytokines in the bronchiolar lavage fluid (BAL) [182]. This mechanism was associated with a reduced ability to traffic antigen-loaded lung dendritic cells to lymph nodes, even though the *CCRL2*$^{-/-}$ dendritic cells were fully able to induce T-cell proliferation in allostimulatory mixed leukocyte reaction.

The number of studies investigating CCRL2 in inflammation is limited. Overall the allergy and lung inflammatory models in mice lacking the CCRL2 receptor show reduced inflammation, which suggests that the presence of CCRL2 indirectly enhances the T_H2 pathways. Importantly, if the key role of CCRL2 is to present chemerin, free chemerin must be responsible for these effects. Yet chemerin levels were only assessed in Monnier *et al.* in a LPS peritonitis model. In contrast to the previous, more recently Mazzon *et al.* reported that mice lacking CCRL2 receptor displayed exacerbated disease in an experimental autoimmune encephalitis (EAE) model. The exacerbated disease phenotype in *CCRL2*$^{-/-}$ was associated with T cells and macrophages being polarised towards T_H1 and M1 pro-inflammatory phenotype [183]. This suggests that the presence of CCRL2 in WT animals dampens the disease in the EAE model, similar to effects seen by other atypical receptors, such as D6 [299]. The lack of ChemR23 receptor and the use of a ChemR23 antagonist suppresses the development of CNS disease in the EAE models [177, 213]. Therefore, if CCRL2 is needed to present chemerin to ChemR23 expressing cells in inflammation, the absence of CCRL2 would also be expected to suppress the inflammatory disease onset not exacerbate it. Taken together, this indicates that the model of CCRL2 presenting chemerin to ChemR23 expressing cells merits further investigation. This is also another indication that the pro or anti-inflammatory actions of chemerin could be disease and location dependent.

5.1.1 Rationale for study

Critical assessment of the published literature has shown that the CCRL2 receptor likely plays a role during inflammation, due to its upregulation in multiple cells type. However, the exact role of CCRL2 in inflammation is still unclear. The main aim of this chapter was to investigate the role of CCRL2 at early time points of acute inflammation using a simple model of zymosan-induced peritonitis. Peritonitis is the inflammation of the peritoneum; a cavity formed from a monolayer of mesothelial cells that contains the abdominal organs. Due to its easy assess, injection of an inflammatory stimulus is widely used as a model to study the acute inflammatory response.

The peritoneum contains approximately 3 million resident cells, which will contribute to the initiation of the inflammatory response [304, 1]. Moreover, cells recruited to the peritoneal cavity and inflammatory mediators produced can be easily recovered by peritoneal lavage. Zymosan is a yeast cell wall component that stimulates the TLR2 and Dectin-1 receptors, leading to a reproducible acute inflammatory response. In this chapter, a 100μg dose of zymosan leads to peak neutrophilia at 4 hours and peak monocytes at 16 hours in the local site of inflammation, the peritoneum. This dose and time points of this model were optimised by a previous lab member, Dr Daniel Regan-Komito (Daniel Regan-Komito, Thesis). Hence, this model was selected, firstly, to assess the role of CCRL2 in leukocyte recruitment and secondly, to assess the mechanism driving any inflammatory phenotype in acute inflammation. The number of animals per experimental group was assessed by a power calculation for most *in vivo* experiments.

5.2 Results

5.2.1 Absence of non-signalling receptor, CCRL2, displays no overt difference in peritoneal resident leukocyte populations under naive conditions.

The main aim of this chapter was to investigate the role of CCRL2 receptor in a standard model of acute inflammation. In order to address this, *CCRL2* knock out mice, back-crossed onto a C57BL/6J background for 12 generation, were used in simple peritonitis models. As the peritoneum is the local site of inflammation for this model, resident leukocyte populations in the peritoneum were assessed in the mice lacking CCRL2 receptor under naive conditions. There were no observed differences in total peritoneal cells when compared to age-matched wild type mice (Figure 5.1). These resident cells included macrophages, which make up a large portion of the peritoneal cells, dendritic cells and B cells (Figure 5.1). Data from our lab has previously shown that resident immune cells in the blood, spleen and bone marrow of *CCRL2*$^{-/-}$ mice display no overt differences under naive conditions (D. Regan-Komito, thesis).

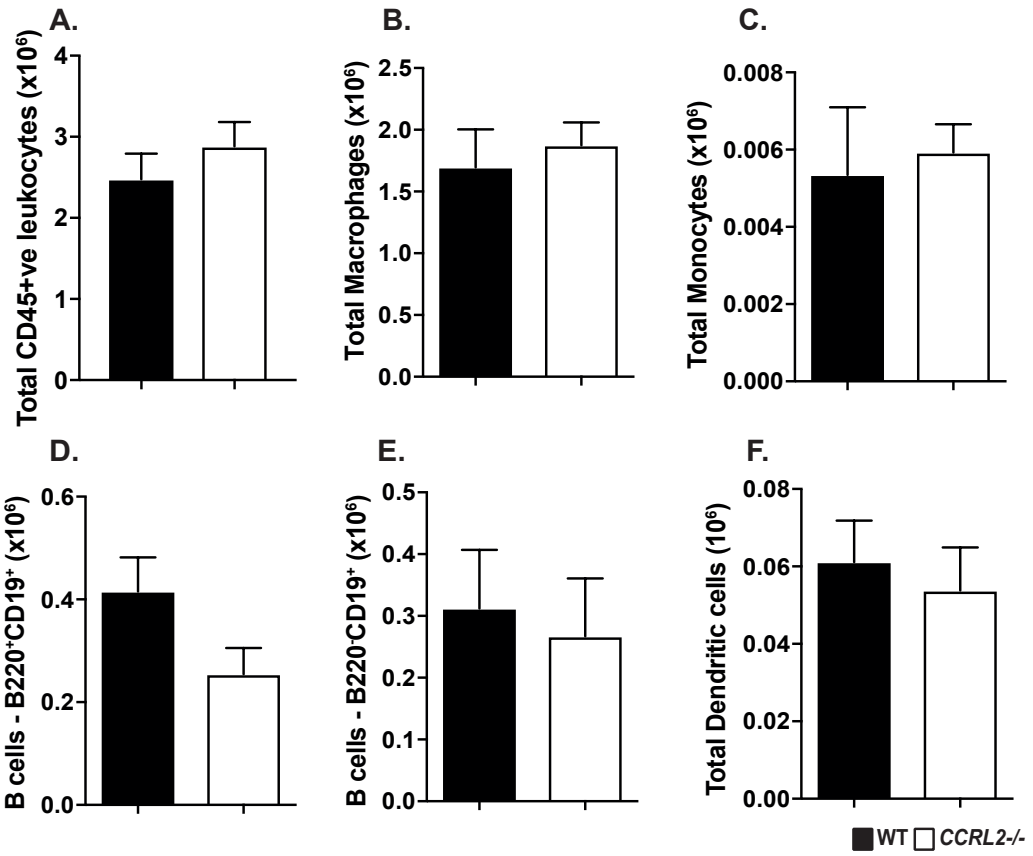


Figure 5.1: Absence of non-signalling receptor, CCRL2, displays no overt difference in peritoneal resident leukocyte populations under naive conditions. 8-10 week old male *CCRL2-/-* and WT mice were euthanised, their peritoneal cavities were lavaged with ice-cold PBS supplemented with 2mM EDTA, and resident cells populations were analysed by flow cytometry and quantified by counting beads. **A.** Total $CD45^+$ leukocytes from resident peritoneal cells. **B.** Macrophages **C.** Monocytes **D.** B cells - $B220^+CD19^+$ **E.** B cells - $B220^-CD19^+$ **F.** Dendritic cells. Error bars represent S.E.M. of 2-8 animals/group. Statistical significance was assessed using unpaired t-tests, no significant $P \geq 0.05$.

5.2.2 Absence of non-signalling chemerin receptor, CCRL2, exacerbates inflammatory responses in zymosan-induced peritonitis.

Zymosan-induced peritonitis (ZIP) is a self resolving inflammatory model of acute inflammation. This is a simple model to monitor leukocyte trafficking and performing multiple time points reveals the kinetics of acute inflammation for this model (Figure 5.2b). Mice lacking the CCRL2 receptor display augmented inflammatory cell recruitment in acute time points of zymosan induced peritonitis, when challenged with 100μg of zymosan for 2, 4 and 16 hours [1]. Total $CD45^+$ peritoneal cells are signifi-

[1]The most data from the 4 hour time point were carried out by Dr Daniel Regan-Komito.

cantly increased from 2-16 hours in *CCRL2*-/- mice, Figure 5.2b. There are striking increases in neutrophil (CD11b, Ly6G, Ly6C) recruitment from 2-16 hours, for example *CCRL2*$^{-/-}$ mice display 6.2 ± 0.54 x10^6 (Mean ± SEM) neutrophils compared to 3.1 ± 0.35 x10^6 in WT mice at 4 hours ZIP, Figure 5.2a,c. Similarly, monocytes (CD11b, Ly6C) at 4 -16 hours ZIP, Figure 5.2d, are significantly increased with 1.85 $\pm 0.18 \times 10^6$ and 1.4 $\pm 0.17 \times 10^6$ at 16 hours in *CCRL2*$^{-/-}$ and WT respectively. In early time points of inflammation, total macrophages (F4/80$^+$) present in the peritoneum, reduce dramatically and begin to recover at 16 hours post-inflammatory onset, also reported by Bystrom *et al.* [269]. The lack of CCRL2 receptor does not seem to differ the macrophage behaviour in 2 and 16 hours of ZIP.

Inflammatory mediators produced in the peritoneal cavity were measured, by ELISA (R&D). CXCL1 cytokine is significantly increased at 2 hours of ZIP in *CCRL2*$^{-/-}$ mice, and as a result of its kinetics, it drops to low levels at later time points [T. Kapellos and D.Regan-Komito, personal communication]. Under naive conditions, chemerin is detected in the peritoneum cavity and shows no difference in levels between *CCRL2*$^{-/-}$ and WT mice. However, chemerin is significantly increased at 2, 4 and 16 hours post inflammatory insult in the *CCRL2*$^{-/-}$ mice. Chemerin levels, in mice lacking CCRL2 receptor, reach their highest levels at 2 hour ZIP where the mean of *CCRL2*$^{-/-}$ is 4.2 ± 0.6 ng/ml compared to 2.4 ± 0.6 ng/ml in WT. They reach their lowest levels at 16 hour ZIP, even lower than naive conditions, at 0.84 ± 0.072 ng/ml and 0.5 ± 0.085 ng/ml, in *CCRL2*$^{-/-}$ and WT mice respectively.

Following inflammation onset by zymosan injection in ZIP, the leukocyte content of blood and spleen were also measured by flow cytometry. Blood neutrophils (CD11b, Ly6G, Ly6C) are significantly elevated in the *CCRL2*$^{-/-}$ mice with 0.56 $\pm 0.03 \times 10^6$ compared to 0.13 $\pm 0.07 \times 10^6$ in the WT mice at the 4 hour ZIP. There are no observed differences in blood neutrophils in the 2 and 16 hours post zymosan injection. Monocytes (CD11b, Ly6C) in blood show no difference in the two genotypes at 2 and 4 hours post zymosan injection, yet at 16 hours, monocytes are significantly increased in the *CCRL2*$^{-/-}$ at 0.19 $\pm 0.017 \times 10^6$ and 0.11 $\pm 0.027 \times 10^6$ in WT mice. Contrarily, neutrophils in spleen show no difference between genotypes, where as monocytes are significantly elevated at 2 hours followed by no difference at 16 hours ZIP. Inflammatory mediators were also measured in the plasma. CXCL1 levels are found to be approximately 3× higher in *CCRL2*$^{-/-}$ mice at 2 hour ZIP. Chemerin levels in plasma are also significantly elevated at 2 hours in *CCRL2*$^{-/-}$ mice.

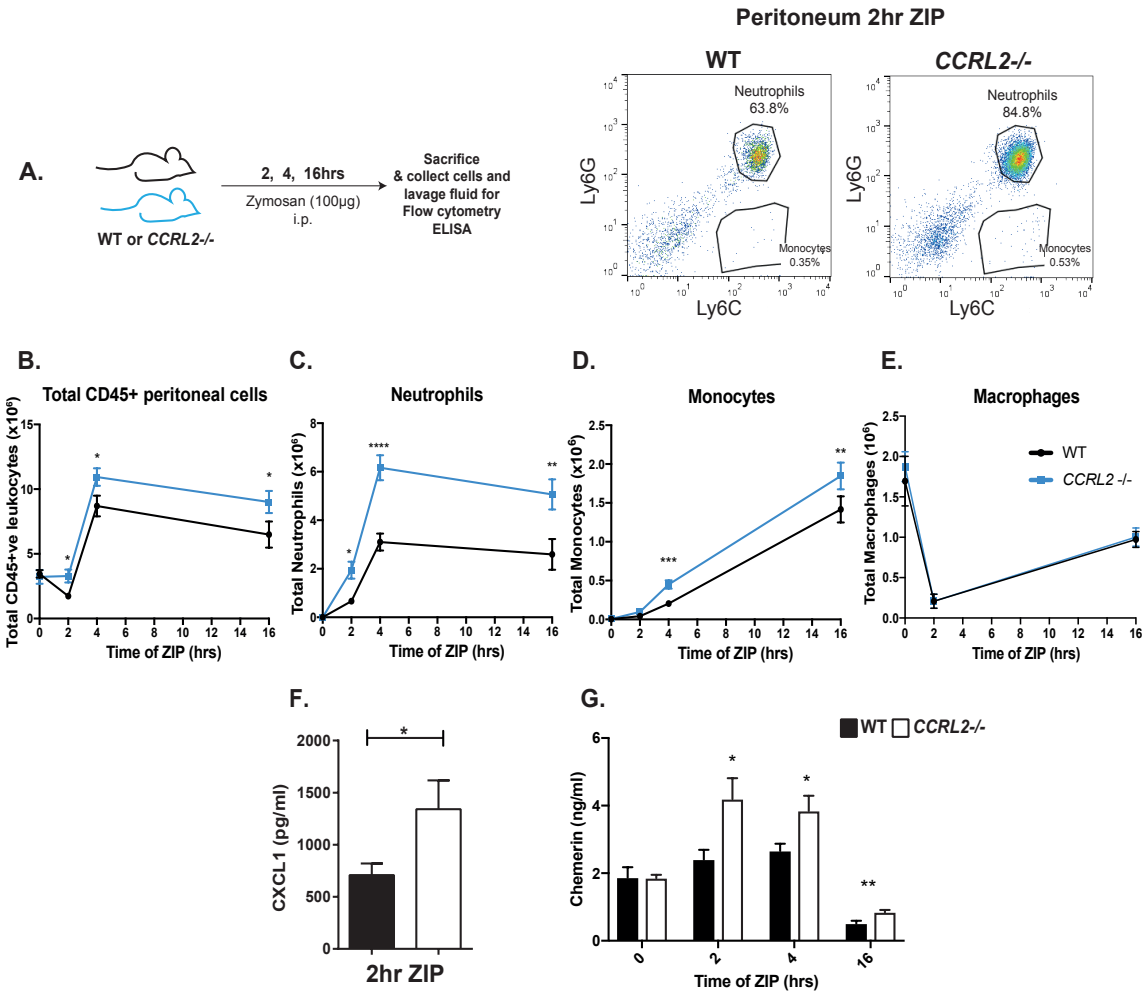


Figure 5.2: The absence of non-signalling receptor, CCRL2, increases leukocyte recruitment to peritoneum during acute zymosan-induced peritonitis. 8-12 week old male *CCRL2*-/- and WT mice were injected i.p. with zymosan (100μg/mouse). Mice were euthanised following inflammatory onset at the indicated time points. Peritoneal cavities were lavaged with ice-cold PBS supplemented with 2mM EDTA, cell populations were analysed by flow cytometry and quantified by counting beads. **A.** Flow diagram of experiment outline. Representative flow cytometry plots of neutrophils and monocytes in the peritoneum following 2 hour zymosan-induced peritonitis (ZIP) in WT and *CCRL2*-/- mice. **B-E.** Total cells present in peritoneum under naive conditions, 2 , 4, and 16 hrs following inflammatory onset; WT in black, *CCRL2*-/- in blue. **B.** Total CD45$^+$ peritoneal cells are significantly increased at 2, 4, and 16 hr time points of ZIP in *CCRL2*-/- mice. **C.** Neutrophils are significantly increased in *CCRL2*-/- following 2 , 4, and 16 hr ZIP time points. **D.** Monocytes are significantly increased in *CCRL2*-/- following 4 and 16 hr ZIP time points. **E.** Macrophages show no differences between groups, under naive conditions and following inflammatory onset. **F-G.** Chemokines and cytokines, present in peritoneal cavities, were measured by ELISA (R&D). **F.** CXCL1 is significantly increased in *CCRL2*-/- at 2hr ZIP time point. **G.** During 2 , 4, 16 hr ZIP time points, there is increased chemerin in peritoneal exudate of *CCRL2*-/- mice. Error bars represent S.E.M. of n=4-12 animals/group. Statistical significance was assessed using unpaired t-tests and two-way ANOVA with Sidak's multiple comparisons correction, $*$ P$\leq$0.05, $**$P$\leq$0.01, $***$P$\leq$0.001, $****$P$\leq$0.0001.

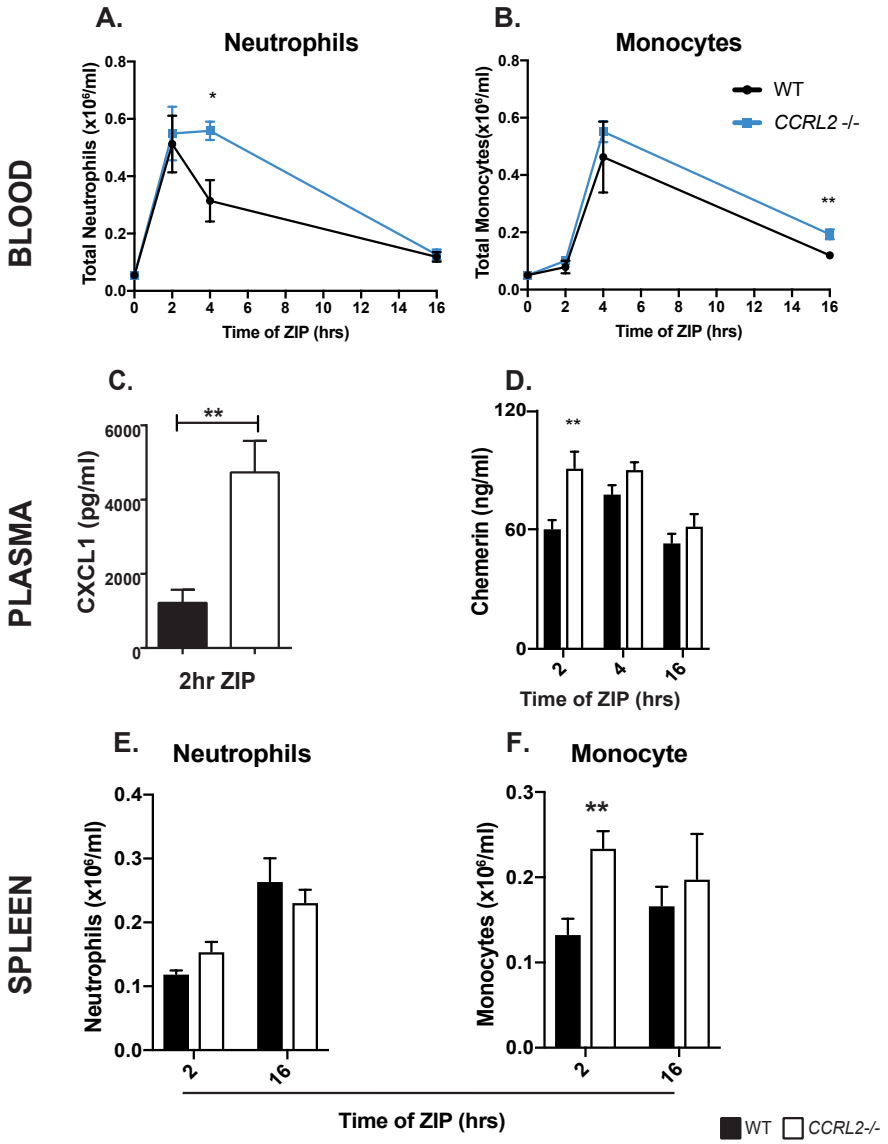


Figure 5.3: The absence of non-signalling receptor, CCRL2, increases leukocyte counts and inflammatory mediators in blood during acute zymosan-induced peritonitis. 8-12 week old male *CCRL2*-/- and WT mice were injected i.p. with zymosan (100μg/mouse). Mice were euthanised following inflammatory onset at the indicated time points. Blood was collected via the posterior vena cava into EDTA coated tubes and spleen was collected with ice-cold PBS. Cells were quantified by counting beads and cell populations were anaylsed by flow cytometry. **A-B.** Concentration of blood cells present under naive conditions, 2, 4, and 16 hrs following inflammatory onset; WT in black, *CCRL2*-/- in blue. **A.** Blood neutrophils are significantly increased in *CCRL2*-/- at 4 hr time point of ZIP. **B.** Blood monocytes are significantly increased in *CCRL2*-/- at 16 hr ZIP time point. **C-D.** Inflammatory mediators were measured in blood plasma by ELISA kits. **C.** CXCL1 and **D.** chemerin are significantly increased in *CCRL2*-/- at 2 hr time point of ZIP. **E.** Spleen neutrophil counts showed no significant differences between groups during varying time points of ZIP. **F.** Spleen monocytes showed significant increases in *CCRL2*-/- at the 2hr time point of ZIP. Error bars represent S.E.M. of n= 4-12 animals/group. Statistical significance was assessed using unpaired t-tests and two-way ANOVA with Sidak's multiple comparisons correction. $*P \leq 0.05$, $**P \leq 0.01$.

5.2.3 Absence of non-signalling receptor, CCRL2, increases leukocyte recruitment to peritoneum during acute thioglycollate induced peritonitis.

In order to establish whether this exaggerated inflammatory response observed in the absence of CCRL2 receptor was inflammogen dependent, the *CCRL2*$^{-/-}$ were challenged with 4% thioglycollate i.p. injection for 1 hour. Thioglycollate broth is a well-established inflammatory stimulus, containing abundant advance glycation end products (AGEs) [305]. It is used to elicit inflammatory macrophages and neutrophils [305, 306]. Early time points of thioglycollate peritonitis model are used to monitor neutrophil recruitment and early inflammatory mediators such as CXCL1 [306]. Similarly to the zymosan-induced peritonitis, *CCLR2*$^{-/-}$ mice treated with thioglycollate i.p. display almost a 2 fold increase in neutrophil recruitment, $0.13\pm0.01 \times 10^6$, to the peritoneum in 1 hour, compared to $0.07\pm0.01 \times 10^6$ neutrophils in WT controls (Figure 5.4c). Once again, CXCL1 and chemerin levels are significantly increased in the peritoneal cavity of knock out mice. Moreover, blood neutrophils and monocytes were also measured but show no overt differences possibly due to the early time point measured (Figure 5.4f-g). Additionally, CXCL1 levels in plasma are not different between genotypes at this time point, however, chemerin levels in plasma are significantly elevated in the *CCRL2*$^{-/-}$ mice.

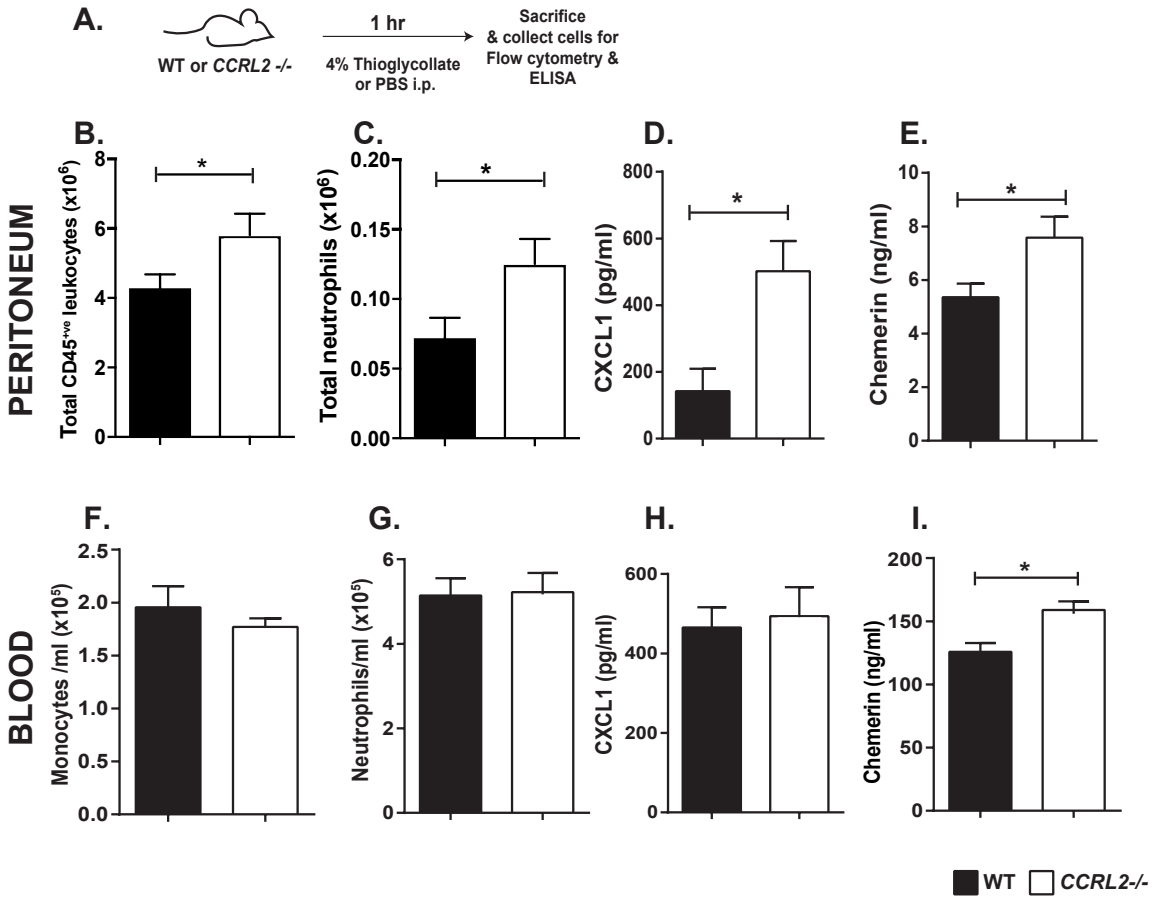


Figure 5.4: The absence of non-signalling receptor, CCRL2, increases peritoneal leukocyte recruitment and inflammatory mediator production. 8-10 week old male *CCRL2*-/- and WT mice were injected i.p. with 4% Thioglycollate broth. Mice were euthanised following 1hr of inflammogen injection. Peritoneal cavities were lavaged with ice-cold PBS supplemented with 2mM EDTA and blood was collected via the posterior vena cava into EDTA coated tubes. Cells were quantified by counting beads and cell populations were analysed by flow cytometry. Mediators present in peritoneal fluid and plasma were analysed by ELISA. **A.** Flow diagram of experiment outline. Cells and mediators present in peritoneum (**B-E.**) and in blood plasma (**F-I.**) at 1hr thioglycollate-induced peritonitis; WT in black, *CCRL2*-/- in white. **B.** *CCRL2*-/- mice show significantly increased total $CD45^+$ leukocytes present in peritoneum. **C.** *CCRL2*-/- mice show significantly increased neutrophil recruitment to the peritoneum. **D.** CXCL1 and **E.** chemerin levels in the peritoneum, are significantly increased in *CCRL2*-/- mice. **F-G.** No differences observed in blood monocytes and neutrophils between two groups at this time point. **H.** CXCL1 levels in plasma show no difference between groups. **I.** Chemerin levels in plasma are significantly increased in *CCRL2*-/- mice. Error bars represent S.E.M. of 5 animals/group. Statistical significance was assessed using unpaired t-tests. $*P \leq 0.05$.

5.2.4 Chemerin blocking antibody treatment attenuates neutrophil recruitment to the local site of inflammation in *CCRL2*$^{-/-}$ mice.

Chemerin is a ligand for the CCRL2 receptor [155, 164]. I observed increases in local and systemic levels of chemerin in *CCRL2*$^{-/-}$ mice following an inflammatory insult by zymosan and thioglycollate peritonitis. This is corroborated by previous reports [171]. Because of these findings, I hypothesised that elevated levels of chemerin in the *CCRL2*$^{-/-}$ mice is exaggerating the acute inflammatory phenotype. Therefore, by blocking the effects of excess chemerin these effects should be reduced. I was able to assess this hypothesis by using a chemerin blocking antibody. The dose of this antibody was selected from a dose response in a ChemR23 activation assay, in Figure 3.10b. The *CCRL2*$^{-/-}$ mice were treated with chemerin blocking antibody prior to inducing ZIP for 4 hours, showed significant reduction in total peritoneal leukocytes and neutrophils compared to *CCRL2*$^{-/-}$ mice treated with a control isotype IgG (Figure 5.5b,c). In the chemerin-blocking antibody group, there are $6.1 \pm 0.33 \times 10^6$ recruited neutrophils and $7.7 \pm 0.52 \times 10^6$ in the isotype IgG-treated group. However, there are no changes to monocyte recruited to the peritoneum between groups. This suggests that, at least in this ZIP time point, blocking chemerin does not affect monocyte recruitment to local site of inflammation. No changes in cells numbers are observed in the blood neutrophil and monocyte between groups (data not shown). Furthermore, peritoneal-lavage fluid was analysed by ELISA for the presence of CXCL1, IL-6 and CCL2 mediators (Figure 5.5e-g). Even though the CXCL1 mediator is present in low levels at 4 hours ZIP, it is significantly decreased in the chemerin-blocking antibody group, while the other mediators show no difference. These results indicate that the elevated levels of chemerin observed in the *CCRL2*$^{-/-}$ mice do contribute, as least partly, to the exaggerated neutrophil recruitment and the increased CXCL1 levels observed during acute inflammation.

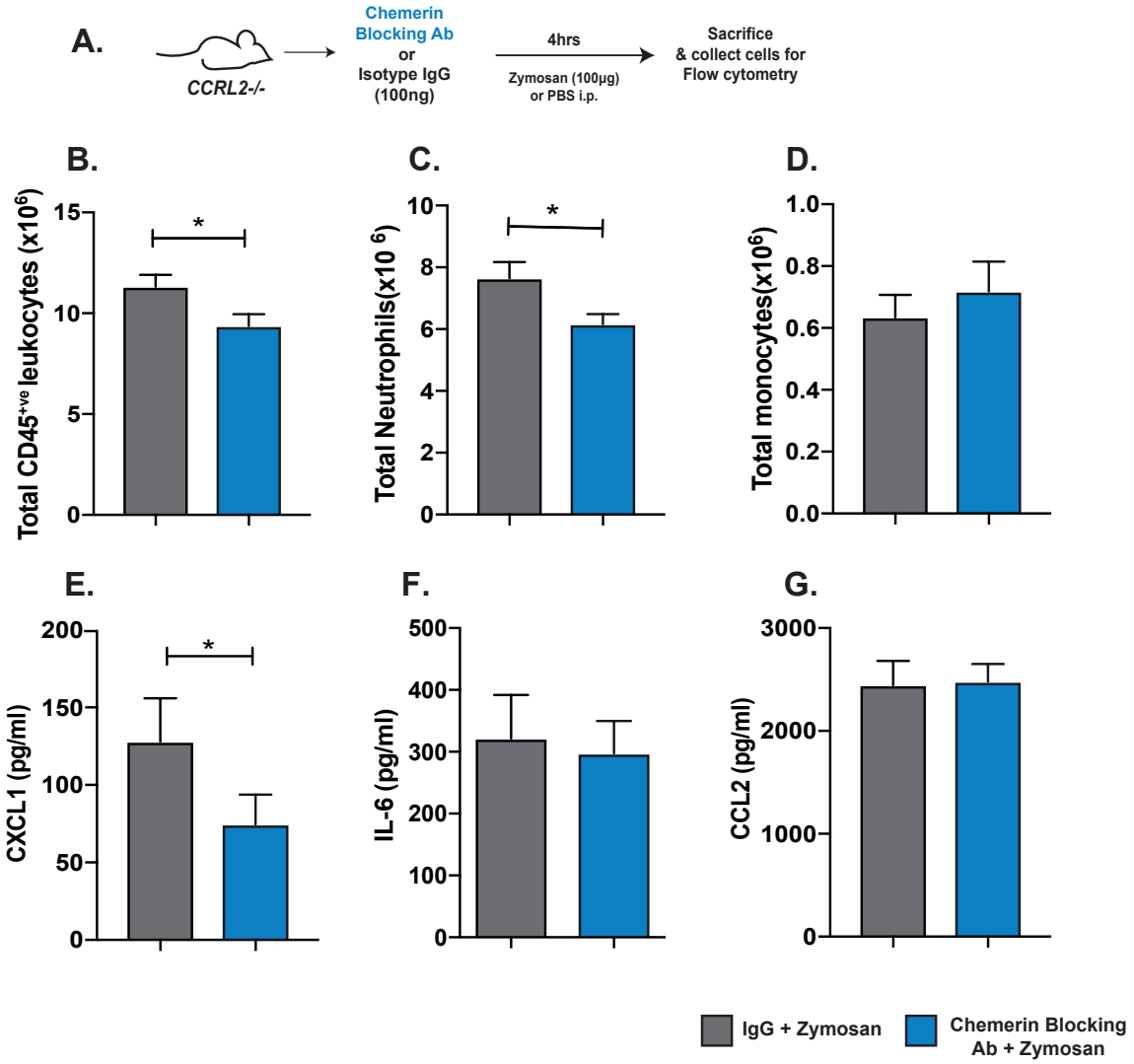


Figure 5.5: Chemerin blocking antibody treatment attenuates neutrophil recruitment to peritoneum in *CCRL2-/-* mice A. 8-10 week old male *CCRL2*-/- mice were treated with 100ng of chemerin blocking antibody (R&D) or IgG isotype control i.p. for 24 hours and 1 hour prior to challenging with zymosan for 4 hrs. Mice were euthanised and their peritoneal cavities were lavaged with ice-cold PBS supplemented with 2mM EDTA. Cells were quantified using counting beads and cell populations were analysed by flow cytometry. *CCRL2*-/- treated with IgG isotype, in grey and treated with chemerin blocking antibody in blue. **B.** Total $CD45^+$ cells and **C.** neutrophils recruited to peritoneum are significantly reduced in chemerin blocking antibody group. **D.** No difference in monocyte recruitment to peritoneum between groups. Mediators in peritoneal fluid were quantified by ELISA (R&D). **E.** CXCL1 levels were significantly reduced in the chemerin blocking antibody group. Yet, **F.** IL-6 and **G.** CCL2 levels were unchanged between groups. Error bars represents S.E.M. of n=8 animals/group. Statistical significance was assessed using unpaired t-tests $*P \leq 0.05$.

5.2.5 Chemerin-treatment exacerbates neutrophil recruitment to local site of inflammation in wild type mice.

Due to the data obtained from the chemerin-blocking antibody experiment described in 5.2.4, it was evident that 'excess' free chemerin in the *CCRL2*$^{-/-}$ mice is contributing to the enhanced inflammatory phenotype of these mice. Additionally, chemerin has been reported to induce the expression of inflammatory mediators, including CXCL1 and CCL2, in vascular endothelial cell, fibroblasts and synoviocytes *in vitro* [209, 188, 208]. Thus, in order to assess whether 'excess' chemerin is able to augment the inflammatory process *in vivo* in a wild type setting, WT mice were pretreated with recombinant chemerin (4μg/mouse) or PBS i.p. prior to 4 hour ZIP. The chemerin-treated group display an approximate 2× increase in total peritoneal leukocytes and neutrophils; with $2.5\pm0.5 \times 10^6$ neutrophils in PBS-treated group and $4.5\pm0.7 \times 10^6$ in the chemerin-treated group, Figure 5.6b,c. Moreover, monocytes present in the peritoneum do not display any changes between groups (Figure 5.6d). Importantly, chemerin-treated mice with PBS injection show no neutrophil or monocyte recruitment to the peritoneum in 4 hour post PBS injection (Figure 5.6c,d). No changes in cell numbers are observed in the blood neutrophil and monocyte between groups (data not shown). Inflammatory mediators of CXCL1, IL6 and CCL2 analysed from peritoneal fluid, in Figure 5.6e-g, all show a $\geq 2\times$ increase in the chemerin-treated group following zymosan injection. Interestingly, the chemerin-treated group, without zymosan, shows increases in CXCL1 levels when compared with PBS injected controls, suggesting that chemerin is promoting the production of CXCL1 in the local site of inflammation.

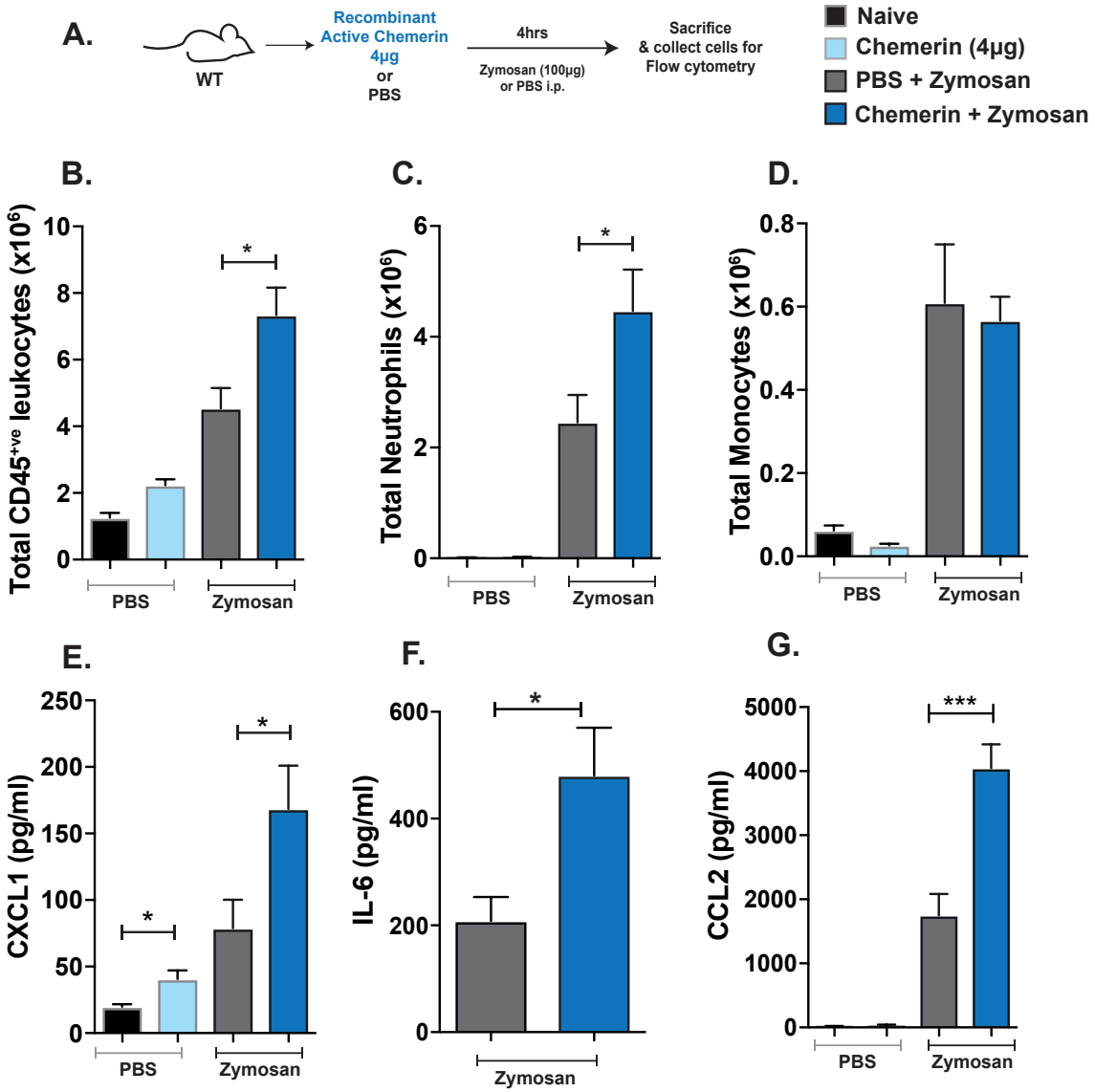


Figure 5.6: Recombinant chemerin pre-treatment exacerbates neutrophil recruitment and mediator production in the peritoneum of wild type mice. A. 8-10 week old male C57BL/6J mice were injected i.p. with recombinant murine chemerin (4μg/mouse) or PBS for 1 hour prior to challenging with zymosan or PBS for 4 hrs. Mice were euthanised and peritoneal cavities were lavaged with ice-cold PBS supplemented with 2mM EDTA. Cells were quantified by counting beads and cell populations were analysed by flow cytometry. **B.** Total $CD45^+$ and **C.** total neutrophils were significantly increased in chemerin-treated zymosan-challenged group. **D.** Monocytes recruited to the peritoneum were unchanged by chemerin pre-treatment. **E-G.** Peritoneal fluid was assessed for mediator content using ELISA (R&D). CXCL1, IL-6 and CCL2 are significantly increased in the chemerin-treated zymosan-challenged group. CXCL1 is significantly increased in chemerin-treated group. Error bars represent S.E.M. of 3-7 animals/group. Statistical significance was assessed using unpaired t-tests. $*P \leq 0.05$, $***P \leq 0.001$.

The pre-treatment dose of recombinant chemerin (4μg), from Figure 5.6, which is not unprecedented [176], could be considered non-physiologically relevant. Therefore, a lower dose of recombinant chemerin (0.5μg/mouse), also previously used [207, 180], was employed for pre-treatment before inducing peritonitis with zymosan in WT mice. Even with the lower dose, the chemerin-treated group (0.5μg/mouse) displays a 1.6 and 2$\times$ increase in total peritoneal leukocytes and neutrophils, with $7.7\pm1.2\times10^6$ and $3.7\pm0.8\times10^6$ neutrophils in the PBS-treated group. Similar to the higher chemerin dose, the monocytes present in the peritoneum also show no change. The inflammatory mediators of IL-6 and CCL2 in the peritoneal fluid are significantly increased, whereas CXCL1 levels do not reach significances in the chemerin-treated group (Figure 5.7e-g). However, CXCL1 measured in plasma shows significant increases in the chemerin-treated group. Chemerin levels in the peritoneal fluid were also measured in order to assess if the chemerin pre-treatment reached more relevant physiological level. The levels of chemerin in the peritoneum are comparable with the 0.5μg pre-treated group and as expected are significantly elevated in the chemerin-treated group. Though, chemerin in plasma did not reach significant difference between groups (Figure 5.7i,j). Finally, blood neutrophils and monocytes were also quantified, yet no changes are observed between groups (data not shown).

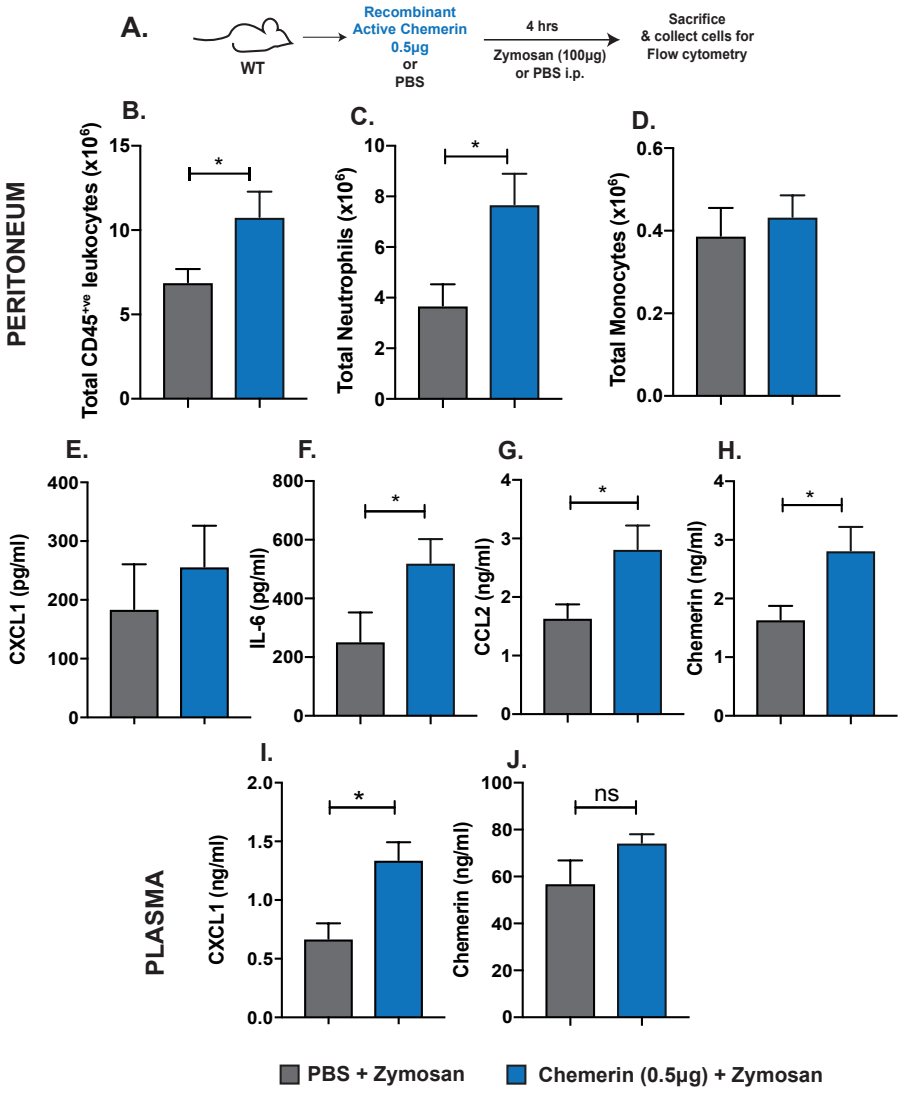


Figure 5.7: A lower concentration of recombinant chemerin pre-treatment exacerbates neutrophil recruitment and mediator production in the peritoneum of wild type mice. **A.** 8-10 week old male C57BL/6J mice were injected i.p. with recombinant murine chemerin (0.5μg/mouse) or PBS for 1 hour prior to challenging with zymosan or PBS for 4 hrs. Mice were euthanised, peritoneal cavities were lavaged with ice-cold PBS supplemented with 2mM EDTA and blood was collected via the posterior vena cava into EDTA coated tubes. Cells were quantified by counting beads and cell populations were analysed by flow cytometry. **B-C.** Total CD45$^+$ and recruited neutrophils are significantly increased in chemerin-treated group. **D.** Monocytes are observed to have no difference between groups. **E-H.** Peritoneal fluid was measured for IL-6, CCL2 and chemerin by ELISA (R&D), all of which are significantly increased in the chemerin-treated group. CXCL1 is not significantly increased in the peritoneum between groups. **I-J.** CXCL1 and chemerin levels in plasma were analysed by ELISA (R&D), where CXCL1 was significantly increased in the chemerin-treated group. Error bars represent S.E.M. of 5 animals/group. Statistical significance was assessed using unpaired t-tests $*P \leq 0.05$.

5.2.6 Real-time chemotaxis of macrophages lacking CCRL2 and ChemR23 receptors.

From previous data in this chapter, I have demonstrated that mice lacking the CCRL2 receptor exhibit exaggerated leukocyte recruitment during acute inflammation. I wanted to assess the migratory behaviour of murine macrophage populations lacking CCRL2 in response to chemerin or to the potent chemoattractant complement fragment C5a, in order to address whether the lack of CCRL2 receptor plays a direct role in leukocyte chemotaxis. The murine macrophage populations used were firstly, Bio-Gel elicited PECs, which contain a mixture of macrophages and neutrophils as seen in Figure 4.5, and secondly, 7-day cultured bone marrow derived macrophages (BMDM), seen in Figure 4.1. The chemotactic cell index in this system is measured from cells adhering to the under-side of gold plated transwell plate [224]. The raw chemotactic cell index traces obtained from the system depict the Bio-Gel PEC traces; from wild type and *ChemR23*$^{-/-}$ and BMDM traces; from wild type and *CCRL2*$^{-/-}$ (Figure 5.8a-b). Both Bio-Gel elicted PECs and BMDM show no differences between WT and *CCRL2*$^{-/-}$ in their chemotaxis towards C5a, chemerin (both 10nM) or C17 peptide (20nM), Figure 5.8c-d. While *ChemR23*$^{-/-}$ macrophages from Bio-Gel elicited PECs show a significant reduction in the delta cell index towards chemerin when compared to WT cells. BMDM cells from *ChemR23*$^{-/-}$ show a reduction in the cell index that does not reach significance (Figure 5.8d). A similar pattern is observed with the C17 peptide.

In chapter 4, Figure 4.1 I showed that BMDM cells treated with pro-inflammatory TLR ligands expressed significantly elevated mRNA levels of the CCRL2 receptor. Due to this finding, BMDM cells were treated with LPS (0.1μg/ml) or vehicle for 16 hours in order to increase the CCRL2 receptor mRNA expression by these cells. WT cells with 16 hour LPS treatment did not display any differences in their migratory behaviour towards C5a, however, *CCRL2*$^{-/-}$ cells display a significant increase towards C5a following LPS-treatment. Both WT and *CCRL2*$^{-/-}$ cells show a non-significant decrease in chemotaxis towards chemerin and C17 following LPS-treatment. This could be due to the slight decrease in ChemR23 receptor protein expression following LPS-treatment seen in Figure 4.1b.

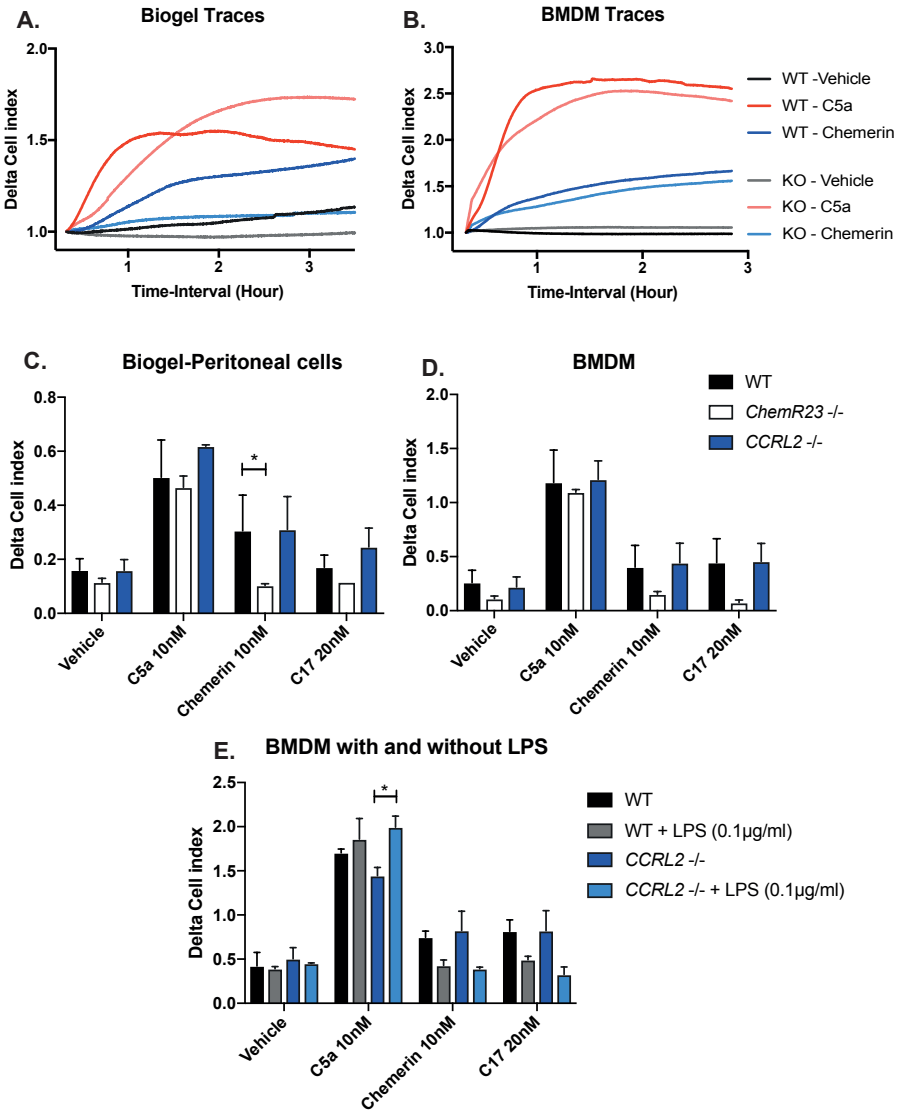


Figure 5.8: Absence of ChemR23 inhibits leukocyte migration towards chemerin whereas the absence of *CCRL2* has no effect in real-time chemotaxis assay. Biogel-elicited murine peritoneal cells or 7 day cultured murine bone-marrow derived macrophages (BMDM) ($4x10^5$) were placed into upper chamber of a CIM-16 plate and allowed to migrate for 3-4 hours, at 37°C, 5% CO_2, towards vehicle, C5a, Chemerin (both 10nM) and C-terminal C17 peptide (20nM). Representative real-time chemotaxis traces towards C5a and Chemerin of (**A.**) biogel-elicited peritoneal cells from WT and *ChemR23*-/- and (**B.**) BMDM from WT and *CCRL2*-/-. **C-D.** Mean S.E.M. of 2-4 biological replicates from WT, *ChemR23*-/- and *CCRL2*-/- cells with 2 technical replicates per condition. **C.** Biogel-elicited peritoneal cells from *CCRL2*-/- show no differences in chemotaxis, where as *ChemR23*-/- shows significant reduction in chemotaxis towards chemerin. **D.** BMDM cells from *CCRL2*-/- and *ChemR23*-/- show similar migration pattern to the Biogel elicited cells. BMDM from WT and *CCRL2*-/- were treated with LPS (0.1μg/ml) for 16 hrs prior to placing into chemotaxis assay. No differences between WT and *CCRL2*-/- with and without LPS for chemotaxis towards chemerin, where as *CCRL2*-/- treated with LPS show significantly higher chemotaxis towards C5a. Statistical significance was assessed by two-way ANOVA with Sidak's multiple comparisons correction, $*P \leq 0.05$.

5.2.7 *In vitro* zymosan and chemerin stimulations of peritoneal mesothelium and resident cells.

From previous data in this chapter, I have demonstrated that mice lacking the CCRL2 receptor exhibit exaggerated CXCL1 production during early time points of acute inflammation. CXCL1 is a potent neutrophil chemoattractant, so higher levels of this chemokine will recruit higher numbers of neutrophils to the site of inflammation. Due to the higher levels of chemerin found locally and systemically and the data from Figures 5.5, 5.6, I hypothesised that chemerin is inducing the production of CXCL1 by cells present in the peritoneum. This function of chemerin has been reported in previous work carried out on vascular endothelial cells and synoviocytes *in vitro*. Hence, peritoneal mesothelium tissue and resident peritoneal cells from WT and *CCRL2*$^{-/-}$ were treated with zymosan (100μg) or zymosan with recombinant chemerin (20nM) for 4 hours *in vitro*. Cell supernatants were collected and CXCL1 levels were quantified by ELISA. There were no differences observed in CXCL1 production between the WT and *CCRL2*-/- mesothelium tissue or resident peritoneal cells (Figure 5.9b,c). Yet, there was a significant increase in the CXCL1 production in the zymosan with chemerin treated mesothelium tissue compared to zymosan alone treatment in *CCRL2*$^{-/-}$ mice, while there is no difference between the WT group.

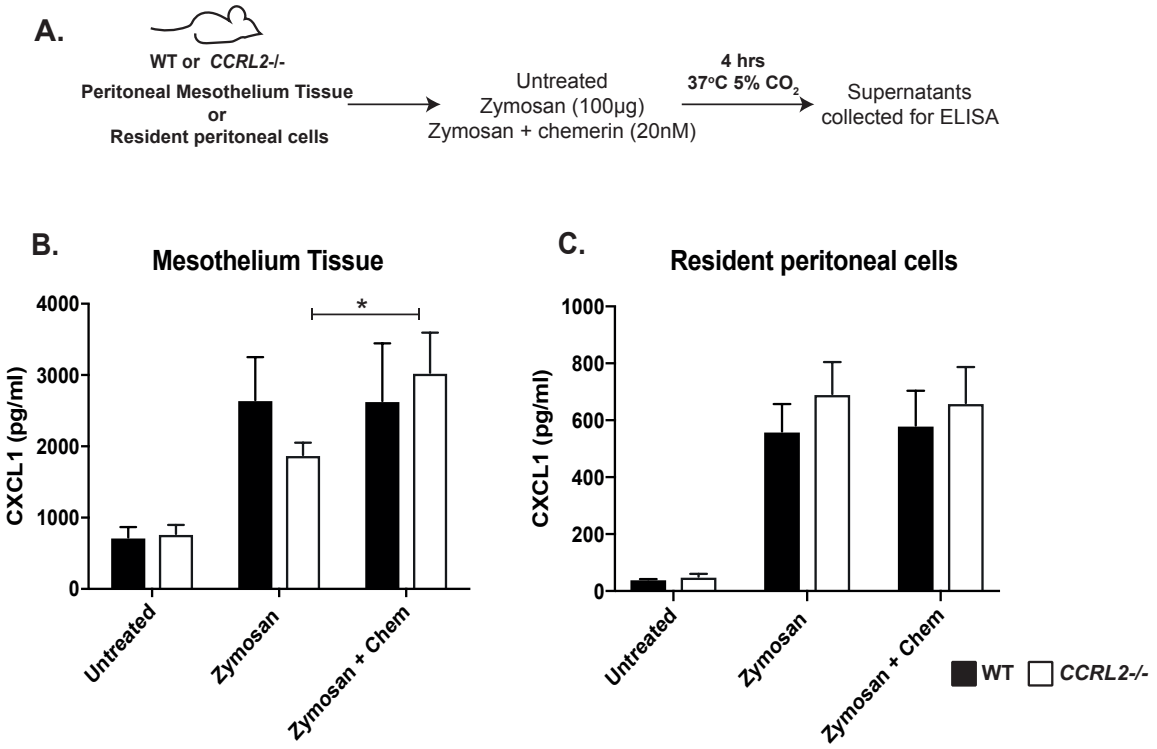


Figure 5.9: The CXCL1 production by WT and *CCRL2*-/- peritoneal mesothelium and resident cells show no differences following *in vitro* stimulations. A. 8-11 week old female *CCRL2*-/- and WT mice were euthanised and their peritoneal cavities were lavaged with ice-cold PBS supplemented with 2mM EDTA. Peritoneal mesothenium tissue was dissected into uniform sizes by a punch biopsy instrument. The dissected mesothelium and resident cells ($8x10^5$) were placed in complete RPMI media and treated *in vitro* with zymosan (100μg) and recombinant murine chemerin (20nM) for 4 hrs at 37°C 5%CO_2, supernatants were collected for analysis by ELISA. **B.** Mesothelium tissue from WT and *CCRL2*-/- shows no difference in the production of CXCL1 following *in vitro* treatments. However, there is a significant increase in the production of CXCL1 by *CCRL2*-/- treated with and without chemerin. **C.** Resident peritoneal cells from WT and *CCRL2*-/- shows no difference in the production of CXCL1 following *in vitro* treatments. Error bars represent S.E.M. of 4-5 biological replicates. Statistical significance was assessed by one-way and two-way ANOVA with Sidak's multiple comparisons correction. $*P \leq 0.05$.

5.2.8 Absence of the chemerin signalling receptor, ChemR23, decreases leukocyte recruitment to the peritoneum during acute zymosan-induced peritonitis.

The ChemR23 receptor has the strongest binding affinity towards chemerin from all its receptors. It mediates the chemotactic effects of chemerin and its activation leads to rapid downstream signalling cascades, which are $G_{\alpha i/o}$ coupled [164]. To confirm this, murine peritoneal macrophages and BMDMs lacking the ChemR23 receptor show defective migration towards chemerin and C-terminal C17 peptide in Figure 5.8. Previous reports of *ChemR23*$^{-/-}$ in different inflammatory models have

shown decreased and increased inflammatory recruitment [178, 307, 180]. Due to the elevated levels of chemerin in the *CCRL2*$^{-/-}$ animals and the general inflammatory phenotype observed in early time points, I wanted to investigate the effect of this acute inflammatory model of ZIP in the absence of ChemR23 receptor. Mice lacking ChemR23 receptor are on a 129S6 stain background used in Cash *et al.*, hence 129S6 WT controls and *ChemR23*$^{-/-}$ were injected with zymosan (100μg/mouse) i.p. for 2 or 16 hour time points. Peritoneal cell populations and inflammatory mediators present in the peritoneum were analysed by flow cytometry and ELISA. Mice lacking the ChemR23 receptor display a reduction in inflammatory cell recruitment in acute time points of zymosan induced peritonitis. Total CD45^{+} peritoneal cells are significantly decreased at 2 hours and non-significantly decreased at 16 hour in *ChemR23*$^{-/-}$ mice, Figure 5.10c. There are significant decreases in neutrophil (CD11b, Ly6G, Ly6C) recruitment at 2 and 16 hours, Figure 5.10b,d. At 16 hours post ZIP injection, *ChemR23*$^{-/-}$ mice display $7.5\pm0.8\times10^{6}$ neutrophils compared to $10\pm1.0\times10^{6}$ in WT mice. Similarly, monocytes (CD11b, Ly6C) at 16 hours ZIP are significantly reduced in *ChemR23*$^{-/-}$ with $1.1\pm0.15\times10^{6}$ and $1.9\pm0.22\times10^{6}$ in *ChemR23*$^{-/-}$ and WT respectively. The lack of ChemR23 receptor does not significantly reduce the recovery of the macrophages population at 16 hours of ZIP (Figure 5.2e). The inflammatory mediators CXCL1 and IL-6, present in the peritoneum, are significantly decreased by $\geq 1.4\times$ in the *ChemR23*$^{-/-}$ mice at the 2 hour ZIP, while CCL2 displays no change between groups (Figure 5.10g-i). Finally, chemerin is significantly increased in the peritoneal fluid of *ChemR23*$^{-/-}$ mice at both 2 and 16 hours post ZIP.

Following inflammatory onset by ZIP, the leukocyte content of blood and spleen were also measured by flow cytometry. Blood neutrophils are significantly reduced in the *ChemR23*$^{-/-}$ mice; with $0.2\pm0.03\times10^{6}$ compared to $0.3\pm0.02\times10^{6}$ in the WT mice at the 2 hour ZIP time point (Figure 5.11a). While there is no observed differences in blood monocytes numbers in blood between the two genotypes at 2 and 16 hours post zymosan injection. Spleen neutrophils and monocytes are significantly decreased in *ChemR23*$^{-/-}$ mice at 2 hours ZIP, and by stark contrast, both neutrophils and monocytes are significantly elevated at 16 hours post ZIP injection (Figure 5.11i,j). The inflammatory mediators CXCL1 and CCL2 in the plasma are significantly increased, while IL-6 is non-significantly increased in *ChemR23*$^{-/-}$ mice. CXCL1 is 1.5$\times$ higher in *ChemR23*$^{-/-}$ mice at the 2 hour ZIP time point (Figure 5.11c). However, at 16 hours, CXCL1 is significantly reduced in *ChemR23*$^{-/-}$ mice. Chemerin is significantly increased at 2 hours ZIP in plasma in *ChemR23*$^{-/-}$ mice, where as in 16 hours, shows no differences between genotypes.

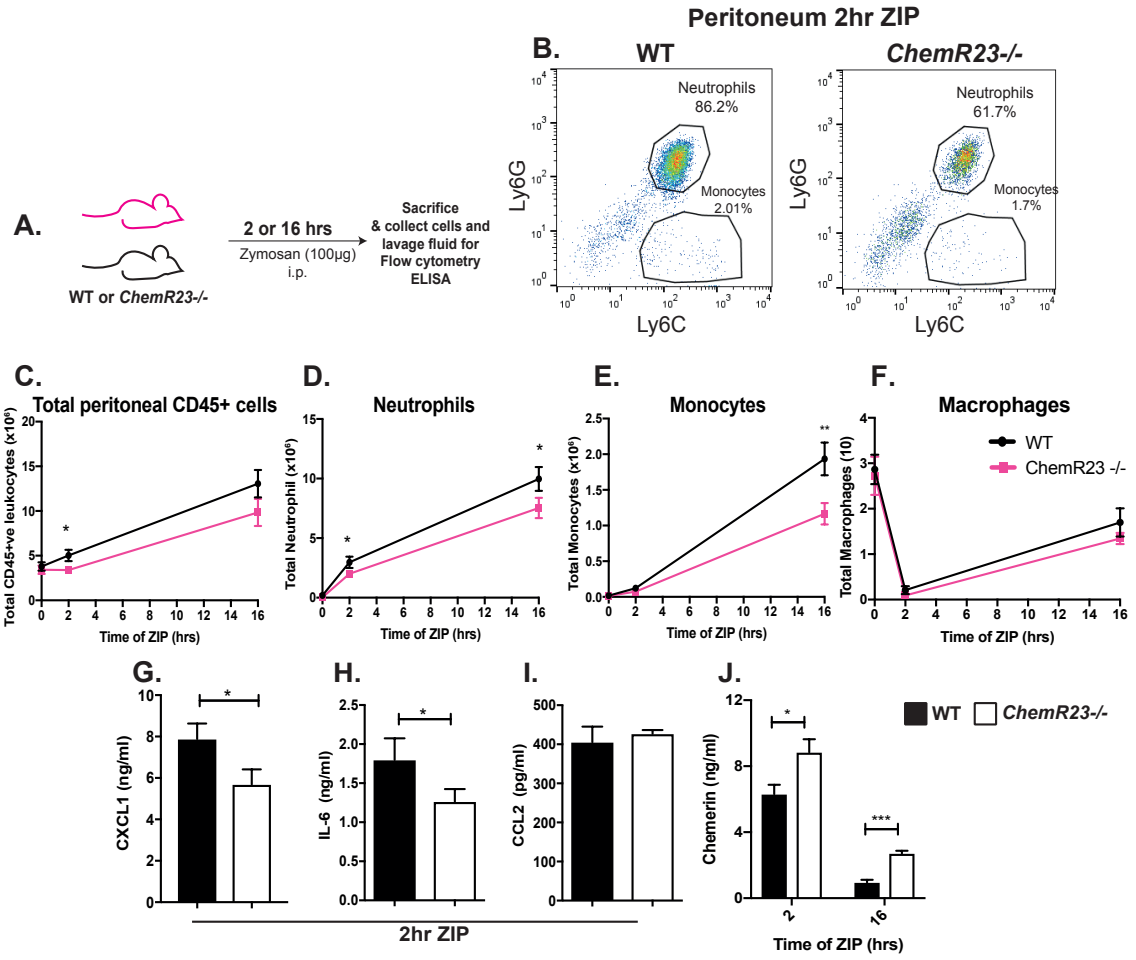


Figure 5.10: The absence of chemerin signalling receptor, ChemR23, decreases leukocyte recruitment to peritoneum during acute zymosan-induced peritonitis. A. 8-11 week old male *ChemR23-/-* and WT mice were injected i.p. with zymosan (100μg/mouse). Mice were euthanised following inflammatory onset at the indicated time points. Peritoneal cavities were lavaged with ice-cold PBS supplemented with 2mM EDTA, cells populations were analysed by flow cytometry and quantified by counting beads. **B.** Representative flow cytometry plots of neutrophils and monocytes in the peritoneum following 2 hour zymosan-induced peritonitis (ZIP) in WT and *ChemR23-/-* mice. **C-F.** Total cells present in peritoneum under naive conditions, 2 and 16 hrs following inflammatory onset; WT in black, *ChemR23-/-* in pink. **C.** Total CD45$^+$ peritoneal cells show no differences under naive conditions. However, at 2 hr time points of ZIP onset, *ChemR23-/-* mice show significant reductions in total CD45$^+$ cells. **D.** Neutrophils are significantly decreased in *ChemR23-/-* following 2 and 16 hr ZIP time points. **E.** Monocyte counts are significantly decreased in *ChemR23-/-* at the 16 hrs ZIP time points. **F.** Macrophages show no significant differences between groups. **G-J.** Chemokines and cytokines, present in peritoneal cavities, were measured by ELISA. **G-H.** CXCL1 and IL-6 are significantly decreased in *ChemR23-/-*, while (**I.**)CCL2 levels do not differ between groups at 2hr ZIP time point. **J.** During 2 and 16 hr ZIP time points, chemerin is increased in *ChemR23-/-* mice. Error bars represent S.E.M. of n=3-7 animals/group. Statistical significance was assessed using unpaired t-tests and two-way ANOVA with Sidak's multiple comparisons correction, $*$ P$\leq$0.05, $***$P$\leq$0.001.

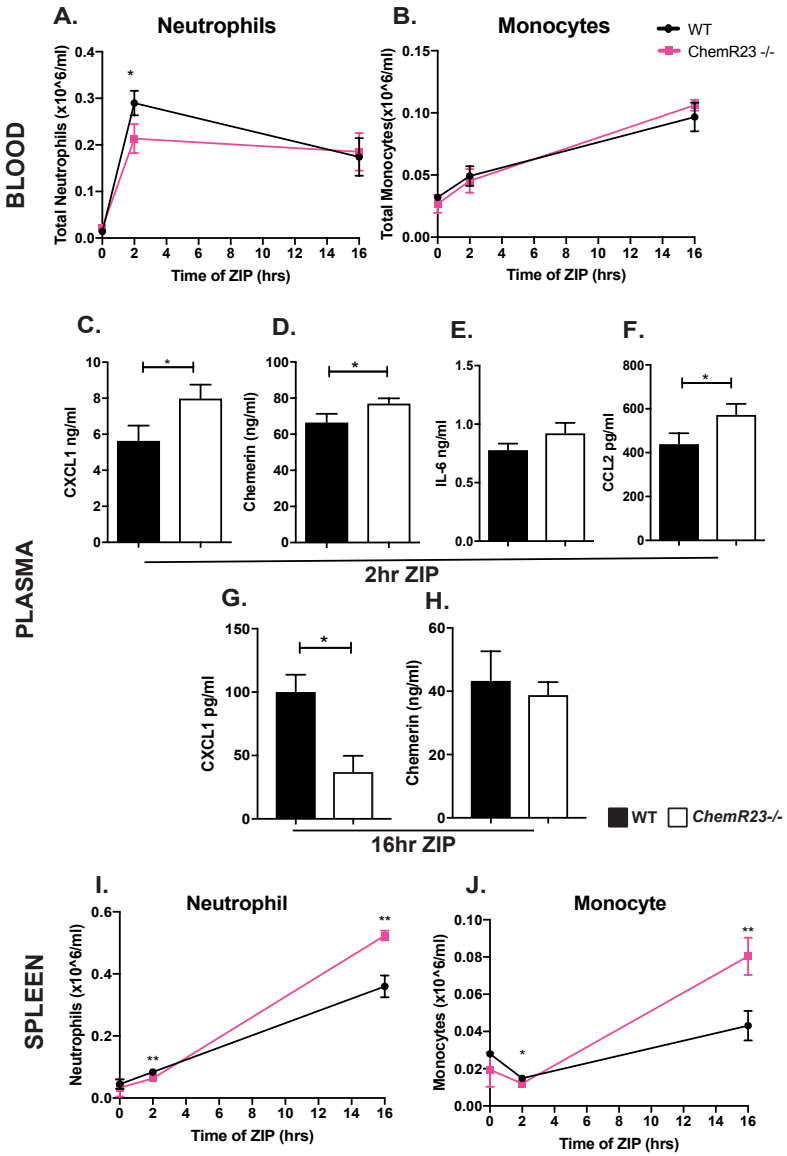


Figure 5.11: The absence of non-signalling receptor, ChemR23, increases leukocytes in spleen and inflammatory mediators in plasma, while reducing neutrophils in blood during acute zymosan-induced peritonitis. 8-12 week old male *ChemR23*-/- and WT mice were injected i.p. with zymosan (100μg/mouse). Mice were euthanised following inflammatory onset at the indicated time points. Blood was collected via the posterior vena cava into EDTA coated tubes and spleen was collected with ice-cold PBS. Cells were quantified by counting beads and cell populations were anaylsed by flow cytometry. **A-B.** Concentration of blood cells present under naive conditions, 2 and 16 hrs following inflammatory onset; WT in black, *ChemR23*-/- in pink. **A.** Blood neutrophils are significantly lower in *ChemR23*-/- at 2 hr time point of ZIP. **B.** Blood monocytes show no significant differences between groups. **C-H.** Inflammatory mediators were measured in blood plasma by ELISA. **C,D,F.** CXCL1, chemerin and CCL2 are significantly increased in *ChemR23*-/- at 2 hr time point of ZIP. **E.** IL-6 shows no significant change at 2hr time point of ZIP. **G.** CXCL1 is significantly reduced at 16 hr ZIP, while, (**H.**) chemerin shows no significant change. **I-J.** Spleen neutrophils and monocytes are significantly decreased at 2hrs and increased at 16hr ZIP in the *ChemR23*-/- mice. Error bars represent S.E.M. of n=4-12 animals/group. Statistical significance was assessed using unpaired t-tests and two-way ANOVA with Sidak's multiple comparisons correction. $*P \leq 0.05$, $**P \leq 0.01$.

5.3 Discussion

The main aims of this chapter were firstly to assess immune cell recruitment in *CCRL2*$^{-/-}$ mice during acute phases of peritoneal inflammation and secondly to investigate the mechanism behind any differences observed between WT and *CCRL2*$^{-/-}$ mice.

5.3.1 The inflammatory phenotype of *CCRL2*$^{-/-}$ mice

With regards to the first aim, I found that *CCRL2*$^{-/-}$ animals exhibit 2 fold increases in neutrophil and monocyte recruitment in comparison to WT animals, during acute inflammatory phases of zymosan-induced peritonitis. Peritonitis is a simple model of inflammation, where an inflammogen is injected intraperitoneally. It is used to monitor leukocyte trafficking in acute instances of inflammation, due to the fact that cell and mediator recovery is easily obtained from the local site of inflammation, the peritoneum. This model is also used in later time points to study the resolution phase of inflammation, where it has been very useful in identifying pro-resolution lipid mediators of inflammation, such as resolvin E1 and lipoxin A4 [308, 280, 309]. Prior to carrying out the ZIP, the resting state of the peritoneal cell populations in both WT and *CCRL2*$^{-/-}$ mice was confirmed to show no differences (Figure 5.1). Immune cells present in blood, spleen and bone marrow were also comparable in the *CCRL2*$^{-/-}$ mice (D.Regan-Komito, Personal communication/unpublished data).

During inflammation, polymorphonuclear cells, neutrophils, are the first cells to be recruited to the site of inflammation to clear the noxious agent. They are followed by a wave of mononuclear cells, monocyte, recruitment which eventually lead to the re-population of resident macrophages in the site of inflammation to restore the tissue homeostatic state [88]. Therefore, in order to thoroughly assess differences in immune cell migration by WT and *CCRL2*$^{-/-}$ mice, multiple time points were analysed during the acute phase of zymosan-induced peritonitis (2, 4, and 16 hours), in Figure 5.2. This process also revealed the cellular kinetics of acute inflammation for this model, whereby total peritoneal cells and total neutrophils present in peritoneum reach their peak at 4 hours post zymosan injection. Total monocyte recruitment reaches its highest at 16 hours while the total peritoneal cells numbers begin to decline between 4 and 16 hours. Resident macrophages constitute the largest proportion of cells in the peritoneum under naive conditions, during inflammation, the proportion of macrophages declines by 9× at 2 hours post zymosan injection and begins recovering at 16 hours, which correlates with the monocyte recruitment to the peritoneum.

CCRL2$^{-/-}$ mice display significantly elevated neutrophils at 2, 4 and 16 hours and significantly increased monocytes at 16 hours post zymosan injection compared to WT controls (Figure 5.2b,c). I also observed systemic changes in neutrophils and monocytes in blood, in the *CCRL2*$^{-/-}$ mice, at 4 and 16 hours, respectively. Finally, there are elevated monocytes in spleen at 2 hours in the *CCRL2*$^{-/-}$ animals (Figure 5.3).

The results obtained from the zymosan-induced peritonitis in *CCRL2*$^{-/-}$mice (Figure 5.2) were confirmed as being stimulus independent by using an alternative well-established inflammogen for peritonitis: thioglycollate brewers broth. Zymosan is a yeast cell wall particle and thus engages the TLR2 and Dectrin-1 receptors for pathogen recognition. Thioglycollate broth contains abundant protein and reducing sugars, which undergo non-enzymatic reactions. This leads to the generation of AGEs which stimulate the RAGE receptor [305]. Both inflammogens establish a higher neutrophil recruitment to the peritoneum of *CCRL2*$^{-/-}$ in early time points of peritonitis (Figure 5.4).

5.3.2 Other inflammatory models in the absence of CCRL2

The role of CCRL2 receptor during inflammation has yet to be fully understood. It is a receptor of interest due to the fact that it is a non-signalling receptor, that is widely expressed by leukocytes, endothelial and epithelial cells and becomes greatly upregulated during inflammation, in Figure 4.1 [171, 301]. As stated previously, one popular model for the function of CCRL2 is to present chemerin to ChemR23 expressing cells. Therefore, the function of CCRL2 should be determined by the function of chemerin and its ability to signal through its other receptors. Several studies investigating the role of CCRL2 *in vivo* have produced conflicting results potentially due to the different type of inflammatory models employed. Zabel *et al.*, Monnier *et al.* and Otero *et al.* show that mice lacking CCRL2 display reduced leukocyte recruitment in an atopic and lung allergy models as well as an acute lung inflammatory model. A very recently published study conducted in two models of inflammatory arthritis reported that CCRL2-deficient mice had a defect in neutrophil recruitment to the site of inflammation [184]. *In vitro* analysis found that CCRL2 could regulate the function of CXCR2 [184].

Contrary to the prior, Mazzon *et al.* reported that mice lacking CCRL2 receptor display exacerbated disease in an EAE model, associated polarisation towards T_H1 and M1 pro-inflammatory phenotype. Finally, my study on CCRL2 using the zymosan-induced peritonitis model, is the first to assess the *in vivo* role of CCRL2 in

early time points of acute inflammation, while the other models have focused on its role in longer term models.

5.3.3 Addressing the mechanism driving the inflammatory phenotype

To address the second aim of this chapter namely the mechanistic basis of increased acute inflammation in *CCRL2*$^{-/-}$ mice, I assessed various inflammatory mediators in local and systemic regions of the ZIP model. In order to begin understanding the mechanism driving the inflammatory phenotype observed in the *CCRL2*$^{-/-}$ mice. This exaggerated leukocyte recruitment correlated with increases in the inflammatory mediator, CXCL1, locally and systemically in early time points of zymosan and thioglycollate induced peritonitis (Figure 5.2f, 5.3c, 5.4). CXCL1 is a potent neutrophil chemoattractant which signals via the CXCR2 and CXCR1 receptor present on neutrophils [310, 311]. During early inflammation, resident macrophages and mast cells in the peritoneum produce CXCL1 and CXCL2 (MIP-2) upon TLR 2, 3, and 4 stimulation, which results in neutrophil recruitment to the site of injury [304, 312]. Similarly, elevated levels of CXCL1, in this model, induced greater neutrophil recruitment as early as 2 hours of ZIP. Neutrophil numbers continue being significantly higher at 4 and 16 hour time points post ZIP in *CCRL2*$^{-/-}$ mice, regardless of the fact that CXCL1 is below detection at these later time points. This is contrary to the experimental findings reported by Del Prete *et al.* where CCRL2 had a role promoting the functions and expression of CXCR2 receptor [184]. Other inflammatory mediators were not found to be different between genotypes at 4 hours (D.Regan-Komito, unpublished data) and the mediators were below the ELISA detection limit at 16 hours.

An important mediator assessed during these experiments, is the CCRL2 ligand, chemerin. Chemerin is produced by multiple sources, including adipocytes, kertinocytes and endothelial cells; its production is upregulated upon TNFα treatment in adipocytes and retinoic acid stimulation in endothelial cells [313, 169, 192]. The *CCRL2*$^{-/-}$ animals display elevated levels of chemerin locally and systemically post zymosan and thioglycollate-induced peritonitis. These results are in agreement with a report by Monnier *et al.* following a LPS-induced peritonitis [171]. It is common to see that in the absence of a receptor, its ligand is usually increased in homeostatic and inflammatory conditions. For example, TNFα is elevated in mice lacking the TNFR1 and 2 receptors [314, 315]. Thus, giving an explanation for the elevated chemerin levels seen in both *CCRL2*$^{-/-}$ and *ChemR23*$^{-/-}$ mice during acute

phase of ZIP (Figure 5.2, 5.10). Regardless of whether CCRL2 lacks classic downstream signalling, these findings suggest that one of the roles of CCRL2 receptor is to maintain 'free' chemerin at a homeostatic level during inflammation. Rather than having to be presented by the CCRL2 receptor, I postulate that 'excess' chemerin observed in *CCRL2*$^{-/-}$ mice will be freely available to bind to the other chemerin receptors, ChemR23 and GPR1, both of which have the ability to activate a downstream signalling cascade. In order to investigate whether chemerin signalling via these other receptors was occuring, I pre-treated *CCRL2*$^{-/-}$ mice with a chemerin blocking antibody, which had been validated in a ChemR23 activation assay in chapter 3 (Figure 3.10). With this experiment, I was able to illustrate that chemerin is actively contributing to the *CCRL2*$^{-/-}$ inflammatory phenotype (Figure 5.5), as the anti-chemerin treatment resulted in a significant decrease in neutrophil peritoneal influx at 4 hour ZIP. Importantly, from the data in chapter 4, I was able to confirm that neutrophils do not express protein or mRNA of the active chemerin receptor ChemR23 and GPR1 but they do express mRNA of CCRL2 (Figure 4.3, 4.5). Additionally, this decrease in neutrophil influx correlates with a significant decrease in the CXCL1 production in the peritoneum (Figure 5.5e). Furthermore, there was no effect on the monocyte influx following anti-chemerin treatment at 4 hour post ZIP. This could indicate that the concentration of chemerin blocking antibody used may not be optimal or that the augmented monocyte recruitment in *CCRL2*$^{-/-}$ at 4 hour ZIP, occurs independent to chemerin. As the levels of CCL2, a potent monocyte chemoattractant protein, were also unchanged between groups, it seems likely that elevated levels of chemerin do not effect the monocyte recruitment directly.

To further investigate the role of 'free' chemerin in acute inflammation, I pre-treated C57BL6 WT mice with recombinant chemerin prior to inducing a 4 hour ZIP. The wild type mice have all functional chemerin receptors, hence the only variable is the excess chemerin. The pre-treatment of recombinant chemerin displays exacerbated neutrophil recruitment and inflammatory mediator production of CXCL1, IL-6 and CCL2 at 4 hour ZIP, with both higher(4μg) and lower (0.5μg) doses (Figure 5.6, 5.7). At the 4 hour time point, *CCRL2*$^{-/-}$ mice show a significant increase in monocyte recruitment to the local site of inflammation, while the WT chemerin-treated mice do not. Despite this, in later time points, the WT chemerin-treated animals may display an increase in the number of monocytes in the peritoneum, probably because they display an increase in CCL2 chemokine at 4 hour ZIP for both doses of chemerin treatments (Figure 5.6, 5.7). As an experimental control, I injected 4μg chemerin alone to confirm that neutrophil recruitment, was not driven by chemerin

alone (Figure 5.6), this was also confirmed from chapter 4, Figure 4.12. However, I found a significant increase in CXCL1 production in the chemerin-treated group vs the PBS injected after 4 hours of PBS injection. Due to the fact that the CXCL1 production is significantly lower than when the animals are induced with zymosan, there are no neutrophils being recruited. I wanted to confirm my findings with a lower dose of recombinant chemerin (0.5μg), to make the concentration of chemerin more physiologically relevant. I confirmed this by quantifying the peritoneal chemerin by ELISA, which showed that chemerin-treated mice had significantly higher chemerin but the levels were comparable to the *CCRL2*$^{-/-}$ mice (Figure 5.7).

Next, I investigated the mechanism using *in vitro* assays to understand the inflammatory phenotype of the *CCRL2*$^{-/-}$ mice. First, I assessed leukocyte migration, using a real-time chemotaxis system, ACEA xCelligence (Roche), in the absence of CCRL2 receptor and while comparing to WT and *ChemR23*$^{-/-}$ cells. In the absence of CCRL2, leukocytes exhibited no change in their migratory abilities, whereas the absence of ChemR23 receptor reduced migration towards chemerin and C-terminal chemerin-derived peptide C17 in both Bio-Gel elicited peritoneal cells and BMDM (Figure5.8). Bio-Gel elicited peritoneal cells (PECs) contain a mixture of 30% macrophages, 40% neutrophils and 10% monocytes. As seen in Figure 4.5, macrophages and monocytes from Bio-Gel elicted PECs express the ChemR23 receptor, the receptor responsible for chemotaxis towards chemerin, whilst neutrophils do not. Furthermore, the adherent nature of macrophages enables the measurement of the chemotactic cell index in the ACEA xCelligence real-time chemotaxis assay, because the chemotaxis measurement is obtained from cells adhering to the gold plated under-side of the transwell plate. From previously published work, it is expected that the macrophage population in Bio-Gel elicted PECs will be responsible for the signals obtained in the ACEA xCelligence real-time chemotaxis assay [316]. By using a second pure macrophage population of 7 day cultured murine BMDM, I observed a similar migratory behaviour, the absence of the CCRL2 receptor does not effect macrophage chemotaxis towards C5a, an anaphylotoxin and potent chemoattractant, and chemerin and derived peptide C17. In the absence of the ChemR23 receptor BMDM show no difference in chemotaxis towards C5a but display a non-significant reduction in migration towards chemerin and derived peptide C17. Moreover, I investigated whether there were any changes to the migration behaviour of BMDM following 16 hour exposure to LPS (0.1μg/ml). BMDM exposed to TLR ligands upregulate their expression of the CCRL2 receptor (Figure 4.1), therefore, I wanted to assess whether the upregulation of CCRL2 made any changes to the migration behaviour of WT BMDM and

CCRL2$^{-/-}$ BMDM as a control. I found that there were no differences in migration towards C5a in LPS-treated WT BMDM compared to untreated WT BMDM. However, the migration towards C5a in LPS-treated *CCRL2*$^{-/-}$ BMDM is significantly upregulated compared to the untreated *CCRL2*$^{-/-}$ BMDM (Figure 5.8e). Both WT and *CCRL2*$^{-/-}$ BMDM display a non-significant decrease in chemotaxis towards chemerin and derived peptide C17 following 16 hour LPS treatment, could be due to the decrease in ChemR23 receptor expression (Figure 4.1).

One important mechanism driving the inflammatory phenotype in my inflammatory model of the *CCRL2*$^{-/-}$ is the increased production of CXCL1, which seems to be affected by the presence of 'excess' chemerin. I hypothesised that 'excess' chemerin in an inflammatory setting stimulates elevated production of CXCL1. Previous work has identified the expression of the CCRL2 receptor on various leukocyte populations, endothelial and epithelial cells [173, 171, 182]. Therefore, in order to identify the cell type responsible for the higher CXCL1 production in the peritoneum of *CCRL2*$^{-/-}$ mice, peritoneal mesothelium tissue, composed of simple squamous epithelial cell, and resident peritoneal cells, composed of leukocytes in Figure 4.6, were treated *in vitro* with zymosan or zymosan with chemerin (20nM) for 4 hours. The CXCL1 production between WT and *CCRL2*$^{-/-}$ mesothelium tissue shows no difference in the zymosan and zymosan with chemerin group. However, there is a significant increase in the chemerin treated group of the *CCRL2*$^{-/-}$ when compared to the *CCRL2*$^{-/-}$ zymosan alone group but this difference was no seen in the WT mesothelium tissue. This indicates that the elevated levels of chemerin do contribute to the increased CXCL1 production in the presence of an inflammatory stimulus by the *CCRL2*$^{-/-}$ mesothelial cells. However, this effect is not recapitulated in the WT mesothelial cells nor is the expression of CXCL1 higher in the *CCRL2*$^{-/-}$ compared to the WT which I would expect. The resident peritoneal cells display no difference in CXCL1 production by the WT and *CCRL2*$^{-/-}$ between the chemerin and zymosan alone treated groups, which suggests that they are not responsible for the augmented CXCL1 production.

As mentioned previously, the inflammatory phenotype observed in the absence of CCRL2 could at least be partly due to the augmented chemerin levels seen in *CCRL2*$^{-/-}$ which are freely available to bind and signal through its other two active receptors, GPR1 and ChemR23. Chemerin binding to ChemR23 receptor mediates a signalling cascade involving MAP kinase, RhoA, ROCK, MEK1/2 and p38 proteins among others [165, 303]. I wanted to assess whether the effects of chemerin in the *CCRL2*$^{-/-}$ were mediated through the ChemR23 receptor. Mice lacking the ChemR23 receptor display a significant reduction in the neutrophil and monocyte recruitment to

the local site of inflammation in both 2 hour and 16 hour zymosan-induced peritonitis (Figure 5.10). There was also a significant reduction in the blood neutrophils at 2 hours post ZIP (Figure 5.11). These results display the opposite effect to what is seen in the mice lacking CCRL2 receptor at the 2 and 16 hour ZIP. Consistent with a reduction in neutrophil influx, the inflammatory mediators present in the peritoneum, CXCL1 and IL-6, are significantly $\geq 1.3\times$ decreased at 2 hour ZIP. Even though CCL2, a monocyte chemoattractant, is unchanged between groups, the monocyte influx is significantly reduced in *ChemR23*$^{-/-}$ mice at 16 hour ZIP. In later time points, CCL2 may be decreased, resulting in the decreased monocyte recruitment observed at 16 hours post ZIP. Or on the other hand, the decrease in monocyte recruitment could be occuring independently of CCL2, even though the CCR2/CCL2 axis is important for monocyte mobilisation [317, 318, 278]. The absence of the ChemR23 receptor will result in the ablation of chemotaxis this could be partially responsible for the reduced monocyte recruitment observed in the *ChemR23*$^{-/-}$ mice. However, there have been conflicting reports about the expression of ChemR23 receptor on human and murine monocytes [319, 280, 281]. Although I have not been able to detect the ChemR23 receptor on blood monocytes (Figure 4.4), I am able to detect it on monocytes recruited to the peritoneum in 4 day Bio-gel elicited PECs (Figure 4.5).

Contrary to the decreases in inflammatory mediators seen in the peritoneum, systemically in the plasma, CXCL1 and CCL2 are significantly upregulated at the 2 hour ZIP, followed by a significant decrease in CXCL1 at 16 hours, whereas CCL2 is under below the detection limit at 16 hours (Figure 5.11). The upregulation of CXCL1 and CCL2 is not reflected on the monocyte recruitment to the peritoneum or the blood. Though the splenic neutrophils and monocytes are both significantly downregulated and then upregulated at 2 and 16 hours ZIP respectively. With this data from the inflammatory mediators in the plasma, I would expect to see augmented neutrophils and monocytes in the blood at later ZIP time points, such as 4 or 16 hours, due to the fact that monocyte mobilisation is CCR2 dependent from the bone marrow [318, 278]. This would then account for the higher levels of neutrophils and monocytes in the spleen at 16 hours ZIP. Elevated levels of chemerin are also observed in the *ChemR23*$^{-/-}$ mice during peritonitis, at 2 and 16 hours ZIP compared to the WT controls. As mentioned earlier, it is common to see elevated levels of a ligand in the absence of a corresponding receptor. One interesting point to note is that the overall levels of chemerin in the 129S6 stain are higher than in the C57BL/6J strain. The peritoneal chemerin levels of WT mice at 2 hour ZIP are 6.3 ± 0.57 ng/ml and 2.4 ± 0.28 ng/ml in 129S6 and C57BL6 respectively. However, the fold increase in

CCRL2$^{-/-}$ is 2× greater than the WT control, while there is only a 1.4× increase measured in the 129S6 *ChemR23*$^{-/-}$ mice. Yet in this instance, the 'excess' chemerin is only able to bind to the other chemerin receptors available, GPR1 and CCRL2 receptors; chemerin is a partial agonist of the GPR1 receptor and CCRL2 does not signal downstream at all [164]. This results in the *ChemR23*$^{-/-}$ mice displaying an overall a reduction in the inflammatory cell recruitment and mediator production to the peritoneum due to the absence of chemerin signalling via the ChemR23 receptor.

The role of ChemR23 receptor during inflammation has been investigated in previous publications, with conflicting results. ChemR23 has been implicated in having anti-inflammatory processes by being the receptor for resolvin E1, an eicosapentaenoic acid-derived lipid mediator, which dramatically reduces inflammation in various disease models [280, 308]. C-terminal chemerin derived peptide, C15, has been implicated in enhancing pro-resolution effects in a low dose zymosan-induced peritonitis and in a wound healing model [175, 286]. Furthermore, Luangsay *et al.* observed that *ChemR23*$^{-/-}$ displayed exacerbated neutrophil and macrophage accumulation in BAL fluid in an acute lung inflammation model induced by transoral instillation of LPS. The treatment with chemerin reduced the accumulated recruitment of inflammatory cells and disease severity in a ChemR23-dependent manner [176]. Using a model of viral pneumonia, Bondue *et al.* showed that *ChemR23*$^{-/-}$ mice had significant increases in mortality, disease severity and neutrophil infiltration to the BAL fluid. This effect was associated with the lack of anti-inflammatory pathways involving ChemR23 receptor expressed by non-leukocytic cells in the lung [178].

Conversely, in agreement with my results from the *ChemR23*$^{-/-}$ peritontis model, Demoor *et al.* showed attenuated inflammation in BAL fluid and lungs of *ChemR23*$^{-/-}$ mice in a model of chronic cigarette smoke-exposed lungs. Inflammatory chemokines and the recruitment of inflammatory cells were significantly decreased as well as a significant delay in T cell accumulation in the lungs [179]. Moreover, *ChemR23*$^{-/-}$ mice displayed decreased inflammatory cell recruitment in an acute lung inflammation model, induced by diesel exhaust particles [181]. In the same publication, Provoost *et al.* performed a house dust mite-induced allergy lung inflammation model on *ChemR23*$^{-/-}$ mice that showed enhanced eosinophilia and T_H2 cytokine production when compared to WT mice. Additionally, a model of dextran sodium sulfate (DSS)-induced colitis carried out on *ChemR23*$^{-/-}$ mice demostrated an attenuated development of clinical illness [180]. Similarly, mice treated with recombinant chemerin in a model of DSS-induced colitis, developed an higher severity of clinical illness, which was assossiated with an M1 macrophage polarisation and suppression

of M2 genes [207]. Finally, Herová *et al.* reported that naive and M1 polarised macrophages express ChemR23, allowing for migration towards site of inflammation via chemerin signalling, while M2 polarised macrophages do not express or migrate towards chemerin. The treatment of M1 macrophages with resolvin E1 converts the M1 via ChemR23 receptor into an alternative polarisation, producing IL-10 and reducing migration towards chemerin, a macrophage phenotype distinctly different from the M2 macrophage phenotype. Even though they did not stimulate macrophages with chemerin, they hypothesise that chemerin acts as a pro-inflammatory mediator in human macrophages and resolvin E1 activates a pro-resolution macrophage phenotype [281].

In conclusion, taking all data into consideration, all the experiments reported in this chapter are consistent with the role of non-signalling CCRL2 receptor is to maintain homeostatic levels of chemerin during the inflammatory process. In my model, chemerin acts as a pro-inflammatory agent in early time points of inflammation, stimulating the production of pro-inflammatory mediators for cell recruitment into local sites of inflammation via the ChemR23 receptor. In this hypothesis, CCRL2, being a non-signalling receptor, is able to act like other non-signalling chemokine receptors, D6 or DARC [307], in dampening the effects of its ligand chemerin. The efficient influx of pro-inflammatory cells to site of inflammation is vital for the effective clearance of invasive pathogens. Thus, the pro-inflammatory actions of chemerin observed in simple zymosan and thioglycollate-induced peritonitis models are important for contributing to the inflammatory process for pathogen clearance. In later time points, when the pathogen is cleared and the pro-resolution process begins to restore the tissue to homeostasis, the ChemR23 receptor may be involved in the enabling the pro-resolution process to occur, through alternate activation of macrophages and other non-leukocyte cells, via chemerin and resolvin E1. Considering the inconsistencies in the literature, the anti-inflammatory actions of ChemR23/chemerin are likely to be site-dependent and dependent on the type of inflammation occurring.

5.3.4 Limitations of the study

One limitation of this study is that the inflammogens used for the peritonitis study, zymosan and thioglycollate, for examining the role of CCRL2 and ChemR23 during acute inflammation, were only stimulating TLR 2, Dectin-1 and RAGE pathogen associated receptors. To fully understand how these receptors regulate inflammation, a wider range of inflammatory agents should be used to identify the various TLR involved *in vivo*. Other inflammagens could include LPS, or inflammatory cytokines

such as IL-1β [320, 309]. This may help identify pathologies where therapeutic intervention targeting CCRL2 or ChemR23 receptor could have clinical value.

A further limitation to this study is that the cell type responsible for the excess production of the pro-inflammatory chemokine, CXCL1, has not been conclusively identified. *In vitro* analysis into this mechanism, reveals that resident leukocyte peritoneal cells are not responsible for excess production of CXCL1 (Figure 5.9). The *CCRL2*$^{-/-}$ mesothelium tissue treated with chemerin produced elevated levels of CXCL1 compared to the zymosan alone, yet no significant difference when compared to the WT. From this result, I speculate that the cells producing higher levels of CXCL1 are resident in the mesothelial lining. In the absence of time restraints, it would have been interesting to generate bone marrow chimeric mice, where bone marrow cells from *CCRL2*$^{-/-}$ or WT mice are transplanted into lethally irradiated mice. This would have helped to identify whether the haematopoietic cells or the non-haematopoietic cells drive the inflammatory phenotype in mice lacking the CCRL2 receptor. In addition to this, treatment of WT murine cells *in vitro* and *in vivo* with an anti-CCRL2 antibody, which has recently become commercially available and published in Del Prete *et al.* [184], would be a useful tool to validate the source of the increased CXCL1 production observed in the zymosan-induced peritonitis.

Furthermore, within this chapter I have been comparing the effect of ZIP in both *CCRL2*$^{-/-}$ and *ChemR23*$^{-/-}$ mice. These knock out mice are on two different background strains, C57BL/6J and 129S6SV respectively. As such, they are genetically distinct. To account for this, each experiment has been analysed independently with its corresponding WT strain control. However, strain discrepancies could be more fully addressed by backcrossing the strains on the same background strain.

Another limitation of this study is that I have only investigated the early events of acute inflammation. The benefit of using zymosan peritonitis is that it is a self resolving inflammatory model, hence its use in identifying various pro-resolution mediators of inflammation. In this study, I have not taken advantage of this aspect of the zymosan-induced peritonitis model, I did not extend my time points to investigate 24, 48 and 72 hours post zymosan injection. At these later time points, the resolution phase of the model, I could investigate the potential anti-inflammatory effects of chemerin using both *CCRL2*$^{-/-}$ and *ChemR23*$^{-/-}$ mice.

Finally, peritonitis models of inflammation do not directly relate to a specific human disease. Sterile peritonitis is occasionally observed in the clinic after leakage of sterile body fluids into the peritoneal cavity after surgery or complications with peritoneal dialysis [321, 322]. Even though this model is ideal for investigating the

principles and the kinetics of acute inflammation, it does not lend itself to a clinically relevant disease process, other than resolving inflammation. Due to elevated serum levels of chemerin in chronic inflammatory diseases, such as coronary artery disease [323], inflammatory bowel disorder [191], metabolic syndrome [324] and rheumatoid artheritis [203, 204], it would be interesting to investigate the role of CCRL2 and ChemR23 receptors in a more clinically relevant disease model in order to assess any potential therapeutic benefits in targeting chemerin and its receptors. [2]

[2]Many of the experiments discussed in this chapter are included in a manuscript submitted to the Journal of Frontiers in Immunology [185].

Chapter 6

Investigating the behaviour of mice lacking CCRL2 receptor

6.1 Introduction

6.1.1 Immunity, the central nervous system and behaviour

There are many well-studied cases in which interactions between a pathogen and its host can lead to behavioural changes in the host. One classic example is that of *Toxoplasma gondii*. *Toxoplasma* is a protozoan parasite that infects a wide range of mammalian species including rodents and humans and the disease it causes is called toxoplasmosis. Evolutionary pressure has helped develop *Toxoplasma*'s ability to effect host behaviour in order to complete the parasite's life cycle [325]. The *Toxoplasma* parasite undergoes asexual reproduction in the host, and can only sexually reproduce in the feline gut. In order for it to get there, the pathogen rodent host must be eaten [325]. Hence, infection with the *Toxoplasma* parasite leads to higher host mobility and exposure [326] and the removal of the innate fear of cats from rodents [327]. The mechanism of action whereby *Toxoplasma* can influence the host behaviour is unknown. Histopathological changes have been observed in the infected hosts where there are cyst-containing regions of the brain which induce local inflammatory profile changes within the brain [328]. Furthermore, significant changes in the levels of neurotransmitters, particularly dopamine, have been observed between infected and uninfected mice [329]. Infections in humans have been linked to behavioural disorders including schizophrenia [325].

More generally, the example of *Toxoplasma* illustrates how the crosstalk between inflammatory pathways and neurocircuits in the central nervous system (CNS) can have a dramatic effect on the behaviour of the host. This crosstalk is able to influence not only the behaviour but also the emotional well-being of an individual.

An imbalance in the interactions between the immune system and the CNS can lead to detrimental effects on mental health. The following brief introduction will discuss how neurotransmitter molecules and inflammatory pathways influence the behavioural changes depicted in depression and anxiety disorders.

Depression and anxiety disorders are in the top ten leading causes of disability worldwide [330]. These disorders are characterised by depressed mood, anhedonia (the lack of motivation to participate in pleasurable activites) and elevated fear and anxiety. Benzodiazepines, discovered in the early sixties were the first commercially available treatment of anxiety and depression. They act on the gamma amino butyric acid (GABA)-A receptor, which is a ligand-gated chloride-selective ion channel. Activation of the GABA receptors has inhibitory actions and thus downregulates neural activation, resulting in sedative and anxiolytic effects [331]. Their actions inhibit the neurotransmission of serotonin and norepinephrine. Nowadays, the major class of anti-depressants prescribed are the selective serotonin or serotonin and norepinephrine reuptake inhibitors (SSRIs or SNRIs). The pharmacological action of these drugs blocks the actions of several serotonin or norepinephrine transporter receptors, thereby treating some forms of depression and anxiety [332]. However, a third of all patients with depression fail to respond to these conventional pharmacological treatments [333]. There is a subset of patients suffering from major depression who display higher levels of inflammatory markers in their plasma, including elevated levels of IL-6 [334, 335] and elevated numbers of circulating leukocytes [336]. Hence, this suggests that there could be an inflammatory component in behavioural and psychological disorders.

The inflammatory response is greatly influenced by the CNS. For instance, in a model of chronic psychosocial stress, catecholamines, such as norepinephrine, are released by sympathetic nerve fibres, which activate the β_3-adrenergic receptors (β_3AR) in the bone marrow. This leads to haematopoietic proliferation, the downregulation of CXCL12 and the subsequent release of myeloid cells to the periphery [337, 338]. This function is beneficial in an evolutionary context; stress induced by the presence of preditors results in the preparation of the immune system to combat injury and subsequent infection [339]. However, repeated psychosocial stress has been shown to promote anxiety-like behaviour in mice in a β-adrenergic receptor-dependent manner. Excess stress results in increased macrophage trafficking to the brain, microglia activation in CNS and higher levels of pro-inflammatory markers including, IL-6, TNFα, CCL2 secreted by microglia [340]. The use of a β-adrenergic receptor antagonist pre-

vents these inflammatory events from occurring [340]. These findings further highlight the strong immune component in the development of the anxiety-like behaviour.

An important mechanism which becomes activated during psychological distress or tissue trauma, is the activation of the hypothalamic-pituitary-adrenal (HPA) axis, which triggers a rapid increase in glucocorticoid production, an immune suppressant. During the events of stress, the hypothalamus also stimulates the production of pro-inflammatory cytokines, such as interleukin-1 (IL-1), TNF and IL-6, which in turn enhances glucocorticoid production. This creates as a positive feedback loop for glucocorticoid production while glucocorticoid receptor signalling activates a negative feedback loop [341]. Disruption to this glucocorticoid receptor results in reduced anxiety and impaired response to stress in mice [342]. Glucocorticoid receptors are expressed in almost every cell type in the body and in general glucocorticoids act to suppress the immune system but they have also been shown to enhance inflammation[341]. For example, administration of glucocorticoids before LPS challenge in rats, enhances the immune response, whereas administration of glucocorticoids following LPS treatment results in a dampened immune response [343]. This indicates that a tightly controlled production of glucocorticoids is necessary for both dampening the inflammatory pathways during inflammation but also in maintaining a balanced cognitive function.

Another mechanism occuring as a result of the crosstalk between the immune system and the CNS, is exhibited by the interplay between proinflammatory mediators and the vagus nerve. Proinflammatory mediators, produced during an inflammatory event, can signal via the vagus nerve to the CNS [344]. The symphathetic nerve fibres then relay the response from the brainstem by releasing catecholamines to lymphoid organs, such as the spleen. The catecholamines can modulate the immune response by promoting dendritic cells to facilitate the development of T helper type 2 (Th2) and Th17 phenotype from $CD4^+$ T cells [345]. The catecholamines can also induce a subset of memory T cells, expressing the β_2-adrenergic receptor, to release acetylcholine. Acetylcholine promotes splenic macrophages to suppress their production of inflammatory cytokines [346].

Furthermore, T cells seem to play a significant role in the maintenance of a positive psychology and cognitive function. The depletion of $CD4^+$ T cells in mice correlates with the cognitive impairment in learning and memory and increased anxitey-like behaviour [347, 348]. The beneficial effects of T cells seems to correlate with the accumulation of T cells producing IL-4 cytokines in the CNS. IL-4 seems to promote

neuroprotective properties by up-regulating neurotrophic factors [349]. Patients suffering from HIV/AIDS disease show a more rapid disease progression when they are in a more stressful environment, have great emotional imbalances and have limited social support [350]. Likewise, patients taking a T-cell immunosuppressive peptide, cyclosporine, following organ transplantation, display a higher occurrence of mood and anxiety disorders [351]. Additionally, another pro-resolution mediator, IL-10, produced by myeloid, B and T cells [352], also seems to play a beneficial role on mood regulation. IL-10 knock-out mice display depressive-like behaviours in mice which are reversed by the administration of IL-10 and over-expression of IL-10 which displayed anti-depressive behavioural phenotype in mice [353]. Taken together, these findings suggest that the activation and production of a balanced anti-inflammatory network is favourable for the effective cognitive function and emotional well-being of mice and humans.

Finally, I would like to give an example of a transgenic mouse, lacking an inflammatory receptor, that displays altered behaviour. The formyl peptide receptors (FPR) belong to a family of sensors which detect microbe-associated molecules. Their main role is to activate the immune response to address the invading pathogen but FPR receptors can also bind to annexin-1 and lipoxin A4; both are pro-resolution lipid mediators. Signalling via these ligands results in dampening of the inflammatory response [68, 124]. Mice lacking FPR1 and 2 receptors display augmented inflammation and higher mortality with pneumococcal meningitis [354]. The lack of either FPR1 or FPR2/3 receptors results in reduced anxiety and fear memory [355, 356]. To conclude, these studies have illustrated that the immune system and the CNS engage in finely tuned communication pathways ensuring our survival against predators and invasive pathogens. An imbalance in the pathways involving the CNS and the immune system can result in disabling psychological effects by the immune system or by invading pathogens. This interplay between the CNS and immune system is yet to be exploited as a therapeutic treatment for mental health disorders. Given the evidence manipulation of the immune system may be beneficial for the third of patients who do not respond to the prescribed treatments.

6.1.2 Rationale of study

Firstly, three independent operators reported altered behaviour by the *CCRL2*$^{-/-}$ mice, including aggression and hyperactivity during handling. Secondly, the chemerin receptors, CCRL2, ChemR23 and GPR1 are all widely expressed in the CNS, including microglial cells, astrocytes and neurons [357, 358, 177, 267]. Thirdly, the lack

of the CCRL2 receptor augments the inflammatory response in mice during acute inflammation, as described in Chapter 5 but also in a CNS autoimmune inflammatory model [183]. Moreover, the antagonism or the lack of ChemR23 reduced disease progression in a CNS autoimmune inflammatory model [213, 177]. This prompted the investigation into the possible altered behaviour of mice lacking the CCRL2 receptor, due to the interlinking relationship between the immune system, the CNS and behaviour described above. The aim of the chapter is to assess the behavioural phenotype of *CCRL2*$^{-/-}$ mice using three well-established behaviour assays and finally observe the morphology of their neuroanatomy.

6.2 Results

6.2.1 Open Field assay

The open field test is a well versed technique in investigating the behaviour in rodents. It provides a controlled environment to assess the exploration and general locomotor activity of mice [359]. Mice were individually placed in the left corner of the gridded open field box and left to explore the environment for 7 minutes. There was no observed difference in the number of rearing (standing on hind legs) between mice but there is a significant decrease in the number of squares crossed by the *CCRL2*$^{-/-}$ mice. There is a significant decrease in the number of times the *CCRL2*$^{-/-}$ mice enter the middle square of the box and the latency entering into the middle square in significantly higher than the WT counterparts.

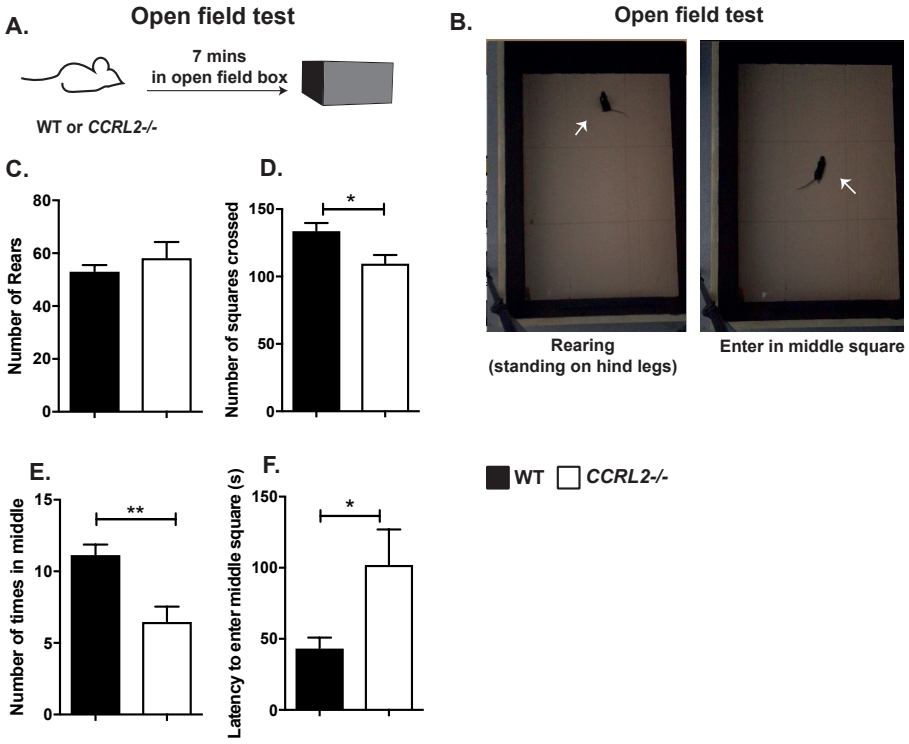


Figure 6.1: Increased anxiety-like behaviour of *CCRL2-/-* mice in the open field test. **A.** 8-10 week old male WT and *CCRL2-/-* mice were placed in open field box for 7 minutes. **B.** Mice were monitored in a gridded open field box for total number of rears (**C.**), total number of squares crossed (**D.**) and number of times entering the middle square (**E.**) in 7 minutes. **F.** Latency to enter the middle square was also quantified. Error bars represent S.E.M. of 6-7 mice/group. Statistical significance was analysed using unpaired t-test $*P \leq 0.05$, $**P \leq 0.01$. Video footage of assay was assessed by 3 independent operators blinded to the genotype of the animals.

6.2.2 Elevated O-Maze test

The elevated O-maze, also known as elevated zero maze, is a well-established technique used to assess anxiety-like behaviour in mice [359]. This test provides the mouse with a choice of spending time in the open, unprotected maze arms, or in the enclosed, protected arms, all elevated approximately 1 metre from the floor. Individual mice are place in the protected 'hidden' arm of the O-maze and left to explore for 5 minutes. There is a non-significant decrease in the time spent in the open 'exposed' arms of the O-maze by the *CCRL2*$^{-/-}$ mice. The number of crosses to the other half of the O-maze is significantly decreased in the *CCRL2*$^{-/-}$ mice.

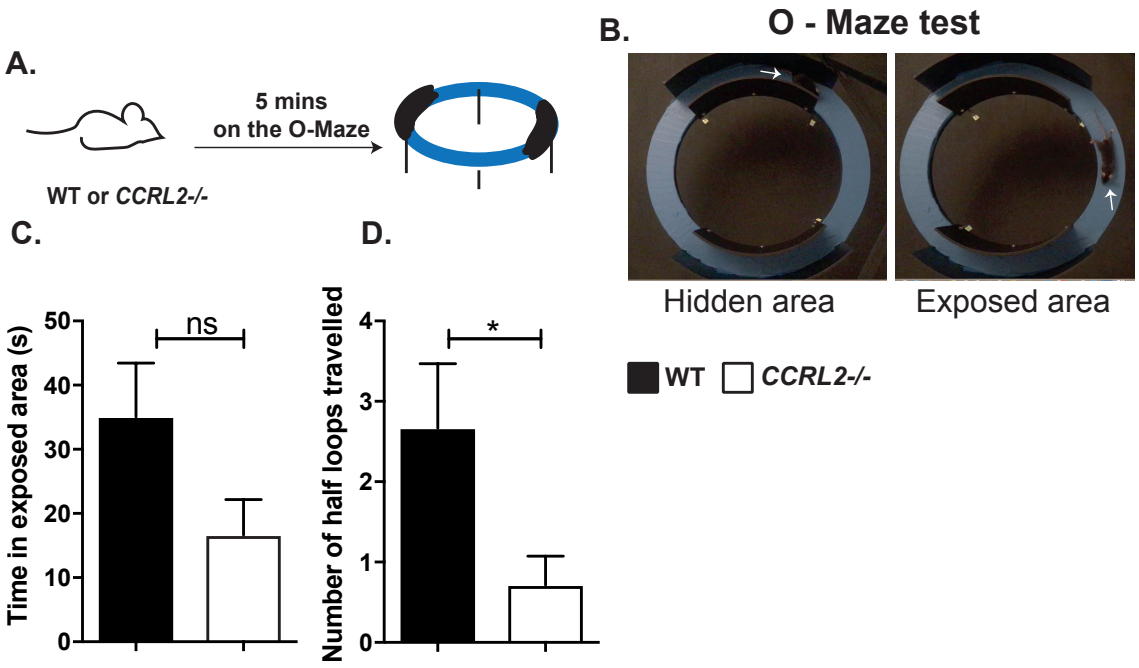


Figure 6.2: Increased anxiety-like behaviour of *CCRL2*-/- in the elevated O-Maze test. **A.** 8-10 week old male WT and *CCRL2*-/- mice were placed in the hidden area of the O-maze. **B.** Mice were monitored for total time spent in exposed area (**C.**) and total number of crosses travelled (**D.**) during 5 minutes. Error bars represent S.E.M. of 6-7 mice/group. Statistical significance was analysed using unpaired t-test ns=$P<0.05$, $*P\leq0.05$.Video footage of assay was assessed by 3 independent operators blinded to the genotype of the animals.

6.2.3 Forced swim test

The forced swim test is a commonly used assay for the study of depressive-like behaviour in rodents. It is based on the assumption that mice, placed in a container filled with water, will make efforts to escape but eventually will exhibit immobility, which in this instance I have described as 'float'. This immobility may be considered a measure for behavioural despair [360]. Mice are placed in a container filled with 30°C water for 2 minutes. The latency until first 'float' in the water is significantly greater in the *CCRL2*$^{-/-}$ mice than in the WT mice. Furthermore, the total time spent floating is significantly lower in the *CCRL2*$^{-/-}$ mice.

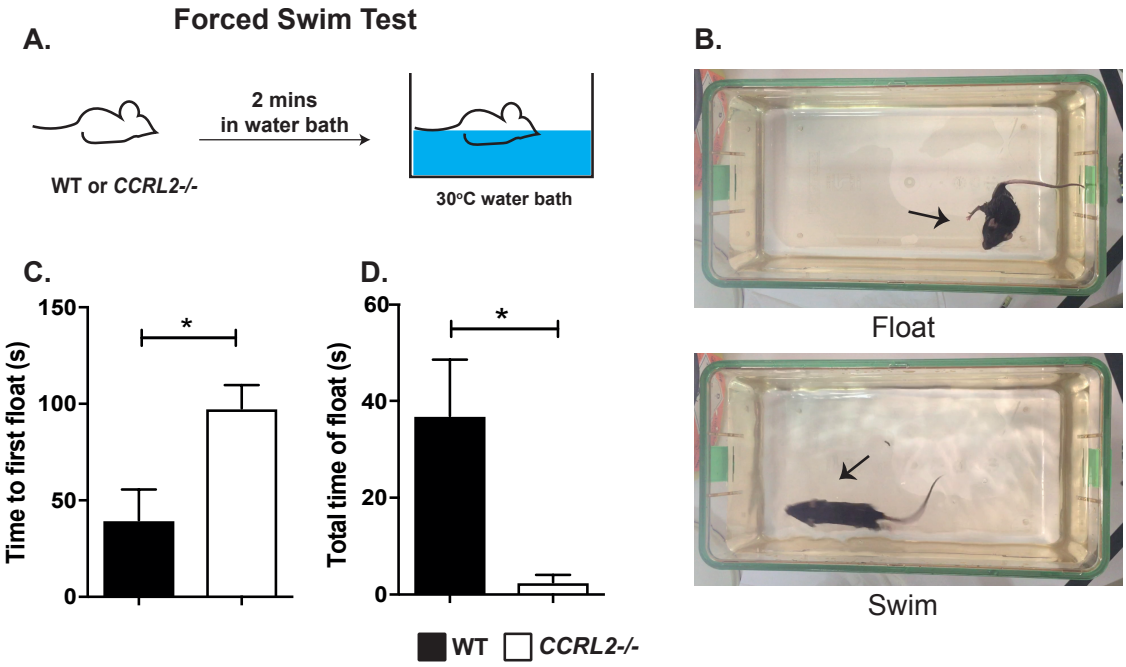


Figure 6.3: Behaviour of *CCRL2*-/- mice in the forced swim test. A. 8-10 week old male WT and *CCRL2*-/- mice were placed in a 30°C water bath. **B.** Mice were monitored for time till first float (**C.**) and total time of float (**D.**) for 2 minutes. Error bars represent S.E.M. of 6-7 mice/group. Statistical significance was analysed using unpaired t-test $*P \leq 0.05$. Video footage of assay was assessed by 3 independent operators that were blinded to the genotype.

6.2.4 Neuroanatomy of *CCRL2*-/- mice

6.2.4.1 Neuronal staining

Due to the differences observed in the behavioural assays by the *CCRL2*$^{-/-}$ mice, I wanted to assess the neuro-anatomy of the *CCRL2*$^{-/-}$ mice. The murine brains were perfused and cryosectioned for immunohistochemistry (IHC) staining with a neuronal nuclei (NeuN) antibody. No morphological differences are observed in the distribution and quantification of neurons in the frontal cortex, midbrain, and cerebellum in the *CCRL2*$^{-/-}$ mice (Figure 6.4).

6.2.4.2 Microglial staining

Microglial cells are self renewing tissue resident macrophages of the brain. Their role is to survey the brain for invading pathogens or debris [361]. Due to the association of neuro-inflammation with changes in behaviour, and the acute inflammatory phenotype of *CCRL2*$^{-/-}$ described in Chapter 5, I decided to quantify and assess the distribution of microglial cells in the brain sections of *CCRL2*$^{-/-}$ mice with ionized calcium-binding adaptor molecule 1 (Iba-1) antibody. There are no morphological

differences observed in the distribution and quantification of microglial cells in the frontal lobe, midbrain and cerebellum by the *CCRL2*$^{-/-}$ mice (Figure 6.5).

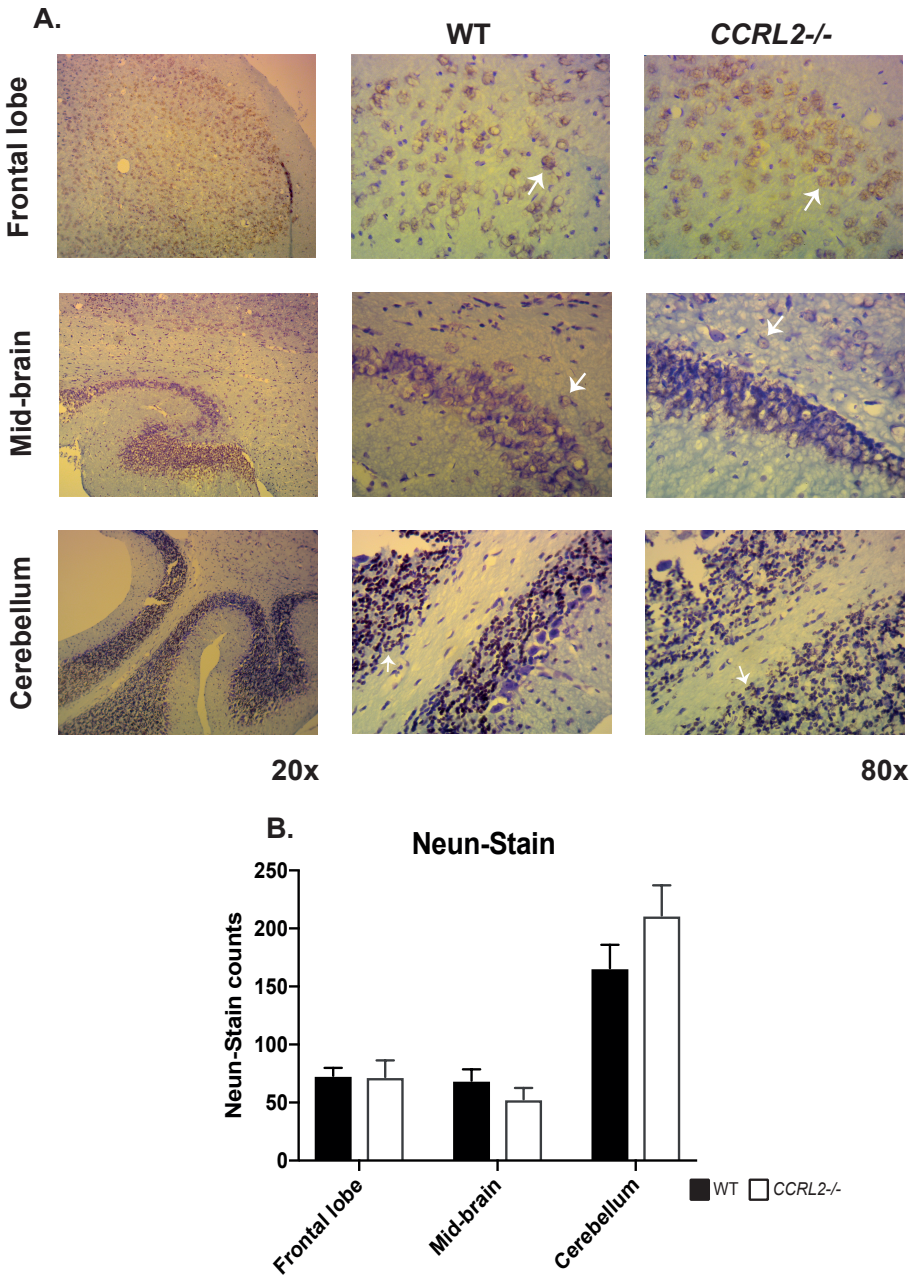


Figure 6.4: Neural architecture and quantification of neural nuclear stain show no differences in the *CCRL2*$^{-/-}$ mice. 8-10 week old male mice from WT and *CCRL2* -/- were euthanised, tissues were fixed by perfusion and brains were cryosectioned for IHC. **A.** Neuronal nuclear protein stain (Neun stain; Abcam) was performed with streptavidin horseradish peroxidase technique and counter-stained haematoxylin, to visualise the neurons in the frontal lobe, mid-brain and cerebellum. Neun stain indicated with white arrows. **B.** Quantified neun-stain shows no difference between groups. Error bars represent S.E.M. of 5-6 mice/group. Statistical significance was analysed by two-way ANOVA with Sidak's multiple comparisons correction, ns=P>0.05.

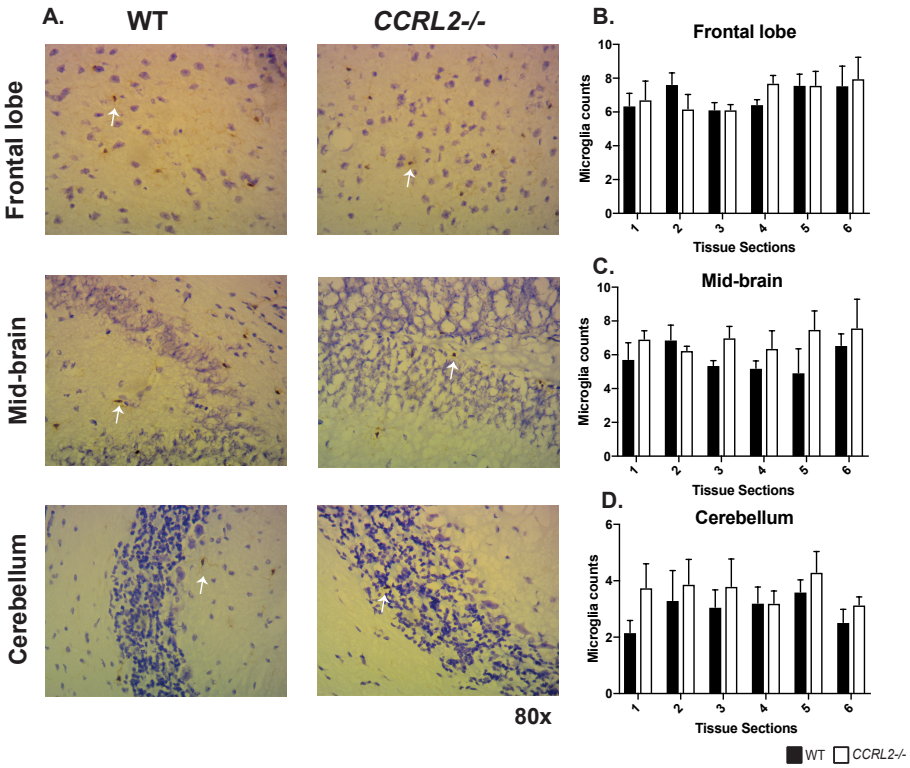


Figure 6.5: Microglial distribution and quantification show no difference in *CCRL2*$^{-/-}$ mice. 8-10 week old male mice from WT and *CCRL2*$^{-/-}$ were euthanised, tissues were fixed by perfusion and brains were cryosectioned for IHC. **A.** Iba-1 stain (Abcam) was performed with streptavidin horseradish peroxidase technique and counter-stained haematoxylin, to visualise microglia in the frontal lobe, mid-brain and cerebellum. Iba-1 staining indicated with white arrows. Quantification of Iba-1 stain, from 6 consecutive 10μm sections, in the frontal lobe (**B.**), mid-brain (**C.**), and cerebellum (**D.**) shows no difference between groups. Error bars represent S.E.M. of 5-6 mice/group. Statistical significance was analysed by two-way ANOVA with Sidak's multiple comparisons correction, ns=P>0.05.

6.2.5 *In vitro* cultured microglia cells express chemerin receptor

Murine microglial cells from p3 C57BL/6 postnatal pups were cultured *in vitro* and treated for 16 hours with various TLR and cytokine ligands. The mRNA expression of chemerin and chemerin receptors was assessed following 16 hour treatments. The cell culture and mRNA samples were a kind gift by Dr. Carlota Recio and Dr. Jie Yin from Prof. Francis Szele (DPAG, Oxford University). The mRNA expression of CCRL2 receptor is significantly elevated following LPS, LPS/IFNγ and PolyI:C treatments. The mRNA expression of ChemR23 is also upregulated by the pro and anti-inflammatory treatments. The mRNA of GPR1 and chemerin expression was observed in one biological set of the microglia sample, illustrated in Figure 6.6c,d.

Chemerin is upregulated by LPS treatment and GPR1 is upregulated PolyI:C treatment.

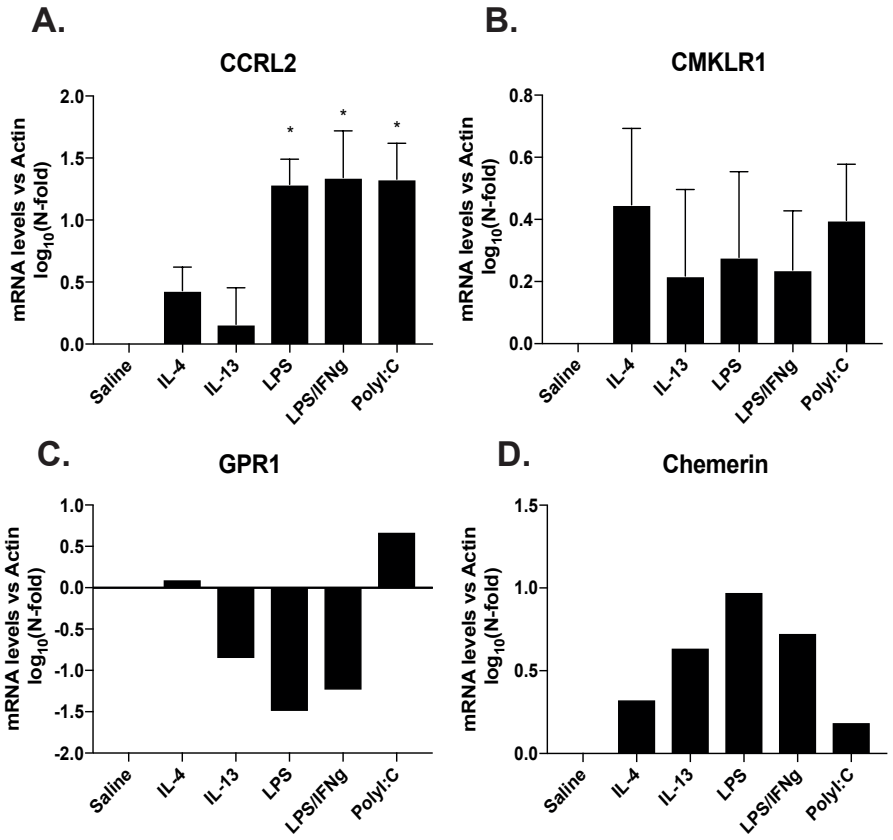


Figure 6.6: mRNA levels of chemerin receptors tend to increase *in vitro* cultured microglial cells following 16 hrs exposure to TLR and cytokine ligands. Tissue cultured microglial cells were treated with TLR and cytokine ligands for 16 hrs, followed by mRNA isolation. Cells culture and mRNA samples were a kind gift from Dr. Carlota Recio and JinYang. mRNA levels of chemerin receptors were obtained by qPCR, normalised to Δcycle value of actin and saline samples. **A-B.** CCRL2 and ChemR23 levels were elevated following treatments. **C-D.** GPR1 and chemerin were detected and elevated following treatment of 1 biological replicate. Error bars represent S.E.M. of 3 biological replicates. Statistical significance was analysed by one-way ANOVA with Dunnett's multiple comparisons test. ns=P>0.05 or $*$P$\leq$0.05.

6.3 Discussion

The main aim of this chapter was to investigate the behavioural phenotype of *CCRL2*$^{-/-}$ mice. Three independent operators noticed hyperactive and aggressive during handling. Because of the association of inflammation with cognitive and psychological disorders and due to the augmented inflammatory phenotype observed in the *CCRL2*$^{-/-}$, described in Chapter 5, I became interested in investigating whether *CCRL2*$^{-/-}$ mice had a behavioural phenotype. The *CCRL2*$^{-/-}$ mice display anxi-

ety and anti-depressive-like behaviour from the pilot behaviour tests employed in this chapter. Their neuroanatomy displayed no gross morphological abnormalities and finally I confirmed that activated microglia cells, with a range of inflammatory mediators and cytokines express the mRNA of three chemerin receptors suggesting that the chemerin system may play a role their functions.

The behaviour of the *CCRL2*$^{-/-}$ mice, under naïve conditions, was assessed by three well-established behavioural assays. The first was the open field test. This is a simple technique to investigate the exploratory-behaviour in a controlled environment, which was a 56×56cm gridded wooden box. Rodents will typically spend a significantly greater time exploring the periphery of the area, than the unprotected central area of the box [359]. The *CCRL2*$^{-/-}$ mice displayed a decrease in the number of times they enter the unprotected area, the middle square of the gridded open field box (Figure 6.1). Due to the significant decrease in the total number of squares crossed by the knock-out mice, it could be argued that the reduced locomotion is the reason for the decreased instances in entering the middle square. However, the increased latency in entering the middle square during the total 7 minute period by the *CCRL2*$^{-/-}$ mice supports the fact that the mice display increased anxiety behaviour.

The second behavioural assay conducted was the elevated O-maze. This technique has a long and successful history in assessing anxiety-like behaviours in mice [359]. Mice have a natural tendency in exploring novel environments, yet they tend to avoid the brightly lit open arms and prefer the darker protected arms. Treatment with anxiolytic drugs results in increased exploration of the open arms [362, 363]. Even though the time *CCRL2*$^{-/-}$ mice spent in the exposed open arm of the O-maze is non-significantly reduced, the total number of crosses to the other protected arm is significantly decreased in the *CCRL2*$^{-/-}$ mice compared to their age-matched wild-type controls (Figure 6.2). This further indicates that mice lacking the CCRL2 receptor display an anxiety-like behaviour.

The third behavioural assay conducted was the forced swim test. It is a well-established technique to investigate the depressive-like behaviours in rodents. Using this technique, many existing and potential antidepressant therapies have been tested for their efficacy [364, 365, 366]. In the water bath, the mice will make efforts to escape but eventually will begin to float and become immobile. The length of the immobility is the measure to indicate behavioural despair [360]. In this instance, mice lacking the CCRL2 receptor display an approximate 18-fold decrease in the total time of float and latency to first float (Figure 6.3). These results indicate that the *CCRL2*$^{-/-}$ mice display an antidepressive-like phenotype, as they keep swimming

when their wild-type controls have already begun to float. Given the previous anxiety-like phenotype observed from the other behavioural experiments and my observation of these mice during handling, where they become aggressive and move very fast when they feel threatened, I postulate that the behaviour observed in the forced swim test may be due to the elevated levels of anxiety rather than antidepressant effects. I would argue that the CCRL2 knockout mice experience a prolonged anxiety which prevents them reaching despair during the 120 second duration of the FST. A similar example is seen in the absence of glucocorticoid receptor in neurons or specifically in the dentate gyrus of the hippocampus. The lack of glucocorticoid receptors results in reduced immobility in the forced swim test [367, 342]. In this case, the authors interpreted this result as a failure to act in an energy-conserving or stress-coping manner. According to this reasoning, immobility behaviour is favourable and a successful passive behavioural strategy [367, 342].

The elevated levels of anxiety observed in these knockout mice may correlate with their augmented inflammatory response in the acute peritonitis model (Figure 5.2). The relation between the immune system and behaviour, provides an evolutionary advantage in human interactions with pathogens and predators. 'Sickness behaviour' displayed during infection is characteristic of depressive symptoms. It is characterised by social avoidance and anhedonia. These characteristics serve to preserve energy resources to fight infection and wound healing [339]. The hypervigilance characteristic of anxiety disorders, serves as a protection from attack and subsequent pathogen exposure [368]. Hence, the exaggerated pro-inflammatory response against infection have been linked to causing various behaviour changes including, the elevated anxiety-like behaviour. For instance, in a model of chronic gastrointestinal inflammation, mice display elevated anxiety-like behaviour, which is reversed by anti-TNFα treatment [369]. Importantly, these changes in behaviour were associated with decreases in brain-derived neurotophic factor (BDNF), which promote neural growth. The significance of neural growth in behaviour will be discussed later in this section. Moreover, a model of LPS-induced peritonitis induces depressive-like behaviour in a indoleamine 2,3-dioxygenase(IDO) dependent manner [370]. IDO is a tryptophan-degrading enzyme in the kynurenine pathway, which is released by dendritic cells and macrophages induced by pro-inflammatory cytokines, including IFNγ and TNF-α [370]. IDO is active in patients suffering from chronic inflammatory disease, and its expression levels have been found to correlate with depressive symptoms. IDO is also expressed in brain endotelial cells, microglia and astrocytes under pro-inflammatory conditions. As tryptophan is needed for the production of the serotonin neurotransmisor, the

over-activity of IDO, indirectly reduces serotonin levels [370]. Insufficient levels of serotonin signalling via the 5-HT1AR receptor, decreases neural dendritic spine density in the dentate gyrus of the brain[371, 372]. The degraded tryptophan-product generated by IDO, kynurenine can be metabolised by macrophage and microglial cells to generate glutamatergic compounds which have been implicated in the causation of depression [370].

Cytokines have also been shown to be directly active on afferent nerves including the vagus nerve. Removal of the vagus nerve decreased the depressant-like phenotype induced by LPS-induced peritonitis, yet it did not effect the cytokine production [344]. Another way in which the immune system affects the CNS, is by the circumventricular organs. The circumventricular organs are structures in the brain that lie outside of the blood brain barrier (BBB), and contain resident macrophages which will respond to circulating PAMPs by producing pro-inflammatory cytokines. These cytokines can enter the BBB by volume diffusion [373]. Cytokines can also gain access to the BBB from the peripheral circulation, by a pH-dependent and saturable influx transport system [374, 375]. The presence of cytokines within the BBB leads to the activation of microglial cells. Activated microglial cells increase proliferation, have altered morphology and cytokine production. In a healthy uninjured brain, microglia typically promote neurogenesis by pruning neurons dentates through phagocytosis [361, 376, 377]. Activated microglia cells do not promote neurogenesis and this results in dysfunctional neuronal growth. Alternatively activated microglia, by treatment with a nonsteroidal anti-inflammatory drug, promotes the repair hippocampal neurogenesis as reported by Monje *et al.* following LPS administration [378]. The administration of a microglial inhibitor, minocycline, blocked the LPS-induced decrease in neurogenesis [379] and improved recognition memory in a model of schizophrenia [380]. Microglial activation has been linked to the progressive brain changes seen in schizophrenia, which have been assessed post mortem [381]. The major impact of microglial activation, or neuroinflammation, is that it invokes alterations in the levels of the neurotrophic factors, important in supporting the neuron longevity, memory formation and neurogenesis [382, 383]. The reduction in neurogenesis is believed to be a direct link to neuroinflammatory disorders, including dementia, Parkinson's disease, Huntington's disease and schizophrenia [384, 385, 386, 387, 381].

The heightened anxiety traits observed in the *CCRL2*$^{-/-}$ mice under naïve conditions, suggest that there be some alterations in the neuron growth. The neuron morphology and quantification was assessed by NeuN antibody, in Figure 6.4, and displayed no overt morphological differences between the WT and knockout animals,

suggesting no gross neural changes. I also assessed microglial cell present in frontal lobe, midbrain and cerebellum, in the naïve state and I did not observe higher number of microglial cells in the *CCRL2*$^{-/-}$ mice (Figure 6.5). It may be useful to assess the neural progenitors present and microglial activation states in order to observe any changes between genotypes.

The expression of the chemerin receptors, CCRL2 and ChemR23, by *in vitro* cultured microglia cells following pro and anti-inflammatory stimuli, suggests a role for chemerin in these cells (Figure 6.6). The ChemR23 and CCRL2 receptors are upregulated in microglia and astrocytes *in vitro* and *in vivo* and is expressed on infiltrating myeloid cells in a EAE model [357, 358, 177]. EAE models the inflammatory aspects of the autoimmune disorder multiple sclerosis, a immune-mediated demyelination disease of the CNS. Chemerin is upregulated in the CNS of EAE model [177]. Aside from showing significant increased demyelination and inflammation in the CNS in the *CCRL2*$^{-/-}$ mice, Mazzon *et al.* also displayed a significant increase in T cell and macrophage polarisation states, to Th1 and M1 respectively, in the *CCRL2*$^{-/-}$ mice [183]. The treatment of chemerin has previously been shown to promote a M1 pro-inflammatory polarisation in macrophages via the ChemR23 receptor and while suppressing the M2 anti-inflammatory polarisation *in vitro* and *in vivo* [281, 207]. Taken together, the anxiety behaviour displayed by the *CCRL2*$^{-/-}$ mice is likely to be due to their pro-inflammatory tendencies. It would be interesting to assess whether the anxiety becomes even more exacerbated during inflammation. Chemerin signalling via the other chemerin receptors may influence the pro-inflammatory polarisation states of immune cells and thus, enhance the anxiety levels in these mice. Finally, the over expression of chemerin may display similar behavioural traits to the ones displayed in the mice lacking the CCRL2 receptor, in which case this would indicate that like other cytokines, chemerin is able to influence the CNS.

6.3.1 Limitations of this study

One major limitation to this study was the limited number of behavioural assays undertaken in this chapter to assess the behaviour of mice lacking the CCRL2 receptor. With this preliminary number of experiments, there is a limited amount that can be interpreted. Due to time restrains, I was not able to address all the behaviour traits observed by the *CCRL2*$^{-/-}$ mice. I was no able to address, the aggression and speed of their movement under threatening conditions. With the existing experiments, I could try to assess the speed of movement in the forced swim test by the *CCRL2*$^{-/-}$ mice. However, additional behaviour tests, such as the social behaviour and novel

object experiment would be necessary to fully confirm and establish a behavioural phenotype by these mice.

Another limitation to the behavioural experiments, as discussed earlier, is applying the correct interpretation of the behaviour displayed. The typically accepted phenomena for the behaviour does not always apply for all instances. Furthermore, it can be difficult to correlate human behaviour with the behaviour of a rodent.

Additionally, it would have been more accurate to assess particular regions of the brain which are known to be affected behaviour, rather than just generally assessing the frontal lobe, midbrain and cerebellum by the IHC of neural and microglial stain. The regions of the brain interpreted was kept consistent, however, focusing on particular regions per section, would increase accuracy of quantification. Moreover, assessing the neuronal progenitors and microglial activation states may be more useful in addressing changes between genotypes, particularly if the mice were undergoing inflammation.

Finally, it may be of interest to investigate the effects of inflammation on the brain of the CCRL2 null mice. Following inflammation, it would be interesting to measure mRNA of inflammatory mediators within brain tissue or stimulate WT and *CCRL2*$^{-/-}$ *in vitro* cultured microglia cells with various inflammatory stimuli in the presence or absence of chemerin and measure any change in inflammatory mediator production and responses.

Chapter 7

Summary and future directions

7.1 Key findings

The first aim of this thesis was to develop and characterise antibodies against chemerin isoforms derived from a phage display library in UCB Pharma. With regards to this, the key findings were :

- 103 unique 'binding' clones were isolated against the C23 peptide pan from round 3 output. From these, 20 were binding clones confirmed by SPR analysis. The 10 best binding clones were selected.

Two subsets of clones were revealed:

- Group 1: clones which could recognise the active C-terminal sequence of chemerin.
- Group 2: clones which could recognise the inactive sequence of C-terminal prochemerin.

The selected scFv clones were cloned onto a mouse Fc vector (UCB) and transiently transfected into mammalian cells for the production and purification of scFv-Fc antibodies for functional characterisation.

- The scFv-Fc clones showed weak affinity towards C-terminal peptides and full length chemerin, particularly during the engagement of only one scFv region.
- Group 1 clones were unable to inhibit chemerin, C17 peptide or streptavidin bound C17 peptide activity at the ChemR23 receptor.
- Group 2 clones were unable to inhibit the cleavage of C23 peptide by neutrophil elastase and cathepsin G proteases.

- Group 2 clones bound non-specifically to multiple proteins in peritoneal exudate. They were unable to demonstrate changes in chemerin quantity between samples, likely due to their non-specific binding.

My second aim was to investigate the expression of chemerin receptors on leukocyte subsets. My findings were:

- BMDM upregulate their expression of CCRL2 mRNA when stimulated with pro-inflammatory mediators. Protein expression should be confirmed by flow cytometry with newly available anti-CCRL2 antibodies.
- Neutrophils do not express ChemR23 protein or mRNA, however they do express CCRL2 mRNA.
- ChemR23 protein was highly expressed on the surface of tissue-resident peritoneal macrophages, bone marrow derived macrophages and dendritic cells and monocytes in 4 day Bio-gel elicited peritoneal cells.
- ChemR23 protein was not expressed in any other myeloid or lymphocyte resident cell in the liver, lung and spleen. Due to the detection of ChemR23 mRNA expression in these tissues, it is hypothesised that non-leukocyte cells are responsible for the detection of ChemR23 mRNA expression.
- The injection of chemerin to the peritoneal cavity recruits pDCs and higher levels of $MHCII^{mid}$ cells. Neutrophils and monocytes are not recruited to the cavity.

The third aim of this thesis was to investigate the role of non-signalling receptor, CCRL2, and the signalling receptor, ChemR23, in an acute inflammatory model of zymosan-induced peritonitis. A schematic representation the functional dynamics between CCRL2 and ChemR23 receptor that were observed in the zymosan-induced peritonitis model of acute inflammation is seen in Figure 7.1. With regards to this aim, my key findings were:

- The absence of the CCRL2 receptor exacerbates the acute phase of inflammation in a zymosan-induced model of peritonitis. Neutrophil and monocyte infiltration were significantly increased at 2 and 4 hours.

- The increase of chemerin levels observed in the *CCRL2*$^{-/-}$ mice was attributed to driving inflammation by the increased expression of pro-inflammatory mediators, such as CXCL1. Chemerin neutralisation in *CCRL2*$^{-/-}$ mice and chemerin treatment in WT mice supported this hypothesis.

- The absence of the ChemR23 receptor abrogated the acute phase of inflammation in the same model, which suggested that the actions of chemerin observed previously were mediated via the ChemR23 receptor.

The final aim of this thesis was to investigate behavioural changes observed in CCRL2 null mice.

- CCRL2 null mice display elevated levels of anxiety compared to age-matched WT mice.

- *CCRL2*$^{-/-}$ mice do not display any gross differences in their neuroanatomy or in the quantity of microglial cells.

7.2 What is the role of chemerin in pathology? Can it be a therapeutic target in human disease?

The ultimate goal of biological scientific research in pathology is to increase our understanding of biological processes in health and disease. One benefit of basic science research is to discover therapeutic targets to intervene in the pathological progression of disease. This leads me to question whether chemerin should be targeted in human disease. As discussed previously, chemerin is a multifunctional protein. It has a role in cell recruitment, as an antibacterial peptide, it has a role in adipogenesis and as a promoter of angiogenesis. Its role during inflammation is disputed. Chemerin is involved with many pathways and its function is dependent on tissue site and stimuli driving the inflammatory process.

The skin is a good example of the complex homeostatic and harmful functions chemerin can exert within a tissue environment. Chemerin is produced by keratinocytes in the epidermis of healthy skin and it is markedly downregulated in the epidermis of patients suffering from the autoimmune skin disorder psoriasis. In contrast, the healthy dermis layer of skin contains low levels of chemerin, but the affected psoriatic dermis is a significant source of chemerin production which leads to the recruitment of pDCs [388]. Early lesions are characterised by the presence of neutrophils

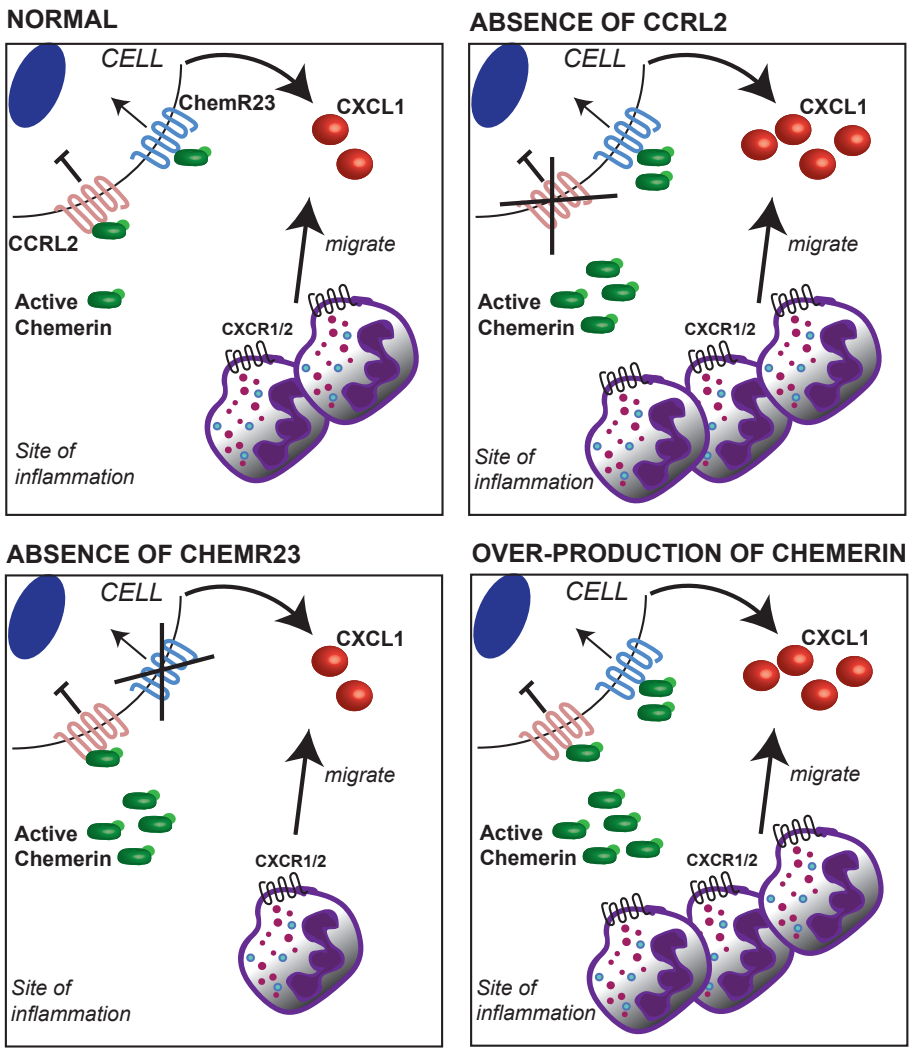


Figure 7.1: The function of CCRL2 and ChemR23 in acute inflammation of zymosan-induced peritonitis. A cell at the site of inflammation responds to active chemerin (green) via the ChemR23(blue GPCR) receptor by producing CXCL1 production (red circles), subsequently promoting neutrophil recruitment via a CXCR1/2 receptor. In the absence of CCRL2, high levels of chemerin have the opportunity to signal via the ChemR23 receptor, thus, causing higher levels of CXCL1. In the absence of ChemR23, there is a lack of response to chemerin, thus, resulting in lower CXCL1 production and migration of neutrophils to site of inflammation. In the over-expression of chemerin, as in some instances of chronic inflammation, there is more signalling via the ChemR23 receptor, thus, resulting in higher levels of CXCL1 and greater neutrophil influx.

and pDCs. Keratinocytes upregulate their production of chemerin in response to bacteria and acute pro-inflammatory mediators, such as IL-1β, and chemerin is required for efficient bacterial clearance in the skin partly driven by its bactericidal effects. However, chemerin production by keratinocytes becomes significantly downregulated in the presence of IL-17 and IL-22, which are key cytokines implicated in psoriasis pathogenesis [169]. The blockade of chemerin in this disease setting may be beneficial by reducing the pDC recruitment which drives the $T_H1/17$ response in the dermis. However, the anti-psoriatic treatment of retinoid-tazarotene, in which chemerin was first discovered, upregulates chemerin levels [152] by keratinocytes in the epidermis and possibly downregulates in the dermis, so blockade of chemerin in the recovery phase of the disease would not be beneficial for psoriasis.

Initially, chemerin acts as a pro-inflammatory mediator, causing recruitment and stimulating the production of pro-inflammatory mediators and exerting anti-bacterial effects. In later time points of inflammation, chemerin could act as anti-inflammatory, further cleavage by serine protease generating peptides for alternative signalling, and or by promoting growth and wound healing [175, 286]. However, in chronic inflammation, where the resolution of inflammation is not achieved, chemerin is consistently reported as being elevated in the serum and in the site of inflammation. These findings support the notion of it being used as a biomarker of inflammation. Therefore, therapeutically neutralising the effects of chemerin in these instances could be beneficial as it could be part of the inflammatory cascade perpetuating the inflammatory process. Many of chemerin's reported functions seemed to be particularly linked with the pathogenesis of atherosclerosis. Yet, the role of chemerin in longer term models of diseases, such as RA and atherosclerosis, have not been studied even though in both of these human diseases, there are elevated levels of chemerin in serum, and chemerin and chemerin receptors expressed locally [389].

The vascular and synovial endothelium, including chondrocytes and fibroblasts express chemerin receptors and express pro-inflammatory cytokines in response to chemerin. Furthermore, vascular endothelial cells stimulated with chemerin have been shown to induce angiogenesis. Smooth muscle cells also express chemerin receptors and chemerin treatment causes contractions, thus increasing hypertension [390], smooth muscle proliferation and migration [391, 392].

In addition to this, cardiovascular disease is closely associated with obesity and glucose metabolism, and interestingly there is a higher cardiovascular risk in RA patients [393]. Excess chemerin may effect homeostatic functions during adipogenesis and glucose tolerance and thus, promoting the onset of perpetuation of cardiovascular

disease. In this context, the blockade of excess chemerin may provide therapeutic benefit in the cardiovascular outcome of RA inflammation.

In diseases such as IBD, MS, SLE, and cancer, the exact pathogenic function of chemerin is unknown. Therefore, further basic research will have to be done to draw a close association of chemerin with these disease even though there already have been some preliminary indications.

Antithetical to the previous discussion, the administration of recombinant chemerin or chemerin peptides seems to have beneficial effects in T_H2 type allergic inflammatory diseases such as asthma or chronic obstructive pulmonary disorder (COPD). Full-length recombinant chemerin and a lipidated chemerin C9 peptide have been reported to exert anti-inflammatory effects in allergic airway inflammation [176, 211, 394]. Further research is required to confirm the mechanism of chemerin's effects in these disease contexts but treatment with chemerin could provide an alternative therapy particularly because there is an unmet clinical need for good long term treatments in asthma and COPD. Hence, chemerin or chemerin peptides either alone or in combination with current therapies like corticosteroids or β-adrenergic receptor agonists may prove beneficial in decreasing airway inflammation [395].

7.3 Future directions

In addition to the future work highlighted at the end of each chapter, I believe to further address the mechanistic actions exerted by chemerin, there is a need to investigate non-leukocyte populations in relation to the pathogenic function of chemerin. Stromal, endothelial and epithelial cells all seem to produce and respond to chemerin via autocrine and paracrine pathways. These cell types are key players involved in the onset and the perpetuation of chronic inflammation and functional insight in relation to chemerin signalling can lead to effective therapeutic targeting chemerin in pathology.

It is important to remember that chemerin receptor global knockouts do not help address specific cell type functions. New transgenic mice, with inducible or cell specific knockouts of chemerin or chemerin receptors, would vastly improve our understanding of the role of chemerin and its receptors in specific cell type linages, such as the endothelium, within a disease setting. In fact, the removal of two or all three chemerin receptors and then comparing them to the single receptor knockouts, within specific disease settings or chronic inflammation, would also illuminate the functional importance of one receptor to another.

Finally, the chemerin field is still lacking the tools to detect different isoforms of chemerin. Chemerin detection by R& D chemerin ELISA kit does not always equate with its bioactivity [180]. Due to the multiple functions exerted by chemerin at different sites of inflammation, these tools would aid the identification of specific isoform functions. Moreover, blocking specific isoforms may also act specifically to improve one area of pathology.

7.4 Conclusion

In this thesis, I found that chemerin is a pro-inflammatory driver of acute inflammation, mediated via signalling of the ChemR23 receptor. The presence of CCRL2 receptor dampens the initial pro-inflammatory effects of ChemR23. These effects of chemerin are mediated through an unidentified cell type, probably located in the site of inflammation. I have proven that it is possible to generate specific antibodies which can differentiate between the prochemerin and the active chemerin C-terminus using human naïve phage display library. In an unexpected observation, I found that the absence of CCRL2 receptor enhances the anxiety behaviour in mice, which could be linked to their augmented inflammatory tendencies possibly within the CNS.

To conclude, chemerin is clearly involved in multiple homeostatic and pathological pathways, which make it an attractive area of research and for potential future therapeutic targeting. At this moment, there is a lack of tools and evidence to fully support any therapeutic application. However, with further investigation, anti-chemerin strategies could be used beneficially in medicine.

Appendix

Conference presentations

Oral Presentations

- **13th World Congress of Inflammation** - London, U.K. 07.2017
  'Investigating the role of chemerin and the non-signalling chemerin receptor, CCRL2, during an acute inflammatory model of peritonitis"
- **UCB PhD day 2016** - London, U.K. 09.2016
  'Developing antibodies against chemerin using phage display technology"
- **Departmental Graduate Symposium** - Oxford, U.K. 07.2016
  'Developing antibodies against chemerin using phage display technology"

Poster Presentations

- **11th ENII EFIS EJI Summer School on Advanced Immunology** - Porto Cervo, Sardinia 05.2016
  'Developing antibodies against chemerin using phage display technology"
- **UCB PhD day 2015** - London, U.K. 10.2015
  'Developing antibodies against chemerin using phage display technology"
- **4th European Congress of Immunology** - Vienna, Austria 09.2015
  'Developing antibodies against chemerin using phage display technology"
- **UCB PhD day 2014** - London, U.K. 10.2014
  'Investigating the function of ChemR23 and chemerin peptides in macrophage and dendritic cells"
- **BSI Oxford Immunology group** - Oxford, U.K. 03.2014
  'Measuring macrophage and dendritic cell functional responses to chemokines using a label free cell impedance assay"

Courses Attended

- Home Office Animal Course Modules 1,2 and 3
  Animal Management and Welfare for Personal Licence Holders
- Writing Skills - Reports
- Biological Safety and Genetic Modification

Publications

Regan-Komito D.*, **Valaris S.***, Kapellos T.S, Taylor L., Greaves D.R.±, Iqbal A.J.± Deletion of non-signalling chemerin receptor CCRL2 exacerbates acute inflammatory responses in vivo. Frontiers of Immunology. *joint first ± joint senior authors - 2017

Abstract

Chemerin is a chemotactic protein that induces migration of several immune cells including macrophages, immature dendritic cells and NK cells. Chemerin binds to three G protein-coupled receptors (GPCRs), including CCRL2. The exact function of CCRL2 remains unclear. Ccrl2 expression is rapidly upregulated during inflammation, but it lacks the intracellular DRYLAIV motif required for classical GPCR downstream signalling pathways and it has not been reported to internalise chemerin upon binding. The aim of this study was to investigate what role if any CCRL2 plays during acute inflammation. Using the zymosan and thioglycollate induced murine models of acute inflammation, we report that mice deficient in the Ccrl2 gene display exaggerated local and systemic inflammatory responses, characterised by increased myeloid cell recruitment. This amplified myeloid cell recruitment was associated with increased chemerin and CXCL1 levels. Furthermore, we report that the inflammatory phenotype observed in these mice is dependent upon elevated levels of endogenous chemerin. Antibody neutralisation of chemerin activity in Ccrl2-/- mice abrogated the amplified inflammatory responses. Importantly, chemerin did not directly recruit myeloid cells but rather increased the production of other chemotactic proteins such as CXCL1. Administration of recombinant chemerin to WT mice prior to inflammatory challenge recapitulated the increased myeloid cell recruitment and inflammatory mediator production observed in Ccrl2-/- mice. We have demonstrated that the absence of Ccrl2 results in increased levels of local and systemic chemerin levels and exacerbated inflammatory responses during acute inflammatory challenge. These results further highlight the importance of chemerin as a therapeutic target in inflammatory diseases.

Bibliography

[1] A. J. Iqbal, E. A. Fisher, and D. R. Greaves. Inflammationa Critical Appreciation of the Role of Myeloid Cells. *Microbiol. Spectr.*, 4(5), oct 2016.

[2] C. Janeway. *Immunobiology 5 : the immune system in health and disease.* Garland Pub, 2001.

[3] T. Kawai and S. Akira. The role of pattern-recognition receptors in innate immunity: update on Toll-like receptors. *Nat. Immunol.*, 11(5):373–384, may 2010.

[4] M. R. Thompson, J. J. Kaminski, E. A. Kurt-Jones, and K. A. Fitzgerald. Pattern recognition receptors and the innate immune response to viral infection. *Viruses*, 3(6):920–40, 2011.

[5] T. Kawai and S. Akira. The roles of TLRs, RLRs and NLRs in pathogen recognition. *Int. Immunol.*, 21(4):317–37, apr 2009.

[6] B. M. J. Owens, T. A. M. Steevels, M. Dudek, D. Walcott, M.-Y. Sun, A. Mayer, P. Allan, and A. Simmons. CD90(+) Stromal Cells are Non-Professional Innate Immune Effectors of the Human Colonic Mucosa. *Front. Immunol.*, 4:307, 2013.

[7] C. Schulz, E. Gomez Perdiguero, L. Chorro, H. Szabo-Rogers, N. Cagnard, K. Kierdorf, M. Prinz, B. Wu, S. E. W. Jacobsen, J. W. Pollard, J. Frampton, K. J. Liu, and F. Geissmann. A lineage of myeloid cells independent of Myb and hematopoietic stem cells. *Science*, 336(6077):86–90, apr 2012.

[8] M. J. Melnicoff, P. K. Horan, E. W. Breslin, and P. S. Morahan. Maintenance of peritoneal macrophages in the steady state. *J. Leukoc. Biol.*, 44(5):367–75, nov 1988.

[9] B. Ajami, J. L. Bennett, C. Krieger, W. Tetzlaff, and F. M. V. Rossi. Local self-renewal can sustain CNS microglia maintenance and function throughout adult life. *Nat. Neurosci.*, 10(12):1538–43, dec 2007.

[10] D. Hashimoto, A. Chow, C. Noizat, P. Teo, M. B. Beasley, M. Leboeuf, C. D. Becker, P. See, J. Price, D. Lucas, M. Greter, A. Mortha, S. W. Boyer, E. C. Forsberg, M. Tanaka, N. van Rooijen, A. García-Sastre, E. R. Stanley, F. Ginhoux, P. S. Frenette, and M. Merad. Tissue-resident macrophages self-maintain locally throughout adult life with minimal contribution from circulating monocytes. *Immunity*, 38(4):792–804, apr 2013.

[11] M. Greter, I. Lelios, P. Pelczar, G. Hoeffel, J. Price, M. Leboeuf, T. M. Kündig, K. Frei, F. Ginhoux, M. Merad, and B. Becher. Stroma-derived interleukin-34 controls the development and maintenance of langerhans cells and the maintenance of microglia. *Immunity*, 37(6):1050–1060, dec 2012.

[12] L. C. Davies, S. J. Jenkins, J. E. Allen, and P. R. Taylor. Tissue-resident macrophages. *Nat. Immunol.*, 14(10):986–995, sep 2013.

[13] J. F. Cailhier, D. A. Sawatzky, T. Kipari, K. Houlberg, D. Walbaum, S. Watson, R. A. Lang, S. Clay, D. Kluth, J. Savill, and J. Hughes. Resident pleural macrophages are key orchestrators of neutrophil recruitment in pleural inflammation. *Am. J. Respir. Crit. Care Med.*, 173(5):540–7, mar 2006.

[14] M. N. Ajuebor, A. M. Das, L. Virág, R. J. Flower, C. Szabó, M. Perretti, J. Savill, J. Hughes, and R. A. Lang. Role of resident peritoneal macrophages and mast cells in chemokine production and neutrophil migration in acute inflammation: evidence for an inhibitory loop involving endogenous IL-10. *J. Immunol.*, 162(3):1685–91, feb 1999.

[15] L. C. Davies, M. Rosas, P. J. Smith, D. J. Fraser, S. A. Jones, and P. R. Taylor. A quantifiable proliferative burst of tissue macrophages restores homeostatic macrophage populations after acute inflammation. *Eur. J. Immunol.*, 41(8):2155–64, aug 2011.

[16] N. Kobayashi, P. Karisola, V. Peña-Cruz, D. M. Dorfman, M. Jinushi, S. E. Umetsu, M. J. Butte, H. Nagumo, I. Chernova, B. Zhu, A. H. Sharpe, S. Ito, G. Dranoff, G. G. Kaplan, J. M. Casasnovas, D. T. Umetsu, R. H. Dekruyff, and G. J. Freeman. TIM-1 and TIM-4 glycoproteins bind phosphatidylserine and mediate uptake of apoptotic cells. *Immunity*, 27(6):927–40, dec 2007.

[17] S. Uderhardt, M. Herrmann, O. V. Oskolkova, S. Aschermann, W. Bicker, N. Ipseiz, K. Sarter, B. Frey, T. Rothe, R. Voll, F. Nimmerjahn, V. N. Bochkov,

G. Schett, and G. Krönke. 12/15-lipoxygenase orchestrates the clearance of apoptotic cells and maintains immunologic tolerance. *Immunity*, 36(5):834–46, may 2012.

[18] M. F. Gurish and K. F. Austen. Developmental Origin and Functional Specialization of Mast Cell Subsets. *Immun. Perspect.*, 37:25–33, 2012.

[19] S. C. Bischoff. Role of mast cells in allergic and non-allergic immune responses: comparison of human and murine data. *Nat. Rev. Immunol.*, 7(2):93–104, feb 2007.

[20] J. S. Marshall. Mast-cell responses to pathogens. *Nat. Rev. Immunol.*, 4(10):787–799, oct 2004.

[21] B. Johnston, A. R. Burns, and P. Kubes. A role for mast cells in the development of adjuvant-induced vasculitis and arthritis. *Am. J. Pathol.*, 152(2):555–63, feb 1998.

[22] M. Kaartinen, A. Penttilä, and P. T. Kovanen. Mast cells in rupture-prone areas of human coronary atheromas produce and store TNF-alpha. *Circulation*, 94(11):2787–92, dec 1996.

[23] P. F. Weller and L. A. Spencer. Functions of tissue-resident eosinophils. *Nat. Rev. Immunol.*, sep 2017.

[24] H. F. Rosenberg, K. D. Dyer, and P. S. Foster. Eosinophils: changing perspectives in health and disease. *Nat. Rev. Immunol.*, 13(1):9–22, nov 2012.

[25] M. H. Shin, Y. A. Lee, and D.-Y. Min. Eosinophil-mediated tissue inflammatory responses in helminth infection. *Korean J. Parasitol.*, 47 Suppl(Suppl):S125–31, oct 2009.

[26] P. C. Fulkerson, C. A. Fischetti, and M. E. Rothenberg. Eosinophils and CCR3 regulate interleukin-13 transgene-induced pulmonary remodeling. *Am. J. Pathol.*, 169(6):2117–26, dec 2006.

[27] P. C. Fulkerson, C. A. Fischetti, M. L. Mcbride, L. M. Hassman, S. P. Hogan, M. E. Rothenberg, and K. F. Austen. A central regulatory role for eosinophils and the eotaxinCCR3 axis in chronic experimental allergic airway inflammation. *PNAS*, 103(44):16418–23, 2006.

[28] J. Y. Cho, M. Miller, K. J. Baek, J. W. Han, J. Nayar, S. Y. Lee, K. McElwain, S. McElwain, S. Friedman, and D. H. Broide. Inhibition of airway remodeling in IL-5-deficient mice. *J. Clin. Invest.*, 113(4):551–60, feb 2004.

[29] C. Blanchard, N. Wang, K. F. Stringer, A. Mishra, P. C. Fulkerson, J. P. Abonia, S. C. Jameson, C. Kirby, M. R. Konikoff, M. H. Collins, M. B. Cohen, R. Akers, S. P. Hogan, A. H. Assa'ad, P. E. Putnam, B. J. Aronow, and M. E. Rothenberg. Eotaxin-3 and a uniquely conserved gene-expression profile in eosinophilic esophagitis. *J. Clin. Invest.*, 116(2):536–47, feb 2006.

[30] J. Chen, A. Schlitzer, S. Chakarov, F. Ginhoux, and M. Poidinger. Mpath maps multi-branching single-cell trajectories revealing progenitor cell progression during development. *Nat. Commun.*, 7:11988, jun 2016.

[31] S. N. Mueller and L. K. Mackay. Tissue-resident memory T cells: local specialists in immune defence. *Nat. Rev. Immunol.*, 16:79–89, 2016.

[32] G. W. Roberts, D. Baird, K. Gallagher, R. E. Jones, C. J. Pepper, J. D. Williams, and N. Topley. Functional effector memory T cells enrich the peritoneal cavity of patients treated with peritoneal dialysis. *J. Am. Soc. Nephrol.*, 20(9):1895–900, sep 2009.

[33] R. Purwar, J. Campbell, G. Murphy, W. G. Richards, R. A. Clark, and T. S. Kupper. Resident Memory T Cells (TRM) Are Abundant in Human Lung: Diversity, Function, and Antigen Specificity. *PLoS One*, 6(1):e16245, jan 2011.

[34] R. A. Clark, K.-i. Yamanaka, M. Bai, R. Dowgiert, and T. S. Kupper. Human skin cells support thymus-independent T cell development. *J. Clin. Invest.*, 115(11):3239–49, nov 2005.

[35] E. E. B. Ghosn, Y. Yang, J. Tung, L. A. Herzenberg, and L. A. Herzenberg. CD11b expression distinguishes sequential stages of peritoneal B-1 development. *Proc. Natl. Acad. Sci.*, 105(13):5195–5200, apr 2008.

[36] C. S. N. Klose and D. Artis. Innate lymphoid cells as regulators of immunity, inflammation and tissue homeostasis. *Nat. Immunol.*, 17(7):765–774, jun 2016.

[37] G. Gasteiger, X. Fan, S. Dikiy, S. Y. Lee, and A. Y. Rudensky. Tissue residency of innate lymphoid cells in lymphoid and nonlymphoid organs. *Science (80-.).*, 350(6263):981–985, nov 2015.

[38] M. L. Robinette, A. Fuchs, V. S. Cortez, J. S. Lee, Y. Wang, S. K. Durum, S. Gilfillan, M. Colonna, L. Shaw, B. Yu, A. Goldrath, S. Mostafavi, A. Regev, E. Y. Kim, D. F. Dwyer, M. B. Brenner, K. F. Austen, A. Rhoads, D. Moodley, H. Yoshida, D. Mathis, C. Benoist, T. Nabekura, V. Lam, L. L. Lanier, B. Brown, M. Merad, V. Cremasco, S. Turley, P. Monach, M. L. Dustin, Y. Li, S. A. Shinton, R. R. Hardy, T. Shay, Y. Qi, K. Sylvia, J. Kang, K. Fairfax, G. J. Randolph, M. L. Robinette, A. Fuchs, and M. Colonna. Transcriptional programs define molecular characteristics of innate lymphoid cell classes and subsets. *Nat. Immunol.*, 16(3):306–317, jan 2015.

[39] C. S. Klose, M. Flach, L. Möhle, L. Rogell, T. Hoyler, K. Ebert, C. Fabiunke, D. Pfeifer, V. Sexl, D. Fonseca-Pereira, R. G. Domingues, H. Veiga-Fernandes, S. J. Arnold, M. Busslinger, I. R. Dunay, Y. Tanriver, and A. Diefenbach. Differentiation of Type 1 ILCs from a Common Progenitor to All Helper-like Innate Lymphoid Cell Lineages. *Cell*, 157(2):340–356, apr 2014.

[40] J. Mjösberg, J. Bernink, K. Golebski, J. J. Karrich, C. P. Peters, B. Blom, A. A. te Velde, W. J. Fokkens, C. M. van Drunen, and H. Spits. The Transcription Factor GATA3 Is Essential for the Function of Human Type 2 Innate Lymphoid Cells. *Immunity*, 37(4):649–659, oct 2012.

[41] S. Sawa, M. Cherrier, M. Lochner, N. Satoh-Takayama, H. J. Fehling, F. Langa, J. P. Di Santo, and G. Eberl. Lineage Relationship Analysis of ROR t+ Innate Lymphoid Cells. *Science (80-.).*, 330(6004):665–669, oct 2010.

[42] J. S. Pober and W. C. Sessa. Evolving functions of endothelial cells in inflammation. *Nat. Rev. Immunol.*, 7(10):803–815, oct 2007.

[43] K. Ashina, Y. Tsubosaka, T. Nakamura, K. Omori, K. Kobayashi, M. Hori, H. Ozaki, and T. Murata. Histamine Induces Vascular Hyperpermeability by Increasing Blood Flow and Endothelial Barrier Disruption In Vivo. *PLoS One*, 10(7):e0132367, jul 2015.

[44] J. S. Pober. Warner-Lambert/Parke-Davis award lecture. Cytokine-mediated activation of vascular endothelium. Physiology and pathology. *Am. J. Pathol.*, 133(3):426–33, dec 1988.

[45] K. A. Birch, B. M. Ewenstein, D. E. Golan, and J. S. Pober. Prolonged peak elevations in cytoplasmic free calcium ions, derived from intracellular stores,

correlate with the extent of thrombin-stimulated exocytosis in single human umbilical vein endothelial cells. *J. Cell. Physiol.*, 160(3):545–554, sep 1994.

[46] K. Egan and G. A. FitzGerald. Eicosanoids and the Vascular Endothelium. In *Vasc. Endothel. I*, pages 189–211. Springer Berlin Heidelberg, Berlin, Heidelberg, 2006.

[47] M. M. Teixeira, T. J. Williams, and P. G. Hellewell. Role of prostaglandins and nitric oxide in acute inflammatory reactions in guinea-pig skin. *Br. J. Pharmacol.*, 110(4):1515–21, dec 1993.

[48] S. M. Prescott, G. A. Zimmerman, and T. M. McIntyre. Human endothelial cells in culture produce platelet-activating factor (1-alkyl-2-acetyl-sn-glycero-3-phosphocholine) when stimulated with thrombin. *Proc. Natl. Acad. Sci. U. S. A.*, 81(11):3534–8, jun 1984.

[49] D. E. Lorant, K. D. Patel, T. M. McIntyre, R. P. McEver, S. M. Prescott, and G. A. Zimmerman. Coexpression of GMP-140 and PAF by endothelium stimulated by histamine or thrombin: a juxtacrine system for adhesion and activation of neutrophils. *J. Cell Biol.*, 115(1), 1991.

[50] S. Massena, G. Christoffersson, E. Hjertstrom, E. Zcharia, I. Vlodavsky, N. Ausmees, C. Rolny, J.-P. Li, and M. Phillipson. A chemotactic gradient sequestered on endothelial heparan sulfate induces directional intraluminal crawling of neutrophils. *Blood*, 116(11):1924–1931, sep 2010.

[51] J. M. Munro, J. S. Pober, and R. S. Cotran. Tumor necrosis factor and interferon-gamma induce distinct patterns of endothelial activation and associated leukocyte accumulation in skin of Papio anubis. *Am. J. Pathol.*, 135(1):121–33, jul 1989.

[52] C. L. Semerad, F. Liu, A. D. Gregory, K. Stumpf, and D. C. Link. G-CSF is an essential regulator of neutrophil trafficking from the bone marrow to the blood. *Immunity*, 17(4):413–23, oct 2002.

[53] E. Kolaczkowska and P. Kubes. Neutrophil recruitment and function in health and inflammation. *Nat. Rev. Immunol.*, 13(3):159–175, feb 2013.

[54] C. Martin, P. C. E. Burdon, G. Bridger, J. C. Gutierrez-Ramos, T. J. Williams, and S. M. Rankin. Chemokines acting via CXCR2 and CXCR4 control the release of neutrophils from the bone marrow and their return following senescence. *Immunity*, 19(4):583–93, oct 2003.

[55] P. Kruger, M. Saffarzadeh, A. N. R. Weber, N. Rieber, M. Radsak, H. von Bernuth, C. Benarafa, D. Roos, J. Skokowa, and D. Hartl. Neutrophils: Between Host Defence, Immune Modulation, and Tissue Injury. *PLOS Pathog.*, 11(3):e1004651, mar 2015.

[56] O. Holz, S. Khalilieh, A. Ludwig-Sengpiel, H. Watz, P. Stryszak, P. Soni, M. Tsai, J. Sadeh, and H. Magnussen. SCH527123, a novel CXCR2 antagonist, inhibits ozone-induced neutrophilia in healthy subjects. *Eur. Respir. J.*, 35(3), 2010.

[57] R. Virtala, A.-K. Ekman, L. Jansson, U. Westin, and L. O. Cardell. Airway inflammation evaluated in a human nasal lipopolysaccharide challenge model by investigating the effect of a CXCR2 inhibitor. *Clin. Exp. Allergy*, 42(4):590–596, apr 2012.

[58] A. W. Segal. The function of the NADPH oxidase of phagocytes and its relationship to other NOXs in plants, invertebrates, and mammals. *Int. J. Biochem. Cell Biol.*, 40(4):604–18, 2008.

[59] E. P. Reeves, H. Lu, H. L. Jacobs, C. G. M. Messina, S. Bolsover, G. Gabella, E. O. Potma, A. Warley, J. Roes, and A. W. Segal. Killing activity of neutrophils is mediated through activation of proteases by K+ flux. *Nature*, 416(6878):291–297, mar 2002.

[60] V. Brinkmann, U. Reichard, C. Goosmann, B. Fauler, Y. Uhlemann, D. S. Weiss, Y. Weinrauch, and A. Zychlinsky. Neutrophil extracellular traps kill bacteria. *Science*, 303(5663):1532–5, mar 2004.

[61] T. A. Fuchs, U. Abed, C. Goosmann, R. Hurwitz, I. Schulze, V. Wahn, Y. Weinrauch, V. Brinkmann, and A. Zychlinsky. Novel cell death program leads to neutrophil extracellular traps. *J. Cell Biol.*, 176(2):231–41, jan 2007.

[62] V. Papayannopoulos, K. D. Metzler, A. Hakkim, and A. Zychlinsky. Neutrophil elastase and myeloperoxidase regulate the formation of neutrophil extracellular traps. *J. Cell Biol.*, 191(3):677–91, nov 2010.

[63] O. Soehnlein, S. Steffens, A. Hidalgo, and C. Weber. Neutrophils as protagonists and targets in chronic inflammation. *Nat. Rev. Immunol.*, 17(4):248–261, mar 2017.

[64] H. L. Wright, R. J. Moots, and S. W. Edwards. The multifactorial role of neutrophils in rheumatoid arthritis. *Nat. Rev. Rheumatol.*, 10(10):593–601, oct 2014.

[65] H. Kamohara, W. Matsuyama, O. Shimozato, K. Abe, C. Galligan, S.-I. Hashimoto, K. Matsushima, and T. Yoshimura. Regulation of tumour necrosis factor-related apoptosis-inducing ligand (TRAIL) and TRAIL receptor expression in human neutrophils. *Immunology*, 111(2):186–94, feb 2004.

[66] C. T. N. Pham. Neutrophil serine proteases fine-tune the inflammatory response. *Int. J. Biochem. Cell Biol.*, 40(6-7):1317–33, 2008.

[67] M. Scannell, M. B. Flanagan, A. DeStefani, K. J. Wynne, G. Cagney, C. Godson, and P. Maderna. Annexin-1 and peptide derivatives are released by apoptotic cells and stimulate phagocytosis of apoptotic neutrophils by macrophages. *J. Immunol.*, 178(7):4595–605, apr 2007.

[68] M. Perretti and J. Dalli. Exploiting the Annexin A1 pathway for the development of novel anti-inflammatory therapeutics. *Br. J. Pharmacol.*, 158(4):936–46, oct 2009.

[69] J. Hettinger, D. M. Richards, J. Hansson, M. M. Barra, A.-C. Joschko, J. Krijgsveld, and M. Feuerer. Origin of monocytes and macrophages in a committed progenitor. *Nat. Immunol.*, 14(8):821–830, jun 2013.

[70] C. V. Jakubzick, G. J. Randolph, and P. M. Henson. Monocyte differentiation and antigen-presenting functions. *Nat. Rev. Immunol.*, 17(6):349–362, apr 2017.

[71] H. Jung, D. S. Mithal, J. E. Park, and R. J. Miller. Localized CCR2 Activation in the Bone Marrow Niche Mobilizes Monocytes by Desensitizing CXCR4. *PLoS One*, 10(6):e0128387, jun 2015.

[72] L. Boring, J. Gosling, S. W. Chensue, S. L. Kunkel, R. V. Farese, H. E. Broxmeyer, and I. F. Charo. Impaired monocyte migration and reduced type 1 (Th1) cytokine responses in C-C chemokine receptor 2 knockout mice. *J. Clin. Invest.*, 100(10):2552–2561, nov 1997.

[73] C.-L. Tsou, W. Peters, Y. Si, S. Slaymaker, A. M. Aslanian, S. P. Weisberg, M. Mack, and I. F. Charo. Critical roles for CCR2 and MCP-3 in monocyte mobilization from bone marrow and recruitment to inflammatory sites. *J. Clin. Invest.*, 117(4):902–9, apr 2007.

[74] H. Raghu, C. M. Lepus, Q. Wang, H. H. Wong, N. Lingampalli, F. Oliviero, L. Punzi, N. J. Giori, S. B. Goodman, C. R. Chu, J. B. Sokolove, and W. H. Robinson. CCL2/CCR2, but not CCL5/CCR5, mediates monocyte recruitment, inflammation and cartilage destruction in osteoarthritis. *Ann. Rheum. Dis.*, 76(5):914–922, may 2017.

[75] C. Jakubzick, E. L. Gautier, S. L. Gibbings, D. K. Sojka, A. Schlitzer, T. E. Johnson, S. Ivanov, Q. Duan, S. Bala, T. Condon, N. van Rooijen, J. R. Grainger, Y. Belkaid, A. Ma'ayan, D. W. Riches, W. M. Yokoyama, F. Ginhoux, P. M. Henson, and G. J. Randolph. Minimal Differentiation of Classical Monocytes as They Survey Steady-State Tissues and Transport Antigen to Lymph Nodes. *Immunity*, 39(3):599–610, sep 2013.

[76] G. Thomas, R. Tacke, C. C. Hedrick, and R. N. Hanna. Nonclassical patrolling monocyte function in the vasculature. *Arterioscler. Thromb. Vasc. Biol.*, 35(6):1306–16, jun 2015.

[77] J. Cros, N. Cagnard, K. Woollard, N. Patey, S.-Y. Zhang, B. Senechal, A. Puel, S. K. Biswas, D. Moshous, C. Picard, J.-P. Jais, D. D'Cruz, J.-L. Casanova, C. Trouillet, and F. Geissmann. Human CD14dim Monocytes Patrol and Sense Nucleic Acids and Viruses via TLR7 and TLR8 Receptors. *Immunity*, 33(3):375–386, sep 2010.

[78] C. Combadiere, S. Potteaux, M. Rodero, T. Simon, A. Pezard, B. Esposito, R. Merval, A. Proudfoot, A. Tedgui, and Z. Mallat. Combined Inhibition of CCL2, CX3CR1, and CCR5 Abrogates Ly6Chi and Ly6Clo Monocytosis and Almost Abolishes Atherosclerosis in Hypercholesterolemic Mice. *Circulation*, 117(13):1649–1657, mar 2008.

[79] H. Wu, R. M. Gower, H. Wang, X.-Y. D. Perrard, R. Ma, D. C. Bullard, A. R. Burns, A. Paul, C. W. Smith, S. I. Simon, and C. M. Ballantyne. Functional Role of CD11c+ Monocytes in Atherogenesis Associated With Hypercholesterolemia. *Circulation*, 119(20):2708–2717, may 2009.

[80] M. Nahrendorf, F. K. Swirski, E. Aikawa, L. Stangenberg, T. Wurdinger, J.-L. Figueiredo, P. Libby, R. Weissleder, and M. J. Pittet. The healing myocardium sequentially mobilizes two monocyte subsets with divergent and complementary functions. *J. Exp. Med.*, 204(12):3037–47, nov 2007.

[81] S. A. Freeman and S. Grinstein. Phagocytosis: receptors, signal integration, and the cytoskeleton. *Immunol. Rev.*, 262(1):193–215, nov 2014.

[82] L. Peiser, S. Mukhopadhyay, and S. Gordon. Scavenger receptors in innate immunity. *Curr. Opin. Immunol.*, 14(1):123–8, feb 2002.

[83] D. R. Greaves and S. Gordon. Thematic review series: the immune system and atherogenesis. Recent insights into the biology of macrophage scavenger receptors. *J. Lipid Res.*, 46(1):11–20, jan 2005.

[84] K. J. Moore, F. J. Sheedy, and E. A. Fisher. Macrophages in atherosclerosis: a dynamic balance. *Nat. Rev. Immunol.*, 13(10):709–721, sep 2013.

[85] J. R. Grainger, J. E. Konkel, T. Zangerle-Murray, and T. N. Shaw. Macrophages in gastrointestinal homeostasis and inflammation. *Pflugers Arch.*, 469(3-4):527–539, apr 2017.

[86] G. Farro, M. Stakenborg, P. J. Gomez-Pinilla, E. Labeeuw, G. Goverse, M. D. Giovangiulio, N. Stakenborg, E. Meroni, F. D'Errico, Y. Elkrim, D. Laoui, Z. M. Lisowski, K. A. Sauter, D. A. Hume, J. A. Van Ginderachter, G. E. Boeckxstaens, and G. Matteoli. CCR2-dependent monocyte-derived macrophages resolve inflammation and restore gut motility in postoperative ileus. *Gut*, pages gutjnl–2016–313144, jun 2017.

[87] T. T. Braga, J. S. H. Agudelo, and N. O. S. Camara. Macrophages During the Fibrotic Process: M2 as Friend and Foe. *Front. Immunol.*, 6:602, 2015.

[88] J. N. Fullerton and D. W. Gilroy. Resolution of inflammation: a new therapeutic frontier. *Nat. Rev. Drug Discov.*, 15(8):551–567, mar 2016.

[89] C. A. Dinarello. Historical Review of Cytokines. *Eur. J. Immunol.*, 37(Suppl 1):S34, 2007.

[90] E. A. Carswell, L. J. Old, R. L. Kassel, S. Green, N. Fiore, and B. Williamson. An endotoxin-induced serum factor that causes necrosis of tumors. *Proc. Natl. Acad. Sci. U. S. A.*, 72(9):3666–70, sep 1975.

[91] M. D. Turner, B. Nedjai, T. Hurst, and D. J. Pennington. Cytokines and chemokines: At the crossroads of cell signalling and inflammatory disease. *Biochim. Biophys. Acta - Mol. Cell Res.*, 1843(11):2563–2582, nov 2014.

[92] R. A. Black, C. T. Rauch, C. J. Kozlosky, J. J. Peschon, J. L. Slack, M. F. Wolfson, B. J. Castner, K. L. Stocking, P. Reddy, S. Srinivasan, N. Nelson, N. Boiani, K. A. Schooley, M. Gerhart, R. Davis, J. N. Fitzner, R. S. Johnson, R. J. Paxton, C. J. March, and D. P. Cerretti. A metalloproteinase disintegrin that releases tumour-necrosis factor-α from cells. *Nature*, 385(6618):729–733, feb 1997.

[93] E. Friedmann, E. Hauben, K. Maylandt, S. Schleeger, S. Vreugde, S. F. Lichtenthaler, P.-H. Kuhn, D. Stauffer, G. Rovelli, and B. Martoglio. SPPL2a and SPPL2b promote intramembrane proteolysis of TNFα in activated dendritic cells to trigger IL-12 production. *Nat. Cell Biol.*, 8(8):843–848, aug 2006.

[94] A. A. Lobito, T. L. Gabriel, J. P. Medema, and F. C. Kimberley. Disease causing mutations in the TNF and TNFR superfamilies: Focus on molecular mechanisms driving disease. *Trends Mol. Med.*, 17(9):494–505, sep 2011.

[95] C. A. Hunter and S. A. Jones. IL-6 as a keystone cytokine in health and disease. *Nat. Immunol.*, 16(5):448–457, apr 2015.

[96] M. Kopf, H. Baumann, G. Freer, M. Freudenberg, M. Lamers, T. Kishimoto, R. Zinkernagel, H. Bluethmann, and G. Köhler. Impaired immune and acute-phase responses in interleukin-6-deficient mice. *Nature*, 368(6469):339–342, mar 1994.

[97] O. Dienz, J. G. Rud, S. M. Eaton, P. A. Lanthier, E. Burg, A. Drew, J. Bunn, B. T. Suratt, L. Haynes, and M. Rincon. Essential role of IL-6 in protection against H1N1 influenza virus by promoting neutrophil survival in the lung. *Mucosal Immunol.*, 5(3):258–266, may 2012.

[98] S. Diehl and M. Rincon. The two faces of IL-6 on Th1/Th2 differentiation. *Mol. Immunol.*, 39(9):531–536, dec 2002.

[99] E. Bettelli, Y. Carrier, W. Gao, T. Korn, T. B. Strom, M. Oukka, H. L. Weiner, and V. K. Kuchroo. Reciprocal developmental pathways for the generation of pathogenic effector TH17 and regulatory T cells. *Nature*, 441(7090):235–238, may 2006.

[100] G. E. White, A. J. Iqbal, and D. R. Greaves. CC Chemokine Receptors and Chronic Inflammation–Therapeutic Opportunities and Pharmacological Challenges. *Pharmacol. Rev.*, 65(1):47–89, jan 2013.

[101] M. Thelen. Dancing to the tune of chemokines. *Nat. Immunol.*, 2(2):129–134, feb 2001.

[102] T. Yoshimura, K. Matsushima, S. Tanaka, E. A. Robinson, E. Appella, J. J. Oppenheim, and E. J. Leonard. Purification of a human monocyte-derived neutrophil chemotactic factor that has peptide sequence similarity to other host defense cytokines. *Proc. Natl. Acad. Sci. U. S. A.*, 84(24):9233–7, dec 1987.

[103] M. Phillipson, B. Heit, P. Colarusso, L. Liu, C. M. Ballantyne, and P. Kubes. Intraluminal crawling of neutrophils to emigration sites: a molecularly distinct process from adhesion in the recruitment cascade. *J. Exp. Med.*, 203(12):2569–75, nov 2006.

[104] A. M. Wengner, S. C. Pitchford, R. C. Furze, and S. M. Rankin. The coordinated action of G-CSF and ELR + CXC chemokines in neutrophil mobilization during acute inflammation. *Blood*, 111(1):42–49, jan 2008.

[105] J. Hol, L. Wilhelmsen, and G. Haraldsen. The murine IL-8 homologues KC, MIP-2, and LIX are found in endothelial cytoplasmic granules but not in Weibel-Palade bodies. *J. Leukoc. Biol.*, 87(3):501–508, mar 2010.

[106] J. K. Roche, T. R. Keepers, L. K. Gross, R. M. Seaner, and T. G. Obrig. CXCL1/KC and CXCL2/MIP-2 are critical effectors and potential targets for therapy of Escherichia coli O157:H7-associated renal inflammation. *Am. J. Pathol.*, 170(2):526–37, feb 2007.

[107] P. Nair, M. Gaga, E. Zervas, K. Alagha, F. E. Hargreave, P. M. O'Byrne, P. Stryszak, L. Gann, J. Sadeh, and P. Chanez. Safety and efficacy of a CXCR2 antagonist in patients with severe asthma and sputum neutrophils: a randomized, placebo-controlled clinical trial. *Clin. Exp. Allergy*, 42(7):1097–1103, jul 2012.

[108] R. B. Moss, S. J. Mistry, M. W. Konstan, J. M. Pilewski, E. Kerem, R. Tal-Singer, A. L. Lazaar, and CF2110399 Investigators. Safety and early treatment effects of the CXCR2 antagonist SB-656933 in patients with cystic fibrosis. *J. Cyst. Fibros.*, 12(3):241–8, may 2013.

[109] T. Yokomizo. Leukotriene B4 receptors: Novel roles in immunological regulations. *Adv. Enzyme Regul.*, 51(1):59–64, 2011.

[110] E. A. Dennis and P. C. Norris. Eicosanoid storm in infection and inflammation. *Nat. Rev. Immunol.*, 15(8):511–23, aug 2015.

[111] W. W. Busse. Leukotrienes and Inflammation. *Am. J. Respir. Crit. Care Med.*, 157(6):S210–S213, jun 1998.

[112] W. L. Smith, Y. Urade, and P.-J. Jakobsson. Enzymes of the Cyclooxygenase Pathways of Prostanoid Biosynthesis. *Chem. Rev.*, 111(10):5821–5865, oct 2011.

[113] E. Ricciotti and G. A. Fitz Gerald. Prostaglandins and inflammation. *Arterioscler. Thromb. Vasc. Biol.*, 31(5):986–1000, may 2011.

[114] H. Hirai, K. Tanaka, O. Yoshie, K. Ogawa, K. Kenmotsu, Y. Takamori, M. Ichimasa, K. Sugamura, M. Nakamura, S. Takano, and K. Nagata. Prostaglandin D2 selectively induces chemotaxis in T helper type 2 cells, eosinophils, and basophils via seven-transmembrane receptor CRTH2. *J. Exp. Med.*, 193(2):255–61, jan 2001.

[115] A. J. Klil-Drori and A. Ariel. 15-Lipoxygenases in cancer: A double-edged sword? *Prostaglandins Other Lipid Mediat.*, 106:16–22, oct 2013.

[116] T. Ochi, Y. Ohkubo, and S. Mutoh. Role of cyclooxygenase-2, but not cyclooxygenase-1, on type II collagen-induced arthritis in DBA/1J mice. *Biochem. Pharmacol.*, 66(6):1055–60, sep 2003.

[117] M. Chen, E. Boilard, P. A. Nigrovic, P. Clark, D. Xu, G. A. FitzGerald, L. P. Audoly, and D. M. Lee. Predominance of cyclooxygenase 1 over cyclooxygenase 2 in the generation of proinflammatory prostaglandins in autoantibody-driven K/BxN serumtransfer arthritis. *Arthritis Rheum.*, 58(5):1354–1365, may 2008.

[118] H. Oida, T. Namba, Y. Sugimoto, F. Ushikubi, H. Ohishi, A. Ichikawa, and S. Narumiya. In situ hybridization studies of prostacyclin receptor mRNA expression in various mouse organs. *Br. J. Pharmacol.*, 116(7):2828–37, dec 1995.

[119] T. Murata, F. Ushikubi, T. Matsuoka, M. Hirata, A. Yamasaki, Y. Sugimoto, A. Ichikawa, Y. Aze, T. Tanaka, N. Yoshida, A. Ueno, S. Oh-ishi, and S. Narumiya. Altered pain perception and inflammatory response in mice lacking prostacyclin receptor. *Nature*, 388(6643):678–682, aug 1997.

[120] K. M. Egan, J. A. Lawson, S. Fries, B. Koller, D. J. Rader, E. M. Smyth, and G. A. Fitzgerald. COX-2-Derived Prostacyclin Confers Atheroprotection on Female Mice. *Science (80-.).*, 306(5703):1954–1957, dec 2004.

[121] T. Kobayashi, Y. Tahara, M. Matsumoto, M. Iguchi, H. Sano, T. Murayama, H. Arai, H. Oida, T. Yurugi-Kobayashi, J. K. Yamashita, H. Katagiri, M. Majima, M. Yokode, T. Kita, and S. Narumiya. Roles of thromboxane A2 and prostacyclin in the development of atherosclerosis in apoE-deficient mice. *J. Clin. Invest.*, 114(6):784–794, sep 2004.

[122] C. N. Serhan, N. Chiang, and T. E. Van Dyke. Resolving inflammation: dual anti-inflammatory and pro-resolution lipid mediators. *Nat. Rev. Immunol.*, 8(5):349–361, may 2008.

[123] F. S. Machado, J. E. Johndrow, L. Esper, A. Dias, A. Bafica, C. N. Serhan, and J. Aliberti. Anti-inflammatory actions of lipoxin A4 and aspirin-triggered lipoxin are SOCS-2 dependent. *Nat. Med.*, 12(3):330–334, mar 2006.

[124] K. J. Ho, M. Spite, C. D. Owens, H. Lancero, A. H. Kroemer, R. Pande, M. A. Creager, C. N. Serhan, and M. S. Conte. Aspirin-Triggered Lipoxin and Resolvin E1 Modulate Vascular Smooth Muscle Phenotype and Correlate with Peripheral Atherosclerosis. *Am. J. Pathol.*, 177(4):2116–2123, oct 2010.

[125] C. N. Serhan. Novel lipid mediators and resolution mechanisms in acute inflammation: to resolve or not? *Am. J. Pathol.*, 177(4):1576–91, oct 2010.

[126] M. Jedrzejczak-Czechowicz, A. Lewandowska-Polak, B. Bienkiewicz, and M. L. Kowalski. Involvement of 15-lipoxygenase and prostaglandin EP receptors in aspirin-triggered 15-hydroxyeicosatetraenoic acid generation in aspirin-sensitive asthmatics. *Clin. Exp. Allergy*, 38(7):1108–1116, jul 2008.

[127] K. Gronert, A. Gewirtz, J. L. Madara, and C. N. Serhan. Identification of a human enterocyte lipoxin A4 receptor that is regulated by interleukin (IL)-13 and interferon gamma and inhibits tumor necrosis factor alpha-induced IL-8 release. *J. Exp. Med.*, 187(8):1285–94, apr 1998.

[128] S. Fiore and C. N. Serhan. Formation of lipoxins and leukotrienes during receptor-mediated interactions of human platelets and recombinant human granulocyte/macrophage colony-stimulating factor-primed neutrophils. *J. Exp. Med.*, 172(5):1451–7, nov 1990.

[129] J. M. Schwab, N. Chiang, M. Arita, and C. N. Serhan. Resolvin E1 and protectin D1 activate inflammation-resolution programmes. *Nature*, 447(7146):869–874, jun 2007.

[130] E. L. Campbell, N. A. Louis, S. E. Tomassetti, G. O. Canny, M. Arita, C. N. Serhan, and S. P. Colgan. Resolvin E1 promotes mucosal surface clearance of neutrophils: a new paradigm for inflammatory resolution. *FASEB J.*, 21(12):3162–3170, oct 2007.

[131] M. Perretti and F. D'Acquisto. Annexin A1 and glucocorticoids as effectors of the resolution of inflammation. *Nat. Rev. Immunol.*, 9(1):62–70, jan 2009.

[132] M. Perretti, H. Christian, S. K. Wheller, I. Aiello, K. G. Mugridge, J. F. Morris, R. J. Flower, and N. J. Goulding. Annexin I is stored within gelatinase granules of human neutrophill and mobilized on the cell surface upon adhesion but not phagocytosis. *Cell Biol. Int.*, 24(3):163–174, mar 2000.

[133] E. B. Babiychuk, K. Monastyrskaya, and A. Draeger. Fluorescent Annexin A1 Reveals Dynamics of Ceramide Platforms in Living Cells. *Traffic*, 9(10):1757–1775, oct 2008.

[134] M. L. Jones, M. A. Alfaleh, S. Kumble, S. Zhang, G. W. Osborne, M. Yeh, N. Arora, J. J. C. Hou, C. B. Howard, D. Y. Chin, and S. M. Mahler. Targeting membrane proteins for antibody discovery using phage display. *Sci. Rep.*, 6(1):26240, sep 2016.

[135] T. Gobbetti, S. M. Coldewey, J. Chen, S. McArthur, P. le Faouder, N. Cenac, R. J. Flower, C. Thiemermann, and M. Perretti. Nonredundant protective properties of FPR2/ALX in polymicrobial murine sepsis. *Proc. Natl. Acad. Sci. U. S. A.*, 111(52):18685–90, dec 2014.

[136] D. H. M. Kusters, M. L. Chatrou, B. A. G. Willems, M. De Saint-Hubert, M. Bauwens, E. van der Vorst, S. Bena, E. A. L. Biessen, M. Perretti, L. J.

Schurgers, and C. P. M. Reutelingsperger. Pharmacological Treatment with Annexin A1 Reduces Atherosclerotic Plaque Burden in LDLR-/- Mice on Western Type Diet. *PLoS One*, 10(6):e0130484, jun 2015.

[137] M. Saraiva and A. O'Garra. The regulation of IL-10 production by immune cells. *Nat. Rev. Immunol.*, 10(3):170–181, mar 2010.

[138] B. Schaljo, F. Kratochvill, N. Gratz, I. Sadzak, I. Sauer, M. Hammer, C. Vogl, B. Strobl, M. Muller, P. J. Blackshear, V. Poli, R. Lang, P. J. Murray, and P. Kovarik. Tristetraprolin Is Required for Full Anti-Inflammatory Response of Murine Macrophages to IL-10. *J. Immunol.*, 183(2):1197–1206, jul 2009.

[139] M. A. Sugimoto, L. P. Sousa, V. Pinho, M. Perretti, and M. M. Teixeira. Resolution of Inflammation: What Controls Its Onset? *Front. Immunol.*, 7:160, 2016.

[140] C. Monaco, J. Nanchahal, P. Taylor, and M. Feldmann. Anti-TNF therapy: past, present and future. *Int. Immunol.*, 27(1):55–62, jan 2015.

[141] P. Chames, M. Van Regenmortel, E. Weiss, and D. Baty. Therapeutic antibodies: successes, limitations and hopes for the future. *Br. J. Pharmacol.*, 157(2):220–33, may 2009.

[142] I. N. Foltz, M. Karow, and S. M. Wasserman. Evolution and emergence of therapeutic monoclonal antibodies: what cardiologists need to know. *Circulation*, 127(22):2222–30, jun 2013.

[143] J. S. Smolen, D. Aletaha, and I. B. McInnes. Rheumatoid arthritis. *Lancet*, 388(10055):2023–2038, oct 2016.

[144] A. E. Koch, S. L. Kunkel, and R. M. Strieter. Cytokines in rheumatoid arthritis. *J. Investig. Med.*, 43(1):28–38, feb 1995.

[145] M. Feldmann and R. N. Maini. Anti-TNFa therapy of rheumatoid arthritis: What Have We Learned? *Annu. Rev. Immunol.*, 19(1):163–196, apr 2001.

[146] D. J. Shealy and S. Visvanathan. Anti-TNF Antibodies: Lessons from the Past, Roadmap for the Future. In *Handb. Exp. Pharmacol.*, number 181, pages 101–129. 2008.

[147] N. Goel and S. Stephens. Certolizumab pegol. *MAbs*, 2(2):137–47, 2010.

[148] A. Nesbitt, G. Fossati, M. Bergin, P. Stephens, S. Stephens, R. Foulkes, D. Brown, M. Robinson, and T. Bourne. Mechanism of action of certolizumab pegol (CDP870): In vitro comparison with other anti-tumor necrosis factor α agents. *Inflamm. Bowel Dis.*, 13(11):1323–1332, nov 2007.

[149] G. Vidarsson, G. Dekkers, and T. Rispens. IgG subclasses and allotypes: from structure to effector functions. *Front. Immunol.*, 5:520, 2014.

[150] M. Suzuki, C. Kato, and A. Kato. Therapeutic antibodies: their mechanisms of action and the pathological findings they induce in toxicity studies. *J. Toxicol. Pathol.*, 28(3):133–9, jul 2015.

[151] Y. Hu, M. J. Turner, J. Shields, M. S. Gale, E. Hutto, B. L. Roberts, W. M. Siders, and J. M. Kaplan. Investigation of the mechanism of action of alemtuzumab in a human CD52 transgenic mouse model. *Immunology*, 128(2):260–70, oct 2009.

[152] S. Nagpal, S. Patel, H. Jacobe, D. DiSepio, C. Ghosn, M. Malhotra, M. Teng, M. Duvic, and R. A. Chandraratna. Tazarotene-induced Gene 2 (TIG2), a Novel Retinoid-Responsive Gene in Skin. *J. Invest. Dermatol.*, 109(1):91–95, jul 1997.

[153] V. Wittamer, J.-D. Franssen, M. Vulcano, J.-F. Mirjolet, E. Le Poul, I. Migeotte, S. Brézillon, R. Tyldesley, C. Blanpain, M. Detheux, A. Mantovani, S. Sozzani, G. Vassart, M. Parmentier, and D. Communi. Specific recruitment of antigen-presenting cells by chemerin, a novel processed ligand from human inflammatory fluids. *J. Exp. Med.*, 198(7):977–85, oct 2003.

[154] G. Barnea, W. Strapps, G. Herrada, Y. Berman, J. Ong, B. Kloss, R. Axel, and K. J. Lee. The genetic design of signaling cascades to record receptor activation. *Proc. Natl. Acad. Sci. U. S. A.*, 105(1):64–9, jan 2008.

[155] B. a. Zabel, S. Nakae, L. Zúñiga, J.-Y. Kim, T. Ohyama, C. Alt, J. Pan, H. Suto, D. Soler, S. J. Allen, T. M. Handel, C. H. Song, S. J. Galli, and E. C. Butcher. Mast cell-expressed orphan receptor CCRL2 binds chemerin and is required for optimal induction of IgE-mediated passive cutaneous anaphylaxis. *J. Exp. Med.*, 205(10):2207–20, sep 2008.

[156] B. A. Zabel, L. Zuniga, T. Ohyama, S. J. Allen, J. Cichy, T. M. Handel, and E. C. Butcher. Chemoattractants, extracellular proteases, and the integrated host defense response. *Exp. Hematol.*, 34(8):1021–1032, aug 2006.

[157] X.-Y. Du, B. A. Zabel, T. Myles, S. J. Allen, T. M. Handel, P. P. Lee, E. C. Butcher, and L. L. Leung. Regulation of chemerin bioactivity by plasma carboxypeptidase N, carboxypeptidase B (activated thrombin-activable fibrinolysis inhibitor), and platelets. *J. Biol. Chem.*, 284(2):751–8, jan 2009.

[158] V. Wittamer, B. Bondue, a. Guillabert, G. Vassart, M. Parmentier, and D. Communi. Neutrophil-Mediated Maturation of Chemerin: A Link between Innate and Adaptive Immunity. *J. Immunol.*, 175(1):487–493, jun 2005.

[159] B. A. Zabel, S. J. Allen, P. Kulig, J. A. Allen, J. Cichy, T. M. Handel, and E. C. Butcher. Chemerin activation by serine proteases of the coagulation, fibrinolytic, and inflammatory cascades. *J. Biol. Chem.*, 280(41):34661–6, oct 2005.

[160] Y. Yamaguchi, X.-Y. Du, L. Zhao, J. Morser, and L. L. K. Leung. Proteolytic Cleavage of Chemerin Protein Is Necessary for Activation to the Active Form, Chem157S, Which Functions as a Signaling Molecule in Glioblastoma. *J. Biol. Chem.*, 286(45):39510–39519, nov 2011.

[161] A. Guillabert, V. Wittamer, B. Bondue, V. Godot, V. Imbault, M. Parmentier, and D. Communi. Role of neutrophil proteinase 3 and mast cell chymase in chemerin proteolytic regulation. *J. Leukoc. Biol.*, 84(6):1530–8, dec 2008.

[162] P. Kulig, T. Kantyka, B. A. Zabel, M. Banas, A. Chyra, A. Stefanska, H. Tu, S. J. Allen, T. M. Handel, A. Kozik, J. Potempa, E. C. Butcher, and J. Cichy. Regulation of chemerin chemoattractant and antibacterial activity by human cysteine cathepsins. *J. Immunol.*, 187(3):1403–10, aug 2011.

[163] T. Yoshimura and J. J. Oppenheim. Chemokine-like receptor 1 (CMKLR1) and chemokine (C-C motif) receptor-like 2 (CCRL2); two multifunctional receptors with unusual properties. *Exp. Cell Res.*, 317(5):674–84, mar 2011.

[164] O. De Henau, G.-N. Degroot, V. Imbault, V. Robert, C. De Poorter, S. Mcheik, C. Galés, M. Parmentier, and J.-Y. Springael. Signaling Properties of Chemerin Receptors CMKLR1, GPR1 and CCRL2. *PLoS One*, 11(10):e0164179, oct 2016.

[165] R. Hart and D. R. Greaves. Chemerin Contributes to Inflammation by Promoting Macrophage Adhesion to VCAM-1 and Fibronectin through Clustering of VLA-4 and VLA-5. *J. Immunol.*, 185(6):3728–3739, sep 2010.

[166] M. Arita, T. Ohira, Y.-P. Sun, S. Elangovan, N. Chiang, and C. N. Serhan. Resolvin E1 selectively interacts with leukotriene B4 receptor BLT1 and ChemR23 to regulate inflammation. *J. Immunol.*, 178(6):3912–7, mar 2007.

[167] T. Ohira, M. Arita, K. Omori, A. Recchiuti, T. E. Van Dyke, and C. N. Serhan. Resolvin E1 receptor activation signals phosphorylation and phagocytosis. *J. Biol. Chem.*, 285(5):3451–61, jan 2010.

[168] A. J. Kennedy, P. Yang, C. Read, R. E. Kuc, L. Yang, E. J. A. Taylor, C. W. Taylor, J. J. Maguire, and A. P. Davenport. Chemerin Elicits Potent Constrictor Actions via ChemokineLike Receptor 1 (CMKLR1), not GProteinCoupled Receptor 1 (GPR1), in Human and Rat Vasculature. *J. Am. Heart Assoc.*, 5(10):e004421, oct 2016.

[169] M. Banas, A. Zegar, M. Kwitniewski, K. Zabieglo, J. Marczynska, M. Kapinska-Mrowiecka, M. LaJevic, B. A. Zabel, and J. Cichy. The Expression and Regulation of Chemerin in the Epidermis. *PLoS One*, 10(2):e0117830, feb 2015.

[170] J. L. Rourke, S. Muruganandan, H. J. Dranse, N. M. McMullen, and C. J. Sinal. Gpr1 is an active chemerin receptor influencing glucose homeostasis in obese mice. *J. Endocrinol.*, 222(2):201–215, jul 2014.

[171] J. Monnier, S. Lewén, E. O'Hara, K. Huang, H. Tu, E. C. Butcher, and B. a. Zabel. Expression, regulation, and function of atypical chemerin receptor CCRL2 on endothelial cells. *J. Immunol.*, 189(2):956–67, jul 2012.

[172] L. Patel, S. Charlton, J. Chambers, and C. Macphee. Expression and functional analysis of chemokine receptors in human peripheral blood leukocyte populations. *Cytokine*, 14(1):27–36, apr 2001.

[173] I. Migeotte, J.-D. Franssen, S. Goriely, F. Willems, and M. Parmentier. Distribution and regulation of expression of the putative human chemokine receptor HCR in leukocyte populations. *Eur. J. Immunol.*, 32(2):494–501, feb 2002.

[174] D. J. Ferland and S. W. Watts. Chemerin: A comprehensive review elucidating the need for cardiovascular research. *Pharmacol. Res.*, 99:351–61, sep 2015.

[175] J. L. Cash, R. Hart, A. Russ, J. P. C. Dixon, W. H. Colledge, J. Doran, A. G. Hendrick, M. B. L. Carlton, and D. R. Greaves. Synthetic chemerin-derived peptides suppress inflammation through ChemR23. *J. Exp. Med.*, 205(4):767–75, apr 2008.

[176] S. Luangsay, V. Wittamer, B. Bondue, O. De Henau, L. Rouger, M. Brait, J.-D. Franssen, P. de Nadai, F. Huaux, and M. Parmentier. Mouse ChemR23 Is Expressed in Dendritic Cell Subsets and Macrophages, and Mediates an Anti-Inflammatory Activity of Chemerin in a Lung Disease Model. *J. Immunol.*, 183(10), 2009.

[177] K. L. Graham, B. A. Zabel, S. Loghavi, L. A. Zuniga, P. P. Ho, R. A. Sobel, and E. C. Butcher. Chemokine-like receptor-1 expression by central nervous system-infiltrating leukocytes and involvement in a model of autoimmune demyelinating disease. *J. Immunol.*, 183(10):6717–23, nov 2009.

[178] B. Bondue, O. Vosters, P. de Nadai, S. Glineur, O. De Henau, S. Luangsay, F. Van Gool, D. Communi, P. De Vuyst, D. Desmecht, and M. Parmentier. ChemR23 dampens lung inflammation and enhances anti-viral immunity in a mouse model of acute viral pneumonia. *PLoS Pathog.*, 7(11):e1002358, nov 2011.

[179] T. Demoor, K. R. Bracke, L. L. Dupont, M. Plantinga, B. Bondue, M.-O. Roy, V. Lannoy, B. N. Lambrecht, G. G. Brusselle, and G. F. Joos. The Role of ChemR23 in the Induction and Resolution of Cigarette Smoke-Induced Inflammation. *J. Immunol.*, 186(9):5457–5467, may 2011.

[180] H. J. Dranse, J. L. Rourke, A. W. Stadnyk, and C. J. Sinal. Local chemerin levels are positively associated with DSS-induced colitis but constitutive loss of CMKLR1 does not protect against development of colitis. *Physiol. Rep.*, 3(8), aug 2015.

[181] S. Provoost, K. C. De Grove, G. L. Fraser, V. J. Lannoy, K. G. Tournoy, G. G. Brusselle, T. Maes, and G. F. Joos. Pro- and Anti-Inflammatory Role of ChemR23 Signaling in Pollutant-Induced Inflammatory Lung Responses. *J. Immunol.*, 196(4), 2016.

[182] K. Otero, A. Vecchi, E. Hirsch, J. Kearley, W. Vermi, A. Del Prete, S. Gonzalvo-Feo, C. Garlanda, O. Azzolino, L. Salogni, C. M. Lloyd, F. Facchetti, A. Mantovani, and S. Sozzani. Nonredundant role of CCRL2 in lung dendritic cell trafficking. *Blood*, 116(16):2942–9, oct 2010.

[183] C. Mazzon, L. Zanotti, L. Wang, A. Del Prete, E. Fontana, V. Salvi, P. L. Poliani, and S. Sozzani. CCRL2 regulates M1/M2 polarization during EAE recovery phase. *J. Leukoc. Biol.*, 99(6):1027–33, jun 2016.

[184] A. Del Prete, L. Martínez-Muñoz, C. Mazzon, L. Toffali, F. Sozio, L. Za, D. Bosisio, L. Gazzurelli, V. Salvi, L. Tiberio, C. Liberati, E. Scanziani, A. Vecchi, C. Laudanna, M. Mellado, A. Mantovani, and S. Sozzani. The atypical receptor CCRL2 is required for CXCR2-dependent neutrophil recruitment and tissue damage. *Blood*, 130(10):1223–1234, sep 2017.

[185] D. Regan-Komito, S. Valaris, T. S. Kapellos, C. Recio, L. Taylor, D. R. Greaves, and A. J. Iqbal. Absence of the Non-Signalling Chemerin Receptor CCRL2 Exacerbates Acute Inflammatory Responses In Vivo. *Front. Immunol.*, 8:1621, nov 2017.

[186] M. Takahashi, Y. Okimura, G. Iguchi, H. Nishizawa, M. Yamamoto, K. Suda, R. Kitazawa, W. Fujimoto, K. Takahashi, F. N. Zolotaryov, K. S. Hong, H. Kiyonari, T. Abe, H. Kaji, S. Kitazawa, M. Kasuga, K. Chihara, and Y. Takahashi. Chemerin regulates β-cell function in mice. *Sci. Rep.*, 1(1):123, dec 2011.

[187] L. Rouger, G. R. Denis, S. Luangsay, and M. Parmentier. ChemR23 knockout mice display mild obesity but no deficit in adipocyte differentiation. *J. Endocrinol.*, 219(3):279–89, dec 2013.

[188] K. Kaneko, Y. Miyabe, A. Takayasu, S. Fukuda, C. Miyabe, M. Ebisawa, W. Yokoyama, K. Watanabe, T. Imai, K. Muramoto, Y. Terashima, T. Sugihara, K. Matsushima, N. Miyasaka, and T. Nanki. Chemerin activates fibroblast-like synoviocytes in patients with rheumatoid arthritis. *Arthritis Res. Ther.*, 13(5):R158, 2011.

[189] V. Berg, B. Sveinbjörnsson, S. Bendiksen, J. Brox, K. Meknas, and Y. Figenschau. Human articular chondrocytes express ChemR23 and chemerin; ChemR23 promotes inflammatory signalling upon binding the ligand chemerin21-157. *Arthritis Res. Ther.*, 12(6):R228, 2010.

[190] D. Stejskal, M. Karpisek, Z. Hanulova, and M. Svestak. Chemerin is an independent marker of the metabolic syndrome in a Caucasian population–a pilot study. *Biomed. Pap. Med. Fac. Univ. Palacky. Olomouc. Czech. Repub.*, 152(2):217–21, dec 2008.

[191] J. Weigert, F. Obermeier, M. Neumeier, J. Wanninger, M. Filarsky, S. Bauer, C. Aslanidis, G. Rogler, C. Ott, A. Schäffler, J. Schölmerich, and C. Buechler. Circulating levels of chemerin and adiponectin are higher in ulcerative colitis and chemerin is elevated in Crohns disease. *Inflamm. Bowel Dis.*, 16(4):630–637, apr 2010.

[192] S. Gonzalvo-Feo, A. Del Prete, M. Pruenster, V. Salvi, L. Wang, M. Sironi, S. Bierschenk, M. Sperandio, A. Vecchi, and S. Sozzani. Endothelial CellDerived Chemerin Promotes Dendritic Cell Transmigration. *J. Immunol.*, 192(5), 2014.

[193] S. Muruganandan, S. D. Parlee, J. L. Rourke, M. C. Ernst, K. B. Goralski, and C. J. Sinal. Chemerin, a novel peroxisome proliferator-activated receptor gamma (PPARgamma) target gene that promotes mesenchymal stem cell adipogenesis. *J. Biol. Chem.*, 286(27):23982–95, jul 2011.

[194] A. E. Adams, Y. Abu-Amer, J. Chappel, S. Stueckle, F. P. Ross, S. L. Teitelbaum, and L. J. Suva. 1,25 dihydroxyvitamin D3 and dexamethasone induce the cyclooxygenase 1 gene in osteoclast-supporting stromal cells. *J. Cell. Biochem.*, 74(4):587–595, sep 1999.

[195] S. Muruganandan, H. J. Dranse, J. L. Rourke, N. M. McMullen, and C. J. Sinal. Chemerin neutralization blocks hematopoietic stem cell osteoclastogenesis. *Stem Cells*, 31(10):2172–2182, oct 2013.

[196] S. Kralisch, S. Weise, G. Sommer, J. Lipfert, U. Lossner, M. Bluher, M. Stumvoll, and M. Fasshauer. Interleukin-1ß induces the novel adipokine chemerin in adipocytes in vitro. *Regul. Pept.*, 154(1-3):102–106, apr 2009.

[197] C. Carlino, E. Trotta, H. Stabile, S. Morrone, R. Bulla, A. Soriani, M. L. Iannitto, C. Agostinis, C. Mocci, M. Minozzi, C. Aragona, G. Perniola, F. Tedesco, S. Sozzani, A. Santoni, and A. Gismondi. Chemerin regulates NK cell accumulation and endothelial cell morphogenesis in the decidua during early pregnancy. *J. Clin. Endocrinol. Metab.*, 97(10):3603–12, oct 2012.

[198] G. Aksan, S. nci, G. Nar, K. Soylu, Ö. Gedikli, S. Yüksel, M. Özdemir, R. Nar, M. Meriç, and M. ahin. Association of serum chemerin levels with the severity of coronary artery disease in patients with metabolic syndrome. *Int. J. Clin. Exp. Med.*, 7(12):5461–8, 2014.

[199] K. Bozaoglu, K. Bolton, J. McMillan, P. Zimmet, J. Jowett, G. Collier, K. Walder, and D. Segal. Chemerin Is a Novel Adipokine Associated with Obesity and Metabolic Syndrome. *Endocrinology*, 148(10):4687–4694, oct 2007.

[200] T.-P. Zhang, H.-M. Li, R.-X. Leng, X.-P. Li, X.-M. Li, H.-F. Pan, and D.-Q. Ye. Plasma levels of adipokines in systemic lupus erythematosus patients. *Cytokine*, 86:15–20, oct 2016.

[201] A. Leiherer, A. Muendlein, E. Kinz, A. Vonbank, P. Rein, P. Fraunberger, C. Malin, C. H. Saely, and H. Drexel. High plasma chemerin is associated with renal dysfunction and predictive for cardiovascular events Insights from phenotype and genotype characterization. *Vascul. Pharmacol.*, 77:60–68, feb 2016.

[202] P. Gu, M. Cheng, X. Hui, B. Lu, W. Jiang, and Z. Shi. Elevating circulation chemerin level is associated with endothelial dysfunction and early atherosclerotic changes in essential hypertensive patients. *J. Hypertens.*, 33(8):1624–1632, aug 2015.

[203] M. M. J. Herenius, A. S. F. Oliveira, C. A. Wijbrandts, D. M. Gerlag, P. P. Tak, and M. C. Lebre. Anti-TNF Therapy Reduces Serum Levels of Chemerin in Rheumatoid Arthritis: A New Mechanism by Which Anti-TNF Might Reduce Inflammation. *PLoS One*, 8(2):e57802, feb 2013.

[204] K. Makrilakis, K. Fragiadaki, J. Smith, P. P. Sfikakis, and G. D. Kitas. Interrelated reduction of chemerin and plasminogen activator inhibitor-1 serum levels in rheumatoid arthritis after interleukin-6 receptor blockade. *Clin. Rheumatol.*, 34(3):419–427, mar 2015.

[205] W. Vermi, E. Riboldi, V. Wittamer, F. Gentili, W. Luini, S. Marrelli, A. Vecchi, J.-D. Franssen, D. Communi, L. Massardi, M. Sironi, A. Mantovani, M. Parmentier, F. Facchetti, and S. Sozzani. Role of ChemR23 in directing the migration of myeloid and plasmacytoid dendritic cells to lymphoid organs and inflamed skin. *J. Exp. Med.*, 201(4), 2005.

[206] S. Parolini, A. Santoro, E. Marcenaro, W. Luini, L. Massardi, F. Facchetti, D. Communi, M. Parmentier, A. Majorana, M. Sironi, G. Tabellini, A. Moretta, and S. Sozzani. The role of chemerin in the colocalization of NK and dendritic cell subsets into inflamed tissues. *Blood*, 109(9):3625–3632, may 2007.

[207] Y. Lin, X. Yang, W. Yue, X. Xu, B. Li, L. Zou, and R. He. Chemerin aggravates DSS-induced colitis by suppressing M2 macrophage polarization. *Cell. Mol. Immunol.*, 11(4):355–66, jul 2014.

[208] K. Eisinger, S. Bauer, A. Schäffler, R. Walter, E. Neumann, C. Buechler, U. Müller-Ladner, and K. W. Frommer. Chemerin induces CCL2 and TLR4 in synovial fibroblasts of patients with rheumatoid arthritis and osteoarthritis. *Exp. Mol. Pathol.*, 92(1):90–96, feb 2012.

[209] K. B. Neves, A. Nguyen Dinh Cat, R. A. M. Lopes, F. J. Rios, A. Anagnostopoulou, N. S. Lobato, A. M. de Oliveira, R. C. Tostes, A. C. Montezano, and R. M. Touyz. Chemerin Regulates Crosstalk Between Adipocytes and Vascular Cells Through NoxNovelty and Significance. *Hypertension*, 66(3):657–666, sep 2015.

[210] L. Wang, T. Yang, Y. Ding, Y. Zhong, L. Yu, and M. Peng. Chemerin plays a protective role by regulating human umbilical vein endothelial cell-induced nitric oxide signaling in preeclampsia. *Endocrine*, 48(1):299–308, feb 2009.

[211] L. Zhao, W. Yang, X. Yang, Y. Lin, J. Lv, X. Dou, Q. Luo, J. Dong, Z. Chen, Y. Chu, and R. He. Chemerin suppresses murine allergic asthma by inhibiting CCL2 production and subsequent airway recruitment of inflammatory dendritic cells. *Allergy*, 69(6):763–74, jun 2014.

[212] B. Bondue, O. De Henau, S. Luangsay, T. Devosse, P. de Nadaï, J.-Y. Springael, M. Parmentier, and O. Vosters. The Chemerin/ChemR23 System Does Not Affect the Pro-Inflammatory Response of Mouse and Human Macrophages Ex Vivo. *PLoS One*, 7(6):e40043, jun 2012.

[213] K. L. Graham, J. V. Zhang, S. Lewén, T. M. Burke, T. Dang, M. Zoudilova, R. A. Sobel, E. C. Butcher, and B. A. Zabel. A Novel CMKLR1 Small Molecule Antagonist Suppresses CNS Autoimmune Inflammatory Disease. *PLoS One*, 9(12):e112925, dec 2014.

[214] J. L. Cash, S. Bena, S. E. Headland, S. McArthur, V. Brancaleone, and M. Perretti. Chemerin15 inhibits neutrophil-mediated vascular inflammation and myocardial ischemia-reperfusion injury through ChemR23. *EMBO Rep.*, 14(11):999–1007, sep 2013.

[215] S.-g. Roh, S.-H. Song, K.-C. Choi, K. Katoh, V. Wittamer, M. Parmentier, and S.-i. Sasaki. ChemerinA new adipokine that modulates adipogenesis via its own receptor. *Biochem. Biophys. Res. Commun.*, 362(4):1013–1018, nov 2007.

[216] K. B. Goralski, T. C. McCarthy, E. A. Hanniman, B. A. Zabel, E. C. Butcher, S. D. Parlee, S. Muruganandan, and C. J. Sinal. Chemerin, a Novel Adipokine That Regulates Adipogenesis and Adipocyte Metabolism. *J. Biol. Chem.*, 282(38):28175–28188, sep 2007.

[217] S. H. Chu, M. K. Lee, K. Y. Ahn, J.-A. Im, M. S. Park, D.-C. Lee, J. Y. Jeon, and J. W. Lee. Chemerin and Adiponectin Contribute Reciprocally to Metabolic Syndrome. *PLoS One*, 7(4):e34710, apr 2012.

[218] J. Kaur, R. Adya, B. K. Tan, J. Chen, and H. S. Randeva. Identification of chemerin receptor (ChemR23) in human endothelial cells: Chemerin-induced endothelial angiogenesis. *Biochem. Biophys. Res. Commun.*, 391(4):1762–1768, jan 2010.

[219] K. Bozaoglu, J. E. Curran, C. J. Stocker, M. S. Zaibi, D. Segal, N. Konstantopoulos, S. Morrison, M. Carless, T. D. Dyer, S. A. Cole, H. H. H. Goring, E. K. Moses, K. Walder, M. A. Cawthorne, J. Blangero, and J. B. M. Jowett. Chemerin, a novel adipokine in the regulation of angiogenesis. *J. Clin. Endocrinol. Metab.*, 95(5):2476–85, may 2010.

[220] M. Banas, K. Zabieglo, G. Kasetty, M. Kapinska-Mrowiecka, J. Borowczyk, J. Drukala, K. Murzyn, B. A. Zabel, E. C. Butcher, J. M. Schroeder, A. Schmidtchen, and J. Cichy. Chemerin Is an Antimicrobial Agent in Human Epidermis. *PLoS One*, 8(3):e58709, mar 2013.

[221] F. M. Marim, T. N. Silveira, D. S. Lima, and D. S. Zamboni. A Method for Generation of Bone Marrow-Derived Macrophages from Cryopreserved Mouse Bone Marrow Cells. *PLoS One*, 5(12):e15263, dec 2010.

[222] X. Jiang, C. Shen, J. Rey-Ladino, H. Yu, and R. C. Brunham. Characterization of murine dendritic cell line JAWS II and primary bone marrow-derived dendritic cells in Chlamydia muridarum antigen presentation and induction of protective immunity. *Infect. Immun.*, 76(6):2392–401, jun 2008.

[223] M. Swamydas and M. S. Lionakis. Isolation, purification and labeling of mouse bone marrow neutrophils for functional studies and adoptive transfer experiments. *J. Vis. Exp.*, (77):e50586, jul 2013.

[224] A. J. Iqbal, D. Regan-Komito, I. Christou, G. E. White, E. McNeill, A. Kenyon, L. Taylor, T. S. Kapellos, E. a. Fisher, K. M. Channon, and D. R. Greaves. A real time chemotaxis assay unveils unique migratory profiles amongst different primary murine macrophages. *PLoS One*, 8(3):e58744, jan 2013.

[225] L. Zhao, Y. Yamaguchi, S. Sharif, X.-Y. Du, J. J. Song, D. M. Lee, L. D. Recht, W. H. Robinson, J. Morser, and L. L. K. Leung. Chemerin158K protein is the dominant chemerin isoform in synovial and cerebrospinal fluids but not in plasma. *J. Biol. Chem.*, 286(45):39520–7, nov 2011.

[226] S. Schultz, A. Saalbach, J. T. Heiker, R. Meier, T. Zellmann, J. C. Simon, and A. G. Beck-Sickinger. Proteolytic activation of prochemerin by kallikrein 7 breaks an ionic linkage and results in C-terminal rearrangement. *Biochem. J.*, 452(2):271–80, jun 2013.

[227] B. A. Zabel, A. M. Silverio, and E. C. Butcher. Chemokine-Like Receptor 1 Expression and Chemerin-Directed Chemotaxis Distinguish Plasmacytoid from Myeloid Dendritic Cells in Human Blood. *J. Immunol.*, 174(1), 2004.

[228] V. Wittamer, F. Grégoire, P. Robberecht, G. Vassart, D. Communi, and M. Parmentier. The C-terminal nonapeptide of mature chemerin activates the chemerin receptor with low nanomolar potency. *J. Biol. Chem.*, 279(11):9956–62, mar 2004.

[229] H. John, J. Hierer, O. Haas, and W.-G. Forssmann. Quantification of angiotensin-converting-enzyme-mediated degradation of human chemerin 145154 in plasma by matrix-assisted laser desorption/ionizationtime-of-flight mass spectrometry. *Anal. Biochem.*, 362(1):117–125, 2007.

[230] G. P. Smith. Filamentous fusion phage: novel expression vectors that display cloned antigens on the virion surface. *Science*, 228(4705):1315–7, jun 1985.

[231] J. Bazan, I. Całkosiński, and A. Gamian. Phage display–A powerful technique for immunotherapy: 1. Introduction and potential of therapeutic applications, dec 2012.

[232] A. Fagerlund, A. H. Myrset, and M. A. Kulseth. Construction and characterization of a 9-mer phage display pVIII-library with regulated peptide density. *Appl. Microbiol. Biotechnol.*, 80(5):925–936, oct 2008.

[233] G. T. Hess, J. J. Cragnolini, M. W. Popp, M. A. Allen, S. K. Dougan, E. Spooner, H. L. Ploegh, A. M. Belcher, and C. P. Guimaraes. M13 Bacteriophage Display Framework That Allows Sortase-Mediated Modification of Surface-Accessible Phage Proteins. *Bioconjug. Chem.*, 23(7):1478–1487, jul 2012.

[234] S. A. Moon, M. K. Ki, S. Lee, M.-L. Hong, M. Kim, S. Kim, J. Chung, S. G. Rhee, and H. Shim. Antibodies against non-immunizing antigens derived from a large immune scFv library. *Mol. Cells*, 31(6):509–513, jun 2011.

[235] V. Stoyanova, R. Aleksandrov, M. Lukarska, D. Duhalov, V. Atanasov, and S. Petrova. Recognition of Vipera ammodytes meridionalis neurotoxin vipoxin and its components using phage-displayed scFv and polyclonal antivenom sera. *Toxicon*, 60(5):802–809, oct 2012.

[236] A. Knappik, L. Ge, A. Honegger, P. Pack, M. Fischer, G. Wellnhofer, A. Hoess, J. Wölle, A. Plückthun, and B. Virnekäs. Fully synthetic human combinatorial antibody libraries (HuCAL) based on modular consensus frameworks and CDRs randomized with trinucleotides. *J. Mol. Biol.*, 296(1):57–86, feb 2000.

[237] W. Chen, Z. Zhu, Y. Feng, and D. S. Dimitrov. A large human domain antibody library combining heavy and light chain CDR3 diversity. *Mol. Immunol.*, 47(4):912–921, jan 2010.

[238] C. Chang, A. Takayanagi, T. Yoshida, and N. Shimizu. Screening of scFv-displaying phages recognizing distinct extracellular domains of EGF receptor by target-guided proximity labeling method. *J. Immunol. Methods*, 372(1-2):127–136, sep 2011.

[239] Z. Duan and H. Siegumfeldt. An Efficient Method for Isolating Antibody Fragments Against Small Peptides by Antibody Phage Display. *Comb. Chem. High Throughput Screen.*, 999(999):1–11, jul 2010.

[240] Z. Assur, W. A. Hendrickson, and F. Mancia. Tools for coproducing multiple proteins in mammalian cells. *Methods Mol. Biol.*, 801:173–87, 2012.

[241] N. Ouerghi, M. K. B. Fradj, M. Khammassi, M. Feki, N. Kaabachi, and A. Bouassida. Plasma chemerin in young untrained men: association with cardio-metabolic traits and physical performance, and response to intensive interval training. *Neuro Endocrinol. Lett.*, 38(1):59–66, feb 2017.

[242] H. R. Hoogenboom. Selecting and screening recombinant antibody libraries. *Nat. Biotechnol.*, 23(9):1105–1116, sep 2005.

[243] R. M. Hoet, E. H. Cohen, R. B. Kent, K. Rookey, S. Schoonbroodt, S. Hogan, L. Rem, N. Frans, M. Daukandt, H. Pieters, R. van Hegelsom, N. C.-v. Neer, H. G. Nastri, I. J. Rondon, J. A. Leeds, S. E. Hufton, L. Huang, I. Kashin, M. Devlin, G. Kuang, M. Steukers, M. Viswanathan, A. E. Nixon, D. J. Sexton, H. R. Hoogenboom, and R. C. Ladner. Generation of high-affinity human antibodies by combining donor-derived and synthetic complementarity-determining-region diversity. *Nat. Biotechnol.*, 23(3):344–348, mar 2005.

[244] C. Rothe, S. Urlinger, C. Löhning, J. Prassler, Y. Stark, U. Jäger, B. Hubner, M. Bardroff, I. Pradel, M. Boss, R. Bittlingmaier, T. Bataa, C. Frisch, B. Brocks, A. Honegger, and M. Urban. The Human Combinatorial Antibody Library HuCAL GOLD Combines Diversification of All Six CDRs According to the Natural Immune System with a Novel Display Method for Efficient Selection of High-Affinity Antibodies. *J. Mol. Biol.*, 376(4):1182–1200, feb 2008.

[245] C. Bee, Y. N. Abdiche, J. Pons, A. Rajpal, and J. Hawkins. Determining the Binding Affinity of Therapeutic Monoclonal Antibodies towards Their Native Unpurified Antigens in Human Serum. *PLoS One*, 8(11):e80501, nov 2013.

[246] P. Decker, D. Isenberg, and S. Muller. Inhibition of caspase-3-mediated poly(ADP-ribose) polymerase (PARP) apoptotic cleavage by human PARP autoantibodies and effect on cells undergoing apoptosis. *J. Biol. Chem.*, 275(12):9043–6, mar 2000.

[247] I. Tikhonov, T. J. Ruckwardt, S. Berg, G. S. Hatfield, and C. David Pauza. Furin cleavage of the HIV-1 Tat protein. *FEBS Lett.*, 565(1-3):89–92, may 2004.

[248] R. S. Thomas, J. E. Liddell, L. S. Murphy, D. M. Pache, and E. J. Kidd. An antibody to the beta-secretase cleavage site on amyloid-beta-protein precursor inhibits amyloid-beta production. *J. Alzheimers. Dis.*, 10(4):379–90, dec 2006.

[249] M. Harries and I. Smith. The development and clinical use of trastuzumab (Herceptin). *Endocr. Relat. Cancer*, 9(2):75–85, jun 2002.

[250] F. M. Yakes, W. Chinratanalab, C. A. Ritter, W. King, S. Seelig, and C. L. Arteaga. Herceptin-induced inhibition of phosphatidylinositol-3 kinase and Akt Is required for antibody-mediated effects on p27, cyclin D1, and antitumor action. *Cancer Res.*, 62(14):4132–41, jul 2002.

[251] M. A. Molina, J. Codony-Servat, J. Albanell, F. Rojo, J. Arribas, and J. Baselga. Trastuzumab (herceptin), a humanized anti-Her2 receptor monoclonal antibody, inhibits basal and activated Her2 ectodomain cleavage in breast cancer cells. *Cancer Res.*, 61(12):4744–9, jun 2001.

[252] P. Paganetti, V. Calanca, C. Galli, M. Stefani, and M. Molinari. β-site specific intrabodies to decrease and prevent generation of Alzheimer's Aβ peptide. *J. Cell Biol.*, 168(6):863–868, mar 2005.

[253] A. Messer and S. N. Joshi. Intrabodies as Neuroprotective Therapeutics. *Neurotherapeutics*, 10(3):447–458, jul 2013.

[254] D. W. Colby, Y. Chu, J. P. Cassady, M. Duennwald, H. Zazulak, J. M. Webster, A. Messer, S. Lindquist, V. M. Ingram, and K. D. Wittrup. Potent inhibition of huntingtin aggregation and cytotoxicity by a disulfide bond-free single-domain intracellular antibody. *Proc. Natl. Acad. Sci. U. S. A.*, 101(51):17616–17621, dec 2004.

[255] L. Renaut, C. Monnet, O. Dubreuil, O. Zaki, F. Crozet, K. Bouayadi, H. Kharrat, and P. Mondon. Affinity Maturation of Antibodies: Optimized Methods to Generate High-Quality ScFv Libraries and Isolate IgG Candidates by High-Throughput Screening. pages 451–461. Humana Press, Totowa, NJ, 2012.

[256] S. E. C. Caoili. Expressing Redundancy among Linear-Epitope Sequence Data Based on Residue-Level Physicochemical Similarity in the Context of Antigenic Cross-Reaction. *Adv. Bioinformatics*, 2016:1276594, 2016.

[257] M.-J. Jacobin, J. Laroche-Traineau, M. Little, A. Keller, K. Peter, M. Welschof, A. Nurden, and G. Clofent-Sanchez. Human IgG Monoclonal Anti-αIIbβ3-Binding Fragments Derived from Immunized Donors Using Phage Display. *J. Immunol.*, 168(4), 2002.

[258] J. C. Blankenship. Bleeding complications of glycoprotein IIb-IIIa receptor inhibitors. *Am. Heart J.*, 138(4 Pt 2):287–96, oct 1999.

[259] P. Bhoria, N. Varma, P. Malhotra, S. Varma, and M. Luthra-Guptasarma. Immunodiagnosis of platelet activation in immune thrombocytopenia through scFv antibodies cognate to activated IIb3 integrins. *MAbs*, 7(6):1212–1220, nov 2015.

[260] X. Peyrassol, T. Laeremans, M. Gouwy, V. Lahura, M. Debulpaep, J. Van Damme, J. Steyaert, M. Parmentier, and I. Langer. Development by Genetic Immunization of Monovalent Antibodies (Nanobodies) Behaving as Antagonists of the Human ChemR23 Receptor. *J. Immunol.*, 196(6):2893–2901, mar 2016.

[261] I. Gantz, Y. Konda, Y. K. Yang, D. E. Miller, H. A. Dierick, and T. Yamada. Molecular cloning of a novel receptor (CMKLR1) with homology to the chemotactic factor receptors. *Cytogenet. Cell Genet.*, 74(4):286–90, 1996.

[262] M. Samson, A. L. Edinger, P. Stordeur, J. Rucker, V. Verhasselt, M. Sharron, C. Govaerts, C. Mollereau, G. Vassart, R. W. Doms, and M. Parmentier. ChemR23, a putative chemoattractant receptor, is expressed in monocyte-derived dendritic cells and macrophages and is a coreceptor for SIV and some primary HIV-1 strains. *Eur. J. Immunol.*, 28(5):1689–700, may 1998.

[263] K. B. Goralski, T. C. McCarthy, E. A. Hanniman, B. A. Zabel, E. C. Butcher, S. D. Parlee, S. Muruganandan, and C. J. Sinal. Chemerin, a Novel Adipokine That Regulates Adipogenesis and Adipocyte Metabolism. *J. Biol. Chem.*, 282(38):28175–28188, sep 2007.

[264] M. Takahashi, Y. Takahashi, K. Takahashi, F. N. Zolotaryov, K. S. Hong, R. Kitazawa, K. Iida, Y. Okimura, H. Kaji, S. Kitazawa, M. Kasuga, and K. Chihara. Chemerin enhances insulin signaling and potentiates insulin-stimulated glucose uptake in 3T3-L1 adipocytes. *FEBS Lett.*, 582(5):573–578, mar 2008.

[265] B. S. Herrera, T. Ohira, L. Gao, K. Omori, R. Yang, M. Zhu, M. N. Muscara, C. N. Serhan, T. E. Van Dyke, and R. Gyurko. An endogenous regulator of inflammation, resolvin E1, modulates osteoclast differentiation and bone resorption. *Br. J. Pharmacol.*, 155(8):1214–1223, dec 2008.

[266] H. Liu, W. Xiong, Q. Liu, J. Zhang, and S. Dong. Chemokine-Like Receptor 1 Regulates the Proliferation and Migration of Vascular Smooth Muscle Cells. *Med. Sci. Monit.*, 22:4054–4061, oct 2016.

[267] A. L. Edinger, T. L. Hoffman, M. Sharron, B. Lee, Y. Yi, W. Choe, D. L. Kolson, B. Mitrovic, Y. Zhou, D. Faulds, R. G. Collman, J. Hesselgesser, R. Horuk, and R. W. Doms. An orphan seven-transmembrane domain receptor expressed widely in the brain functions as a coreceptor for human immunodeficiency virus type 1 and simian immunodeficiency virus. *J. Virol.*, 72(10):7934–40, oct 1998.

[268] A. Marchese, J. M. Docherty, T. Nguyen, M. Heiber, R. Cheng, H. H. Heng, L. C. Tsui, X. Shi, S. R. George, and B. F. O'Dowd. Cloning of human genes encoding novel G protein-coupled receptors. *Genomics*, 23(3):609–18, oct 1994.

[269] J. Bystrom, I. Evans, J. Newson, M. Stables, I. Toor, N. van Rooijen, M. Crawford, P. Colville-Nash, S. Farrow, and D. W. Gilroy. Resolution-phase macrophages possess a unique inflammatory phenotype that is controlled by cAMP. *Blood*, 112(10):4117–27, nov 2008.

[270] H. Singh-Jasuja, A. Thiolat, M. Ribon, M.-C. Boissier, N. Bessis, H.-G. Rammensee, and P. Decker. The mouse dendritic cell marker CD11c is down-regulated upon cell activation through Toll-like receptor triggering. *Immunobiology*, 218(1):28–39, jan 2013.

[271] O. Weinmann, R. Gutzmer, J. Zwirner, M. Wittmann, K. Langer, M. Lisewski, S. Mommert, A. Kapp, and T. Werfel. Up-regulation of C5a receptor expression and function on human monocyte derived dendritic cells by prostaglandin E2. *Immunology*, 110(4):458–65, dec 2003.

[272] D. Yang, Q. Chen, S. Stoll, X. Chen, O. M. Z. Howard, and J. J. Oppenheim. Differential Regulation of Responsiveness to fMLP and C5a Upon Dendritic Cell Maturation: Correlation with Receptor Expression. *J. Immunol.*, 165(5), 2000.

[273] J. Q. Davies and S. Gordon. Isolation and Culture of Murine Macrophages. In *Basic Cell Cult. Protoc.*, pages 091–104. Humana Press, New Jersey, 2005.

[274] X. Zhang, R. Goncalves, and D. M. Mosser. The isolation and characterization of murine macrophages. *Curr. Protoc. Immunol.*, Chapter 14:Unit 14.1, nov 2008.

[275] J. Vandesompele, K. De Preter, F. Pattyn, B. Poppe, N. Van Roy, A. De Paepe, and F. Speleman. Accurate normalization of real-time quantitative RT-PCR data by geometric averaging of multiple internal control genes. *Genome Biol.*, 3(7):34.1–34.11, jun 2002.

[276] M. W. Robinson, C. Harmon, and C. O'Farrelly. Liver immunology and its role in inflammation and homeostasis. *Cell. Mol. Immunol.*, 13(3):267–76, may 2016.

[277] B. A. Zabel, M. Kwitniewski, M. Banas, K. Zabieglo, K. Murzyn, and J. Cichy. Chemerin regulation and role in host defense. *Am. J. Clin. Exp. Immunol.*, 3(1):1–19, 2014.

[278] V. Bronte and M. J. Pittet. The spleen in local and systemic regulation of immunity. *Immunity*, 39(5):806–18, nov 2013.

[279] B. A. Zabel, A. M. Silverio, and E. C. Butcher. Chemokine-like receptor 1 expression and chemerin-directed chemotaxis distinguish plasmacytoid from myeloid dendritic cells in human blood. *J. Immunol.*, 174(1):244–51, jan 2005.

[280] M. Arita, F. Bianchini, J. Aliberti, A. Sher, N. Chiang, S. Hong, R. Yang, N. A. Petasis, and C. N. Serhan. Stereochemical assignment, antiinflammatory properties, and receptor for the omega-3 lipid mediator resolvin E1. *J. Exp. Med.*, 201(5), 2005.

[281] M. Herová, M. Schmid, C. Gemperle, and M. Hersberger. ChemR23, the Receptor for Chemerin and Resolvin E1, Is Expressed and Functional on M1 but Not on M2 Macrophages. *J. Immunol.*, 194(5), 2015.

[282] B. A. Zabel, T. Ohyama, L. Zuniga, J.-Y. Kim, B. Johnston, S. J. Allen, D. G. Guido, T. M. Handel, and E. C. Butcher. Chemokine-like receptor 1 expression by macrophages in vivo: Regulation by TGF-β and TLR ligands. *Exp. Hematol.*, 34(8):1106–1114, aug 2006.

[283] T. Maier, M. Güell, and L. Serrano. Correlation of mRNA and protein in complex biological samples. *FEBS Lett.*, 583(24):3966–3973, dec 2009.

[284] T. Shimada, M. Matsumoto, Y. Tatsumi, A. Kanamaru, and S. Akira. A novel lipopolysaccharide inducible C-C chemokine receptor related gene in murine macrophages. *FEBS Lett.*, 425(3):490–4, apr 1998.

[285] A. D. A. Cassado, M. R. D'Império Lima, and K. R. Bortoluci. Revisiting mouse peritoneal macrophages: heterogeneity, development, and function. *Front. Immunol.*, 6:225, 2015.

[286] J. L. Cash, M. D. Bass, J. Campbell, M. Barnes, P. Kubes, and P. Martin. Resolution Mediator Chemerin15 Reprograms the Wound Microenvironment to Promote Repair and Reduce Scarring. *Curr. Biol.*, 24(12):1406–1414, jun 2014.

[287] M. O. Freire, J. Dalli, C. N. Serhan, and T. E. Van Dyke. Neutrophil Resolvin E1 Receptor Expression and Function in Type 2 Diabetes. *J. Immunol.*, 198(2), 2017.

[288] C. S. McKimmie, A. R. Fraser, C. Hansell, L. Gutiérrez, S. Philipsen, L. Connell, A. Rot, M. Kurowska-Stolarska, P. Carreno, M. Pruenster, C.-C. Chu, G. Lombardi, C. Halsey, I. B. McInnes, F. Y. Liew, R. J. Nibbs, and G. J. Graham. Hemopoietic Cell Expression of the Chemokine Decoy Receptor D6 Is Dynamic and Regulated by GATA1. *J. Immunol.*, 181(5), 2008.

[289] X. Zhang. Regulatory functions of innate-like B cells. *Cell. Mol. Immunol.*, 10(2):113–121, mar 2013.

[290] T. N. Hartmann, M. Leick, S. Ewers, A. Diefenbacher, I. Schraufstatter, M. Honczarenko, and M. Burger. Human B cells express the orphan chemokine receptor CRAM-A/B in a maturation-stage-dependent and CCL5-modulated manner. *Immunology*, 125(2):252–62, oct 2008.

[291] J. Wanninger, S. Bauer, K. Eisinger, T. S. Weiss, R. Walter, C. Hellerbrand, A. Schäffler, A. Higuchi, K. Walsh, and C. Buechler. Adiponectin upregulates hepatocyte CMKLR1 which is reduced in human fatty liver. *Mol. Cell. Endocrinol.*, 349(2):248–54, feb 2012.

[292] R. B. Bressan, P. S. Dewari, M. Kalantzaki, E. Gangoso, M. Matjusaitis, C. Garcia-Diaz, C. Blin, V. Grant, H. Bulstrode, S. Gogolok, W. C. Skarnes, and S. M. Pollard. Efficient CRISPR/Cas9-assisted gene targeting enables rapid and precise genetic manipulation of mammalian neural stem cells. *Development*, 144(4):635–648, feb 2017.

[293] A. E. Cardona, E. P. Pioro, M. E. Sasse, V. Kostenko, S. M. Cardona, I. M. Dijkstra, D. Huang, G. Kidd, S. Dombrowski, R. Dutta, J.-C. Lee, D. N. Cook, S. Jung, S. A. Lira, D. R. Littman, and R. M. Ransohoff. Control of microglial neurotoxicity by the fractalkine receptor. *Nat. Neurosci.*, 9(7):917–924, jul 2006.

[294] P. Fan, H. Kyaw, K. Su, Z. Zeng, M. Augustus, K. C. Carter, and Y. Li. Cloning and Characterization of a Novel Human Chemokine Receptor. *Biochem. Biophys. Res. Commun.*, 243(1):264–268, feb 1998.

[295] P. Joost and A. Methner. Phylogenetic analysis of 277 human G-protein-coupled receptors as a tool for the prediction of orphan receptor ligands. *Genome Biol.*, 3(11):63.1–63.16, oct 2002.

[296] G. Graham, M. Locati, A. Mantovani, A. Rot, and M. Thelen. The biochemistry and biology of the atypical chemokine receptors. *Immunol. Lett.*, 145(1-2):30–38, jul 2012.

[297] M. Leick, J. Catusse, M. Follo, R. J. Nibbs, T. N. Hartmann, H. Veelken, and M. Burger. CCL19 is a specific ligand of the constitutively recycling atypical human chemokine receptor CRAM-B. *Immunology*, 129(4):536–546, apr 2010.

[298] A. M. Fra, M. Locati, K. Otero, M. Sironi, P. Signorelli, M. L. Massardi, M. Gobbi, A. Vecchi, S. Sozzani, and A. Mantovani. Cutting Edge: Scavenging of Inflammatory CC Chemokines by the Promiscuous Putatively Silent Chemokine Receptor D6. *J. Immunol.*, 170(5), 2003.

[299] A. Mantovani, R. Bonecchi, and M. Locati. Tuning inflammation and immunity by chemokine sequestration: decoys and more. *Nat. Rev. Immunol.*, 6(12):907–918, dec 2006.

[300] N. Brouwer, M. Zuurman, T. Wei, R. Ransohoff, H. Boddeke, and K. Biber. Induction of glial L-CCR mRNA expression in spinal cord and brain in experimental autoimmune encephalomyelitis. *Glia*, 46(1):84–94, apr 2004.

[301] C. L. Galligan, W. Matsuyama, A. Matsukawa, H. Mizuta, D. R. Hodge, O. M. Z. Howard, and T. Yoshimura. Up-regulated expression and activation of the orphan chemokine receptor, CCRL2, in rheumatoid arthritis. *Arthritis Rheum.*, 50(6):1806–1814, jun 2004.

[302] J. Auer, M. Bläss, H. Schulze-Koops, S. Russwurm, T. Nagel, J. R. Kalden, M. Röllinghoff, and H. Beuscher. Expression and regulation of CCL18 in synovial fluid neutrophils of patients with rheumatoid arthritis. *Arthritis Res. Ther.*, 9(5):R94, 2007.

[303] J. L. Rourke, H. J. Dranse, and C. J. Sinal. CMKLR1 and GPR1 mediate chemerin signaling through the RhoA/ROCK pathway. *Mol. Cell. Endocrinol.*, 417:36–51, dec 2015.

[304] K. De Filippo, R. B. Henderson, M. Laschinger, and N. Hogg. Neutrophil Chemokines KC and Macrophage-Inflammatory Protein-2 Are Newly Synthesized by Tissue Macrophages Using Distinct TLR Signaling Pathways. *J. Immunol.*, 180(6), 2008.

[305] Y. M. Li, G. Baviello, H. Vlassara, and T. Mitsuhashi. Glycation products in aged thioglycollate medium enhance the elicitation of peritoneal macrophages. *J. Immunol. Methods*, 201(2):183–8, feb 1997.

[306] D. R. Call, J. A. Nemzek, S. J. Ebong, G. L. Bolgos, D. E. Newcomb, and D. G. Remick. Ratio of Local to Systemic Chemokine Concentrations Regulates Neutrophil Recruitment. *Am. J. Pathol.*, 158(2):715–721, feb 2001.

[307] G. J. Graham. D6 and the atypical chemokine receptor family: Novel regulators of immune and inflammatory processes. *Eur. J. Immunol.*, 39(2):342–351, feb 2009.

[308] C. N. Serhan, S. Hong, K. Gronert, S. P. Colgan, P. R. Devchand, G. Mirick, and R.-L. Moussignac. Resolvins. *J. Exp. Med.*, 196(8), 2002.

[309] M. J. Paul-Clark, T. van Cao, N. Moradi-Bidhendi, D. Cooper, and D. W. Gilroy. 15-epi-lipoxin A4mediated Induction of Nitric Oxide Explains How Aspirin Inhibits Acute Inflammation. *J. Exp. Med.*, 200(1), 2004.

[310] J. Lee, G. Cacalano, T. Camerato, K. Toy, M. W. Moore, and W. I. Wood. Chemokine binding and activities mediated by the mouse IL-8 receptor. *J. Immunol.*, 155(4), 1995.

[311] S. R. McColl and I. Clark-Lewis. Inhibition of Murine Neutrophil Recruitment In Vivo by CXC Chemokine Receptor Antagonists. *J. Immunol.*, 163(5), 1999.

[312] K. De Filippo, A. Dudeck, M. Hasenberg, E. Nye, N. van Rooijen, K. Hartmann, M. Gunzer, A. Roers, and N. Hogg. Mast cell and macrophage chemokines CXCL1/CXCL2 control the early stage of neutrophil recruitment during tissue inflammation. *Blood*, 121(24), 2013.

[313] S. D. Parlee, J. O. McNeil, S. Muruganandan, C. J. Sinal, and K. B. Goralski. Elastase and Tryptase Govern TNFα-Mediated Production of Active Chemerin by Adipocytes. *PLoS One*, 7(12):e51072, dec 2012.

[314] C. Keller, P. Keller, M. Giralt, J. Hidalgo, and B. K. Pedersen. Exercise normalises overexpression of TNF-α in knockout mice. *Biochem. Biophys. Res. Commun.*, 321(1):179–182, aug 2004.

[315] K. Teoman Uysal, S. M. Wiesbrock, G. Khan, and S. Hotamisligil. Functional Analysis of Tumor Necrosis Factor (TNF) Receptors in TNF--Mediated Insulin Resistance in Genetic Obesity*. *Endocrinology*, 139(12):4832–4838, 1998.

[316] L. Taylor, I. Christou, T. S. Kapellos, A. Buchan, M. H. Brodermann, M. Gianella-Borradori, A. Russell, A. J. Iqbal, and D. R. Greaves. Primary Macrophage Chemotaxis Induced by Cannabinoid Receptor 2 Agonists Occurs Independently of the CB2 Receptor. *Sci. Rep.*, 5(1):10682, sep 2015.

[317] H. Jung, D. S. Mithal, J. E. Park, R. J. Miller, S. Anaya-O'Brien, and N. Turner. Localized CCR2 Activation in the Bone Marrow Niche Mobilizes Monocytes by Desensitizing CXCR4. *PLoS One*, 10(6):e0128387, jun 2015.

[318] N. V. Serbina and E. G. Pamer. Monocyte emigration from bone marrow during bacterial infection requires signals mediated by chemokine receptor CCR2. *Nat. Immunol.*, 7(3):311–317, mar 2006.

[319] B. A. Zabel, A. M. Silverio, and E. C. Butcher. Chemokine-Like Receptor 1 Expression and Chemerin-Directed Chemotaxis Distinguish Plasmacytoid from Myeloid Dendritic Cells in Human Blood. *J. Immunol.*, 174(1), 2004.

[320] M. Steinmüller, M. Srivastava, W. A. Kuziel, J. W. Christman, W. Seeger, T. Welte, J. Lohmeyer, and U. A. Maus. Endotoxin induced peritonitis elicits monocyte immigration into the lung: implications on alveolar space inflammatory responsiveness. *Respir. Res.*, 7(1):30, feb 2006.

[321] R. G. Holzheimer. Management of secondary peritonitis. In *Surg. Treat. Evidence-Based Probl.* Zuckschwerdt, 2001.

[322] J. A. Akoh. Peritoneal dialysis associated infections: An update on diagnosis and management. *World J. Nephrol.*, 1(4):106–22, aug 2012.

[323] M. Herová, M. Schmid, C. Gemperle, C. Loretz, and M. Hersberger. Low dose aspirin is associated with plasma chemerin levels and may reduce adipose tissue inflammation. *Atherosclerosis*, 235(2):256–262, aug 2014.

[324] M. Lehrke, A. Becker, M. Greif, R. Stark, R. P. Laubender, F. von Ziegler, C. Lebherz, J. Tittus, M. Reiser, C. Becker, B. Göke, A. W. Leber, K. G. Parhofer, and U. C. Broedl. Chemerin is associated with markers of inflammation and components of the metabolic syndrome but does not predict coronary atherosclerosis. *Eur. J. Endocrinol.*, 161(2):339–44, aug 2009.

[325] J. P. Webster. The effect of Toxoplasma gondii on animal behavior: playing cat and mouse. *Schizophr. Bull.*, 33(3):752–6, may 2007.

[326] J. Gatkowska, M. Wieczorek, B. Dziadek, K. Dzitko, and H. Dlugonska. Behavioral changes in mice caused by Toxoplasma gondii invasion of brain. *Parasitol. Res.*, 111(1):53–8, jul 2012.

[327] M. Berdoy, J. P. Webster, and D. W. Macdonald. Fatal attraction in rats infected with Toxoplasma gondii. *Proc. R. Soc. B Biol. Sci.*, 267(1452):1591–1594, aug 2000.

[328] D. Arsenijevic, L. Girardier, J. Seydoux, H. R. Chang, and A. G. Dulloo. Altered energy balance and cytokine gene expression in a murine model of chronic infection with Toxoplasma gondii. *Am. J. Physiol.*, 272(5 Pt 1):E908–17, may 1997.

[329] H. H. Stibbs. Changes in brain concentrations of catecholamines and indoleamines in Toxoplasma gondii infected mice. *Ann. Trop. Med. Parasitol.*, 79(2):153–7, apr 1985.

[330] T. Vos and Others. Global, regional, and national incidence, prevalence, and years lived with disability for 301 acute and chronic diseases and injuries in 188 countries, 19902013: a systematic analysis for the Global Burden of Disease Study 2013. *Lancet*, 386(9995):743–800, aug 2015.

[331] C. E. Griffin, A. M. Kaye, F. R. Bueno, A. D. Kaye, and A. D. Kaye. Benzodiazepine pharmacology and central nervous system-mediated effects. *Ochsner J.*, 13(2):214–23, 2013.

[332] G. J. Marek, L. L. Carpenter, C. J. McDougle, and L. H. Price. Synergistic Action of 5-HT2A Antagonists and Selective Serotonin Reuptake Inhibitors in Neuropsychiatric Disorders. *Neuropsychopharmacology*, 28(2):402–412, feb 2003.

[333] A. J. Rush, M. H. Trivedi, S. R. Wisniewski, A. A. Nierenberg, J. W. Stewart, D. Warden, G. Niederehe, M. E. Thase, P. W. Lavori, B. D. Lebowitz, P. J. McGrath, J. F. Rosenbaum, H. A. Sackeim, D. J. Kupfer, J. Luther, and M. Fava. Acute and Longer-Term Outcomes in Depressed Outpatients Requiring One or Several Treatment Steps: A STAR*D Report. *Am. J. Psychiatry*, 163(11):1905–1917, nov 2006.

[334] M. Maes, H. Y. Meltzer, E. Bosmans, R. Bergmans, E. Vandoolaeghe, R. Ranjan, and R. Desnyder. Increased plasma concentrations of interleukin-6, soluble interleukin-6, soluble interleukin-2 and transferrin receptor in major depression. *J. Affect. Disord.*, 34(4):301–9, aug 1995.

[335] G. E. Hodes, M. L. Pfau, M. Leboeuf, S. A. Golden, D. J. Christoffel, D. Bregman, N. Rebusi, M. Heshmati, H. Aleyasin, B. L. Warren, B. Labonté, S. Horn, K. A. Lapidus, V. Stelzhammer, E. H. F. Wong, S. Bahn, V. Krishnan, C. A. Bolaños-Guzman, J. W. Murrough, M. Merad, and S. J. Russo. Individual differences in the peripheral immune system promote resilience versus susceptibility to social stress. *Proc. Natl. Acad. Sci.*, 111(45):16136–16141, nov 2014.

[336] M. Maes, M. Van der Planken, W. J. Stevens, D. Peeters, L. S. DeClerck, C. H. Bridts, C. Schotte, and P. Cosyns. Leukocytosis, monocytosis and neutrophilia: hallmarks of severe depression. *J. Psychiatr. Res.*, 26(2):125–34, apr 1992.

[337] T. Heidt, H. B. Sager, G. Courties, P. Dutta, Y. Iwamoto, A. Zaltsman, C. von Zur Muhlen, C. Bode, G. L. Fricchione, J. Denninger, C. P. Lin, C. Vinegoni, P. Libby, F. K. Swirski, R. Weissleder, and M. Nahrendorf. Chronic variable stress activates hematopoietic stem cells. *Nat. Med.*, 20(7):754–758, jul 2014.

[338] G. E. Hodes, V. Kana, C. Menard, M. Merad, and S. J. Russo. Neuroimmune mechanisms of depression. *Nat. Neurosci.*, 18(10):1386–1393, sep 2015.

[339] A. H. Miller and C. L. Raison. The role of inflammation in depression: from evolutionary imperative to modern treatment target. *Nat. Rev. Immunol.*, 16(1):22–34, dec 2015.

[340] E. S. Wohleb, M. L. Hanke, A. W. Corona, N. D. Powell, L. ', T. M. Stiner, M. T. Bailey, R. J. Nelson, J. P. Godbout, and J. F. Sheridan. Cellular/Molecular -Adrenergic Receptor Antagonism Prevents Anxiety-Like Behavior and Microglial Reactivity Induced by Repeated Social Defeat. *J. Neurosci.*, 31(17):6277–88, 2011.

[341] D. W. Cain and J. A. Cidlowski. Immune regulation by glucocorticoids. *Nat. Rev. Immunol.*, 17(4):233–247, feb 2017.

[342] F. Tronche, C. Kellendonk, O. Kretz, P. Gass, K. Anlag, P. C. Orban, R. Bock, R. Klein, and G. Schütz. Disruption of the glucocorticoid receptor gene in the nervous system results in reduced anxiety. *Nat. Genet.*, 23(1):99–103, sep 1999.

[343] M. G. Frank, Z. D. Miguel, L. R. Watkins, and S. F. Maier. Prior exposure to glucocorticoids sensitizes the neuroinflammatory and peripheral inflammatory responses to E. coli lipopolysaccharide. *Brain. Behav. Immun.*, 24(1):19–30, jan 2010.

[344] R. M. Bluthé, V. Walter, P. Parnet, S. Layé, J. Lestage, D. Verrier, S. Poole, B. E. Stenning, K. W. Kelley, and R. Dantzer. Lipopolysaccharide induces sickness behaviour in rats by a vagal mediated mechanism. *C. R. Acad. Sci. III.*, 317(6):499–503, jun 1994.

[345] B.-J. Kim and H. P. Jones. Epinephrine-primed murine bone marrow-derived dendritic cells facilitate production of IL-17A and IL-4 but not IFN-γ by CD4+ T cells. *Brain. Behav. Immun.*, 24(7):1126–1136, oct 2010.

[346] M. Rosas-Ballina, P. S. Olofsson, M. Ochani, S. I. Valdés-Ferrer, Y. A. Levine, C. Reardon, M. W. Tusche, V. A. Pavlov, U. Andersson, S. Chavan, T. W. Mak, and K. J. Tracey. Acetylcholine-synthesizing T cells relay neural signals in a vagus nerve circuit. *Science*, 334(6052):98–101, oct 2011.

[347] J. Kipnis, H. Cohen, M. Cardon, Y. Ziv, and M. Schwartz. T cell deficiency leads to cognitive dysfunction: implications for therapeutic vaccination for schizophrenia and other psychiatric conditions. *Proc. Natl. Acad. Sci. U. S. A.*, 101(21):8180–5, may 2004.

[348] L. Rattazzi, G. Piras, M. Ono, R. Deacon, C. M. Pariante, and F. D'Acquisto. CD4 but not CD8 T cells revert the impaired emotional behavior of immunocompromised RAG-1-deficient mice. *Transl. Psychiatry*, 3(7):e280, jul 2013.

[349] N. C. Derecki, A. N. Cardani, C. H. Yang, K. M. Quinnies, A. Crihfield, K. R. Lynch, and J. Kipnis. Regulation of learning and memory by meningeal immunity: a key role for IL-4. *J. Exp. Med.*, 207(5), 2010.

[350] J. Leserman, J. M. Petitto, H. Gu, B. N. Gaynes, J. Barroso, R. N. Golden, D. O. Perkins, J. D. Folds, and D. L. Evans. Progression to AIDS, a clinical AIDS condition and mortality: psychosocial and physiological predictors. *Psychol. Med.*, 32(6):1059–73, aug 2002.

[351] R. Pudlo, M. Piegza, M. Zakliczyński, and M. Zembala. The Occurence of Mood and Anxiety Disorders in Heart Transplant Recipients. *Transplant. Proc.*, 41(8):3214–3218, oct 2009.

[352] K. N. Couper, D. G. Blount, and E. M. Riley. IL-10: The Master Regulator of Immunity to Infection. *J. Immunol.*, 180(9), 2008.

[353] A. R. Mesquita, M. Correia-Neves, S. Roque, A. G. Castro, P. Vieira, J. Pedrosa, J. A. Palha, and N. Sousa. IL-10 modulates depressive-like behavior. *J. Psychiatr. Res.*, 43(2):89–97, dec 2008.

[354] S. Oldekamp, S. Pscheidl, E. Kress, O. Soehnlein, S. Jansen, T. Pufe, J. M. Wang, S. C. Tauber, and L.-O. Brandenburg. Lack of formyl peptide receptor 1 and 2 leads to more severe inflammation and higher mortality in mice with of pneumococcal meningitis. *Immunology*, 143(3):447–61, nov 2014.

[355] J.-L. Gao, E. H. Schneider, E. L. Dimitrov, F. Haun, T. M. Pham, A. H. Mohammed, T. B. Usdin, and P. M. Murphy. Reduced fear memory and anxiety-like behavior in mice lacking formylpeptide receptor 1. *Behav. Genet.*, 41(5):724–33, sep 2011.

[356] I. Gallo, L. Rattazzi, G. Piras, T. Gobbetti, E. Panza, M. Perretti, J. W. Dalley, and F. D'Acquisto. Formyl peptide receptor as a novel therapeutic target for anxiety-related disorders. *PLoS One*, 9(12):e114626, 2014.

[357] N. Brouwer, M. Zuurman, T. Wei, R. Ransohoff, H. Boddeke, and K. Biber. Induction of glial L-CCR mRNA expression in spinal cord and brain in experimental autoimmune encephalomyelitis. *Glia*, 46(1):84–94, apr 2004.

[358] M. W. Zuurman, J. Heeroma, N. Brouwer, H. W. Boddeke, and K. Biber. LPS-induced expression of a novel chemokine receptor (L-CCR) in mouse glial cells in vitro and in vivo. *Glia*, 41(4):327–336, mar 2003.

[359] K. R. Bailey and J. N. Crawley. *Anxiety-Related Behaviors in Mice*. CRC Press/Taylor & Francis, 2009.

[360] R. Yankelevitch-Yahav, M. Franko, A. Huly, and R. Doron. The forced swim test as a model of depressive-like behavior. *J. Vis. Exp.*, (97), mar 2015.

[361] A. Nimmerjahn, F. Kirchhoff, and F. Helmchen. Resting Microglial Cells Are Highly Dynamic Surveillants of Brain Parenchyma in Vivo. *Science (80-.).*, 308(5726):1314–1318, may 2005.

[362] L. E. Gonzalez and S. E. File. A five minute experience in the elevated plus-maze alters the state of the benzodiazepine receptor in the dorsal raphe nucleus. *J. Neurosci.*, 17(4):1505–11, feb 1997.

[363] K. Singh, M. Bishnoi, and S. Kulkarni. Elevated Zero-maze: A paradigm to evaluate anti-anxiety effects of drugs. *Methods Find. Exp. Clin. Pharmacol.*, 29(5):343, jun 2007.

[364] S. Wieland and I. Lucki. Antidepressant-like activity of 5-HT1A agonists measured with the forced swim test. *Psychopharmacology (Berl).*, 101(4):497–504, aug 1990.

[365] J. F. Cryan, M. E. Page, and I. Lucki. Differential behavioral effects of the antidepressants reboxetine, fluoxetine, and moclobemide in a modified forced swim test following chronic treatment. *Psychopharmacology (Berl).*, 182(3):335–344, nov 2005.

[366] S. D. Mague, A. M. Pliakas, M. S. Todtenkopf, H. C. Tomasiewicz, Y. Zhang, W. C. Stevens, R. M. Jones, P. S. Portoghese, and W. A. Carlezon. Antidepressant-Like Effects of κ-Opioid Receptor Antagonists in the Forced Swim Test in Rats. *J. Pharmacol. Exp. Ther.*, 305(1), 2003.

[367] B. Korte, S. Mechiel, De Kloet, E. Ronald, Buwalda, Bauke, Bouman, Stephan D., Bohus. Antisense to the glucocorticoid receptor in hippocampal dentate gyrus reduces immobility in forced swim test. *Eur. J. Pharmacol.*, 301:19–25, 1996.

[368] G. M. Slavich and M. R. Irwin. From stress to inflammation and major depressive disorder: A social signal transduction theory of depression. *Psychol. Bull.*, 140(3):774–815, may 2014.

[369] P. Bercik, E. F. Verdu, J. A. Foster, J. Macri, M. Potter, X. Huang, P. Malinowski, W. Jackson, P. Blennerhassett, K. A. Neufeld, J. Lu, W. I. Khan, I. CorthesyTheulaz, C. Cherbut, G. E. Bergonzelli, and S. M. Collins. Chronic Gastrointestinal Inflammation Induces Anxiety-Like Behavior and Alters Central Nervous System Biochemistry in Mice. *Gastroenterology*, 139(6):2102–2112.e1, dec 2010.

[370] J. C. O'Connor, M. A. Lawson, C. André, M. Moreau, J. Lestage, N. Castanon, K. W. Kelley, and R. Dantzer. Lipopolysaccharide-induced depressive-like behavior is mediated by indoleamine 2,3-dioxygenase activation in mice. *Mol. Psychiatry*, 14(5):511–522, may 2009.

[371] W. Yan, C. C. Wilson, and J. H. Haring. Effects of neonatal serotonin depletion on the development of rat dentate granule cells. *Dev. Brain Res.*, 98(2):177–184, feb 1997.

[372] O. Cases, T. Vitalis, I. Seif, E. De Maeyer, C. Sotelo, and P. Gaspar. Lack of Barrels in the Somatosensory Cortex of Monoamine Oxidase ADeficient Mice: Role of a Serotonin Excess during the Critical Period. *Neuron*, 16(2):297–307, feb 1996.

[373] L. Vitkovic, J. P. Konsman, J. Bockaert, R. Dantzer, V. Homburger, and C. Jacque. Cytokine signals propagate through the brain. *Mol. Psychiatry*, 5(6):604–15, nov 2000.

[374] T. Suzuki, A. Ohmuro, M. Miyata, T. Furuishi, S. Hidaka, F. Kugawa, T. Fukami, and K. Tomono. Involvement of an influx transporter in the blood-brain barrier transport of naloxone. *Biopharm. Drug Dispos.*, 31(4):n/a–n/a, may 2010.

[375] E. G. Gutierrez, W. A. Banks, and A. J. Kastin. Murine tumor necrosis factor alpha is transported from blood to brain in the mouse. *J. Neuroimmunol.*, 47(2):169–76, sep 1993.

[376] R. C. Paolicelli, G. Bolasco, F. Pagani, L. Maggi, M. Scianni, P. Panzanelli, M. Giustetto, T. A. Ferreira, E. Guiducci, L. Dumas, D. Ragozzino, and C. T. Gross. Synaptic Pruning by Microglia Is Necessary for Normal Brain Development. *Science (80-.).*, 333(6048), 2011.

[377] A. Sierra, J. M. Encinas, J. J. P. Deudero, J. H. Chancey, G. Enikolopov, L. S. Overstreet-Wadiche, S. E. Tsirka, and M. Maletic-Savatic. Cell Stem Cell Microglia Shape Adult Hippocampal Neurogenesis through Apoptosis-Coupled Phagocytosis. 2010.

[378] M. L. Monje, H. Toda, and T. D. Palmer. Inflammatory Blockade Restores Adult Hippocampal Neurogenesis. *Science (80-.).*, 302(5651):1760–1765, dec 2003.

[379] G. N. Bastos, T. Moriya, F. Inui, T. Katura, and N. Nakahata. Involvement of cyclooxygenase-2 in lipopolysaccharide induced impairment of the newborn cell survival in the adult mouse dentate gyrus. *Neuroscience*, 155(2):454–462, 2008.

[380] K. Liaury, T. Miyaoka, T. Tsumori, M. Furuya, S. Hashioka, R. Wake, K. Tsuchie, M. Fukushima, E. Limoa, A. J. Tanra, and J. Horiguchi. Minocycline improves recognition memory and attenuates microglial activation in Gunn rat: A possible hyperbilirubinemia-induced animal model of schizophrenia. *Prog. Neuro-Psychopharmacology Biol. Psychiatry*, 50:184–190, apr 2014.

[381] L. E. Laskaris, M. A. Di Biase, I. Everall, G. Chana, A. Christopoulos, E. Skafidas, V. L. Cropley, and C. Pantelis. Microglial activation and progressive brain changes in schizophrenia. *Br. J. Pharmacol.*, 173(4):666–80, feb 2016.

[382] J. Fan, D. Char, G. J. Bagby, M. C. Gelato, and C. H. Lang. Regulation of insulin-like growth factor-I (IGF-I) and IGF-binding proteins by tumor necrosis factor. *Am. J. Physiol.*, 269(5 Pt 2):R1204–12, nov 1995.

[383] S.-E. Park, M. Lawson, R. Dantzer, K. W. Kelley, and R. H. McCusker. Insulin-like growth factor-I peptides act centrally to decrease depression-like behavior of mice treated intraperitoneally with lipopolysaccharide. *J. Neuroinflammation*, 8(1):179, dec 2011.

[384] P. D. Bruen, W. J. McGeown, M. F. Shanks, and A. Venneri. Neuroanatomical correlates of neuropsychiatric symptoms in Alzheimer's disease. *Brain*, 131(9):2455–2463, aug 2008.

[385] H. J. Rosen, S. C. Allison, G. F. Schauer, M. L. Gorno-Tempini, M. W. Weiner, and B. L. Miller. Neuroanatomical correlates of behavioural disorders in dementia. *Brain*, 128(Pt 11):2612–25, nov 2005.

[386] H. Ilieva, M. Polymenidou, and D. W. Cleveland. Noncell autonomous toxicity in neurodegenerative disorders: ALS and beyond. *J. Cell Biol.*, 187(6):761–772, dec 2009.

[387] A. Monji, T. Kato, and S. Kanba. Cytokines and schizophrenia: Microglia hypothesis of schizophrenia. *Psychiatry Clin. Neurosci.*, 63(3):257–65, jun 2009.

[388] C. Albanesi, C. Scarponi, S. Pallotta, R. Daniele, D. Bosisio, S. Madonna, P. Fortugno, S. Gonzalvo-Feo, J.-D. Franssen, M. Parmentier, O. De Pità, G. Girolomoni, and S. Sozzani. Chemerin expression marks early psoriatic skin lesions and correlates with plasmacytoid dendritic cell recruitment. *J. Exp. Med.*, 206(1):249–258, jan 2009.

[389] C. G. Kostopoulos, S. G. Spiroglou, J. N. Varakis, E. Apostolakis, and H. H. Papadaki. Chemerin and CMKLR1 expression in human arteries and periadventitial fat: a possible role for local chemerin in atherosclerosis? *BMC Cardiovasc. Disord.*, 14(1):56, dec 2014.

[390] S. W. Watts, A. M. Dorrance, M. E. Penfold, J. L. Rourke, C. J. Sinal, B. Seitz, T. J. Sullivan, T. T. Charvat, J. M. Thompson, R. Burnett, and G. D. Fink. Chemerin Connects Fat to Arterial Contraction. *Arterioscler. Thromb. Vasc. Biol.*, 33(6):1320–1328, jun 2013.

[391] W. Xiong, Y. Luo, L. Wu, F. Liu, H. Liu, J. Li, B. Liao, and S. Dong. Chemerin Stimulates Vascular Smooth Muscle Cell Proliferation and Carotid Neointimal Hyperplasia by Activating Mitogen-Activated Protein Kinase Signaling. *PLoS One*, 11(10):e0165305, oct 2016.

[392] H. Kunimoto, K. Kazama, M. Takai, M. Oda, M. Okada, and H. Yamawaki. Chemerin promotes proliferation and migration of vascular smooth muscle and increases mouse blood pressure. *Am. J. Physiol. - Hear. Circ. Physiol.*, 309(5):ajpheart.00820.2014, aug 2015.

[393] P. H. Dessein, L. Tsang, A. J. Woodiwiss, G. R. Norton, A. Solomon, and K. Reddi. Circulating concentrations of the novel adipokine chemerin are associated with cardiovascular disease risk in rheumatoid arthritis. *J. Rheumatol.*, 41(9):1746–54, sep 2014.

[394] J. R. Doyle, S. T. Krishnaji, G. Zhu, Z.-Z. Xu, D. Heller, R.-R. Ji, B. D. Levy, K. Kumar, and A. S. Kopin. Development of a membrane-anchored chemerin receptor agonist as a novel modulator of allergic airway inflammation and neuropathic pain. *J. Biol. Chem.*, 289(19):13385–96, may 2014.

[395] P. J. Barnes. New anti-inflammatory targets for chronic obstructive pulmonary disease. *Nat. Rev. Drug Discov.*, 12(7):543–559, jun 2013.